"UNIVERSITAT POLITÈCNICA DE CATALUNYA"

DEPARTMENT OF ELECTRICAL ENGINEERING

DOCTORAL THESIS

NOVEL PIEZOELECTRIC TRANSDUCERS FOR HIGH VOLTAGE MEASUREMENTS

Author: Industrial Engineer ALFREDO VÁZQUEZ CARAZO

Supervisor: Doctor Industrial Engineer RICARD BOSCH TOUS

A thesis submitted to the E.T.S.E.I. Barcelona

of the *"Universitat Politècnica de Catalunya" (U.P.C)*

for the degree of

DOCTOR OF ENGINEERING

Barcelona, January 2000

DOCTORAL THESIS

NOVEL PIEZOELECTRIC TRANSDUCERS FOR HIGH VOLTAGE MEASUREMENTS

Author: **Industrial Engineer ALFREDO VÁZQUEZ CARAZO**

Supervisor: **Doctor Industrial Engineer RICARD BOSCH TOUS**

Examining Committee:

Chairman: **Dr. Luis Humet Coderch**
Catedrático de Universidad of the Department of Electrical Engineering of E.T.S.E.I.Barcelona, Universitat Politècnica de Catalunya (Spain)

Secretary: **Dr. Antonio Conejo Navarro**
Catedrático de Universidad of the Department of Electrical and Electronics of the E.T.S. Ing. Ind., Universidad Castilla-La Mancha (Spain).

Members: **Dr. Carlos Álvarez Bel**
Profesor Titular of the Department of Electrical Engineering of the E.T.S. Ing. Ind., Universidad Politécnica de Valencia (Spain).

Dr. Daniel Guyomar
Professor of the Laboratorie de Génie Électrique et Ferroélectricité of the INSA de Lyon (France).

Dr. Dragan Damjanovic
Senior Lecturer of the Ceramic Laboratory, Materials Department of the Swiss Federale Institute of Technology (EPFL) (Switzerland).

Barcelona, January 2000
(For Graduation April 2000)

To my family

Contents

List of Figures and Tables

Preface

In June of 1996 I completed the five years of the degree in Industrial Engineering, Electrical speciality, in the *Universitat Politècnica de Catalunya*. A requirement for obtaining my Degree was the development of a Final Project in an aspect relative to the Electrical Engineering. In order to complete this requirement, since 1995 I have been working with Prof. Dr. Eng. Ricard Bosch Tous in the development of a novel transducer for measuring High Voltages, based in the use of piezoelectric materials.

Our interest for the piezoelectricity came from a previous doctoral work, also directed by Dr. Bosch, developed by Prof. Dr. Eng. Jesús Álvarez Flórez. In his Thesis, Dr. Álvarez developed successfully a novel resonant step-up transformer for ignition in internal combustion motors.

The ideas about resonant transformers presented in the thesis of Dr. Álvarez were taken as a first approach for the development of an instrument piezoelectric transducer, i.e. a step-down transformer with a very high accuracy. Nevertheless, the use of resonant transformers was early abandoned owing to the low accuracy and the power requirements for exciting the device in its resonance.

Once the resonant alternative was ruled out, the work was concentrated in non-resonant structures. In 1996 I presented my Final Project work, under the title “Development of a piezoelectric transformer. Experimental Analysis for being applied in the measurement of high voltage”. In that work a non-resonant configuration, which had experimentally successfully been tested, was presented as the first prototype of instrument transformer.

In September of 1996, the *Universitat Politècnica de Catalunya* (UPC) applied a solicitude for patenting the developed technology which in September of 1998 was conceded (register number ES2118042 A). In January of 1997, the project was chosen as the third best Final Project in Industrial Engineering in the UPC. Later on, in March of 1997, the work obtained a mention in the Creativity Awards of 1998, conceded by the *Col.legi d’Enginyers de Catalunya*.

In January of 1997, I gained a scholarship for the Ministry of Education and Culture from Spain for working as a research student in the Electrical Department of the UPC. From then, I have been working in the field of novel transducer for measuring High Voltage and particularly in piezoelectric transducers.

The research work gathered in this doctoral thesis has been developed mainly in the Electrical Department of the UPC. Nevertheless, several of the results obtained are a consequence of the short-term research visit undertaken for the author at different research centres of international prestige in the area of high voltage and piezoelectric technology.

In 1997 I visited for three months the University of Southampton for enhancing my knowledge in high voltage. From September of 1998 to March of 1999 I visited the Ceramic Laboratory of the Swiss Federal Institute of Technology, working in piezoelectric applications. In September of 1999 and until the end of December of that year, I was working in Murata Manufacturing Co. Ltd., one of the best companies in the field of the piezoelectric materials and their applications.

This thesis contains the result of the research carried along this period of time.

Acknowledgements

I would like to express my deepest gratitude to my Ph.D. supervisor, Prof. Dr. Eng. Ricard Bosch Tous of the Department of Electrical Engineering at the *Universitat Politècnica de Catalunya*, for giving me the opportunity to develop my research work under his direction.

I also want to extend my grateful thanks to Prof. A.E. Davies and Dr. George Chen from the University of Southampton (England), to Prof. Nava Setter, Dr. Dragan Damjanovic, Dr. Enrico Colla and Dr. Pedro Durán from the Swiss Federal Institute of Technology of Lausanne (Switzerland), and to Mr. Yukio Sakabe and Mr.Akira Ando from Murata Manufacturing Co. Ltd. (Japan), for giving me the opportunity to do research in their centres.

I would especially like to mention Ranjita Dhital for its wholehearted support during those difficult moments I encountered while doing my thesis and for her accurate revision of my English.

I would also like to acknowledge to all my colleagues in the Electrical Department for their valuable suggestions during the development of my thesis, especially to Eng. Sergio Herraiz, Eng. Carlos Gómez, Eng. Jordi Aragón and Mr. Andreas Sumper for their important contribution to my research work.

I would also like to express my heartfelt thanks to Mr. Vicente Zueras for their help in developing ideas and for the useful discussions about the manufacturing process of the prototypes.

I would also like to express my thanks to all the industrial partners which have collaborating in one or other moment, in the development of this thesis: Laboratorio Electrotécnico,s.c.c.l, Epoxima.s.l., Philips Components, Morgan Matroc, CeramTec, AMP.

I would like to send my warm regards to my family and to all my friends for their help and support along this time.

Finally, I wish to express my appreciation for the support of the Ministry of Education and Culture, Spain, for the support in the scholarship that has permitted me the development of my research work.

Summary

A prerequisite for safe and stable operation of an electric power system is the accurate and reliable measurement of the system parameters, in particular, current and voltage. Conventionally, this has been achieved on High Voltage (H.V.) systems by expensive, bulky iron-core transformers and also by capacitor transformers. Both of them are increasingly coming under review (chapter 1) in modern power system due to their cost, safety implications for personnel and surrounding plant if failure occurs, installation time and indeed substation land requirements. Research effort into viable alternatives to instrument transformers has been ongoing for many years to reduce the cost and improve the safety and accuracy of this devices.

In the last years, this research has accelerated due to the new requirements of the modern metering and protection systems based on electronic and microprocessor devices. This trend in the modern systems has allowed the development of novel transducers where the accuracy, the reliability and the safety has been significantly improved.

The main alternative incorporate optic fibre viewed as the most realistic method of providing cheap and safe isolation between the chosen sensor at phase potential and earth. The sensor itself is, in the case of current measurement, based on the Faraday effect while in the case of the voltage measurement is generally a Pockels or Kerr effect device measuring a fraction of the actual phase voltage by employing a capacitive voltage divider.

In parallel to the development of the optical alternative other different transducers have been studied based on the properties offer for new materials and technologies developed in the last years. A clear example of new emergent technologies is found in the piezoelectricity (chapter 2).

In just over 100 years piezoelectricity has moved from a laboratory curiosity to big business. During this period, several technologies have been developed to utilise the piezoelectric effect. In turn, each of these technologies has become an essential component in many kinds of electronic products. The U.S. piezoelectric industry, good mirror for analyse the international technologic development, has gone through several boom and bust cycles. However, new applications are emerging for piezoelectricity because of the developments in piezoelectric ceramics and polymers. Even though piezoelectric quartz crystal still holds the largest market segment, several new piezoelectric ceramic and piezoelectric polymer materials are being developed that represent good, attractive market segments in terms of growth, competition, and investment.

This thesis proposes an alternative for the measurement in High Voltage environments by using the piezoelectric technology. The thesis was initially concentrated in the alternative of the voltage measurement, but the successfully results in this field have open the way to propose alternatives for measuring current.

Accordingly, the present thesis develops a novel instrument transformer based on the mechanical forces developed for the piezoelectric materials under the influence of an electric field. The transformer consists of an actuator piezoelectric column and a sensor piezoelectric column. The actuator column is connected to the a.c. High Voltage to be measured. This electrical voltage produces the generation of mechanical forces within the material. The forces can be measured by means of the piezoelectric sensor and convert it back into a low electrical signal which can drive an electronic protection or measuring system.

The main areas covered by the thesis are:

- Development of the active materials (actuator and sensor columns) adapted to the High Voltage measurement requirements.
- Development of the passive material (housing and prestress system) which permit withstand the blocking stresses generated by the active material.

- Development of prototypes of instrument piezoelectric transformer
- Laboratory prototype tests.
- General characterisation of the constructed prototypes.

The novel piezoelectric transformer herein treated is of wide application in electrical networks for measuring, providing both advantageous accuracy and large transformation ratio. Furthermore, It is expected to reduce the volume, weight and manufacturing cost of the traditional electromagnetic transformers.

The thesis is structured in fourth main parts and two appendixes. First part provides a general overview about the state of the art in instrument transformer and piezoelectricity (Chapters 1 and 2). Second part describes the research on voltage transducers (Chapters 3 to 8). Third part is related to current transducers (Chapter 9). Fourth part gathers the conclusions (Chapter 10). More detailed below is described the content of each chapter.

Chapter 1 give an overview to the to the H.V. measurement techniques, commenting the existing (classical) technologies and the more advanced systems proposed as alternatives.

Chapter 2 presents a short summary of the most relevant aspect of the piezoelectric technology, providing the necessary mathematical tools for understanding the contents of the thesis.

Chapter 3 examines the *resonant transformers* that represent the start point of the research. The chapter analyses the applicability and limitations of this kind of transducer for being applied as instrument transformers.

Chapter 4 gathers the first purpose of instrument piezoelectric transformer, the development of the first prototype and their experimental evaluation. *Blocking* state is view as the most feasible alternative.

Chapter 5 presents the development of a second improved prototype, which is introduced to solve some mounting problems that affect the first prototype. The idea of the piezoelectric transformer with *double column* (actuator-sensor) is concluded as the optimum to made this king of devices. Nevertheless quantities of problems related to material selection are already existing.

Chapter 6 makes an analysis of commercially available PZT composition making an experimental review to the characteristics affecting the behaviour of the transformer. *Hard material* is concluded as appropriate for actuator construction while a novel composition of SBT material is used for sensor application.

Chapter 7 provides a description for the calculation and construction of an accurate piezoelectric transformer. Several conclusions are given to take into consideration in future research. A new, more advanced prototype is constructed and evaluated its expected theoretical response.

Chapter 8 covers the experimental characterisation of the novel piezoelectric transducer for high voltage application.

Chapter 9 is reserved to make an attempt to the possibilities in current transducer. Two prototypes are described and successfully tested.

Chapter 10, finally, presents the contributions and conclusions from the present work and the suggestion for future work.

FIRST PART:

BACKGROUND

Chapter 1

Introduction: An overview to the measure and protection in High Voltage

1 Introduction: An overview to the measure and protection in High Voltage

1.1. Monitoring of a bulk electric delivery system

In the *measuring*, *counting*, *control* and *protection* (relaying) field of power supply, it is well known the need of monitoring the electrical potential and current in the conductors of the transmission lines and the conductors connected to substation power transformers. These measurements are transmitted to a central station [1,2,3] for the control of the entire power system to assist the dispatch operator and other bulk network functions depending on the so-called Power Control Centre.

Systems for the monitoring and the management of electricity networks are composed basically of four sub-systems (Figure 1.1)

S1 Instrument transformer for measuring currents and voltages.
S2 System for transmitting the signals from instrument transformers to protection and control systems.
S3 Protection and measuring systems.
S4 Software for protection and control system.

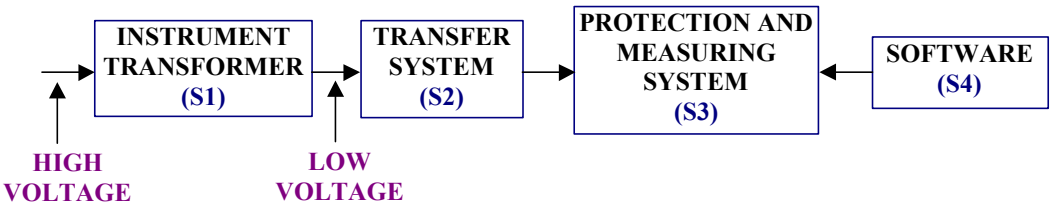

Figure 1.1. *The four sub-systems for the monitoring and for the management of networks* [4,5]

1.2. Instrument Transformers

Instrument transformers, as the name suggests, are used with measuring and protective equipment in order to monitor electrical parameters such as current and voltage or to use these parameters to activate protection schemes. They are thus used with ammeters, voltmeters, energy meters, power factor meters, wattmeters, etc., for the measurement of current and voltage, and with protective relays for tripping circuit breakers in the event of faults.

Their role in electrical systems is of primary importance for various reasons concerning to safety, accuracy, and standardisation (Figure 1.2):

1. *Safety:* The use of instrument transformers isolates measuring and protective circuits from the system, and thus they may be insulated for a low voltage, instead of the much higher system voltage. Measuring and protective devices (S3 in Figures 1.1 and 1.2) can be located at a centralised point, thus offering ease of operation and safety to personnel.

2. *Accuracy:* The primary criterion governing the performance of instrument transformers is accuracy. It is the accuracy which determines the size of the instrument transformer rather than temperature rise requirements. The accuracy of instrument transformers is strictly defined over the operating range depending upon their application. The transformed secondary current or voltage must bear an almost exact correlation with the primary parameters to be transformed, within the limits of accuracy as defined in the various standards.

3. *Standardisation*: They are a mean of 'stepping down' current and voltage to measurable values. Thus, a current of 600 A flowing in a system can be measured by using a 600/5 current transformer (CT for short) in connection with a 5 A ammeter. Similarly, the 5 A or 1 A output of a CT can be connected to a relay. A voltage transformer, also termed potential transformer (VT or PT, the terms are used interchangeably in this thesis) can be used to step down a system voltage of, say 36 kV, to a measurable value of 110 V and can be connected to meters or relays. Thus measuring and protective devices can be standardised on one value of current and voltage.

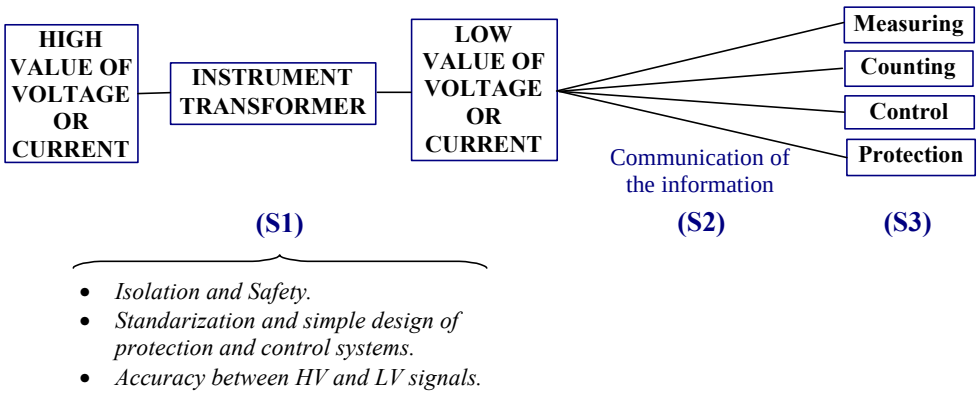

Figure 1.2. Role of the instrument transformer in electrical systems

1.3. Technology trend in the protection and measurement systems (S3, cf. Fig 1.2)

The technology evolution in the protection and control systems (S3) has changed the requirements of the instrument transformers (S1) and the communication of the information (S2) [4-7]. To investigate the requirements of the instrument transformers a good knowledge of the protection systems must be achieved. Table 1.1 shows a classification of the protection systems in accordance with the basic technology.

Fuses are the oldest and simplest protection devices. Their operation is based on sacrificing a little element of the system to keep the rest out of danger. Fuses are connected directly to a line which need to be protected from a short-circuit current and their response depends on the calibre and fusion curve chosen. When the fuse actuates the service stops and it does not start

again until it is replaced. Because of its simplest operating principle, fuses are the most reliable protection system. This is because they are already a essential device in the protection field.

The Direct Electromagnetic Relays, were the next devices introduced for protecting. They could continue in service after actuating and also they allowed one to adjust some of the response characteristics. Their operation was based on the force generated for a coil driving directly for the current of the circuit to be protected, to open the spring of a disconnection mechanism. The limitation of this devices were establish for the magnitude of the voltage or current where were applied. Precisely, the name of *direct* indicated the directed connection of the relays to the voltage or current to be measured.

The evolution of the electrical network [8] motivated an significant increase in the voltage levels and the short-circuit power, and stability requirements were more and more demanding. Hence, devices with more short-circuit power and protection relays which were more reliable and accurate were necessary, appearing then the *Indirect Electromagnetic Relays*. The indirect electromagnetic relays were driven by the secondary current and voltage proportioned from 'instrument' transformers and in their operation used electromagnetic technology based on moving contact members activated by electromagnetic forces.

Until the 70's, the electromagnetic relays were the only systems widely used for protection. During this period appeared the first *moving-coil relays* incorporating resistors, capacitors and diodes which represented the first step towards the analogue electronic. Since the end of the 70's, combination of electronic measurement units with auxiliary electromagnetic devices were used for protecting.

Table 1.1. *Protection and Control technologies* [4-7]

	Technologies	**Examples**
Static Technologies	(0) Fuses	Fuses
	(1) Electromechanical technology	Direct Relays Indirect Electromagnetic Relays Moving-coil Relays
Dynamic Technologies	(2) Analogue technology	Electronic Relays
	(3) Digital technology	Protections with digital logic (no user-programmable).
	(4) Microprocessor technology (Numerical technology)	Protections incorporating microprocessors (capacity of memorisation, programmable, multi-task, etc.)

Analogue Technology is involved in protection utilising the acquisition of analogue signals by a traditional method (amplifier + filtering + comparator). This technology allows one to reduce the power necessary from the instrument transformer. This is due to these relays do not need to excite neither coils of high impedance nor moving contact members as cylinders or induction discs, but only to energise the little input transformers of the protection devices, which adapts the magnitudes to values appropriated for the electronic circuits. This has allowed the power requirements of instrument transformers to be reduced.

During the 80's and before the analogue technology totally removed the older electromagnetic technology, the *Digital Technology* was introduced in the protection field. In contrast to analogue technology, digital used A/D converters for acquiring the signals coming from the

instrument transformers before inputting in a digital circuit. The first digital relays were similar to the previous ones and, like them, only allowed some adjusts.

Later on, the *microprocessor* –so called *numerical technology*- has been incorporated in the measuring field, allowing new tasks to the protection and measuring systems, such as: the possibility of being programmed and operated in function to logic programs, the capacity to register parameters, the aptitude for solving calculations and deriving different magnitudes, the ability of communication with a PC, etc.

Figure 1.3. illustrates relay-technology trends. The increase in relay systems with digital signal processing and microprocessors and the elimination of electromechanical relays implies the revision of the requirements on instrument transformers in relation to protection. There is a similar trend in revenue metering and the first electronics meters for measuring energy consumption are already in service.

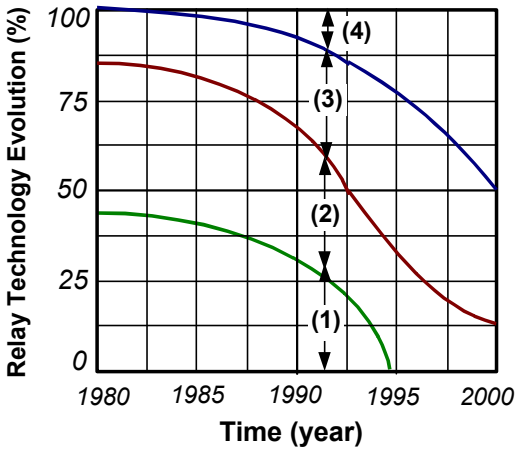

Figure 1.3. *Market shares of the relay technology* [4].

1.4. New requirements for instrument transformers

1.4.1. Voltage transformers (VT)

For a long time, winding type voltage transformers (VT) have been used to measure voltage for the control and the protection of electric power systems.

However, with the recent demand for larger capacity in electric power systems, transmission voltage becomes higher, and hence the distance of insulation increases. This leads to an increase in size of VT.

On the other hand, burden of VTs can be reduced due to the shift in technology (Table 1.2) as following is briefly commented in the next two points (IEC Standard 185, 186 [4]):

- reducing the input power by a factor of at least 5 when replacing electromechanical (1) by static relays with analogue (2) or digital (3) electronics,

- reducing the input power by a factor of at least 10 when replacing static relays with analog (2) or digital (3) electronics by relays with microprocessor-based technology.

Table 1.2. *Voltage transformer requirements* [4]. (Arrow indicates the energy flux from High voltage to Low voltage (S1) to (S3)).

			Protection Input Voltage Required for the Relay	Relay Input Power (Power for Measuring)	Intermediate Transformer in the Input of the Relay (Power to activate the Relay)	Voltage Sensor (Instrument Transformer) Output
				(S3) ←		**(S1)**
Type of Relay		(1) Electromechanical Relay Technology	110 V $\frac{110}{\sqrt{3}}$ V	10 ... 30 VA	1 ... 5 VA	11 ... 35 VA
	Static Technology	(2) Electronic Analog Relay Technology	110 V $\frac{110}{\sqrt{3}}$ V	1 ... 3 VA	1 ... 5 VA	2 ... 8 VA
		(3) Electronic Digital Relay Technology	110 V $\frac{110}{\sqrt{3}}$ V	0.1 ... 0.5 VA	1 ... 5 VA	2 ... 6 VA
		(4) Microprocessor based Technology		0.1 ... 0.5 VA	Unnecessary because connection is software compensated	0.1 ... 0.5 VA

Furthermore the introduction of digital and microprocessor control protection systems requires the elimination of electromagnetic interference in voltage measuring systems.

Under these circumstances, some investigations have been performed to develop voltage measuring systems for being adapted to the new requirements.

1.4.2. Current transformers

Conventional current transducers are transformers (CTs) with copper wire windings and iron cores, are now widely used in power systems. For high-voltage applications, porcelain insulators and oil-impregnated materials have to be used to provide insulation between the primary bus and the secondary windings. The insulation structure has to be designed carefully to avoid electric field stresses which could eventually cause insulation breakdown. The electric current path of the primary bus has to be designed properly to minimise the mechanical forces on the primary conductors for through faults. The reliability of conventional high-voltage CTs has been questioned by engineers at some utility companies who have been experienced violent destructive failures of these CTs which caused fires and impact damage to adjacent apparatus in the switch yard, electric damage to relays, and power service disruptions [9-10].

With the short circuit capacities of power systems getting larger and the voltage levels going higher, the conventional CT becomes more and more bulky and costly. Although the introduction of SF_6 insulated CTs in recent years has improved reliability, it has not reduced the cost of this type of CT.

In addition to the concerns mentioned above, other performance limitations of the conventional CT have raised more concerns [11, 12]. The saturation of the iron core under fault current and the low frequency response of the conventional CT make it difficult to obtain accurate current signals under power system transient conditions. This is specially so for those currents with

transient DC components, which aid a remanent flux condition in the core and may cause inappropriate functioning of relays. The saturation of the iron core also reduces the dynamic range of the CT. In power systems, the electric current is much smaller (<1KA) under normal operating conditions than under fault conditions (>10KA). Because of the small dynamic range of conventional CTs, more than one CT is needed at one location to cover the requirement of metering and relaying.

With computer control techniques and digital protection devices being introduced into power systems, conventional CTs have caused further difficulties, as they are likely to introduce electromagnetic interference through the ground loop into the digital systems.

Furthermore, the standard 5A low burden secondary configuration is not compatible with the new technology which uses analogue to digital converters requiring low voltage input at the front end. Table 1.3 shows the reduction on the burden requirements of CTs.

Table 1.3. *Current transformer requirements* [4]. (Arrows indicate the energy flux from High voltage to Low voltage (S1) to (S3)).

			Protection Relay	Intermediate Transformer Input	Transfer-system input (losses) (Cable 2×2.3 mm diameter 50 m long)	Current sensor output
			(S3) ←		(S2) ←	(S1)
Type of Relay		(1) Electromechanical Relay Technology	1A 10 ... 30 VA 5A 10 ... 30 VA	1 ... 5 VA 1 ... 5 VA	1A :0.5 VA 5A :12 VA	12 ... 36 VA 23 ... 47 VA
	Static Technology	(2) Electronic Analog Relay Technology	1A 1 ... 3 VA 5A 1 ... 3 VA	1 ... 5 VA 1 ... 5 VA	1A :0.5 VA 5A :12 VA	3 ... 9 VA 13 ... 14 VA
		(3) Electronic Digital Relay Technology	1A 0.1 ... 0.5 VA 5A 0.1 ... 0.5 VA	0.1 ... 0.5 VA 0.1 ... 0.5 VA	1A :0.5 VA 5A :12 VA	1 ... 2 VA 13 ... 14 VA
		(4) Microprocessor based Technology	1A 0.1 ... 0.5 VA 5A 0.1 ... 0.5 VA	not necessary	1A :0.5 VA 5A :12 VA	1 VA 13 VA

1.4.3. Comments

The lower power consumption of the current protection systems (0.1-0.5VA, cf. tables 1.2 and 1.3) and electronic revenue-metering, is encouraging motivating the appearance of new high-voltage sensor and current transformers. At the same time there are higher demands for operation reliability as a result of interconnection of networks, and an increase in the measuring points is being purposed in the new standards of high voltage networks. Thus, low output (0.5VA) and low cost voltage and current sensors will be necessary.

Different technologies try to play the role of the classical electromagnetic technology. At present different alternatives are being tested, such as the Rogoswski coil (the toroidal coil without magnetic core), the Faraday-Pockels sensors, or using the microprocessor based technology to reconstruct or calculate the curve of the secondary of the electromagnetic transformer. This is also the aim of this Thesis, to develop a novel system to measure high voltage.

1.5. Instrument Transformer Technologies

1.5.1. Introduction

The instrument transformer technology has changed following the evolution in the protection and metering systems. Until 1975 basic technologies used in high voltage measurements were the *electromagnetic* (for voltage and current measurement) and the *capacitive* (for voltage measurement). During the 80's, evolutions were regarding to the reduction of dimensions, increase of reliability, security and accuracy by means of selection of new materials, and construction techniques, e.g. new solid dielectric materials for the housing and new magnetic materials for the cores. However, the theoretical aspects continued being the same.

Since the end of 80's, the trend in the requirements of the protection and control systems [8] allowed the research of novel sensors for measuring high voltage and currents. An example of this evolution is the electro-optical instrument transformer [9,10] which opens the door to a new concept in the systems for monitoring a bulk electric delivery system.

In the present section an overview of the different instrument transformer technologies is given.

1.5.2. Electromagnetic Instrument Transformers

- **Voltage Transformers (VTs)**

Voltage transformers (VTs), operate under the same principle as power transformers, *the electromagnetic induction between two electric circuits by means of a mutual magnetic flux*.

The standards establishing the performances of the voltage transformer define it as: *an instrument transformer in which the secondary voltage is substantially proportional to the primary voltage and differs in phase from it by an angle which is approximately zero for appropriate direction of the connections.*

The VT usually consists of two electric windings (the primary and secondary circuits), both wound around a magnetic core (Figure 1.4). The number of turns of each winding characterises both circuits: N_1 is the number of turns of the primary circuit, and N_2 is the number of turns of the secondary circuit.

The operation principle of a V.T. [13,14] is based on the Faraday Induction Law. In accordance with this law, when the primary winding is connected in parallel with the alternative high voltage to be measured (Figure 1.5), a magnetic flux is created as indicated in the equation (1.1):

$$u_1(t) = N_1 \cdot \frac{d\phi_1(t)}{dt} = N_1 \cdot \frac{d\phi_c(t)}{dt} \qquad (1.1)$$

This magnetic flux is guided by the magnetic core, which links the primary and secondary windings, and induces a secondary voltage given by equation (1.2):

$$u_2(t) = N_2 \cdot \frac{d\phi_c(t)}{dt} \qquad (1.2)$$

Thus, it is possible to measure the primary high voltage $u_1(t)$ by means of the secondary voltage, $u_2(t)$, which is proportionally reduced and galvanically insulated from the high voltage part. The relationship between the primary voltage and the induced secondary voltage (transformation ratio) is given in equation (1.3).

$$u_2(t) = u_1(t) \cdot \frac{N_2}{N_1} \tag{1.3}$$

The secondary voltage causes a current $i_2(t)$ to flow in the secondary circuit when a load is connected. The current $i_2(t)$ is determined by the total impedance of the secondary circuit (ideally, for the load). The current in the primary is also depending of the load and can be obtained considering that power in both sides is kept constant (no losses):

$$p(t) = u_1(t) \cdot i_1(t) = u_2(t) \cdot i_2(t) \tag{1.4}$$

$$i_1(t) = i_2(t) \cdot \frac{u_2(t)}{u_1(t)} \tag{1.5}$$

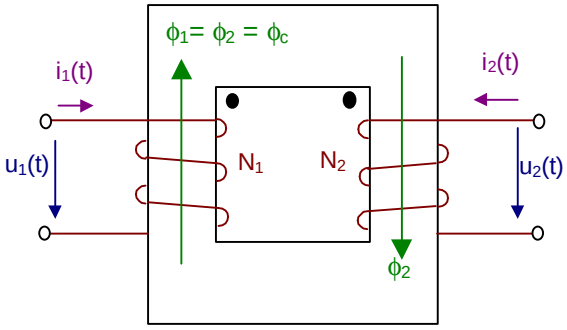

Figure 1.4. *Ideal model of a VT. Resistance of winding and non-linearity of core have not been considered.*

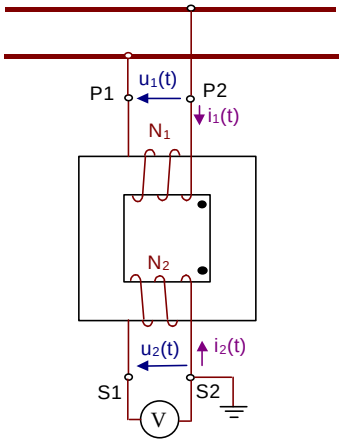

Figure 1.5. *VT connected to the voltage to be measured and with the associate measure system.*

In spite of the similarities between the power and voltage transformers, there are still considerable differences between them. For instance, the main criterion behind choosing the primary and secondary winding gauges is the limit on temperature rise in the case of power transformers and the limitation on errors (i.e., reduction of voltage drops) in the case of voltage transformers. The size of the power transformer depends on the rated capacity, whereas the capacity or burden of the VTs is very low, and size is determined by the system voltage on which the VT is to be used. For a given burden, the VT will be much larger than a power transformer of similar rating. Thus, the exciting current of a VT will also be much larger relative to the burden. Where oil is used in the case of VT's, it is for insulation as opposed to power transformers, where its primary purpose is for cooling.

The accuracy depends on the leakage reactance and the winding resistances which determine how the errors vary as the burden on the secondary increases. The permeability and the power dissipation of the core affect the exciting current and hence the errors at zero burden. The core material used affects the physical size of the transformer with a smaller size being possible if cold-rolled grain-oriented steels are used as opposed to hot rolled steels. If cut cores are used, the saturation flux density is much higher.

Standards for voltage transformers (see cf. 1.6) specify errors that must not be exceeded for various classes of accuracy. Limitation in errors leads to limits of watt loss and magnetising current. The effect of this is to reduce the working flux density of the voltage transformer as compared to the power transformer. Care must also be taken in designing the winding, as the winding resistance and reactance affect errors.

• Current Transformers (CTs)

The current transformer is an instrument transformer in which the secondary current, in normal conditions, is substantially proportional to the primary current and differs in phase from it by an angle which is approximately zero for an appropriate direction of the connections.

Current transformers usually include a magnetic core structure (Figure 1.6) having a winding disposed thereon (the secondary circuit). The core and winding assemble are suitable placed in the magnetic field created by the current to be measured (the primary circuit). N_1 is the number of turn of the primary winding and N_2 is the number of turn of the secondary winding. The resistances of the primary, secondary winding are indicated respectively by R_1, R_2 while Z_c is the burden impedance.

The theoretical principle of the current transformer [13, 14] is similar to the voltage transformer and also explained for the Faraday Induction Law. Nevertheless, the operation of the transformer is quite different.

The primary winding is connected in series with the current to be measured (Figure 1.7). The voltage drop in the primary winding caused for the current is perfectly negligible because the primary current $i_1(t)$ is injected from a current source (the network). This primary current $i_1(t)$ induces a magnetic flux $B(t)$ which is guided through the magnetic core.

$$\Phi_1(t) = \int_S B(t) \cdot dS = B.S = \frac{\mu_0 \cdot I_1 \cdot N_1}{L_1} \cdot S \tag{1.6}$$

where the integral has been solved considering the magnetic flux $B(t)$ with constant magnitude, B, and to be at right angle to the section of the core, the equation. I_1 represents the magnitude of $i_1(t)$.

The flux will be alternative if the primary current is alternative. Thus, a change in the current will produce a change in the surrounding flux, and a voltage will be induced into the secondary winding of the current transformer.

$$u_2(t) = \frac{d\Phi_1(t)}{dt} = N_2 \cdot S \cdot \frac{dB(t)}{dt} \tag{1.7}$$

This voltage causes a secondary current $i_2(t)$ to flow through the secondary circuit that is exactly equal to the primary ampere-turns (ideal transformer) and in precise opposition to them. Furthermore this current is dielectrically insulated from the current flowing through the primary circuit. Equation 1.8 provides its value for the case of a resistive burden.

$$i_2(t) = \frac{u_2(t)}{R_2 + R} \tag{1.8}$$

From the Ampere Law (equation 1.9), the ampere-turns generated for the primary current, $N_1 \cdot i_1(t)$, as is the case for whatever transformer, are compensated by the amperes-turns generated for the secondary current, $N_2 \cdot i_2(t)$, and the amperes-turns, $N_1 \cdot i_0(t)$, need to generate the induction $B(t)$ inside the core. This may be written as indicated equation 1.9

$$\oint B \cdot d\ell = m_0 \cdot \sum_{n=1}^{n=N} I_n \qquad \rightarrow \qquad N_1 \cdot i_1(t) + N_1 \cdot i_0(t) + N_2 \cdot i_2(t) = 0 \tag{1.9}$$

The current transformer is dimensioned to require a very low contribution of magnetizing current, $i_o(t)$, (in general around 1% of the primary current). Thus the Ampere law may be written

in a good approximation as is indicated in equation (1.10), which provides the basic transformer ratio for a current transformer.

$$N_1 \cdot i_1(t) + N_2 \cdot i_2(t) = 0 \quad \rightarrow \quad I_2 = \frac{N_2}{N_1} \cdot I_1 \tag{1.10}$$

From equations (1.8), (1.9) and (1.10) one can establish the transformer ratio as:

$$u_2(t) = \frac{N_2}{N_1} \cdot i_1(t) \cdot (R_2 + R) \tag{1.11}$$

If the secondary is left in open circuit ($R \rightarrow \infty$) the secondary voltage will increase at a dangerous ways since the primary current is constant. This is because, it is necessary to keep the secondary under short circuit or with the load connected when it is in operation.

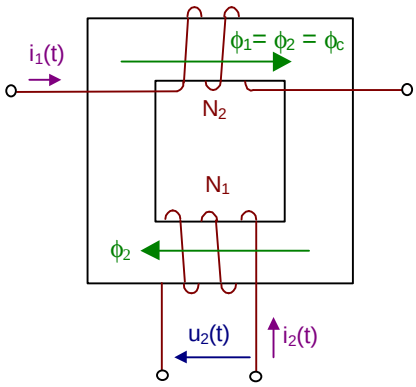

Figure 1.6. *Ideal electromagnetic current transformer. Resistance of winding and non-linearity of core have not been considered.*

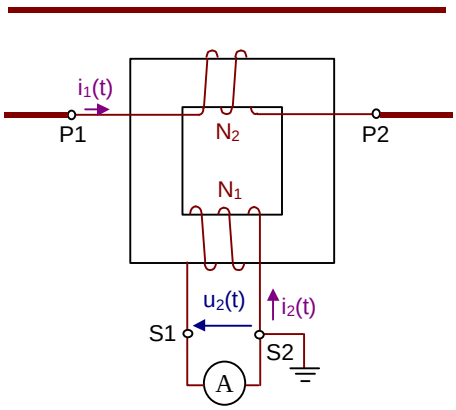

Figure 1.7. *Current Transformer connected to the voltage to be measured and with the associate measure system.*

• Consideration for electromagnetic transformers

In voltage transformers (VTs), the primary current is determined by the load connected to the secondary. Nevertheless, in the current transformers (CTs) the primary is connected in series (Figure 1.7) with the line whose current is to be indicated. In this way, the primary current of the CT is in no way controlled by the condition of the secondary circuit. This fact, represents a cardinal difference between voltage and current transformers.

This leads to a variable flux operation in the CTs as opposed to a constant flux operation in the VTs and power transformers. Thus:

(a) In electromagnetic voltage (and power) transformers, where the voltage $u_1(t)$ is, in average, a constant value U_1, the secondary current is the cause (determined by the burden) and the primary current is the effect. The aim is to modify the factors which establish the power.

(b) In electromagnetic current transformers, the primary current is the cause (is a fixed value measured from the network) and the secondary is the effect. The aim is to obtain a proportionality as accurate as possible between currents.

• Construction of instrument transformers

As mentioned earlier, the size of the instrument transformers depends mainly on the system voltage. Often, the primary insulation will be much larger in volume than the primary winding itself. Figure 1.8 provides a classification of instrument transformers in function of different parameters

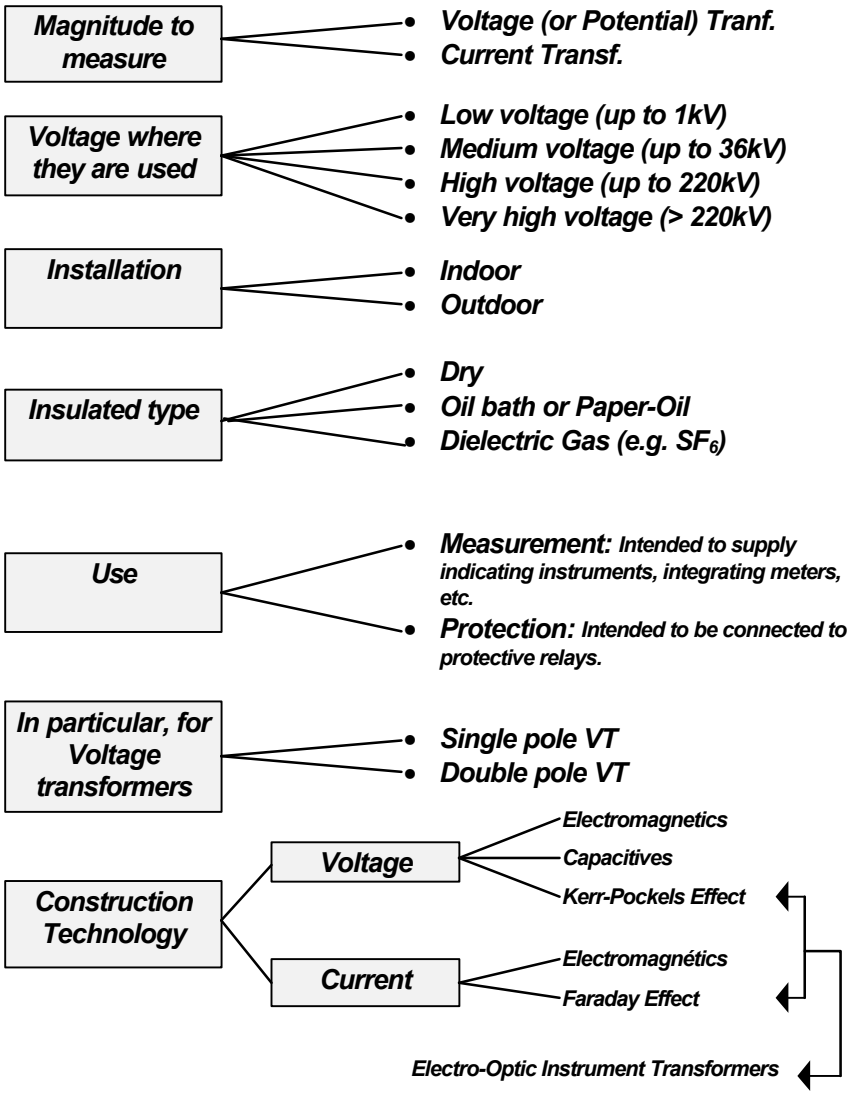

Figure 1.8 *Classification of instrument transformers*

Although oil-filled designs (Figures 1.9-1.11) were being used earlier, this type of construction is being phased out now for system voltages up to 36 kV. Cast resin is used as the major insulating medium for electromagnetic CTs and VTs (Figures 1.12-1.14)

CTs and VTs with OIL BATH or PAPEL-OIL INSULATOR

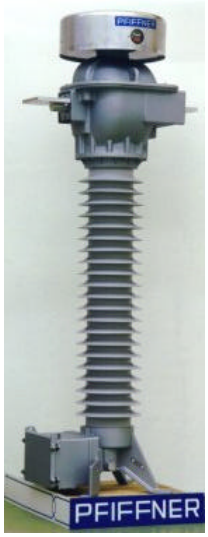

Figure 1.9. *Current Transformer JOF145-type. Nominal current 100 to 2400 A. Nominal voltage 145kV. Insulator of porcelain or silicon. Courtesy of Pfiffner Instrument Transformer, Ltd.*

Figure 1.10. *72kV to 145kV two bushing voltage transformer. Insulated with oil/paper. Courtesy of Haefely-Trench group.*

Figure 1.11. *72kV to 145kV single core, single coil magnetic voltage transformer. Insulation of Paper-Oil and a porcelain insulator. Courtesy of Alstom.*

VTs and CTs in CAST RESIN DESIGN

Figure 1.12. *12 to 36 kV resin insulated voltage transformers for outdoor use. Line to ground (left) and line to line (right) execution. Courtesy of Alstom*

Figure 1.13. *3.3 to 11kV Single phase double pole VT. Courtesy of Kappa Electricals.*

Figure 1.14. *Current transformer in cast resin design for high voltage insulation up to 36kV and current rating up to 15000A. Courtesy of Pfiffner Instrument Transformer, Ltd.*

1.5.3. Capacitor Voltage Instrument Transformers (CVTs)

- **Principle of operation of a CVT**

When system voltages are too high (>150kV) for conventional electromagnetic VT to be constructed comfortably, capacitor voltage transformers are used. These consist basically of a couple of capacitors connected in series that act as a voltage divider (Figure 1.15.a). If the current taken by the burden was negligible compared to that taken by the series-connected capacitors, the error of division of current would be very low and highly efficient voltage transformer would be obtained.

However, this is never the case in practice, and the output voltage is affected by the burden, Z_b, at the tapping point and as the burden current becomes larger the error of division could be prohibitive. This means that the secondary voltage decreases and a phase error is introduced. Compensation for these errors is introduced in the form of an inductance, which is connected in series with the burden. The value of the inductance is such as to cause resonance with the capacitance value of both the capacitors at the supply frequency (Figure 1.15.b).

From a practical point of view, however, the inductance possesses some resistance which limits the output which can be obtained. If the usual phase – neutral value of 110 V / $\sqrt{3}$ is to be obtained from a high system voltage, the value of capacitance required would be very high if the errors are to be kept within limits.

A higher output could be obtained by choosing a higher tapping voltage for a given value of high voltage capacitor. Later, this voltage can be transformed by using an intermediate instrument voltage transformer, which also reduces the burden current flowing in the capacitor transformer (Figure 1.15.c).

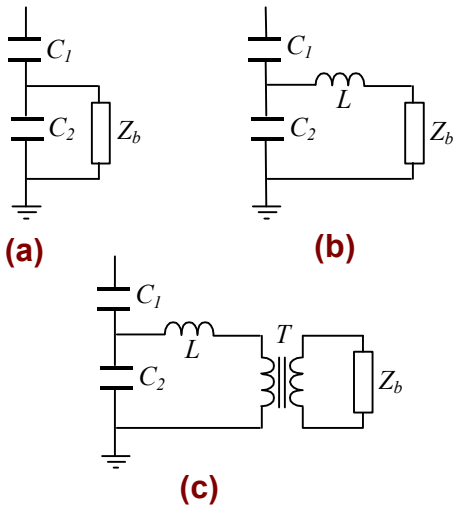

Figure 1.15. *Development of the Voltage Transformer Capacitor (C.V.T)*

The basic circuit may be varied by using an inductance either as a separate unit or as a leakage reactance in the intermediate transformer. The two capacitors cannot conveniently be made to close tolerances and hence tappings are provided on the intermediate transformer, or through a separate auto transformer in the secondary circuit, for the adjustment of ratio. The tuning inductance can be adjusted by tappings, a separate tapped inductance, by the adjustment of gaps in the iron cores or by shunting with variable capacitances.

• Voltage protection of an auxiliary capacitor

The CVT is a series resonant circuit in series with the burden impedance. Although there is little source impedance, the voltage drop, and hence the corresponding voltage at the tapping point, increases with output current. If the burden impedance were short-circuited, the rise in the inductance voltage would be limited only by the inductance losses and possible saturation. This value could be very high and hence a *spark gap* is connected across the auxiliary capacitor. (Figure 1.16).

The voltage on the auxiliary capacitor is rated for continuous service at the higher value. The spark gap is set to flash over at twice this higher value. It is provided so as to limit the short circuit current that can be delivered by the VT and the fuse protection of the secondary has to be designed accordingly. The tapping point must be earthed before any adjustments are made.

A view of a commercial capacitive instrument transformer is displayed in Figure 1.17.

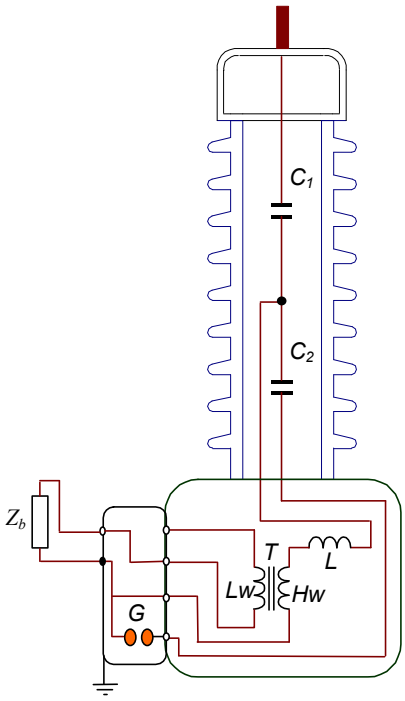

Figure 1.16. *Schematic of a capacitive voltage transformer (CVT). C_1 and C_2 are the capacitive divisors; L is the resonant inductance; Hw is the H.V. winding; Lw is the LV winding; G is the protection spark gap.*

Figure 1.17. *Capacitor Voltage Transformer with insulation of film-oil and external porcelain insulator. It is designed by stacking capacitors and incorporates a magnetic VT in the output. Voltage range : 72kV to 765kV. Courtesy of Alstom.*

1.5.4. Electro-optical instrument transformers

The use of inductive potential transformers encounters difficulties when relatively high voltages are measured and involves a very high expenditure for the required insulation. Thus the use of inductive voltage transformers is not desirable for measuring very high voltages because of the cost inherent in their application.

Capacitive voltage transformers can be used for measuring very high voltages with less initial expense. However, such transformers have the fundamental disadvantage that saw-tooth oscillations tend to appear and the suppression of these oscillations requires additional devices that entail rather considerable additional cost.

The electro-optical measuring sensors [15] utilise the knowledge that linearly polarized light which passes through materials that are situated in strong electric or magnetic fields is rotated in its polarization plane with respect to the field.

- **Optical Voltage Measuring System**

The basic principal of the optical voltage transformer (OVT) is to modulate the irradiance of the light – directed to the OVT by an optical fibre – according to the potential difference between the HV-line and the ground potential. The modulation of the light is accomplished by placing a material – that has an optical property (the birefrigence), which is sensitive to the electrical field strength (Pockels effect) inside the OVT. [16,17]

As shown in Figure 1.18, the voltage sensor consists of three lenses, a polarizer, a quarter-wave plate, a Pockels cell and an analyser. The measuring principle is based in the so-called Pockels effect.

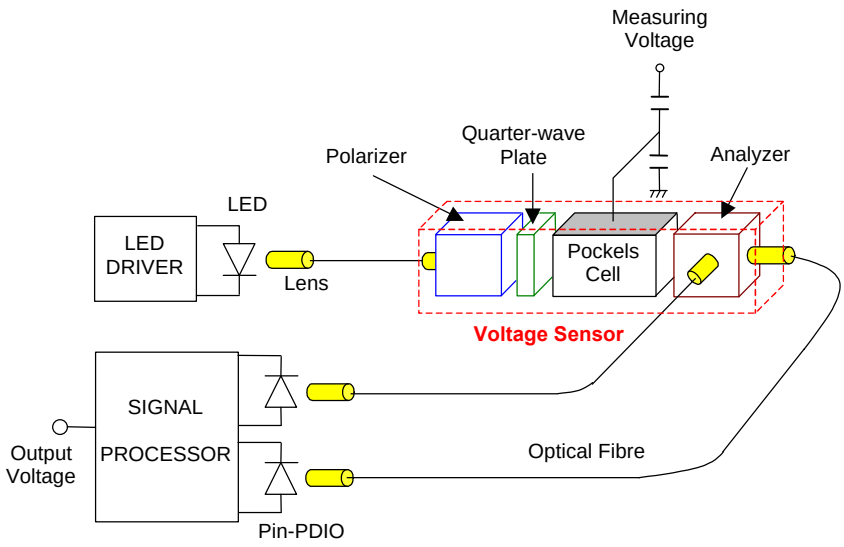

Figure 1.18. *Schematic configuration for optical voltage measuring system*

A voltage up to about 3000V_{rms} is apply between the upper and bottom electrodes of the Pockels cell. This voltage is selected by a capacitor divider from the measuring voltage. Then a light which intersect perpendicularly the applied voltage is conducted through the Pockels cell. This light is emitted from LED with a constant intensity. The ligh beam collimated with the lens is linearly polarized through the polarizer. The quarter-wave plate changes the linearly polarized light to a circular one. Then the circular polarized light change to a elliptically light in the Pockels cell by the linear electrooptic effect which is called the Pockels effect. This ellipticity of the

elliptically polarized light is split into two components polarized perpendicular to each other by the analizer, the optical axis of which makes an angle of 90º with that of the polarizer, the light beams split into two components are guided to two PIN-PDIO through lenses and optical fibres. Assuming that the ellipticity is much smaller than 1, intensity J_1 and J_2 of the light beams measured with two PIN-PDIO is given as follows in (1.12) and (1.13).

$$J_1 = \frac{J_0}{2}(1 + m_v \cdot \sin(w \cdot t)) \quad (1.12)$$

$$J_2 = \frac{J_0}{2}(1 - m_v \cdot \sin(w \cdot t)) \quad (1.13)$$

where:

J_0 = light beam intensity in front of the analyser

w = angular frequency of the applied voltage

$m_v = \frac{2p \cdot n_0^3 \cdot g_{41} \cdot \ell \cdot V_{in}}{l \cdot d}$ is the modulation depth of component light

n_0 = refractive index of Pockels cell without applied voltage

V_{in} = amplitude of applied voltage

g_{41} = electro-optical coefficient of the Pockels cell

ℓ = optical path length of Pockels cell

d = distance between electrodes

Both signals are driving to the signal processor unit where the following calculation is carried out and the output voltage V_{out} is obtained (1.14).

$$V_{out} = \frac{J_1 - \bar{J}_2}{\bar{J}_2} - \frac{J_2 - \bar{J}_2}{\bar{J}_2} = k \cdot V_{in} \cdot \sin(w \cdot t) \quad (1.14)$$

Then the applied voltage $V_{in} \cdot \sin(\omega t)$ can be measured by detecting the output voltage V_{out}.

The optical voltage sensor comprises crystal, the distribution of refractive index of which depends on electrical field, wires for leading the electric field onto the surface of the crystal, polarizers aligned on both sides of crystal, and phase shift phase to detect changes in the distribution of the refractive index, and optical fibres for routing light through the construction formed by polarizers and the crystal. The inner cavity surrounding crystal of the sensor is filled with a transparent material that has low extinction coefficient and dielectric constant, like silicone.

• Optical Current Measuring System

Optical current transducer uses the magneto-optic or Faraday effect. In 1845 Michael Faraday discovered that when a block of glass is subjected to a strong magnetic field, it becomes optically active. When plane-polarized light is sent through glass in a direction parallel to the applied magnetic field, the plane of vibration is rotate [18-23]

As shown in Figure 1.19, the current sensor consists of three lenses, a polarizer, a Faraday cell and an analyser. Faraday cell may be built by using borosilicate crown glass, for instance. As shown in Figure 1.19, the current sensor has a feature that the conductor current is measured by making the light beam circulate around the conductor.

The current measuring principle is as follows: After the light beam emitted from LED is guided to the current sensor, it is linearly polarized through the polarized in the same manner as with the voltage sensor. The linearly polarized light beam is made to circulate through the Faraday cell as the broken lines shown in Figure 1.19. When the light beam is made to circulate around the

conductor through the Faraday cell, the magnetic field generated by the conductor current causes the rotation of the polarization plane of the light beam by the Faraday effect. When the light beam makes a round of the conductor, the polarization rotation angle of the light beam is given by the equation (1.15).

$$j = n_e \cdot \int_{\ell} H_{\ell} \cdot d\ell \tag{1.15}$$

where

H_{ℓ} = component of magnetic field strength in the direction of the light beam

n_e = Veldet constant of Borosilicate crown glass

ℓ = optical path length trough Faraday cell

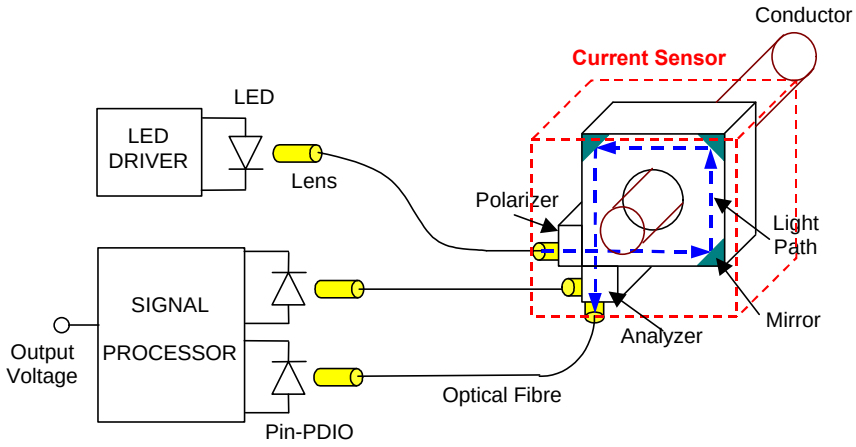

Figure 1.19. *Schematic configuration for optical current measuring systems*

The linearly polarized light with the polarization rotation angle given in equation (1.15) is split into two components polarized perpendicular to each other by the analyser, the optical axis of which makes an angle of 45º with that of the polarizer. The light beams split into two components are guided to two PIN-PDIO through lenses and optical fibres. Assuming $\varphi << 1$, intensity J_1 and J_2 of the light measured with two PIN-PDIO is given as follows in (1.16) and (1.17).

$$J_1 = \frac{J_0}{2}(1 + m_i \cdot \sin(w \cdot t)) \tag{1.16}$$

$$J_2 = \frac{J_0}{2}(1 - m_i \cdot \sin(w \cdot t)) \tag{1.17}$$

where

ω = angular frequency of conductor current

$m_i = 2 \cdot n_e \cdot I_{in}$ = modulation depth of light beams

I_{in} = amplitude of the conductor current

As the calculation of the output voltage from the signal processor is carried out just in the same manner as with the voltage measuring system, the output voltage V_{out} is obtained as follows (1.18):

$$V_{out} = 4 \cdot n_e \cdot I_{in} \cdot \sin(w \cdot t) \tag{1.18}$$

According to equation (1.18), the conductor current $I_{in} \cdot \sin(\omega \cdot t)$ can be measured by detecting the output voltage V_{out}.

Figure 1.20 displays a prototype of optical transformer which combined the Pockels and Faraday effects for measuring both current and voltage.

Figure 1.20. *525 kV Optical combined metering unit installed at Bonneville Power Administration - Keeler substation [USA]. Courtesy of Alstom.*

1.6. Specifications for instrument transformers

Specifications of instrument transformers are based on different international standards specifying the different tests and measurements necessaries to classify the transformers. The performance of the instrument transformer is defined in terms of *accuracy limits* over the range of operation. The next Table 1.4 indicates some of the international and national standards on instrument transformers.

Table 1.4. *Instrument Transformer Standards*

	Voltage Transformer		Current Transformer	
Standard	**Standard number**	**Year**	**Standard number**	**Year**
International Electrotechnical Commission	IEC: 186	1987	IEC: 185	1987
American	ANSI: C.57.13	1978	ANSI: C.57.13	1978
Spanish	UNE: 21088-2	1995	UNE: 21088-1	1995
British	BS: 7625	1993	BS: 7626	1993
Indian	IS: 3156	1992	IS: 2705	1992
Australian	AS: 1243	1982	AS: 1675	1986

- **Tests**

The test to which the instrument transformer are subjected are basically the accuracy tests, dielectric insulation tests, temperature rise tests and impulse test, and always taking into consideration the voltage factor. Due to the extension of the subject, here we only give (Table 1.5) the values associated to the dielectric and lighting tests demanding for IEC, ANSI and UNE standards.

Table 1.5. *Test specified for different standards.*

UNE 21088			IEC 185 and 186				ANSI C57-13		
U_{max} (kV)	Power frequency withstand voltage (kV_{rms})	Lighting impulse voltages (kV_{peak})	U_{max} (kV)	Power frequency withstand voltage (kV_{rms})	Lighting impulse voltages (kV_{peak})	Switching impulse voltages (kV_{peak})	Insulation Class (kV)	Power frequency withstand voltage (kV_{rms})	Lighting impulse voltages (kV_{peak})
0,6	3		0,72	3			0,6	4	10
1,2	6		1,2	6					
2,4	11								
3,6	16	45	3,6	10	40		2,4	15	45
7,2	22	60	7,2	20	60		4,8	19	60
12	28	75	12	28	75		8,32	26	75
							13,8	34	95
17,5	38	95	17,5	38	95		13,8	34	110
							18	40	125
24	50	125	24	50	125		25	50	150
36	70	170	36	70	170		34,5	70	200
52	95	250	52	95	250		46	95	250
72,5	140	325	72,5	140	325		69	140	350
							92	185	450
123	230	550	123	230	550		115	230	550
145	275	650	145	275	650		138	275	650
170	325	750	170	325	750		161	325	750
							196	395	900
245	460	1050	245	460	1050		230	460	1050
			300	460	1050	850			
			362	510	1175	950	287	575	1300
420	680	1550	420	630	1425	1050	315	630	1425
							345	690	1550
525	740	1675	525	680	1550	1175	400	800	1800
			765	975	2400	1550	460	920	2050

1.7. Conclusions

The advances in the protection and measuring systems have motivated new requirements in the instrument transformers. This evolution has been affected, mainly, due to the characteristics of the secondary transducers. Microprocessor (numeric) and digital technologies convert the measure in an information codified by means of a voltage of electronic level (from some mV up to some volts). The classic code in the form of a voltage or current with a certain power is now going to be abandoned.

Thus, the new transducers will have to improve their accuracy, safety, electromagnetic interference, stability and frequency and transient response in order to be of the same standard as the protection and measurement systems.

At present, optical transducers have been introduced as the great advance in the H.V. measurement. The utilisation of novel materials may improve their actual features. Nevertheless, its application passes through a costly inversion and a high dependence from the output electronic necessary. Their pros and contras have been evaluated in comparison to the electromagnetic and capacitive existing technologies. For very high voltage levels it has been considered as the more promising technology.

However the cost of the optical technology increases when the voltages goes down and other solutions should be encouraged. The characteristics of the piezoelectric transducer described in this thesis may give an alternative answer.

Table 1.6. *Existing Instrument Transformer Technologies. A comparison.*

Technologies				
	Electromagnetic		**Capacitive**	**Optical**
	VTs	**CTs**	**CVTs**	**OVT** and **MOVT**
Principle of Actuation	Measure of Voltage by using the Induction Faraday Law	Measure of Current by using the Induction Faraday Law	Measure of Voltage by using a Capacitive Divisor in resonance with and inductive outputing VT.	Measure of the Voltage and Current by using the Pockels effect and the Faraday effect, respectively.
	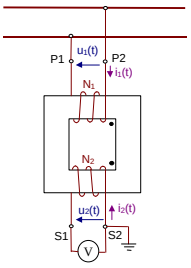	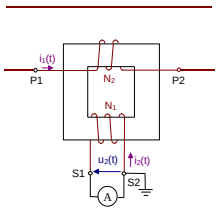	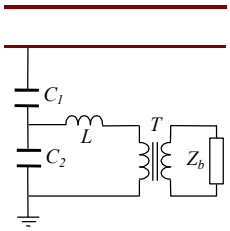	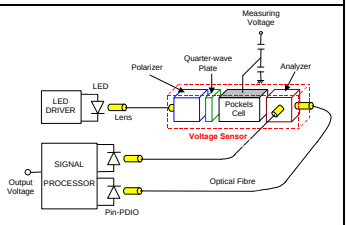 Pockels Effect 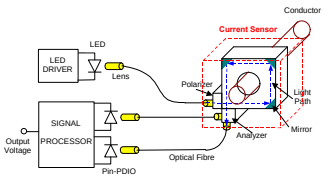 Faraday Effect
Active Materials	• Use of conductive materials and magnetic materials		• Use of dielectric material (capacitors) and electromagnetic transformers.	• Use of Electro-Optic materials.
Constructive Aspects	• Complex process of winding • High dimensions depending on the voltage. Large/Heavy requiring substantial supports.		• High dimensions depending on the voltage.	• No winding • The dimension of the sensor is not depending on the voltage. Small and light weight (sensor weight less than 2 pounds)
Application	• Voltage up to 150kV (approx)		• Voltage higher than 150kV (cost reasons)	• Voltage higher than 150kV (cost reasons)
Characteristics	• Price very elevated for very high voltage. • Frequency measurement limited at 1500Hz (approx.). It does not allow the measurement of the lightning test. • Accuracy is limited to 0.3% • Saturation under faults • Ferroresonance effects in the primary • Subjected to electromagnetic interference • Potential for catastrophic failure due to the oil insulator		• Reasonable cost for very high voltage • Frequency measurement limited at 500Hz, or less. • They allows injecting high frequency signals for communication or protection • Ferroresonance in the secondary • It does not allow the accurate measurement of harmonics.	• Wide frequency band, up to several MHz. (allows the measurement of the lightning test). • Accuracy is only limited by electronics. • No saturation under fault conditions. • No resonance effects. • Immunity to EMI. • Does not contain oil, therefore can not explode. • The price can be significantly elevated because the tecnology used.

1.8. References

[1] *Substation Control and Protection Project*, Appendix C, EPRI, 1989.

[2] Suzuki, M., Tsukui, R., Sano, Y., Yoshida, T., *Development of a Substation Digital Protection and Control System Using Fiber-Optic Local Area Network,* IEEE 1988.

[3] *The Overall Impact of Digital Techniques for Transmission Systems (Substation Control)*, CYGRE SC35WG06, 1988.

[4] *Analysis of the new IEC drafts for 185 (44-1) and 186 (44-2) instrument transformers in relation to the requirements of modern protection systems.* N.Korponay, R.Minkner, Revue General d'Electricité, April 1990.

[5] *IEC* – Standards: 185, 186 and 44-3

[6] *IEC* – drafts for revision of: 185 (44-1), 186 (44-2) and (44-3).

[7] *Relays.* Type LZ95, Modures, solid-state distance relay. Vol. I 08 02.03, ABB

[8] *Development trends in the technology of High Voltage.* Components for AC and DC transmission lines and substations. 87 JC-11. IEEE/CSEE Joint Conference on High Voltage transmission Systems in China, Beijing, October 17-22, 1987.

[9] J.R.Boyle, et al, *The Tennessee Valley Authority's (TVA's) experience and action plans with freestanding oil-filled current transformers (CTs)*, IEEE Trans., Vol PWRD-3, No. 4, October 1988, pp 1769-1775.

[10] B.C.Hydro, *Optical fiber optical current transducer*, CEA 189 T 353, July 1990.

[11] IEEE power system relay committee, *Gapped core current transformer characteristics and performance*, IEEE Trans. Vol. PWRD-5, No. 4, November 1990, pp 1732-1740

[12] IEEE power system relay commitee, *Relay performance considerations with low ratio CTs and high fault current*, IEEE Trans. Vol. PWRD-8, No. 3, July 1990. pp 884-897

[13] Instrument Transformers. A Reference Manual. Kappa Electricals. Madras, India, 1996.

[14] E.Ras, Transformadores de potencia, de medida y de protección. Barcelona, Marcombo, 1991.

[15] M.Kanoi, G.Takahashi, T.Sato, M.Higaki, E.Mori, K.Okumura, *Optical Voltage and Current Measuring System for Electric Power Systems*, IEEE Trans. on Power Delivery, Vol. PWRD-1, No. 1, January 1986, pp 91-97.

[16] Nicolas A.F.Jaeger and Farnoosh Rahmatian, *Integrated Optics Pockels Cell High-Voltage Sensor*, IEEE Trans on Power Delivery, Vol.10, No. 1, January 1995, pp 127-134.

[17] Lars Hofmann Christensen, *Design, construction, and test of a passive optical prototype high voltage instrument transformer*, IEEE Trans. on Power Delivery, Vol. 10, No. 3, July 1995, pp. 1332-1337.

[18] Information BBC: Three head type CT's with fiber optic connection between (S1) and (S3) in operation. Year 1987; Customer: Imatran; Country: Finnland.

[19] G.Mastner, M.Maschek and B.Tomic. *A new family of electronic current transducers*. CIGRE SC 34 meeting; Turku Finnland, June 1987.

[20] G.W.Day, A.H.Rose, *Faraday Effect Sensors: The State of the Art*, Proc SPIE, 985 (1988)

[21] *Optical Current Transducers for Power Systems: A Review*, IEEE Trans. on Power Delivery, Vol. 9, No. 4, October 1994.

[22] Braun, A., and Zinkernagel, J., *Optoelectronic electricity meter for high-voltage lines*. IEEE Trans. Instr. & Meas., 1973. IM-22(4): pp 394-399.

[23] H.Katsukawa, H.Ishikawa, H.Okajima, T.W.Cease, *Development of an Optical Current Transducer with a Bulk Type Faraday Sensor for Metering*, IEEE Trans on Power Delivery, Vol. 11, No.2, April 1996, pp 702-707.

Chapter 2

An Overview to the Piezoelectric Technology

2 An Overview to the Piezoelectric Technology

2.1. Introduction

Materials technology has had such a profound impact on the evolution of human civilisation that historians have defined distinct time periods by the materials that were dominant during these eras (e.g. the *Stone Age*, the *Bronze Age*, and the *Iron Age*).

Today, the current *Synthetic Materials Age* or so-called *Engineering Materials Age* is identified by plastic, composites and other well designed, man-made engineering materials with superior performance over traditional materials. However, these engineering materials and structures have been regarded as 'dumb' since they normally have been pre-processed and designed to offer only limited set of responses to external stimuli. Such responses are usually non-optimal for any single set of conditions, but optimised to best fulfil the range of scenarios to which a material or structure may be exposed [1].

In the more recent years, with the advancement of several emerging technologies, such as biotechnology, biomimetics, nanotechnology, and information technology, the dawn of the 21st century will witness the emergence of the *Smart Materials Age* [2].

Smart materials systems are nonliving systems that integrate the functions of sensing, actuation, logic and control to respond adaptively to changes in their condition on the environment to which they are exposed, in an useful and usually repetitive manner. Smart materials are part of the smart systems-functional materials for a variety of engineering applications. They possess both sensing and actuating functions.

Many existing engineering materials can be employed as sensor and actuator materials if being properly designed. They include piezoelectric ceramics and polymers, shape memory alloys, optical fibres and conductive polymers, etc. Each of them can suit the specific potential requirements of the future smart materials systems.

In this chapter, the general characteristics of piezoelectric materials are reviewed. The chapter stars with a brief historical introduction followed by an introduction to the macroscopic and microscopic aspects which confirm the piezoelectricity. Later on, a general review to the terminology based in the hysteresis behaviour of the ferroelectric material and some aspect of processing materials are given. The chapter concluded with an overview to the linear mathematical theory of piezoelectric and the technical limitations of their applications.

2.2. Piezoelectricity. A brief history

Piezoelectricity derives its name from the Greek word “piezein”, to press. When a piezoelectric crystal is strained by an applied stress, an electric polarisation is produced within the material, which is proportional to the magnitude and sign of the strain – this is the *direct piezoelectric effect*. The converse effect takes place when a polarising electric field produces an elastic strain in the same material (*converse piezoelectric effect*).

Actually, human has had contact with the piezoelectricity for ages. It is well known that primitive human used the *flint*, a variety of quartz, to produce fire by applying a mechanical impact. In fact flint was the main material during the *Stone Age* because of its also good properties as cutting material which were useful to construct tools and arms. The property of the material as ‘lighter’ was precisely an accidental discovery during the processes of manufacturing tools. Later on, and before the invention of the matches the material continued being used as lighter knocking it again iron. However, this particular and useful property of the flint to produce fire was not evaluated from a rigorous point of view.

The first serious experimental work on piezoelectricity was performed by Pierre and Jacques Curie in 1880 [3]. The demonstration of this effect was first discovered in single crystals such as quartz. Their experiments consisted of a conclusive measurement of surface charges appearing on specially prepared crystals (tourmaline, quartz, topaz, cane sugar and Rochelle salt among them) which were subjected to mechanical stress. The Curie brothers did not, however, predict that crystals exhibiting the direct piezoelectric effect (electricity from applied stress) would also exhibit the converse piezoelectric effect (stress in response to applied electric field). This property was mathematically deduced from fundamental thermodynamic principles by Lippmann in 1881. The Curies immediately confirmed experimentally the existence of the ‘converse effect’, and continued on to obtain quantitative proofs of the complete reversibility of electro-elasto-mechanical deformation in piezoelectric crystal.

The first serious application work on piezoelectricity devices took place during World War I. In 1917, P. Langevin and French co-workers began to perfect an ultrasonic submarine detector. Their transducer was a mosaic of thin quartz crystals glued between two steel plates (the composite having a resonant frequency of about 50kHz), mounted in a housing suitable for submersion. Working on past the end of the war, they did achieve their goal of emitting a high frequency ‘chirp’ underwater and measuring depth by timing the return echo. The strategic importance of their achievement was not overlooked by any industrial nation, however, and since that time the development of sonar transducers, circuits, systems, and materials has never ceased.

The success of sonar stimulated intense development activity on all kinds of piezoelectric devices, both resonating and non-resonating. Most of the classic piezoelectric applications with which we are now familiar (microphones, accelerometers, ultrasonic transducers, bender element actuators, phonograph pick-ups, signal filters, etc) were conceived and reduced to practice. It is important to remember, however, that the materials available at the time (limited to single crystal, both natural and synthetics) often limited device performance and certainly limited commercial exploitation.

During World War II, in the U.S., Japan and the Soviet Union, isolated research groups working on improved capacitor materials discovered than certain artificial polycrystalline anisotropic formations (prepared by sintering metallic oxide powders) exhibited dielectric constants up to 100 times higher than common cut crystals, as was the case of the barium titanate (polycrystalline). Due to the randomly distributed and macroscopically averaged distribution of the thousands little-single-crystals, the materials did not display a macroscopic piezoelectric effect.

However, it was not until 1946 [4] that scientist discovered that this type of polycrystalline materials (commonly known as ceramic ferroelectrics), could be made piezoelectric by application of an electric field; a process which is called poling. The discovery of this easily manufactured piezoelectric materials with astonishing performance characteristics touched off a revival of intense research and development into piezoelectric devices.

In 1954, Jaffe *et al.* reported the important discovery of the lead zirconate titanate (PZT) solid-solution which possessed improved piezoelectric properties [5]. The significant feature of PZT is its phase diagram, which is characterised by a boundary, known as the morphotropic phase boundary (MPB), between a tetragonal phase and a rhombohedral one at a zirconate content of about 52%. This feature, which is exploited in commercial compositions, facilitates applications in many different areas.

Other different compositions have been analysed to improve the properties of the PZT, in general by applying new components to the basic PZT.

In 1969 was discovered the strong piezo and pyroelectricity of uniaxially drawn polyvinylidene fluoride (PVDF) after poling in a suitable electrical field. It is also known that other plastic, such as nylon or PVC display piezoelectric effect but with less intensity than the PVDF.

Since beginning of 80's different novel materials have been piezoelectrically studied. In particular composites of ceramics and polymers and grain-oriented glass-ceramics (a composite of a glassy phase and one or more crystalline phase) have a brilliant future.

2.3. The piezoelectric effect

In crystals having piezoelectric properties, mechanical quantities such as stress (T) or strain (S), and electrical quantities such as electric field (E), electric displacement (flux density) or polarisation (P), are interrelated. This phenomenon is called *electromechanical coupling*.

2.3.1. Direct and converse effects

If a force is applied to a piezoelectric material, surface charge is induced by the dielectric displacement and therefore an electric field is built up. On applied electrodes this field can be tapped as electrical voltage (Figure 2.1). If the electrodes are shorted, the surface charge balance out by a current (Figure 2.2). This effect is known as *direct piezoelectric effe*ct.

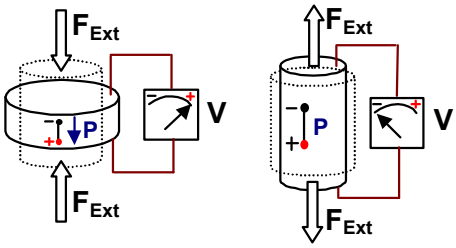

Figure 2.1. *Direct effect with the piezoelectric material in open circuit.*

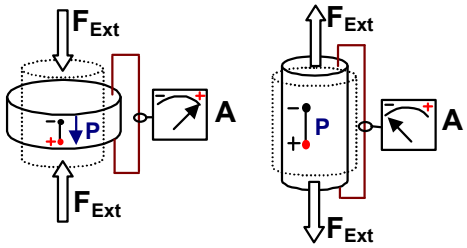

Figure 2.2. *Direct effect with the piezoelectric material shorted.*

Conversely, if an electric field acts on a piezoelectric body it becomes distorted. If this distortion is prevented (blocking total or partially the material), an elastic tension *T* occurs. A force *F* is thereby applied to the device, which prevents the distortion of the piezoelectric body (Figure 2.3). This reversal of the direct piezoelectric effect is defined as *indirect or converse*

piezoelectric effect. In practice, the direct piezoelectric effect is used in static as well as dynamic operation (Figure 2.4).

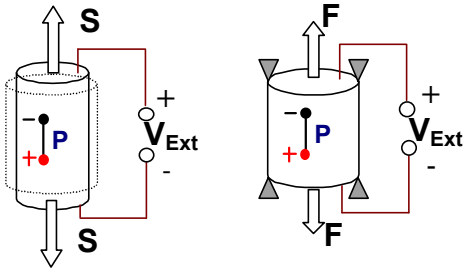

Figure 2.3. *Converse effect. (Left: Free displacement; right: Blocking force)*

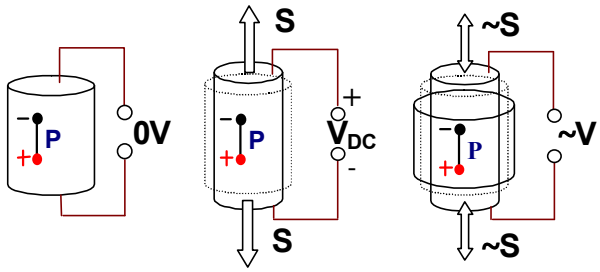

Figure 2.4. *Static (in the middle) and dynamic (right) operation in the converse effect*

2.3.2. Why does piezoelectricity exist?

The piezoelectric effect is exhibited by a number of naturally and synthetics *single crystals* under two different behaviours. Materials such as quartz exhibited a zero polarisation when the external electric or mechanical field is removed. In opposite, other single crystal materials such as Rochelle salt, barium titanate, and others show a remanent polarisation without any external stress. Moreover, the direction of the polarisation could be reversed by application of an inverse electric field. In this case, a hysteresis field appears and the material is called *ferroelectric*.

The origin of the piezoelectric effect in all both type of crystal is common and related to an asymmetry in the cell unit and the resultant generation of electric dipoles due to the mechanical distortion leading to a net polarisation at the crystal surface. The effect is practically linear, i.e. the polarisation varies directly with the applied stress, and direction-dependent, so that compressive and tensile stresses will generate electric fields and hence voltages of opposite polarity. It is also reciprocal, so that if the crystal is exposed to an electric field, it will experience an elastic strain causing its length to increase or decrease according to the field polarity.

A ferroelectric single crystal, when grown, has multiple regions with uniform polarisation called *ferroelectric domains* (or *Weiss domains*). Within a domain, all the electric dipoles are aligned in the same direction. There may be many domains in a crystal separated by boundaries called *domain walls*. Adjacent domains can have their polarisation vectors in antiparallel directions or at right angles to one another. The boundaries between these domains are, correspondingly, known *as 180º or 90º domain walls*. A single domain can be obtained by domain wall motion made possible by the application of a sufficiently high electric field, the process known as *poling*.

For example, Figure 2.5 shows the crystal structure of barium titanate. Above a certain temperature (which is called *Curie temperature*) of 120ºC, the prototype crystal structure is cubic, with Ba^{2+} ions at the cube corners, O^{2-} ions at the face centres and Ti^{4+} ion at the body centre, as shown in Figure 2.5(a). Below the Curie temperature, the structure is slightly deformed, with Ba^{2+} and Ti^{4+} ions displaced relatively to the O^{2-} ions, thereby creating a dipole, as shown in Figure 2.5(b). Thus, we may visualise each pair of positive and negative ions as an electric dipole, and the *spontaneous polarisation* (dipole moment per unit volume) as due to an assembly of these dipoles, which point in the same direction. If the value of the spontaneous polarisation P_S depends on the temperature, this is called the pyroelectric effect. In ferroelectric materials the magnitude and direction of P_S can be reversed by an external electric field.

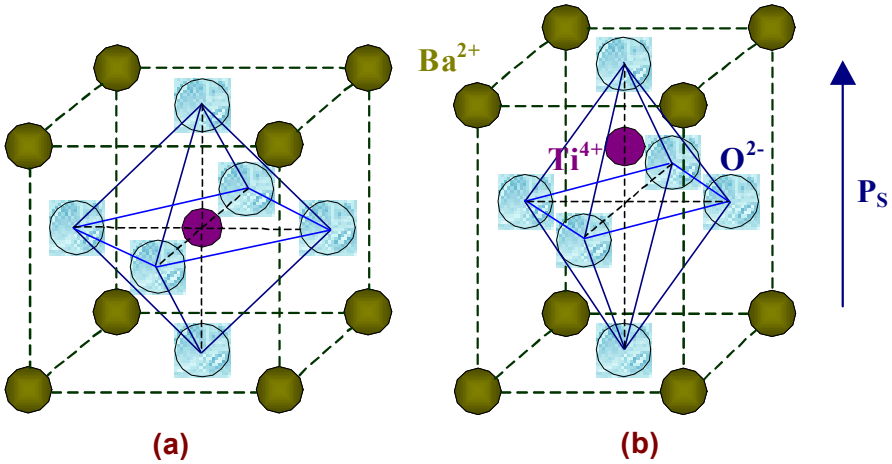

Figure 2.5. *The crystal structure of perovskite barium titanate. (a) Above the Curie temperature the unit cell is cubic; (b) below the Curie temperature the unit cell structure is tetragonal with Ba^{2+} and Ti^{4+} ions displaced relative to the O^{2-}*

Besides the crystals mentioned above, an important group of piezoelectric materials synthesised in laboratory are the *ferroelectric ceramics*, of which PZT is an example. Ferroelectric materials can be considered as a mass of minute single crystals. Globally the ferroelectric ceramic does not possess any piezoelectric properties owing to the random orientations of the ferroelectric domains in the ceramics before poling (Figure 2.6(a)).

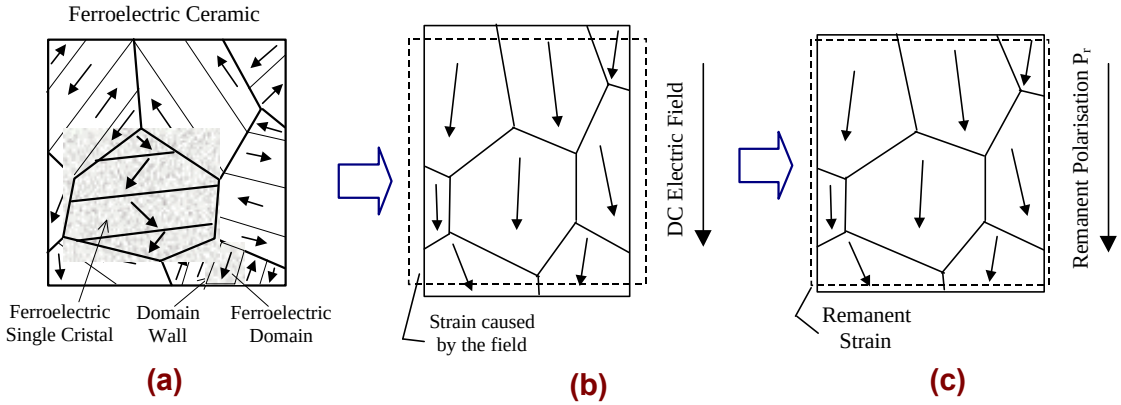

Figure 2.6. *Schematic illustration of the poling process.*

During poling, a DC electric field is applied on the ferroelectric ceramic sample to force the domains to be oriented or 'poled'. While domains cannot be perfectly aligned with the field except when the grain or crystal is coincidentally oriented in the field direction, their polarisation vectors can be aligned to maximise the components resolved in the field direction (Figure 2.6(b)). After poling, the electric field is removed and a *remanent polarisation*, *Pr*, and remanent strain are maintained in the sample, and the sample exhibits piezoelectricity (Figure 2.6(c)). However, a very strong field could lead to the reversal of the polarisation in the domain, known as domain switching.

2.4. Dielectric hysteresis curve. Terminology

Polarisation, which is usually denoted by *P*, is related to electric displacement (or electric flux density) *D* through the linear expression:

$$D_i = P_i + e_0 \cdot E_i$$

where the subscript *i* represents any of the three co-ordinates x, y, and z, and e_0 is the permittivity of free space, equal to 8.854×10^{-12} F/m.

A consequence of the resistance to domain switching in ferroelectric materials is that polarisation is hysteretic, which mean that *D* and *P* are non-linear functions of *E* and may depend on the previous history of the material. Concretely the polarisation *P* is a double-valued function of the applied electric field *E*, and so is not precisely reversible with field. Upper part of Figure 2.7 shows the relation between *P* and *E* for a commercial ferroelectric material. This curve is known as *dielectric hysteresis curve*.

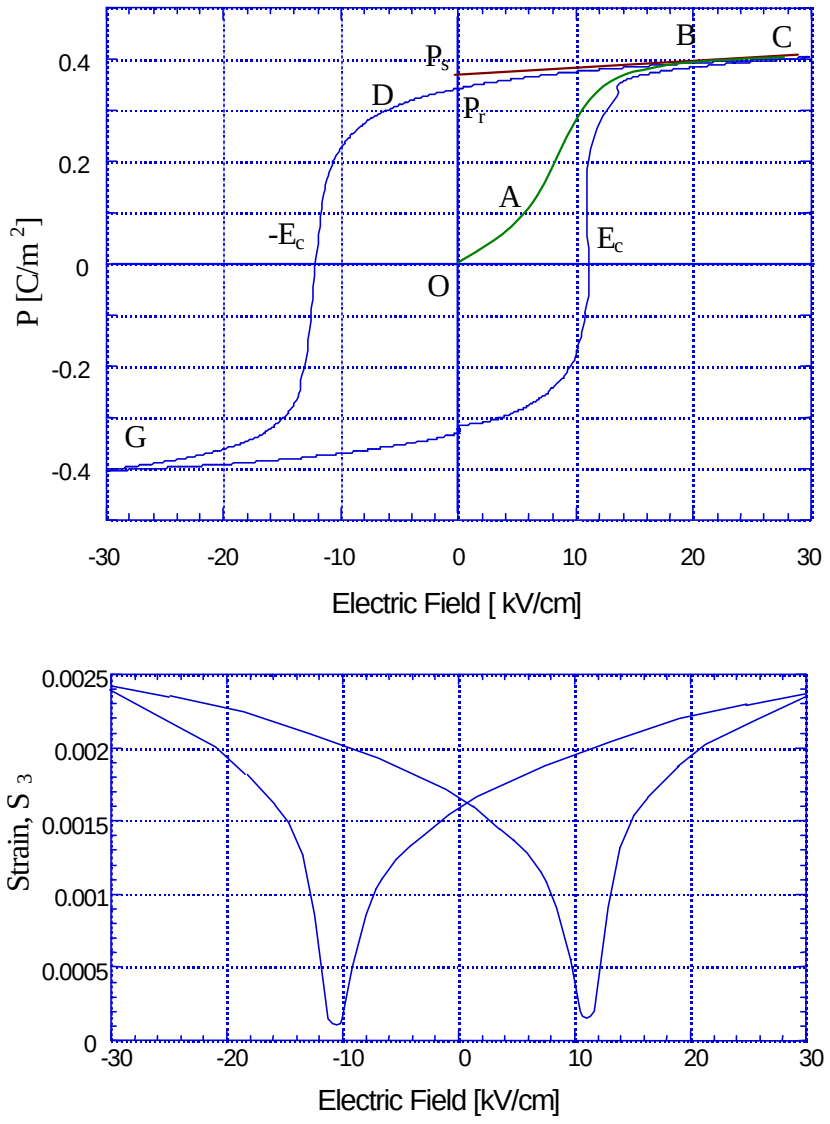

Figure 2.7. *(Upper part of figure): Dielectric hysteresis loop of PZT-5 from Morgan Matroc; (Lower part figure): Deformation loop of PZT-5 in the poling direction, $S_3(E_3)$*

If an initially unpolarised sample of PZT is subjected to an increasing electric field at a temperature slightly below its Curie point, the dipoles become increasing aligned with the field and polarisation will follow the curve shown in top of Figure 2.7. If the electric field applied is small, only a linear relationship between P and E is observed because the field is not large enough to switch any domain and the crystal will behave as a normal dielectric material (*paraelectric*). This case corresponds to the segment OA of the top of Figure 2.7. As the electric strength increases, a number of negative domains, which have a polarisation opposite to the direction of the field, will be switched over in the positive direction along the field, and domain orientation begins to take place. This results in a sharply rising P with increasing field E, and the polarisation will increase rapidly (segment AB) until all the domains are aligned in the positive direction (segment BC). This is a state of saturation in which the crystal is composed of just a single domain. The material is then said to have reached its *saturation polarisation*.

As the field strength decreases, the polarisation will generally decrease but does not return back to zero (at point D in top of Figure 2.7). When the field is reduced to zero, some of the domain will remain aligned in the positive direction and the crystal will exhibit a *remanent polarisation* P_r. The extrapolation of the linear segment BC of the curve back to the polarisation axis (at the point E) represents the value of the *spontaneous polarisation,* P_S. The remanent polarisation in a crystal cannot be removed until the applied field in the opposite direction reaches a certain value (at the point F). The strength of the field required to reduce the polarisation P to zero is called *the coercive field strength* E_C. Further, increasing the field in the negative direction will cause a complete alignment of the dipoles in this direction and the cycle can be completed by reversing the field direction once again.

The curve traced out in upper part of Figure 2.7 is known as the *hysteresis curve*. Its shape varies for the different PZT materials (Figure 2.9 is the hysteresis curve for PZT5) but the remanent polarisation is generally around 0.3- 0.35 C/m^2 for all PZT materials.

The lower part of Figure 2.7 shows the variation of the sample's relative deformation S_3 (i.e. in the direction of polarisation) with electric field, and it can be seen that this also exhibits a hysteresis effect corresponding precisely with the effect observed for polarisation.

2.5. Linear Theory of Piezoelectricity

Figure 2.7 shown the hysteretic behaviour of ferroelectric materials. Nevertheless, operation of the ferroelectric material is restricted to the so-called *linear range*, represented approximately by the CD segment. It can be seen than as bigger the electric field applied, bigger the non-linearity displayed.

The behaviour of piezoelectric materials in the linear range can be explained by the *linear theory of piezoelectricity* which is introduced in this section. In the case of non-ferroelectric materials, like quartz, this theory is very accurate. In the case of ferroelectric materials is necessary to take into account the limitations of the application as will be comment later. As a general rule, the application of linear theory of piezoelectricity is limited for the resonance of the materials, their depolarisation and for other non-linear effects such as hysteresis.

2.5.1. Conventional Assignment

The material constants listed in the data sheets are standard values determined on defined bodies (corresponding to the IEEE Standard on Piezoelectricity 1978, [8]). In accordance with this convention, orthogonal X,Y and Z (also 1,2,3) axes are customarily used as a basis for identifying the elasto-piezo-dielectric coefficients of a material. The Z direction is determined as

the polarisation direction. The numbers 4, 5 and 6 describe the mechanical shear stress which acts tangentially to the areas defining the co-ordinate system. As represented in the Figure 2.8, they can be understood as rotations around each axis.

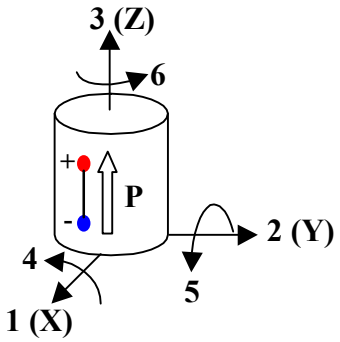

Figure 2.8. *Conventions for Axes*.

2.5.2. Basic Equations

In general, the *Direct Piezoelectric Effect* (so-called Sensor effect) in a single crystal can be described by a matrix which explains the polarisation developed by the crystal when an external stress (normal, T_1 to T_3 , and shear, T_4 to T_6) is applied onto the piezoelectric material.

A particular case of the direct piezoelectric effect is when the measure of the polarisation is made at external electric field E=0 (shorted). In this case, the polarisation developed is equal to the free charge *q* appeared in the electrodes, as given by equation (2.1).

$$P_i = q_i = d_{ij} \cdot T_j \tag{2.1}$$

In equation (2.1), q_i represents the linear free charge developed at the normal surface to the *i* direction. Equation (2.1) can also be expressed as:

$$\begin{Bmatrix} q_1 \\ q_2 \\ q_3 \end{Bmatrix} = \begin{bmatrix} d_{11} & d_{12} & d_{13} & d_{14} & d_{15} & d_{16} \\ d_{21} & d_{22} & d_{23} & d_{24} & d_{25} & d_{26} \\ d_{31} & d_{32} & d_{33} & d_{34} & d_{35} & d_{36} \end{bmatrix} \cdot \begin{Bmatrix} T_1 \\ T_2 \\ T_3 \\ T_4 \\ T_5 \\ T_6 \end{Bmatrix} \tag{2.2}$$

In equations (2.1) and (2.2), the polarisation vector is equal to the free charge in the electrodes due to the hypothesis of external electric field zero (or piezoelectric shorted).

Previous equation (2.1) is completely true in single crystals and, in such a case, it represents the polarisation generated in the material when a mechanical stress is applied. The piezoelectric coefficients, d_{ij}, will indicate the intensity of polarisation in each direction.

When a ferroelectric material is used, a change in the spontaneous polarisation $(P_S)_i$ replaces P_i. If the consideration of linear range is taking into account, the equivalent expression for ferroelectric materials is given by

$$\left(P_{TOTAL}\right)_i = \left(P_S\right)_i + d_{ij} \cdot T_j \tag{2.3}$$

In practice P_S is considered only in the poling direction because in the transversal directions is negligible. Thus $(P_S)_i = P_3$.

The *Converse Piezoelectric Effect* (so-called Actuator effect) described the strain generated in a piezoelectric material when it is subjected to an external electric field E_i. In particular if the material is not clamped (free-displacement condition, T_{ij}=0), the converse effect can be expressed as:

$$S_i = d_{ij}^{\theta,T} \cdot E_j \tag{2.4}$$

or more explicitly:

$$\begin{Bmatrix} S_1 \\ S_2 \\ S_3 \\ S_4 \\ S_5 \\ S_6 \end{Bmatrix} = \begin{bmatrix} d_{11}^{\theta,T} & d_{12}^{\theta,T} & d_{13}^{\theta,T} \\ d_{21}^{\theta,T} & d_{22}^{\theta,T} & d_{23}^{\theta,T} \\ d_{31}^{\theta,T} & d_{32}^{\theta,T} & d_{33}^{\theta,T} \\ d_{41}^{\theta,T} & d_{42}^{\theta,T} & d_{43}^{\theta,T} \\ d_{51}^{\theta,T} & d_{52}^{\theta,T} & d_{53}^{\theta,T} \\ d_{61}^{\theta,T} & d_{62}^{\theta,T} & d_{63}^{\theta,T} \end{bmatrix} \cdot \begin{Bmatrix} E_1 \\ E_2 \\ E_3 \end{Bmatrix} \tag{2.5}$$

In the previous equations (2.4) and (2.5), the coefficient $d_{ij}^{\theta,T}$ is called, the *charge piezoelectric coefficient*. This coefficient indicates the intensity of the deformation in the *i*-direction, S_i, when a electric field is applied in the direction *j*, E_j. Its dimension is: $\left[m/V\right]$. The superscript indexes are used to indicate the quantities that are kept constant or zero. The piezoelectric coefficient d_{ij} are identical to those for the direct effect.

2.5.3. Constitutive Equations

In *general*, a linear dielectric can withstand at the same time external conditions of temperature, mechanical stress and electric field. In this case, it is possible to analyse the mechanical and the electrical behaviour of the material and later coupling both results.

• Mechanical behaviour of a piezoelectric material

The strain **S** describes *the mechanical linear behaviour* (Hooke law approximation) of a piezoelectric material subjected to an electric field **E**, a stress **T** and a thermal variation Δq. This is shown in the next matrix as:

$$\begin{Bmatrix} S_1 \\ S_2 \\ S_3 \\ S_4 \\ S_5 \\ S_6 \end{Bmatrix} = \begin{bmatrix} d_{11}^{q,T} & d_{12}^{q,T} & d_{13}^{q,T} \\ d_{21}^{q,T} & d_{22}^{q,T} & d_{23}^{q,T} \\ d_{31}^{q,T} & d_{32}^{q,T} & d_{33}^{q,T} \\ d_{41}^{q,T} & d_{42}^{q,T} & d_{43}^{q,T} \\ d_{51}^{q,T} & d_{52}^{q,T} & d_{53}^{q,T} \\ d_{61}^{q,T} & d_{62}^{q,T} & d_{63}^{q,T} \end{bmatrix} \cdot \begin{Bmatrix} E_1 \\ E_2 \\ E_3 \end{Bmatrix} + \begin{bmatrix} s_{11}^{E,q} & s_{12}^{E,q} & s_{13}^{E,q} & s_{14}^{E,q} & s_{15}^{E,q} & s_{16}^{E,q} \\ s_{21}^{E,q} & s_{22}^{E,q} & s_{23}^{E,q} & s_{24}^{E,q} & s_{25}^{E,q} & s_{26}^{E,q} \\ s_{31}^{E,q} & s_{32}^{E,q} & s_{33}^{E,q} & s_{34}^{E,q} & s_{35}^{E,q} & s_{36}^{E,q} \\ s_{41}^{E,q} & s_{42}^{E,q} & s_{43}^{E,q} & s_{44}^{E,q} & s_{45}^{E,q} & s_{46}^{E,q} \\ s_{51}^{E,q} & s_{52}^{E,q} & s_{53}^{E,q} & s_{54}^{E,q} & s_{55}^{E,q} & s_{56}^{E,q} \\ s_{61}^{E,q} & s_{62}^{E,q} & s_{63}^{E,q} & s_{64}^{E,q} & s_{56}^{E,q} & s_{66}^{E,q} \end{bmatrix} \cdot \begin{Bmatrix} T_1 \\ T_2 \\ T_3 \\ T_4 \\ T_5 \\ T_6 \end{Bmatrix} + \begin{Bmatrix} a_1^{E,T} \\ a_2^{E,T} \\ a_3^{E,T} \\ a_4^{E,T} \\ a_5^{E,T} \\ a_6^{E,T} \end{Bmatrix} \cdot \Delta q \tag{2.6}$$

The coefficient a is the thermal expansion coefficient, defined as:

$$a_i^{E,T} = \left[\frac{\partial S_i}{\partial q}\right]_{E,T=\text{const}} = \left[\frac{1}{^\circ K}\right] \tag{2.7}$$

• Electric behaviour of a piezoelectric material

Similarly, *the electric response* of the material is described by the linear polarisation **P** generated in the material due to mechanical, electrical or thermal deformation, and is given by equation (2.8):

$$\begin{Bmatrix} D_1 \\ D_2 \\ D_3 \end{Bmatrix} = \begin{bmatrix} d_{11}^{E,q} & d_{12}^{E,q} & d_{13}^{E,q} & d_{14}^{E,q} & d_{15}^{E,q} & d_{16}^{E,q} \\ d_{21}^{E,q} & d_{22}^{E,q} & d_{23}^{E,q} & d_{24}^{E,q} & d_{25}^{E,q} & d_{26}^{E,q} \\ d_{31}^{E,q} & d_{32}^{E,q} & d_{33}^{E,q} & d_{34}^{E,q} & d_{35}^{E,q} & d_{36}^{E,q} \end{bmatrix} \cdot \begin{Bmatrix} T_1 \\ T_2 \\ T_3 \\ T_4 \\ T_5 \\ T_6 \end{Bmatrix} + \begin{bmatrix} e_{11}^{T,q} & e_{12}^{T,q} & e_{13}^{T,q} \\ e_{21}^{T,q} & e_{22}^{T,q} & e_{23}^{T,q} \\ e_{31}^{T,q} & e_{32}^{T,q} & e_{33}^{T,q} \end{bmatrix} \cdot \begin{Bmatrix} E_1 \\ E_2 \\ E_3 \end{Bmatrix} + \begin{Bmatrix} p_1^{T,E} \\ p_2^{T,E} \\ p_3^{T,E} \end{Bmatrix} \cdot \Delta q \qquad (2.8)$$

The coefficient *p* is the pyroelectric coefficient, defined as:

$$p_i^{T,E} = \left[\frac{\partial D_i}{\partial q} \right]_{T,E=\text{const}} = \frac{C}{°K \cdot m^2} \qquad (2.9)$$

• Global response: Coupling of both mechanical and electrical behaviour

The piezoelectric coefficients, d_{ij}, are identical for both electrical and mechanical response. This means that piezoelectricity involves the interaction between the electrical and mechanical behaviour of the medium.

Hence, it is possible to express the *global response* by a matrix that coupled both behaviours. This matrix is called *the elasto-piezo-dielectric matrix*, and is indicated in equation (2.10).

$$\begin{Bmatrix} S_1 \\ S_2 \\ S_3 \\ S_4 \\ S_5 \\ S_6 \\ D_1 \\ D_2 \\ D_3 \end{Bmatrix} = \begin{bmatrix} s_{11}^{E,T} & s_{12}^{E,T} & s_{13}^{E,T} & s_{14}^{E,T} & s_{15}^{E,T} & s_{16}^{E,T} & d_{11}^{T,\theta} & d_{12}^{T,\theta} & d_{13}^{T,\theta} \\ s_{21}^{E,T} & s_{22}^{E,T} & s_{23}^{E,T} & s_{24}^{E,T} & s_{25}^{E,T} & s_{26}^{E,T} & d_{21}^{T,\theta} & d_{22}^{T,\theta} & d_{23}^{T,\theta} \\ s_{31}^{E,T} & s_{32}^{E,T} & s_{33}^{E,T} & s_{34}^{E,T} & s_{35}^{E,T} & s_{36}^{E,T} & d_{31}^{T,\theta} & d_{32}^{T,\theta} & d_{33}^{T,\theta} \\ s_{41}^{E,T} & s_{42}^{E,T} & s_{43}^{E,T} & s_{44}^{E,T} & s_{45}^{E,T} & s_{46}^{E,T} & d_{41}^{T,\theta} & d_{42}^{T,\theta} & d_{43}^{T,\theta} \\ s_{51}^{E,T} & s_{52}^{E,T} & s_{53}^{E,T} & s_{54}^{E,T} & s_{55}^{E,T} & s_{56}^{E,T} & d_{51}^{T,\theta} & d_{52}^{T,\theta} & d_{53}^{T,\theta} \\ s_{61}^{E,T} & s_{62}^{E,T} & s_{63}^{E,T} & s_{64}^{E,T} & s_{65}^{E,T} & s_{66}^{E,T} & d_{61}^{T,\theta} & d_{62}^{T,\theta} & d_{63}^{T,\theta} \\ d_{11}^{E,T} & d_{12}^{E,T} & d_{13}^{E,T} & d_{14}^{E,T} & d_{15}^{E,T} & d_{16}^{E,T} & \varepsilon_{11}^{T,\theta} & \varepsilon_{12}^{T,\theta} & \varepsilon_{13}^{T,\theta} \\ d_{21}^{E,T} & d_{22}^{E,T} & d_{23}^{E,T} & d_{24}^{E,T} & d_{25}^{E,T} & d_{26}^{E,T} & \varepsilon_{21}^{T,\theta} & \varepsilon_{22}^{T,\theta} & \varepsilon_{23}^{T,\theta} \\ d_{31}^{E,T} & d_{32}^{E,T} & d_{33}^{E,T} & d_{34}^{E,T} & d_{35}^{E,T} & d_{36}^{E,T} & \varepsilon_{31}^{T,\theta} & \varepsilon_{32}^{T,\theta} & \varepsilon_{33}^{T,\theta} \end{bmatrix} \cdot \begin{Bmatrix} T_1 \\ T_2 \\ T_3 \\ T_4 \\ T_5 \\ T_6 \\ E_1 \\ E_2 \\ E_3 \end{Bmatrix} \qquad (2.10)$$

The previous matrix is so-called *d-form constitutive equation* and usually is represented in a compact form as shown equation (2.11) in Table 2.1.

The choice of independent variables (one mechanical, **T**, and one electrical, **E**) is arbitrary. A given pair of piezoelectric matrix equations corresponds to a particular choice of independent variables. Equations (2.11) to (2.14) show other possible constitutive matrix-equations using different independent variables.

Table 2.1. *Set of constitutive equations for a piezoelectric material*

Independent Variables	Type	Piezoelectric Relation	Form
[T], [E]	Extensive	$\begin{Bmatrix}[\mathbf{S}]\\[\mathbf{D}]\end{Bmatrix} = \begin{bmatrix}[s^E] & [d]\\ [d] & [e^T]\end{bmatrix} \cdot \begin{Bmatrix}[\mathbf{T}]\\[\mathbf{E}]\end{Bmatrix}$ (2.11)	d-form
[S], [D]	Intensive	$\begin{Bmatrix}[\mathbf{T}]\\[\mathbf{E}]\end{Bmatrix} = \begin{bmatrix}[c^D] & [-h]\\ [-h] & [b^S]\end{bmatrix} \cdot \begin{Bmatrix}[\mathbf{S}]\\[\mathbf{D}]\end{Bmatrix}$ (2.12)	h-form
[T],[D]	Mixed	$\begin{Bmatrix}[\mathbf{S}]\\[\mathbf{E}]\end{Bmatrix} = \begin{bmatrix}[s^D] & [g]\\ [-g] & [b^T]\end{bmatrix} \cdot \begin{Bmatrix}[\mathbf{T}]\\[\mathbf{D}]\end{Bmatrix}$ (2.13)	g-form
[S], [E]	Mixed	$\begin{Bmatrix}[\mathbf{T}]\\[\mathbf{D}]\end{Bmatrix} = \begin{bmatrix}[c^E] & [-e]\\ [e] & [e^S]\end{bmatrix} \cdot \begin{Bmatrix}[\mathbf{S}]\\[\mathbf{E}]\end{Bmatrix}$ (2.14)	e-form

As a particular case, if the material is non-piezoelectric, d_{ij} = 0, the electrical and mechanical behaviour are no-coupled.

[**E**] and [**D**] (so called electric tensors) are first-order tensors (vectors); [**S**] and [**T**] (so-called mechanical tensors) are second-order tensors (matrix 3×3); [**d**],[**g**],[**e**] and [**h**] (the piezoelectric coefficients) are third-order tensors (matrix 6×3); [**e**], [**b**] (the dielectric coefficients) are second-order tensors (3×3 matrix), and [**s**],[**c**] (elastic coefficients) are four-order tensors (6×6 matrix).

In the above mentioned constitutive equations, thermal effect has not been considered and it must be included if pyroelectric materials are considered.

2.5.4. Interpretation of the Elasto-Piezo-Dielectric Coefficients

• Piezoelectric Coefficients

The piezoelectric coefficient d_{ij} is known as *piezoelectric strain coefficient*. Since the *d* coefficient is equivalent for the direct and the converse effect, it is possible to use two equivalent expressions to define it, as shown equation (2.15).

$$d_{ij}^{q} = \begin{cases} = \left[\dfrac{\partial S_j}{\partial E_i}\right]_{D,q=cte} = {}^{m}\!/_{V} & \textit{Converse effect (Sensor)} \\ = \left[\dfrac{\partial D_i}{\partial T_j}\right]_{S,q=cte} = {}^{C}\!/_{N} & \textit{Direct effect (Actuator)} \end{cases} \quad (2.15)$$

Since piezoelectric material can be anisotropic, their physical constants (elasticity, permittivity and piezoelectric coefficients) are tensor quantities and relate to both the direction of the applied stress, electric field, etc., and to the directions perpendicular to these. For this reason the coefficients are generally given with two subscript indices which refer to the direction of the two related quantities (e.g. stress and strain for elasticity, displacement and electric field for permittivity). A superscript index is used to indicate a quantity that is kept constant.

For piezoelectric coefficients, which refer an electric quantity and a mechanical quantity, the first subscript indicates the direction of the considered electrical quantity (displacement or electric field) and the second subscript indicates the direction of the considered mechanical quantity (stress or strain).

The next matrix indicated the structure off the *d*-matrix for three important cases of piezoelectric materials: the single crystal quartz, the ferroelectric ceramics PZT and the ferroelectric polymer PVDF.

Mono-crystal α-Quartz

$$d_{quartz} = \begin{bmatrix} d_{11} & -d_{11} & 0 & d_{14} & 0 & 0 \\ 0 & 0 & 0 & 0 & -d_{14} & -2d_{11} \\ 0 & 0 & 0 & 0 & 0 & 0 \end{bmatrix}$$

$$d_{11} = 2.3.10^{-12}\ C/N$$
$$d_{14} = -0.7.10^{-12}\ C/N$$

(2.16)

$BaTiO_3$, PZT, PLZT, and other polycrystalline ferroelectrics.(Poling axis = 3)

$$d_{PZT} = \begin{bmatrix} 0 & 0 & 0 & 0 & d_{15} & 0 \\ 0 & 0 & 0 & d_{15} & 0 & 0 \\ d_{31} & d_{31} & d_{33} & 0 & 0 & 0 \end{bmatrix}$$

(2.17)

PVDF (piezoelectric polymer)

$$d_{PVDF} = \begin{bmatrix} 0 & 0 & 0 & 0 & d_{15} & 0 \\ 0 & 0 & 0 & d_{24} & 0 & 0 \\ d_{31} & d_{32} & d_{33} & 0 & 0 & 0 \end{bmatrix}$$

(2.18)

The rest of piezoelectric coefficients have an analogous definition, as is indicated in the next equations

Piezoelectric voltage coefficient

$$g_{ij}^{q} = \begin{cases} = \left[\frac{\partial S_j}{\partial D_i}\right]_{E,q=cte} = \frac{m^2}{C} & \textit{Converse effect} \\ = \left[-\frac{\partial E_i}{\partial T_j}\right]_{S,q=cte} = \frac{V.m}{N} & \textit{Direct effect} \end{cases}$$

(2.19)

Piezoelectric stiffness coefficient

$$h_{ij}^{q} = \begin{cases} = \left[\frac{\partial E_i}{\partial S_j}\right]_{D,q=cte} = \frac{V}{m} & \textit{Direct effect} \\ = \left[\frac{\partial T_j}{\partial D_i}\right]_{S,q=cte} = \frac{N}{C} & \textit{Converse effect} \end{cases}$$

(2.20)

Piezoelectric e coefficient

$$e_{ij}^{q} = \begin{cases} = \left[\frac{\partial D_i}{\partial S_j}\right]_{E,q=cte} = \frac{C}{m^2} & \textit{Direct effect} \\ = \left[-\frac{\partial T_j}{\partial E_i}\right]_{S,q=cte} = \frac{N/m}{V} & \textit{Converse effect} \end{cases}$$

(2.21)

• Elastic coefficients

In order to express the relation between the mechanical strain and the stress, two elastic coefficients can be considered: the compliance and the stiffness.

The compliance *s* of a material is defined as the strain produced per unit of applied stress. It can be measured at electric field constant or at electric charge constant as is indicated in the next equations:

Elastic compliance coefficient s_{ij} :

$$s_{ij}^{E,q} = \left[\frac{\partial S_i}{\partial T_j}\right]_{E,q=cte} = \frac{m^2}{N} \quad \textit{Compliance at } E = cte \textit{ or zero (short - circuit)}$$
$$s_{ij}^{D,q} = \left[\frac{\partial S_i}{\partial T_j}\right]_{D,q=cte} = \frac{m^2}{N} \quad \textit{Compliance at } D = cte \textit{ or zero (open - circuit)} \tag{2.22}$$

The first subscript refers to the direction of strain, the second to the direction of stress. For example: s_{23}^{E} is the compliance for a normal stress about axis 3 and accompanying strain in direction 2 under conditions of electric field constant (o zero).

Similarly it is defined the stiffness coefficient as:

Elastic stiffness coefficient c_{ij} :

$$c_{ij}^{E,q} = \left[\frac{\partial T_j}{\partial S_i}\right]_{E,q=cte} = \frac{N}{m^2} \quad \textit{Stiffness at } E = const \textit{ or zero (short - circuit)}$$
$$c_{ij}^{D,q} = \left[\frac{\partial T_j}{\partial S_i}\right]_{D,q=cte} = \frac{N}{m^2} \quad \textit{Stiffness at } D = const \textit{ or zero (open - circuit)} \tag{2.23}$$

• Dielectric coefficients

The absolute *permittivity* (or dielectric constant) is defined as the dielectric displacement per unit of electric field. It is followed of two subscripts: the first subscript gives the direction of the dielectric displacement, the second gives the direction of the electric field. It can be measured at free displacement (T=0) or at blocking force (S=0) as is illustrated in equation (2.24).

$$e_{ij}^{S,q} = \left[\frac{\partial D_i}{\partial E_j}\right]_{S,q=cte} = \frac{F}{m} \quad \textit{Permittivity at } D = const \textit{ o zero (blocking force)}$$
$$e_{ij}^{T,q} = \left[\frac{\partial D_i}{\partial E_j}\right]_{T,q=cte} = \frac{F}{m} \quad \textit{Permittivity at } T = const. \textit{ or zero (free displacement)} \tag{2.24}$$

The Data handbook tables give values for the relative permittivity $\varepsilon/\varepsilon_0$, i.e. the ratio of absolute permittivity to the permittivity of free space (8.85×10^{-12}F/m).

It is also possible to define another dielectric coefficient as:

$$b_{ij}^{S,q} = \left[\frac{\partial E_j}{\partial D_i}\right]_{S,q=cte} = \frac{m}{F} \quad \textit{Impermittivity at } D = const. \textit{ or zero (blocking force)}$$
$$b_{ij}^{T,q} = \left[\frac{\partial E_j}{\partial D_i}\right]_{T,q=cte} = \frac{m}{F} \quad \textit{Impermittivity at } T = const. \textit{ or zero (free displacement)} \tag{2.25}$$

2.6. Linear theory limitations

It has been previously commented that different aspects limit the application of the linear theory of piezoelectricity. Following we considered each of them.

• Electrostriction

In general the response of piezoelectric materials has a quadratic component which is superposed to the linear behaviour. This component depends on a coefficient called *electrostrictive coefficient*. For piezoelectric materials this coefficient is usually lower than the linear piezoelectric coefficient but they can be very significant when the electric field is increased.

• Depolarisation

After its poling treatment a PZT ceramic will be permanently polarised, and care must therefore be taken in all subsequent handling to ensure that the ceramic is not depolarised, since this will result in partial or even total loss of its piezoelectric properties. The ceramic may be depolarised electrically, mechanically or thermally.

Electrical depolarisation: Exposure to a strong electric field of opposite polarity to the poling field will depolarise the material. The field strength required for starting the depolarisation depends, among other things, on the material grade, the time the material is subjected to the depolarising field and the poling temperature.

Mechanical depolarisation: Mechanical depolarisation occurs when the mechanical stress on a piezoelectric element becomes high enough to disturb the orientation of the domains and hence destroy the alignments of the dipoles. The safety limits for mechanical stress vary considerably with material grade.

Thermal depolarisation: If a piezoelectric element is heated to its Curie point, the domains become disordered and the element becomes completely depolarised. A piezoelectric element can therefore function for long period without marked depolarisation only at temperatures well below the Curie point. A safe operating temperature would normally be about half way between 0ºC and the Curie point.

• Frequency limitations

All the physical systems have an associate frequency natural of vibration. When the system is exposed to a periodic serial of impulses (such as electrics, mechanics, acoustics, etc) with a frequency in the vicinity of the natural frequency, the system will oscillate with very high amplitudes. In general a body mechanically exited will response with a mechanical resonance. However, if the material is piezoelectric an electrical resonance can be achieved when the material is driven with a mechanical field. On the other hand, high mechanical deformations can be produced when the material is electrically driven. Hence, an electrical signal with a frequency very close to the mechanical natural frequency of the system will produce a resonance.

Figure 2.9 shows the typical frequency response of a piezoelectric disc. It displays the different resonance peaks. In general the linear response can be considered up to a half of the first resonance of the system.

The resonance frequency will depend on the characteristics of the piezoelectric material and the mechanical and electrical conditions of environment.

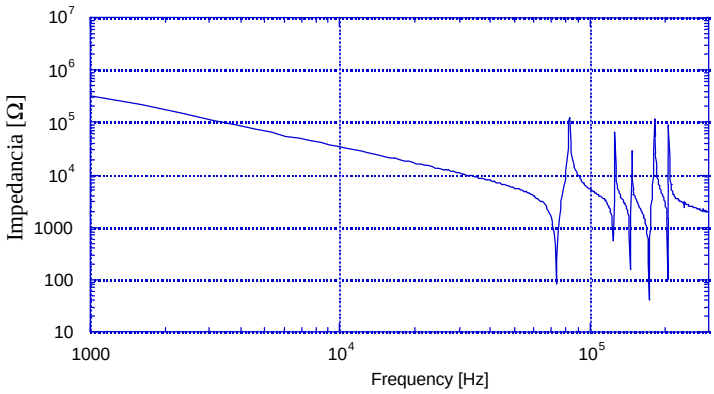

Figure 2.9. *Impedance of a PZT disc as a function of frequency*

2.7. Coupling factor k

Piezoelectric materials couple electric and mechanic fields. Thus, it is possible to use this kind of materials introducing an electrical energy and obtaining a mechanical one, or vice versa. Then, it is necessary to have a coefficient for measuring the effectiveness with which electrical energy is converted into mechanical energy or the opposite case. This coefficient is the coupling factor k_{eff} and is defined at frequencies below the resonant frequency of the piezoelectric body as:

$$k_{eff}^2 = \frac{\textit{energy converted}}{\textit{input energy applied to the material}} \tag{2.26}$$

In the direct piezoelectric effect, the coefficient k is defined as:

$$k_{eff}^2 = \frac{\textit{electrical energy}}{\textit{mechanical energy driven to the material}} \tag{2.27}$$

As for the converse piezoelectric effect, k will be defined as:

$$k_{eff}^2 = \frac{\textit{mechanical energy generated}}{\textit{electrical energy driven to the material}} \tag{2.28}$$

A study of the values of k_{eff} shows that for modern piezoelectric ceramics, up to 50% of the stored energy can be converted at low frequencies. The values of k_{eff}^2 quoted in tables, however, are usually theoretical maxim, based on precisely defined vibration modes of ideal (i.e. unrealistic) specimens of the material. In practical transducers, the coupling factors are usually lower.

The coupling coefficient k_{eff} describes energy conversion in all directions. When only conversions in specific directions are taken into account, the resulting coupling factor is indicated by subscripts. For instance, k_{33} is the coupling factor for longitudinal vibrations of a very long, very slender rod (in theory infinitely long, in practice, with a length/diameter ratio > 10) under the influence of a longitudinal electric field. k_{31} is the coupling factor for longitudinal vibrations of long rod under the influence of a transverse electric field, and k_{15} describe shear mode vibrations o a piezoelectric body.

Special cases of the coupling factor are the planar coupling factor k_p and the thickness coupling factor k_t.

The planar coupling factor k_p of a thin disc represents the coupling between the electric field in direction 3 (parallel to the disc axis) and simultaneous mechanical effects in directions 1 and 2 (Figure 2.10) that result in radial vibrations. This is known as radial coupling.

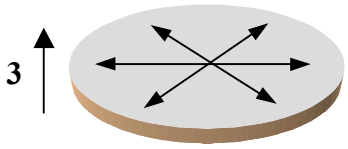

Figure 2.10. *Planar oscillations of a thin disc of piezoelectric material*

The thickness coupling factor k_t represents the coupling between an electric field in direction 3 and the mechanical vibrations in direction 3 of a thin, planar object of arbitrary contour (i.e. an object whose surface dimensions are large compared with its thickness).

The resonant frequency of the thickness mode of a thin planar object is far higher that of its transverse mode.

The coupling factor k_{eff} can be expressed as a quotient of energy densities

$$k_{eff}^2 = \frac{\frac{1}{2} e^T E^2 - \frac{1}{2} e^S E^2}{\frac{1}{2} e^T E^2} \tag{2.29}$$

In the equation (2.29), the term $\frac{1}{2} e^T E^2$ represents the total stored energy density for the freely deforming piezoelectric body (T=0). The term $\frac{1}{2} e^S E^2$ represents the electrical energy density when the body is constrained (S=0). The difference between these two terms (numerator) equals the stored, converted, mechanical energy.

This energy can often be extracted and the unconverted energy can also be recovered. Although a high k is desirable for efficient transduction, k^2 should not be thought of as a measure of efficiency (this is defined as the ratio of the usefully converted power to the input power), since the unconverted energy is not necessarily lost (converted into heat) and can in many cases be recovered.

The real efficiency is the ratio of the converted useful energy to the energy taken up by the transducer, and a properly tuned and well-adjusted transducer operating in its resonance region can achieve efficiencies of well over 90%. Well outside its resonance region, however, its efficiency could be very low.

2.8. Piezoelectric Materials Processing

A large number of natural and synthetic materials are available at present for use in piezoelectric and pyroelectric devices. A basic classification is shown in the Table 2.2:

Table 2.2. *Classification of the piezoelectric materials*

Type of piezo-aterial	Examples
Single crystals (non-ferroelectric[1] and ferroelectrics[2])	*Naturals:* Quartz[1], Zinc Blende (sphalerite), Boracite, Tourmaline, Topaz, Sugar, Rochelle Salt[2], Pyrite *Synthetics:* Ammonium dihydrogen phosphate (ADP), Ethylene diamine tartrate (EDT), Barium titanate single crystal ($BaTiO_3$) [2], Potassium dihydrogen phosphate (KDP)[2]
Ferroelectric Ceramics (Polycrystalline Ferroelectrics)	$BaTiO_3$ (ceramic), PZT, PLZT, SBT, PBT, NBT
Ferroelectric Polymers	PVDF
Ferroelectric Composites	1-3 PZT-polymer composite
Grain-oriented Glass-Ceramics	$2BaO\text{-}3SiO_2\text{-}TiO_2$

2.8.1. Single Crystals

Because of their natural asymmetric structure, the single crystal materials exhibit the piezoelectric effect without further processing. As previously commented, two different behaviours can be found in single crystals: *Non-ferroelectric single crystals* and *ferroelectric single crystals*.

• Non-ferroelectric single crystals

Non-ferroelectric single crystals exhibit a zero polarisation when the external electric or mechanical field is removed. Moreover it is not possible to switch the sense of the polarisation of the material.

Quartz (polymorph of SiO_2), the most widely used single-crystal piezoelectric occurs naturally. Quartz belongs to the so-called group of non-ferroelectric single crystals. This means that it is not possible to switch the sense of the polarisation of the material.

Limited quantities of rigorously inspected natural quartz, without flaws or twinned regions, are accepted for device use. The majority of single-crystal quartz is prepared in laboratory by the hydrothermal technique of growth from hot H_2O solution under pressure. Typical conditions include temperatures of 670 K (397 ºC), pressures of 170MPa, and the presence of a few percent of NaOH or Na_2CO_3 in the solution acting as 'mineralizers' to increase the solubility of the quartz. By filling the vessel with solution to about 80% of the volume, the required pressure is automatically achieved on raising the temperature. The growth vessel, often referred to as an autoclave or bomb, consist of a thick-walled steel container typically 4 m long, 25 cm internal diameter and 10 cm thick. Elaborate seals are based on Bridgman's unsupported area principle. The driving force for growth is a temperature gradient of about 50 K. Solution occurs from crushed natural quartz feed material in the lower and hotter region. The solution is carried by convection into the upper region, where the reduced solubility at the lower temperature results in deposition of quartz on thin seed plates. A typical growth rate of 1 mm per day produces 4 cm $\times$ 4 cm $\times$ 15 cm crystal in a 20 day period.

Too high a growth rate can produce imperfections and cracking. Growth orientations in commonly used seeds are cut parallel or close to the basal plane (001) or to the minor rhombohedral phase (011), the latter giving a growth rate of about half the former. The addition

of lithium salts to the growth solution reduces the OH content of the quartz, causing a marked improvement in the electromechanical properties.

Quartz crystals are the most stable of all piezoelectric materials. Its piezoelectric sensitivity is independent of temperature, time and mechanical stress. Due to this, quartz is ideal for applications requiring high accuracy, as the case of resonators. One of the disadvantages is the low coupling factor k, and because of this, this material is not useful for applications where it is necessary a high efficiency in the energy conversion.

- **Ferroelectric single-crystals**

Ferroelectric single crystals have a remanent polarisation without any external stress applied. Moreover, the direction of the polarisation could be reversed by application of an inverse electric field.

A large of ferroelectric single crystals is available at present for use in piezoelectric devices. The most essential feature of this class of materials is the presence of a spontaneous polarisation without an external electric field usually acting on the material. In this way, the behaviour of ferroelectrics with respect to an electric field displays a certain analogy with that of ferromagnetic materials with respect to a magnetic field (Figure 2.11)

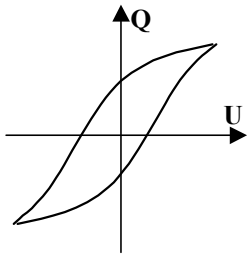

Figure 2.11. *Hysteresis loop of a ferroelectric*

Rochelle salt was the first substance in which the ferroelectricity was observed. Ferroelectric properties of Rochelle salt manifest themselves only on mono-crystal samples along one definitive crystalline axis. Rochelle salt was studied in detail in the Soviet Union by I.Kurchatov, P.Kobeko *et al.* in 1930-1934 and used to develop the first theories of ferroelectric phenomena.

Today several hundreds of substances are known which possess ferroelectric properties. An especially high scientific and technical importance is attached to the discovery of the ferroelectric properties of barium titanate $BaTiO_3$ by the outstanding Soviet physicist Academician B.Vul made in 1943. Barium titanate exhibits a number of advantages over the formerly known ferroelectrics, such as a high mechanical strength, resistance to heat and moisture, presence of ferroelectric properties within a broad range of temperatures and also ease of manufacturing. Barium titanate has attracted universal attention of researchers and has found a wide practical application.

Barium titanate is obtained by roasting equimolecular quantities of titanium dioxide TiO_2 and barium oxide BaO (in practice, barium oxide is introduced in the form of barium carbonate $BaCO_3$ dissociated during heating into BaO and CO_2 that escapes from the sphere of reaction).

Later on, a number of ferroelectrics similar to barium titanate have been discovered (strontium, cadmium and zinc titanates, lead zirconate and solid solutions of the substances of this group and also several niobates and tantalates).

2.8.2. Ceramics

Apart from monocrystals, certain artificial polycrystalline anisotropic formations possess piezoelectric properties. Barium titanate and similar materials, for example, display ferroelectric properties also in polycrystalline prepared by conventional ceramic processes. These materials are frequently referred to as ferroelectric ceramic materials and make them very attractive because of the difficulties and cost of growing single crystals

In a typical PZT production process, the appropriate amounts of lead, zirconium and titanium oxides together with a few percent of modifying additives such as MnO, Nb_2O_5, CaO or Sb_2O_5 are mechanically mixed with water. After drying and pre-reaction (calcination) at temperatures between 800ºC-1000ºC, another wet milling normally follows to eliminate aggregations. Following, organic binders are added and the resultant slurry is spray dried. Shaped ceramics are fabricated by pressing and firing, typically for 1-2 hours at approximately 1100ºC-1300ºC in air. Due to the random polarity of all the individual crystallites the material does not exhibit piezoelectricity and have to be preliminarily poling to reveal their piezoelectric properties. By the poling process the sample will remain with a remanent polarisation.

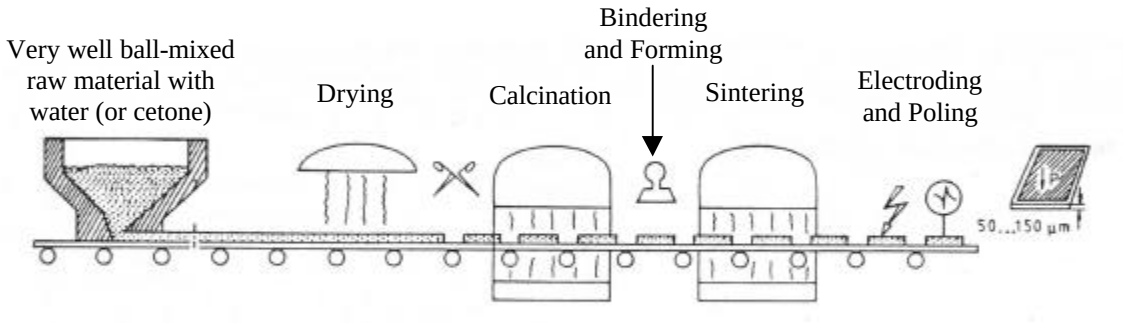

Figure 2.12. *Standard mixed-oxide method utilised for PZT manufacturing.*

Transparent piezoelectric ceramics are produced by adding lanthanum oxide in the PZT process and employing hot pressing for long periods to give lead-lanthanum zirconate-titanate (PLZT).

2.8.3. Polymer Films

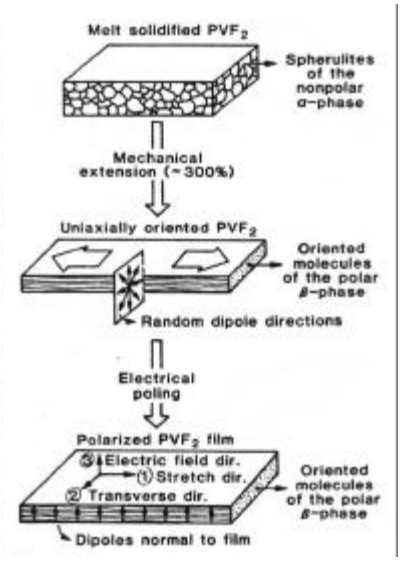

Figure 2.13. *Poling process of a polymer PVDF*

The piezoelectric and related properties of several polymers, such as polyvinylidene fluoride oriented film (PVF_2, also called PVDF), develop fully only when the material has been mechanically and electrically stressed. As cast from the melt, PVF_2 crystallises in the non-polar α form.

On mechanical deformation (typically by stretching or rolling to five times the length), the polar β form is produced by a change in the conformation of the polymer chains, resulting a planar zigzag arrangement with all fluorine atoms on one side and all hydrogen atoms on the other side of the chain. Subsequent poling in an electric field produces parallel dipole orientation.

2.9. References

[1] Friend, C., *Smart Materials: The Emerging Technology*, Materials World, 4 [1], pp. 16-18, 1996.

[2] Gahdhi. M.V. and Thompson, B.S., Smart Materials and Structures, Champman & Hall, London (1992).

[3] Curie, J., and Curie, P., *Development par compression de l'electricite polaire dans les cristaux hemiedres a faces inclinees*, Bulletin de la Societe Mineralogique de France, 3, pp. 90-93, 1880.

[4] Cady, W.G., *Piezoelectricity*, McGraw-Hill, NewYork, 1946

[5] Jaffe, B., Roth, R.S., and Marzullo, S., *Piezoelectric Properties of Lead Zirconate-Titanate Solid-Solution Ceramics*, J.Appl. Phys., 25 [6] 809-810 (1954).

[6] Ikeda, T., Fundamentals of piezoelectricity. Oxford University Press (1990).

[7] Uchino, K., Piezoelectric actuators and ultrasonic motors. Kluwer Academic Publishers. (1997).

[8] IEEE Standard 176-1978, *Standard on Piezoelectricity*.

[9] J. W. Waanders, Piezoelectric Ceramics. Properties and applications. Philips Components

SECOND PART:

VOLTAGE TRANSDUCERS

Chapter 3

State of the Art of Piezoelectric Transformers. Possibilities as Instrument Transformer

3 State of the Art of Piezoelectric Transformers. Possibilities as Instrument Transformer

3.1. Introduction

A piezoelectric transformer, from a general point of view, consists of a body of piezoelectric material where two regions are considered: *driving region* and *driven region*. Both regions are mechanically matched but electrically isolated. In the driving region – so called *input region* – a mechanical vibration is generated from an electrical driving current. This mechanical vibration is transmitted to the driven region - so called *output region* - where it is reconverted back into an electrical signal.

In this way, the piezoelectric transformer may be characterised as a two steps process involving an initial piezoelectric conversion of electrical energy into mechanical energy followed, by a reconversion of the mechanical energy back into electrical energy. The mechanical energy referred to is in the form of vibrational energy. Figure 3.1. displays an schematic of the electrical to electrical energy by using an acoustic vibration.

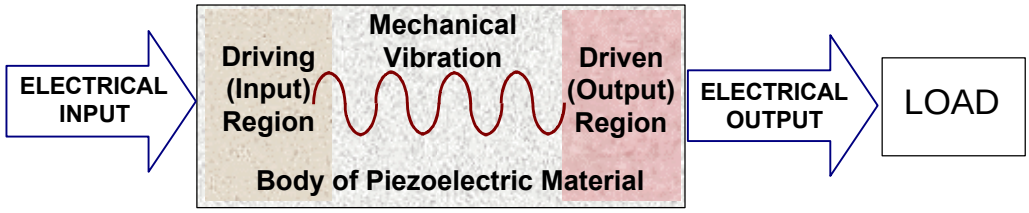

Figure 3.1. *The operation of a piezoelectric transformer is characterised by an electrical to electrical conversion by means of a mechanical vibration.*

In this chapter a review of the state of the art of piezoelectric transformers is given. At present, the applications of the transformers using piezoelectric technology have taken advantage of the properties of the piezoelectric materials operating in *resonance*. As a result, these types of devices are usually known as *Resonant Piezoelectric Transformers*.

A general description of resonant transformers, their evolution and performances are gathered in the following sections. A final discussion about their possibilities and limitations to be applied as measuring transformers and an introduction to the technology of the *Non-Resonant Piezoelectric Transformers* will be done.

3.2. Resonant Piezoelectric Transformers

Resonant Piezoelectric Transformers utilising the piezoelectric effect are known in the technical literature. These kind of transformers can be defined as a passive electrical energy transfer device or transducer employing the piezoelectric properties of a material operated at one of its resonance frequencies, to achieve the transformation of voltage or current or impedance.

Piezoelectric transformers have recently replaced wound-type electromagnetic transformers for generating high voltage in the power circuits for certain electronic applications. These piezoelectric transformers offer numerous advantages over ordinary *electromagnetic transformers*, including a compact and slim shape, rugged construction, and high efficiency and reliability in a comparably smaller package. Piezoelectric transformer are particularly well suited for high voltage applications.

A lot of effort have been put in to make the switching frequency of a switching power source higher to provide a more compact electronic equipment. An electromagnetic transformer has been used here for the switching power source. As the switching frequency is increased, the power loss due to *hysteresis loss*, the *eddy current*, and the loss due to the *skin effect* of the conductor are sharply increased, resulting in a considerably low efficiency of the transformer. Accordingly, the upper limit of the practical frequency of the electromagnetic transformer is at most 500 kHz.

In contrast to the general electromagnetic transformer, the resonant piezoelectric transformer is used in a resonant mode and has a number of advantages as follows:

1. The size of the transformer can be made smaller since the energy density at the same frequency is higher.

2. The transformer can be made non-flammable.

3. There are no electromagnetic interference due to the electromagnetic induction of the transformer.

Thanks to these advantages, resonant piezoelectric transformers are now finding applications in a variety fields including photocopiers, back-lights for liquid crystal displays, flat panel displays, power converters, CRT displays, and the like.

3.2.1. The Rosen-type Piezoelectric Transformer

• Introduction

The first proposal of a piezoelectric transformer correspond to Charles A. Rosen and Keith Fish, (1954) with the U.S. application, Serial No. 401,812, assigned to the General Electric Company [1,2]. At present, the literature refers it as *Rosen-type transformer* one of the embodiments described by Rosen and Fish in the mentioned application. It consists of a thin rectangular piezoelectric body having two regions which are transversely polarised with respect to one another, Figure 3.2.

• Description

In structure, the Rosen-type piezoelectric transformer includes a body of piezoelectric material, having electrodes applied to the body for the application of input potentials, and electrodes

applied to the body for the removal of the potential developed in the body upon the application of input potentials.

Referring more specifically to Figure 3.2, it shows a piezoelectric transformer comprising of a piece of piezoelectric material in the shape of a rectangular parallelepiped, and having a driving region **1** (*input*) and a driven region **2** (*output*). The driving and driven regions may be formed separately, and then fastened together by a suitable cement, such as one of the epoxy resins. However, it is preferable that they be made from a single piece of piezoelectric material as illustrated in Figure 3.2. The opposite faces **3** of the driving region **1** are covered with a metallic coating such as silver, for example, to provide a pair of input terminals, one of which is connected to ground at **4**. In similar manner, the end **5** of the driven region **2** remote from the driven region is also coated with silver to provide an output terminal for the transducer (the other output terminal being the common ground at **4**). The device is energised by a source of alternating current as shown at **6**.

The driving and the driven regions are provided with dissimilar polarisation. Arrows indicate the direction of polarisation of each region. The driving region **1** has a polarisation perpendicular to the long dimension, and the driven region **2** has a polarisation in the longitudinal direction. Thus, both polarisation vectors are at right angles with respect to one another.

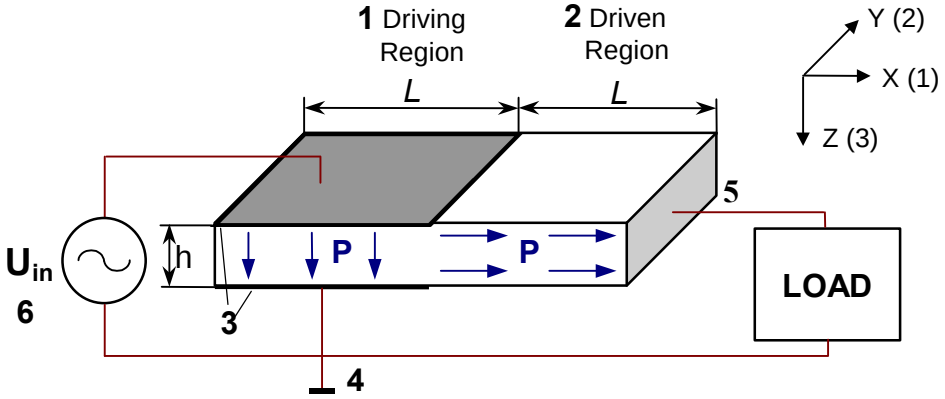

Figure 3.2. *Rosen-type piezoelectric transformer*

• Operation

In the operation of the piezoelectric resonant transformer an alternating current from the source **6** is applied to the driving region **1**, which is transverse to the longitudinal axis of the body (X-axis). The direction of the field is parallel to the direction of the polarisation of the driving region **1**. Application of an alternating potential to the driving region consequently brings about an alteration in the thickness dimension of the body.

This strain, by virtue of Poisson's coupling within the material, also produces a strain in the longitudinal dimension of the body, and then longitudinal mechanical vibrations. The vibration of the body is accompanied by strains along the longitudinal axis. Particularly, if the body is chosen to resonate with an anti-node at either end in the fundamental mode at a frequency equal to the frequency of the applied potentials, then a periodic potential appears between the driven (output) electrodes. The electrode junctions furnish these potentials to the high impedance load device.

If the frequency of the driving alternating current is non-resonant, there will be losses in the transmission of the vibration. In this case the output voltage will be lower than the input voltage.

On the contrary, if the driving current to the piezoelectric transformer has a frequency corresponding to a mechanical frequency of the device, the vibration produced in the driving

region will be very high. This vibration will be transmitted to the output region and the voltage generated will also be elevated.

Figure 3.3 shows the distribution of mechanical stress and particle displacement in a piezoelectric transformer excited at the fundamental vibrational mode [3]. As a result of selecting a high mechanical quality factor Q_m, the particle displacement is nearly sinusoidal. The displacement, for the fundamental mode, exhibits a node (zero displacement) exactly in the middle of the transformer.

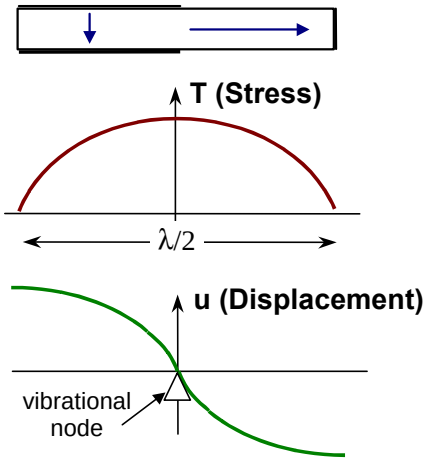

Figure 3.3. *Distribution of mechanical stress and particle displacement in a piezoelectric transformer excited at its fundamental vibrational mode.*

Compared with the classical electromagnetic transformer, the piezoelectric 'resonant' transformer is a narrow band device. This means that it has to be operated in mechanical resonance to achieve efficient transformation.

The unloaded voltage transformation ratio (U_2 / U_1) is determined by the dimension of the transducers, their effective coupling factors (K_{eff}) and the mechanical quality factor (Q_m), by [3,4]:

$$r = \frac{U_{out}}{U_{in}} = \frac{4}{p^2} \cdot k_{31} \cdot k_{33} \cdot Q_m \cdot \frac{L}{t} = \frac{4}{p^2} \cdot \frac{|d_{31} \cdot g_{33}|}{\sqrt{s_{11}^E \cdot s_{33}^E}} \cdot Q_m \cdot \frac{L}{t} \qquad (3.1)$$

For example, the material utilised for Philips Components for piezoelectric transformer is PXE 43. This material is a hard PZT ceramic suitable for power applications. It has excellent power handling capabilites: a power density higher than 25 Watts/cm^3 without thermal problems is achievable. In the Table 3.1 some parameters of PXE43 are given.

Table 3.1. *Properties of the PXE43*

Q_m^E	tan δ	d_{31}[C/N]	g_{33} [V-m/N]	s_{11}^E [Pa^{-1}]	s_{33}^E [Pa^{-1}]	e_{33}^T / e_0
1000	2.10^{-3}	100.10^{-12}	27.10^{-3}	11.10^{-12}	13.10^{-12}	1000

Considering a geometrical ratio *L/t = 24/2*, the transformer voltage ratio, *r*, will approximately be *1190*.

- **Driving**

A sine wave signal is the best way of driving piezoelectric transformers. However, generating a sine wave requires more complicated electronics than a square wave. Therefore using a square wave voltage in combination with a technique to minimise the switching loss is preferable.

Such a technique is the so called *Zero Voltage Switching, ZVS*. Figure 3.4 shows the general principle. A DC-voltage is converted into a square wave voltage, which is applied to the piezoelectric transformer. The generated voltage at the output is supplied to the load. Depending on the application it may be rectified first. Unlike magnetic transformers, piezoelectric transformers are very sensitive to variations in load. Such variations will generally lead to a shift in the resonant frequency, which makes frequency tracking necessary. Therefore some feedback from the piezoelectric transformer or from the load will be indispensable.

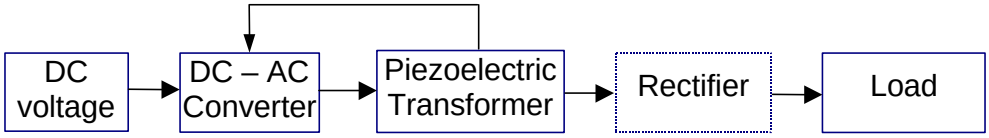

Figure 3.4. *General principle for driving a piezoelectric resonant transformer*

Figures 3.5 shows the simplest topology for driving piezoelectric transformers. Other topologies can be found elsewhere [3]

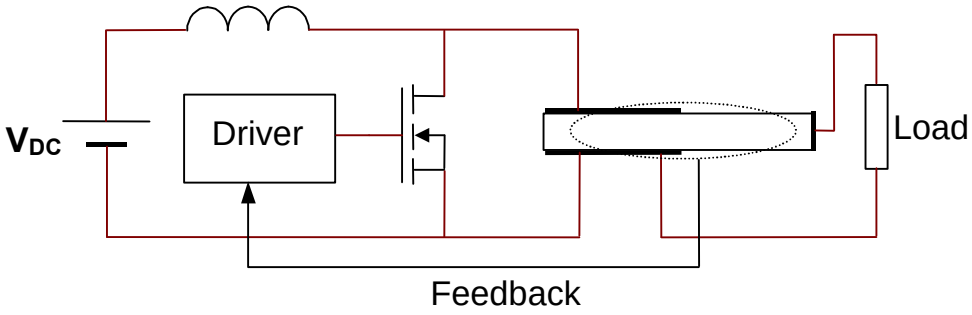

Figure 3.5. *Class E-amplifier driving a piezoelectric resonant transformer*

3.2.2. Different Topologies of the Rosen-type Piezoelectric Resonant Transformer. Evolution

The previously described Rosen-type piezoelectric transformer is the best known and the only one commercially available [3] and used. However, there were other different configurations proposed by Rosen and Fish in 1954 [1,2]. Figures 3.6 up to 3.10 show some of the embodiments proposed also by Rosen & Fish in their patent [1,2].

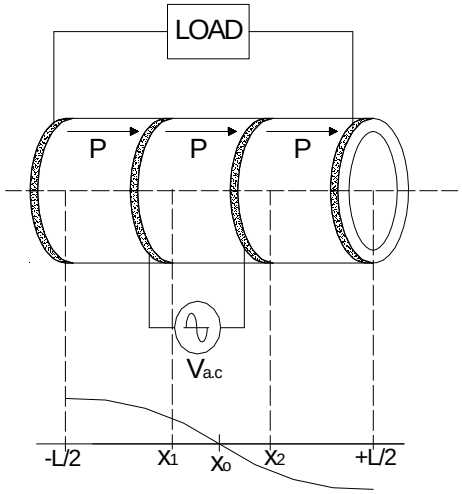

Figure 3.6 *Tubular piezoelectric transformer*

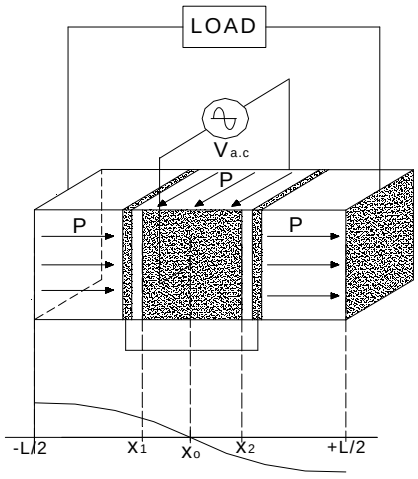

Figure 3.7. *Piezoelectric transformer of elongated rectangular construction*

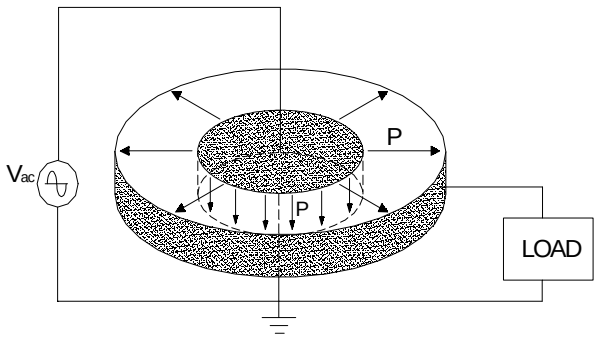

Figure 3.8. *Piezoelectric transformer constructed in a double poled disc*

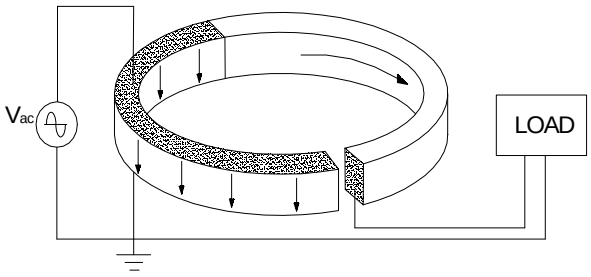

Figure 3.9. *Piezoelectric transformer constructed in a very narrow double poled ring*

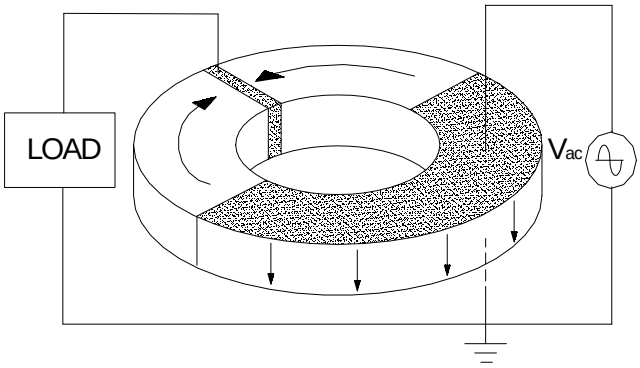

Figure 3.10. *Piezoelectric transformer constructed in a ring double poled*

3.3. Trend in the resonant transformer technology

Piezoelectric resonant transformers have some limitations that have led to intense work on improving their configurations. This limitations are discussed below:

1. *Modification of the resonant frequency due to the high "Q" of the material.* A problem encountered in the manufacture of piezoelectric transformers for certain electronic applications involves assuring that the transformer is driven at its resonant frequency. The *Q* property (*Q* is defined as the centre frequency divided by the bandwidth) of piezoelectric type transformers is extremely high compared to the *Q* values of electromagnetic transformers. Values of several hundred or more are not unusual for piezoelectric type transformers.

   Since high *Q* values are associated with narrow bandwidth, maintaining the resonant frequency for a piezoelectric type transformer (high *Q*) becomes considerably more difficult than maintaining the resonant frequency for a magnetic type transformer (low *Q*).

   In most applications, the transformer must be operated at or very near its resonant frequency. In some applications, frequency errors of less than 0.5% can be detrimental and render the transformer inoperable. Thus, the ability to track frequency through a voltage feedback can be of great importance for many applications. The ability to keep a transformer 'on frequency' may be necessary to assure the operation of the transformer.

   Unfortunately, there are many ways in which a transformer's resonant frequency may change during operation of the device. The resonant frequency of the piezoelectric transformer may be affected by many factors such as the output load variation, drive level, mounting technique, and temperature.

   For example, since a large amount of light is required for back-lighting a colour liquid crystal display, a cold cathode fluorescent lamp (abbreviated 'CFL' hereinafter) is ordinarily used as a light source. Since this CFL has a high impedance on the order of 100kΩ, a stray capacitance C_{st} is created between the CFL and a metallic reflecting plate provided in proximity of the CFL so as to cover the CFL. This stray capacitance C_{st} is parasitic in parallel to the CFL, and can be estimated to be on the order of 10pF for one CFL. Here, assuming that the first order mode frequency of the piezoelectric transformer is on the order of 100kHz, a synthesised impedance of the stray capacitance C_{st} and the CFL drops on the order of 61kΩ.

2. *The output of the piezoelectric transformer changes dependently upon a load impedance connected to the piezoelectric transformer*. Figure 3.11, illustrates an example of the output characteristics of the piezoelectric transformer discussed previously (Figure 3.2). As will be apparent from Figure 3.11, if the piezoelectric transformer is connected to a load having a high impedance in the order of 1MΩ, a high step-up ratio can be obtained, and therefore, a large output power can be achieved. On the other hand, if the impedance of the load connected to the piezoelectric transformer is not greater than 100kΩ the output greatly drops and the step-up ratio becomes not greater than 10.

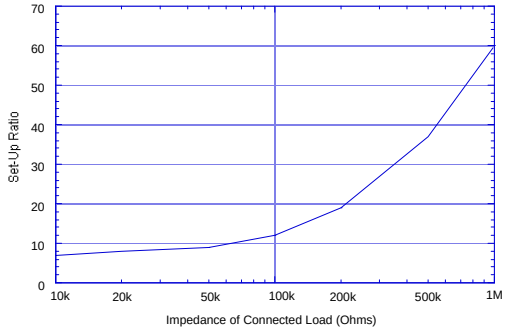

Figure 3.11. *Influence of the load in the ratio transformation*

Output impedance of the Piezoelectric Transformer

$$Z_{2,out} = \frac{1}{C_{d2} \cdot w} = \frac{1}{(1 - k_{33}^2) \cdot e_0 \cdot e_r \cdot \frac{W \cdot t}{L_{out}} \cdot 2p \cdot f}$$

C_{d2} = constrain capacitance of secondary side of piezoelectric transformer.
k_{33} = electromechanical coupling coefficient in a 33 polarisation direction of piezoelectric material.
ε_0 = vacuum permittivity
ε_r = relative permittivity of piezoelectric material
w = width of piezoelectric transformer
t = thickness of piezoelectric transformer
L_{out} = inter-electrode distance on of secondary side of piezoelectric transformer
f = driving frequency
ω = driving angular frequency

The load causing the output characteristics to start to abruptly elevate is called a matching load, where the piezoelectric transformer output impedance matches with the load impedance. Namely, in order to improve the output characteristics of the piezoelectric transformer, it is sufficient if the following relation is satisfied

output impedance < connected load impedance

In order to meet this requirement, it is necessary to reduce the piezoelectric transformer output impedance to prevent adverse influence due to the connected load.

In the present state, since an input voltage for the back-light inverter is on the order of DC 12V, the step-up ratio of the order of 10 times in entirely insufficient to obtain the output voltage on the order of 350V required to light-up the CFL. To solve this problem,

1. it could be considered to enlarge the input voltage of the piezoelectric transformer; or

2. to re-design the piezoelectric transformer, by taking for example a stacked system into a consideration.

In order to realise the first countermeasure (1), it is necessary to elevate the power of a voltage supply of an upper system of the back light inverter, for example, a personal computer, or to increase the number of step-up circuits provided before the piezoelectric transformer. However, the former approach is against a recent low voltage inclination in a field including an LSI (large scaled integrated circuit). The latter approach results in an increased number of parts and in a cost-up. In addition, the latter approach is against a down-sizing and thinning inclination of the inverter and hence the display, which should be realised for a down-sizing request for an overall system. Thus, the first countermeasure (1) will loss and industrial merit and therefore is not acceptable.

The second countermeasure (2) may be realised by stacking a required number of ceramic layers each having a film thickness on the order of a few 10μm. This is carried out by using of a green sheet method, so that it is possible to elevate an input electric field strength, whereby shortage of the set-up ratio is overcome and therefore a large output voltage can be obtained.

Several configurations which improves the stability of the resonant piezoelectric transformer have been proposed. Several companies have commercialised piezoelectric transformers incorporating feedback control and novel designs, such as NEC Corporation [5,6,7], Philips Components [3], Matsushita Electric Industrial Co., Murata Manuf. Co. Ltd [8], etc. As a particular example, Figure 3.15 shows one configuration patented by Motorola Inc. [9].

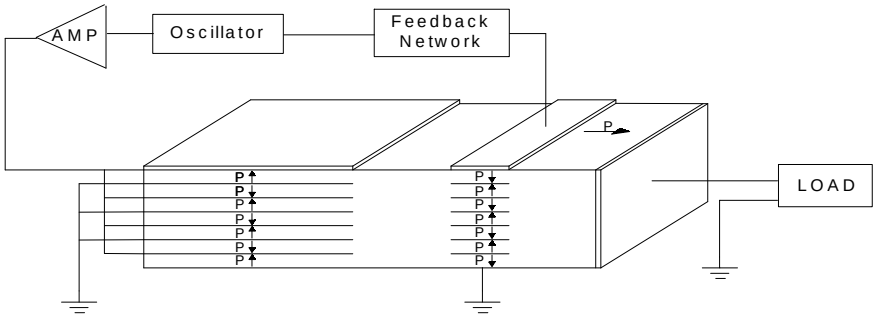

Figure 3.12. *Stack Piezoelectric Transformer (Motorola Inc.* [9]*)*

3.4. Resonant transformers for measuring. Limitations and Conclusions

After reviewing the characteristics of the Resonant Transformers, their applicability as a measuring device is analysed in the following section. In particular the possibility to operate as an instrument transformer is considered.

Some of the requirements demanding for a reliable measure transducer have been previously commented as:

1. Capability to reduce the primary electrical magnitude to very low levels for driving the secondary protection and measuring systems

2. Capacity to dielectrically separate the primary and the secondary circuits, guaranty safety for the personal in charge and for the systems connected to the secondary.

3. To have a very accurate transformer ratio between the primary and secondary levels, also in a wide frequency band.

Resonant Piezoelectric Transformers reviewed in this chapter may be initially considered to be applied for measuring and protecting applications. It is apparent that it should be sufficient to change the driving and driven electrodes in the Rosen-type transformer (Figure 3.2) in order to output a low voltage by inputting a high voltage.

However, in spite of a reduction of the primary voltage is possible, there are other several aspects which limit the use of the Resonant-type Piezoelectric Transformers for measuring applications, such as:

1. In the high voltage measurements, the main frequency of the electrical magnitudes to be measured is 50Hz (or 60 Hz in USA). This frequency is very low to excite the piezoelectric material in its resonance and very big dimensions should be necessaries.

2. The resonant piezoelectric transformer is a narrow band transformer and may only operate very close to their resonant frequencies. This make impossible the measurements of signals with harmonics so they requiere a wide band operation transducer.

3. Accuracy is the main feature in measurement fields. This is not provided when the piezoelectric materials are working in resonance as previously mentioned.

The above considerations limit the application of a Resonant Piezoelectric Transformers for the measuring field.

A more reliable technology for being adapted to measurement would be the *Non-Resonant*. Non-Resonant devices offer interesting properties for applications requiring high precision as is the case of the measuring field (see Table 3.2), such as accuracy and wide frequency band.

Within the technical literature there are no descriptions about Non-Resonant Transformers. This kind of device basically should work under the same principle that the Resonant Transformer, i.e. an electrical to electrical conversion between an inputting and an outputting signal.

One of the aims of the present Thesis is to develop Non-Resonant structures for being apply as Instrument Transformer. Following Table 3.2. summarises the properties of the Resonant and Non-Resonant Transformers and their possibilities of being apply as Instrument Transformers.

Table 3.2. *Comparison of the properties of the Resonant and Non-Resonant piezoelectric technologies and their aptitudes for measuring.*

	Resonant Piezoelectric Technology	Non-Resonant Piezoelectric Technology
General Properties	Excellent energetic efficiencies	Low energetic efficiency
	High transformer ratios (in the meaning of high mechanical or electrical output magnitudes)	Low transformation ratios
	Narrow frequency band operation	Wide frequency band operation
	Low accuracy and low linearity due to the low stability of the transformer ratio in the resonance range	High accuracy and linearity. The transformer ratio is non-frequency dependent (in the linear range).
Applicability as Instrument Transformer	The instabilities of the Resonant devices make this devices not applicable when a high accuracy want to be obtained.	Non-resonant devices are useful in applications where a high accuracy in demanding. Moreover they offer a wide band frequency and a natural step-down response.
General Applications	Applications are in the field of high voltage power supply in TV sets, where a certain variation in the output voltage is allowed since a breakdown voltage is the objective.	Two types of wide applications use this kind of technology: Actuators devices and Sensor devices.

3.5. References

[1] United States patent 2,830,274. *Electromechanical Transducer*, Charles A. Rosen, east Syracuse, Keith A. Fish, Baldwinsville, and Herbert C. Rothenbert, De Witt, N.Y., assignors to General Electrical Company. Apr. 8, 1858.

[2] U.S. application, Serial Number 401, 812, *Electromechanical Transducer*, in the name of Charles A. Rosen and Keith Fish, and assigned to the General Electrical Company, filed January 4, 1954.

[3] Application Note, *Piezoelectric Transformers*, Philips Components, 1996.

[4] Kenji Uchino, Piezoelectric Actuators and Ultrasonic Motors, Kluwer Academic Publisher, Massachusetts, USA, 1997.

[5] United States Patent US5118982, *Thickness mode vibration piezoelectric transformer,* Takeshi Inoue, Osamu Ohnishi, Nobuo Ohde, asignee to NEC Corporation, Japan, Jun 1992

[6] United States Patent US5241236, *Piezoelectric Ceramic Transformer Being Driven with Thickness extensional Vibration,* Yasuhiro Sasaki, Kaneo Uehara, Takeshi Inoue, asignee to NEC Corporation, Japan, Aug. 1993

[7] European Patent Application EP0706227, *Piezoelectric transformer having high conversion efficiency,* Tagami Saturo, asignee to NEC Corporation, Japan, Apr. 1996

[8] United States Patent US5903086, *Piezoelectric transformer*, Koji Ogiso, Akira Ando, assignee to Murata Manufacturing Co. Ltd. (Japan), May 1999

[9] United States Patent US5872419, *Piezoelectric transformer with voltage feedback*, Hall dale G., Mech Harold W., Vaughn Gary L., Forst Donald, Phillips James R., assignee to Motorola Inc. (USA), Feb. 1999

Chapter 4

First Experiences on ‘Non-Resonant Instrument Piezo-Transformers’

4 First Experiences on 'Non-Resonant Instrument Piezo-Transformers'

4.1. Introduction

In 1994, under the context of a Final Degree Project [1], it was started at the Universitat Politècnica de Catalunya (UPC), Spain, an intense research work in the field of novel structures for instrument transformers. The work took advantage of the background on piezoelectricity and piezoelectric resonant transformers achieved by the staff at the laboratory thanks to a previous Thesis developed by Dr. J.Álvarez in 1990 [2].

In his Thesis, Dr. Álvarez developed a system to convert electrical energy into energy by using the properties of the piezoelectric materials working in resonance. The developed device operated as a set-up transformer of very low frequency wide band, as a result of its resonance. The device was successfully applied in the ignition of internal combustion engines.

Nevertheless, and as it has already mentioned in Chapter 3 (and it will be analysed in this Chapter again), resonant piezoelectric devices were shown inappropriate for accurate devices such as those destined to measurements. Consequently, the research was concentrated on *Non-Resonant* structures.

This chapter introduces the first work performed on the development of 'Non-Resonant Piezoelectric' structures for being applied in the field of the instrument transformers. Three different structures were purposed:

(1) *The free displacement column*

(2) *The single blocking column*

(3) *The two-blocked* (or actuator-sensor) *columns*.

Two experimental prototypes were constructed and experimentally tested to verify the behaviour of the different configurations. The theoretical approaches and the experimental results obtained are gathered along this chapter.

The two-blocked columns structure was finally concluded as the most reliable for being apply to instrument transformers. Different types of configurations are described as alternatives to be used for a definitive prototype.

4.2. Resonance and Non-Resonance in Piezoelectric transducers

Dynamic behaviour of piezoelectric transducers may be regarded in a first approximation (Figure 4.1) as *weakly damped linear oscillators* (a spring mass systems with a single degree of freedom). An oscillator of this kind is modelled by the classical second order differential equation:

$$m \cdot \frac{d^2x}{dt^2} + R \cdot \frac{dx}{dt} + k \cdot x = F(x,t) \qquad (4.1)$$

where R = damping constant of the piezoelectric transducer, m = mass of the parts joined rigidly to the piezoelectric and the resonating mass of the material, k = spring characteristic of the piezoelectric element. $F(x,t)$ is the force vibration of the damped system generated when an a.c. voltage is applied to the metallic electrodes of the transducer.

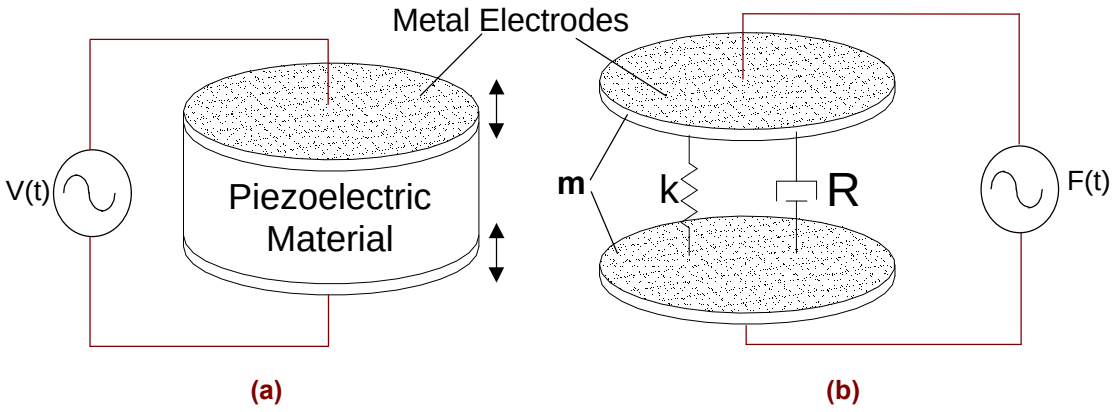

Figure 4.1. *(a) Piezoelectric transducer excited by a.c. voltage and (b) its mechanical model*

If this weakly damped oscillator is excited once and then left to itself (Figure 4.2), it performs a dying out oscillation with a natural angular frequency w_n in accordance with:

$$x = A \cdot \exp(-d \cdot t) \cdot \cos(w_n \cdot t - j) \qquad (4.2)$$

where $d = \frac{R}{2 \cdot m}$ is the dying out constant. The *degree of damping* x result from the relation:

$$x = \frac{d}{w_0} = \frac{R}{2 \cdot m \cdot w_0} \qquad (4.3)$$

where $\omega_0 = 2\pi f_0 = \sqrt{s / m}$ is the characteristic angular frequency of the undamped oscillator with the same storage characteristics m and s (calculated value).

The natural angular frequency $\omega_n = 2\pi f_n$ of the weakly damped oscillator is always somewhat lower than the characteristic angular frequency w_0 due to the damping effects. It amounts to:

$$w_n = w_0 \cdot \sqrt{1 - x^2} \qquad (4.4)$$

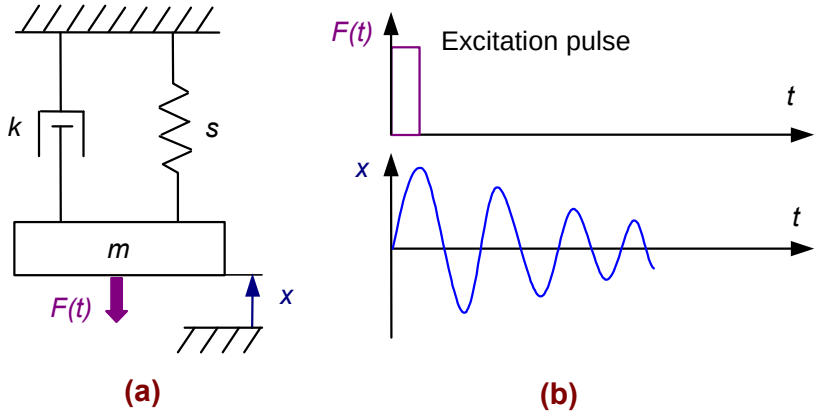

Figure 4.2. *Damped mechanical oscillatory system as equivalent diagram for a piezoelectric material*

When the system is excited artificially, the amplitude and phase of the output signal are function of the frequency, changing as soon as the natural frequency is approached or exceeded. According to the familiar equations from vibration theory, the amplitude x in relation to the value x_o is:

$$\frac{x}{x_0} = \frac{1}{\sqrt{\left(1-\left(\frac{w}{w_n}\right)^2\right)^2 + \left(2\cdot x\cdot\frac{w}{w_n}\right)^2}} \tag{4.5}$$

with x_o = amplitude in frequency range $f<<f_n$. Instead of w_o, w_n has been inserted, this is admissible with weak damping ($\xi<<1$), since according to equation (4.4) $\omega_n \approx \omega_o$.

The resonance step-up x_{max}/x_o is reached at the resonant angular frequency w_{max}:

$$w_{max} = w_o \cdot \sqrt{1-2x^2} \tag{4.6}$$

In general the damping of a piezoelectric transducer is indicated by means of the *Q-factor*, which indicates the sharpness of the resonance. The Q-factor of a ceramic piezoelectric material is in the order of 100 – 800. For quartz transducers, this factor is around 10^4 -10^6. The Q-factor may be obtained from the damping factor as:

$$Q = \frac{w_0 \cdot m}{R} = \frac{1}{2\cdot x} \tag{4.7}$$

Thus, the transfer function (equation (4.5)) can be expressed as:

$$G(w) = \frac{x}{x_0} = \frac{1}{\sqrt{\left(1-\left(\frac{w}{w_n}\right)^2\right)^2 + \left(\frac{1}{Q}\cdot\frac{w}{w_n}\right)^2}} \tag{4.8}$$

Figure 4.3. shown a typical resonance curve where it has been drawn the relative increase of the displacement of the system in reference with the initial x_0 displacement far below its resonance.

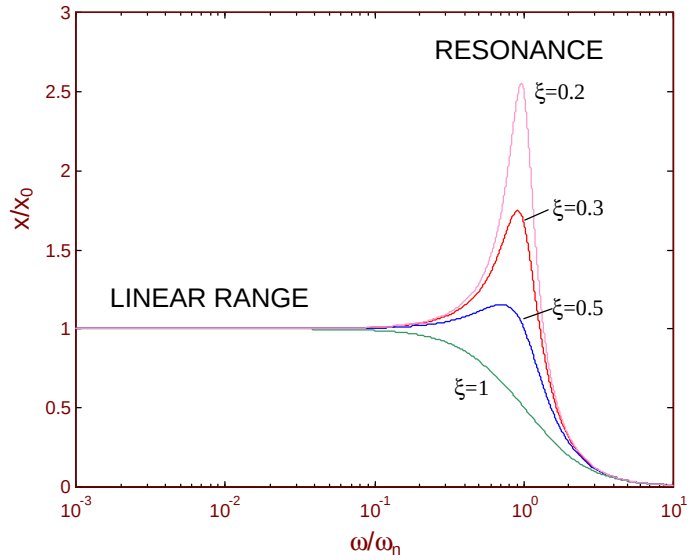

Figure 4.3. *Frequency response $x/x_o = f(w/w_n)$ with degree of damping x as parameter.*

The phase of the output signal lags behind the phase of the excitation by j, whereby (Figure 4.4)

$$\tan j = \frac{2x\,\frac{w}{w_n}}{1-\left(\frac{w}{w_n}\right)^2} \tag{4.9}$$

In Figure 4.4. is illustrated the modification of the phase for a damped system, with different levels of damping.

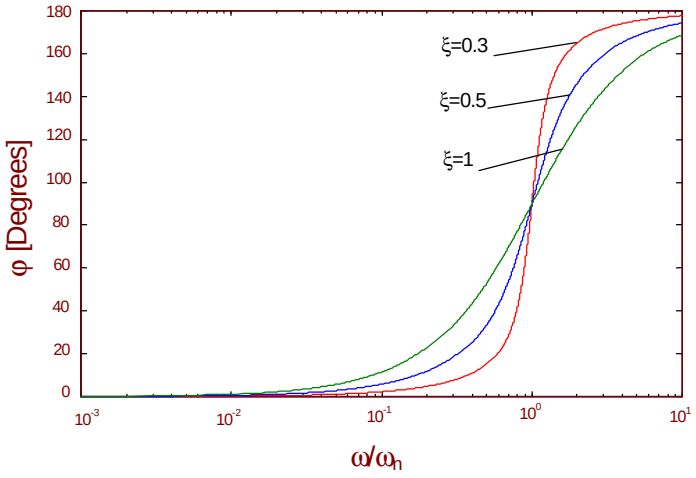

Figure 4.4. *Phase angle $j = f(w/w_n)$ with degree of damping x as parameter.*

• Operation Modes of a Piezoelectric Transducer

From Figures 4.3-4.4 two different operations for a piezoelectric transducer can be observed depending on the frequency of the driving signal.

1. *Resonant Piezoelectric Devices*, when the driving electrical signal excites one of the modes of vibration of the piezoelectric body. As it has been previously commented (Chapter 3), these devices are characterised by:

   Advantages:

   - Excellent energetic efficiencies
   - High transformation ratios (in the meaning of high mechanical or electrical output magnitudes).

   Disadvantages:

   - Narrow frequency band device
   - Low accuracy and low linearity because of low stability of transformation ratio in the resonance range.

   Applications are in the field of high voltage power supply in TV sets, where a certain variation in the output voltage is allowed since a breakdown voltage is the objective.

2. *Non-Resonant Piezoelectric Devices*, when the driving electrical signal has a frequency very far from the fundamental vibration mode. These kind of devices are characterised by:

   Advantages:

   - High accuracy and linearity.
   - Transformation ratio non frequency-dependent (in the linear range).
   - Wide frequency band operation.

   Disadvantages:

   - Low efficiency transformation
   - Low transformation ratios

   Applications will take advantage of the linearity between input and output. This may be interesting in the field of instrument transformers, where both a high step down transformation and a high accuracy are required.

In general, resonant piezoelectric devices are very efficient but with poor accuracy. In contrast, non-resonant piezoelectric devices are very accurate, offer a natural step down response and have a wide frequency band. These properties of the non-resonant made them adequate for applications requiring high accuracy, as is the case of the instrument transformers.

This properties will exploited in the following sections to develop some structures of Non-Resonant devices for being used for measurement applications.

4.3. Start Point in the construction of an instrument piezoelectric transformer: A free displacement column

4.3.1. Operation Principle

Let us consider a column built by piling up piezoelectric discs, each of them characterised by their mechanical, electrical and piezoelectric properties in the poling direction (3-axis), which is taken as the working direction of the system. These properties are summarised below:

- Density of the material: r [kg/m^3]
- Strain piezoelectric coefficient: d_{33} [C/N]=[m/V]
- Relative permittivity: e_{33} [F/m]
- Mechanical compliance: s_{33} [m^2/N]

If such a piezoelectric column is driven by a sinusoidal electric voltage at 50Hz, the discs will start to vibrate. If the poling vectors of each disc are aligned in the same direction, all the discs of the column will displace in compression and tension in unison. Considering that this frequency is far below the first resonance (then, working in the linear range), the mechanical longitudinal strain of the column will be proportional to the applied voltage and with its same frequency (50Hz).

In the particular case that the column is fixed in one end and unloaded in the other end, the free strain of the column is estimated by using the linear relationship for the converse piezoelectric effect, indicated in equation (4.10). This configuration is named as *Free Displacement Column* and is illustrated in Figure 4.5.

$$S_3(t) = \frac{\Delta L}{L} = d_{33} \cdot E_z(t) = d_{33} \cdot E_{z,max} \cdot cos(w \cdot t) \qquad (4.10)$$

The free elongation in the x or y direction (for the transversal effect) can also be calculated as

$$S_1(t) = S_2(t) = \frac{\Delta x}{x_O} = \left(\frac{\Delta y}{y_O}\right) = d_{31} \cdot E_z(t) \qquad (4.11)$$

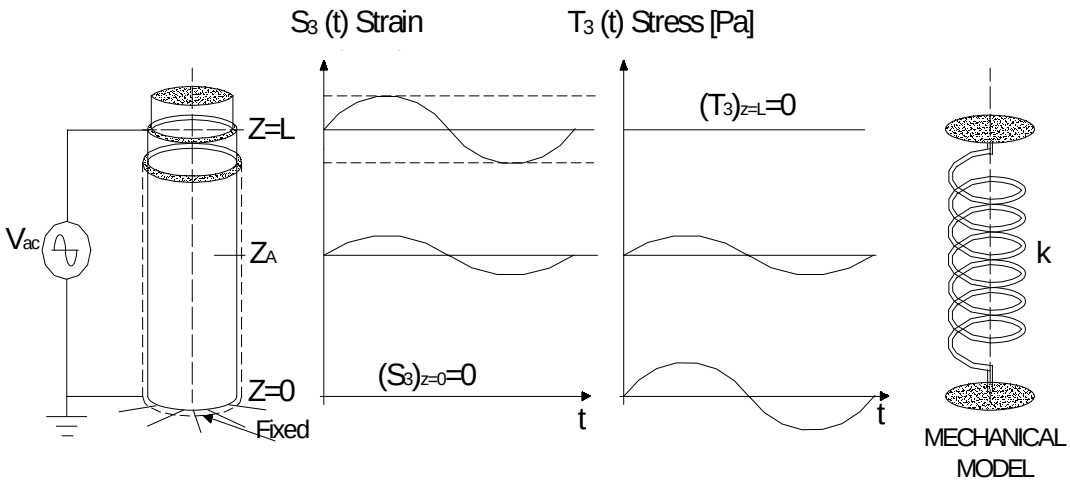

Figure 4.5. *Piezoelectric column operating in Free Displacement Mode*

Figure 4.5 shows both the longitudinal stress and the longitudinal strain in the material. In the free end of the column, the stress T_3 will be zero while the strain S_3 will be maximum (4.10), if it is supposed that there is no air-resistance. In the fixed point, the stress T_3 will be maximum and the strain S_3 will be zero:

Free End: $T_3 = 0$ $S_3(t) = d_{33} \cdot E_{z,max}(t)$

Fixed End: $T_{3,\text{fixed end}}(t) = \frac{d_{33}}{s_{33}^E} \cdot E_3(t)$ $S_3 = 0$ (4.12)

In particular, for a certain point A of the column, strain and stress will be related by the piezoelectric constitutive equation (4.13):

$$S_{3,Point\ z_A}(t) = s_{33}^E \cdot T_{3,Point\ z_A}(t) + d_{33} \cdot E_{3,Point\ z_A}(t) \tag{4.13}$$

Hence, if the possible hysteresis of the piezoelectric material is ignored, the free strain generated at the free end of the column may be used as a good accurate measure of the high voltage applied.

4.3.2. Measuring the Free Displacement

The strain is not of a magnitude useful to activate a mechanic or electronic measuring device and it is necessary to convert it back, for example, into a mechanical force or into an electrical signal.

With this purpose, different techniques for strain measurements are available, such as resistance strain gauges, linear variable differential transformers (LVDT), optical sensors, spring-based sensors, etc. [3,4,5].

Figures 4.6 to 4.8 illustrates some techniques used for the measurement of the free displacement. These techniques do not modify the magnitude to be measured, thereby they are so-called as no-invading. In general, they use passive sensors which require an input power energy to perform the measurement. Figure 4.6 purposes the measure of the strain by using the variation of a voltage influenced for the characteristic of a electrical resistance gauge join in the piezoelectric column. In Figure 4.7 the measurement of the strain is performed by using the modification of the inductance in a coin were a high frequency current is driven. Figure 4.8 uses a optical sensor for measuring the strain.

Figures 4.9 and 4.10 illustrate two systems based in the measurement of the deformation of a secondary calibrated structure (such as a spring or a stainless steel structure). This techniques, however, modify the displacement to be measured. They measure the force developed for the system.

NO-INVADING TECHNIQUES FOR MEASURING THE FREE-DISPLACEMENT

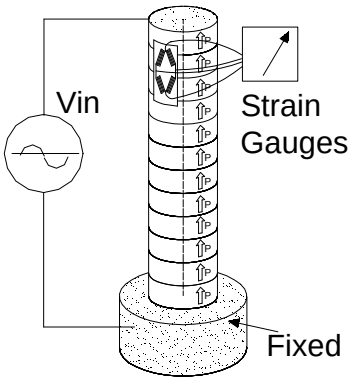

Figure 4.6. *A strain gauge allows the free-displacement. The strain gauge converts the stress into an electrical signal.*

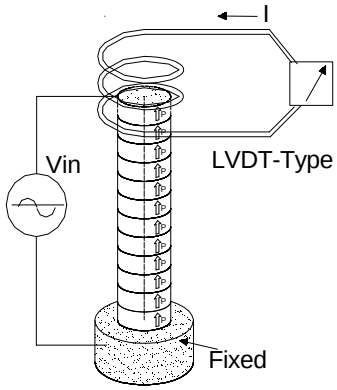

Figure 4.7. *The modification of the inductance in a coil excited at 112kHz when a cylinder of aluminium (placed at the end of the piezoelectric column) vibrates, allows the measure of the free displacement.*

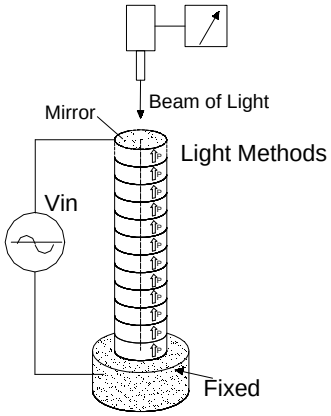

Figure 4.8. *The use of techniques based on the light is another alternative for an accurate measurement of the free displacement. However, this technique is very costly.*

INVADING TECHNIQUES. THEY CONVERT THE DISPLACEMENT IN A PROPORTIONAL FORCE. HOWEVER THEY MODIFY THE REAL DISPLACEMENT IN FREE CONDITIONS

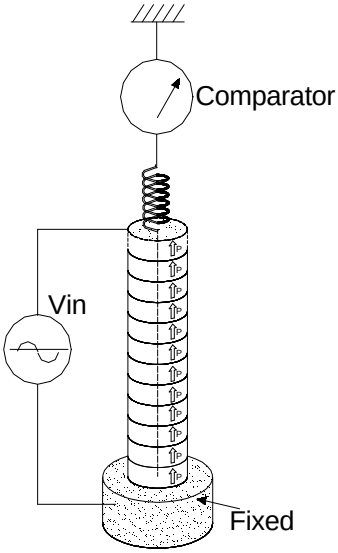

Figure 4.9. *A spring-based device converts the deformation of the column into a movement in the needle. However, the spring introduces an opposite force $F=F_{spring}\,x$, which modifies the free displacement state.*

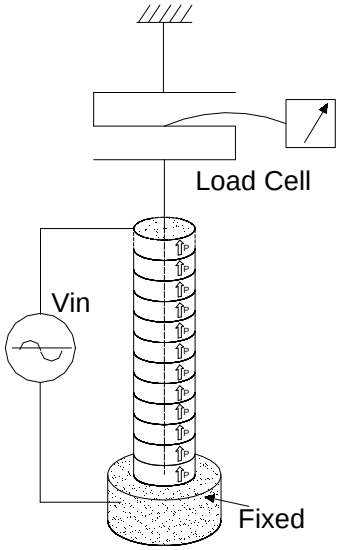

Figure 4.10. *A load cell uses the deformation of a calibrated structure to excite an internally placed strain gauge and to obtain an electrical signal proportional to the deformation. However, the displacement of the column is converted into a deformation force, and the free displacement is modified.*

4.3.3. Evaluation

The use of the Free Displacement Structure as instrument transformer, leads to important difficulties regarding to mechanical stability of the column, fatigue and depoling problems. These problems appear when no-invading techniques are used in the secondary sensor because it is necessary to keep the secondary end without fixation, i.e. totally free, as is commented below:

No-Invading Techniques

- The electrical connection of the high voltage electrode in the free end is complicated if the hypothesis of free displacement must be guaranteed.

- A very long piezoelectric column fixed in only one end will be very unstable, more when this kind of column is built by stacking individual discs, as will be commented upon later. For instance, if horizontal operation is required, an important fatigue in the column will appear.

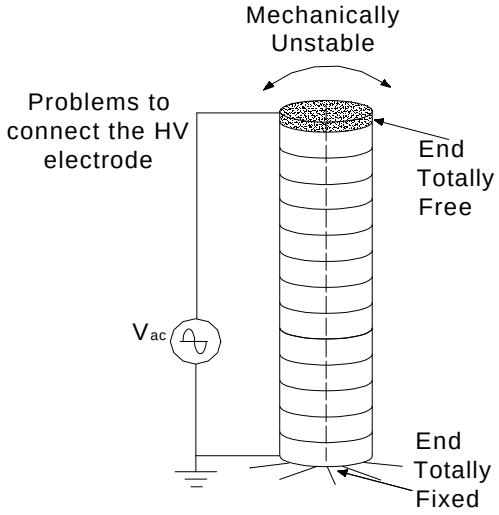

Figure 4.11. *Application of the free displacement configuration is limited due to dimensional instability and electrodes connection.*

- In free displacement the column is not under prestress. This will introduce coupling problem between discs and mechanical fatigue (and probably depoling) in the column. This will be discussed in Chapter 5.

To overcome these problems, one alternative is to use the previously mentioned Invading Techniques as secondary sensor. However, this introduce other difficulties:

- The free displacement structure is totally changed for a partially limited structure, and equations (4.10) to (4.13) are not valid any more.

- Furthermore, the use of spring-based sensors or load cells is limited a very low frequencies and limited operation cycles, due to mechanical fatigue.

The above mentioned difficulties can be surmounted (1) by using a structure where displacement are limited (no mechanical fatigue) and (2) by incorporating a sensor with capability to operate in a very high frequency range and during long operation cycles. The next section approachs this matter.

4.4. Single blocking piezoelectric column

4.4.1. Operation Principle

A *single blocking piezoelectric column* is defined as a column of piezoelectric material fixed between two perfectly rigid pieces. In this situation strain of the column is completely limited. Figure 4.12 shows a piezoelectric blocking column fixed between two conductive pieces. These pieces actuate at the same time as blocking pieces and as electrodes for driving the input voltage.

Piezoelectric column can be constructed by a single piece of material (*bulk column*) or by piling up different pieces of the same material with less thickness (*stacked column*), as is shown in Figure 4.12. The use of a single piece of material is limited to thin actuators, while piling up individual disc is the solution when a certain required length is necessary.

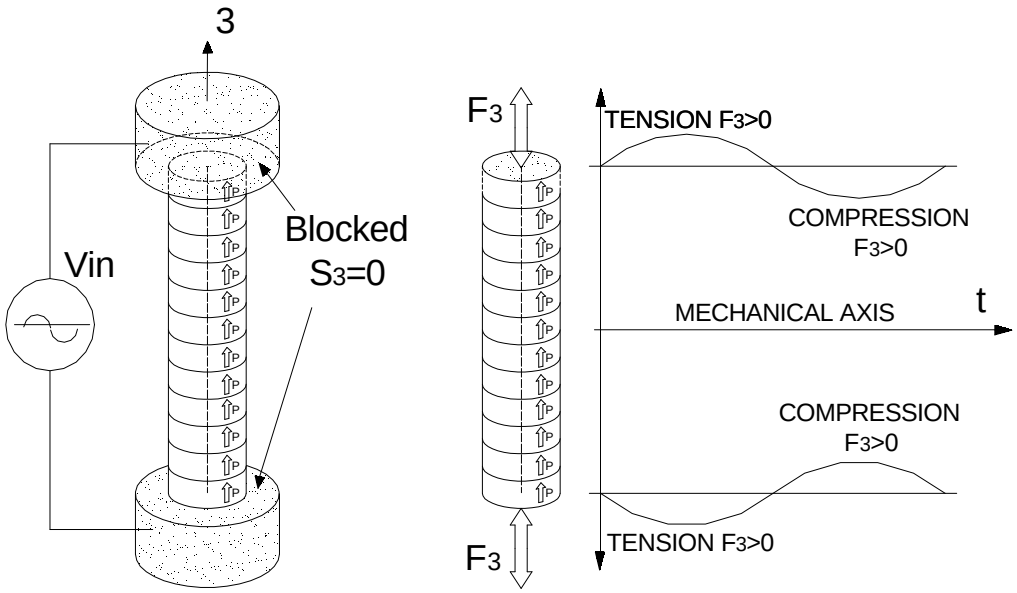

Figure 4.12. *Blocking piezoelectric column*

If in this condition an electric voltage is applied to the external electrodes, a force will appear in both ends of the blocked column. This force may be calculated by considering the condition of null longitudinal deformation, $S_3 = 0$, in all the column, as indicated equation (4.14)

$$T_3(t) = \frac{d_{33}}{s_{33}^E} \cdot E_3(t) \tag{4.14}$$

$$F_{3,Blocked}(t) = \frac{d_{33}}{s_{33}^E} \cdot \frac{A}{t} \cdot V_{in}(t) \tag{4.15}$$

Equations 4.14 and 4.15 show that stress and force developed by the column are proportional to the driving voltage V_{in}. In this way, force generated may be used as a means for measuring voltages.

4.4.2. Measuring the blocking force (secondary sensor)

In order to convert back the force generated into a useful electric signal which could drive the measurement devices, a force sensor is required. Nevertheless, the measurement of *blocking force* requires a very stiff sensor which guarantees that deformations are not introduced in the set-up. The best force sensors for measuring blocking force are the *piezoelectric sensors* (see Appendix 2).

Of course, the piezoelectric sensor has to be placed mechanically matched with the piezoelectric column which generates the force. With this consideration, the initial idea was to use one of the discs belonging to the column operating as a sensor. Since both, the column which converts the electric input voltage to force and the sensor which converts it back into an electric signal belong to the same piezoelectric structure, this configuration was named the *Single-Column Piezoelectric Transformer* (see section 4.4). Figure 4.13 illustrates this idea.

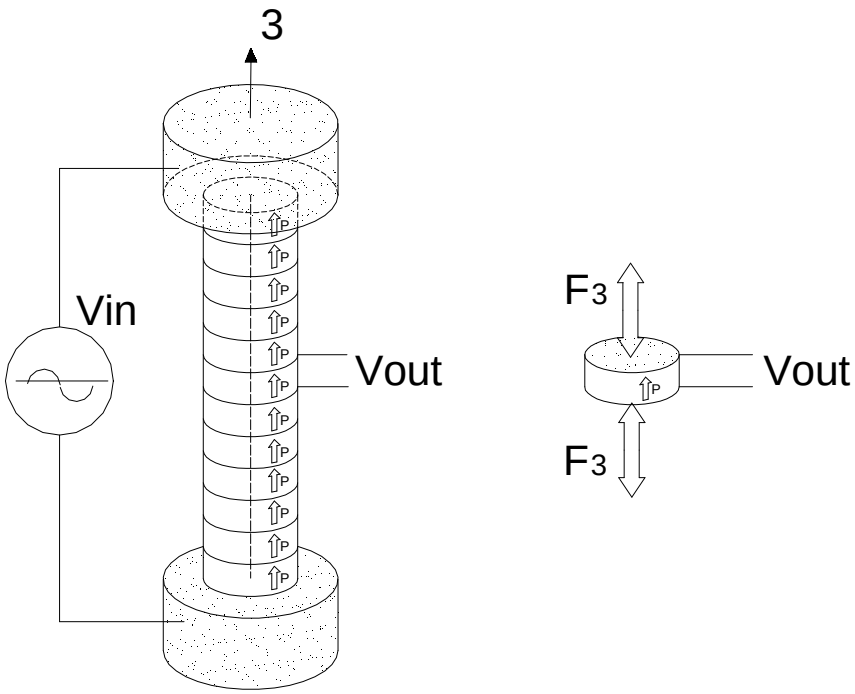

Figure 4.13. *'Single-Column Piezoelectric Transformer': A piezoelectric force sensor is used for converting the blocking force in an electrical signal.*

In this way, if an alternating driving voltage is applied to the column, a periodical force in each of the discs of the column will appear. Equation (4.15), previously indicated, provides the mathematical expression for this force. In particular, the *sensor disc* experiments this force in their both sides and will produce an electric charge, *Q*. If this electric charge is measured under open circuit conditions (see Appendix 1) an equivalent open circuit voltage will be obtained (depending on the capacitance of the piezoelectric material). The relationship between the voltage obtained and the force generated by the column is given in equation (4.16):

$$V_{output}(t) = -F_{3,Blocking}(t) \cdot g_{33,Sensor} \cdot \frac{t_{Sensor}}{A_{Sensor}} \qquad (4.16)$$

Substituting the value of $F_{3,Blocking}(t)$ obtained in expression (4.15), and solving for the transformation ratio V_{output}/V_{input}, we obtain:

$$V_{output}(t) = -\frac{d_{33} \cdot g_{33}}{s_{33}^{E}} \cdot \frac{t}{L} \cdot V_{input}(t) = -\frac{d_{33}^{2}}{\varepsilon_{33}^{T} \cdot s_{33}^{E}} \cdot \frac{t}{L} \cdot V_{input} = -k_{33}^{2} \cdot \frac{t}{L} \cdot V_{input} \quad (4.17)$$

$$r_t = \frac{V_{input}}{V_{output}} = -\frac{1}{k_{33}^{2}} \cdot \frac{L}{t} \quad (4.18)$$

In the previous equation (4.18) for r_t, the piezoelectric column has been assumed to be composed with all the disc of the same material (homogeneous). Otherwise, the piezoelectric coefficients d_{33}, e_{33}^{T}, s_{33}^{E} should be evaluated for each type of piezoelectric material.

In the next section the previous theoretical discussion is practically implemented in an experimental prototype, PIEZOTRF1, of non-resonant piezoelectric transformer.

4.5. Prototype of single-column piezoelectric transformer: PIEZOTRF1

4.5.1. Design criterions

PIEZOTRF1 represents the first experimental prototype of a piezoelectric device for measuring high voltages. It uses the non-resonant characteristics of a piezoelectric stacked column working in blocking configuration.

The main goal of the PIEZOTRF1 design was to obtain a versatile configuration which allowed one to test a variety of parameters, such as the input/output transformation ratio, the type of material used, and the influence of the applied static prestress.

From an engineering point of view, the prototype was dielectrically dimensioned to withstand high electric voltages up to 170kV, which is the standard lighting test for 36kV-type instrument transformer (see Table 1.5, Chapter 1). Mechanically, the prototype was dimensioned to withstand forces of 60N/kV, which were estimated as the maximum for the blocking situation from equation (4.15).

4.5.2. Prototype construction

PIEZOTRF1 prototype consists of a central piezoelectric body and an external dielectric housing molded with epoxy resin. The construction process was divided in two stages: (i) Construction of the piezoelectric body, (ii) Injection of epoxy resin to provide the dielectric housing.

The piezoelectric body is the *active* part of the device. It is constructed by piling up single piezoelectric discs. The number of discs required was determined by considering the depolarisation resistance of the piezoelectric material and the maximum electric field to be applied. The design rule is indicated in equation (4.19), and it is based in the consideration that the electric field is homogeneously distributed along the column. Under this supposition, every disc should withstand the same electric field strength ($E=V_{in}/L$).

$$E_{max} < E_{depolarisation} \qquad L > \frac{E_{max}}{E_{depolarisation}} \quad (4.19)$$

where E_{max} is the maximum expected electric field to be applied, $E_{depolarisation}$ is the maximum electric field that the piezoelectric material can withstand and L is the calculated necessary length.

In the design of the PIEZOTRF1, a maximum electric voltage of 170kV was considered, which corresponds with the voltage for the lightning test demanding for the instrument voltage standards (see Chapter 1, Table 1.5). The maximum depolarisation field for the used piezoelectric material, PXE-41, is 1000V/mm. Consequently, the length of the column should be:

$$L > \frac{170\text{kV}}{1\text{kV/mm}} = 170\text{mm} \tag{4.20}$$

PXE-41, from Philips Components, is a ***hard-type*** piezoelectric ceramic material. This means that the material has a high resistance against the depolarisation compared to soft materials, which have a depolarisation resistance of only 300-500 V/mm (see Chapter 5). Discs of 10mm of PXE-41 were, thus, chosen for constructing the piezoelectric column. These discs were the thicker available from Philips Components. The diameter was chosen as 25.4mm. Hence, the number of required discs, N, was:

$$N > \frac{L}{t} = \frac{170\,\text{mm}}{10\,\text{mm}} = 17\ \text{disc} \tag{4.21}$$

Although initially the design of the column was planed to be performed with a completally homogeneous column (18 disc of PXE-41), finally it was decided to incorporate a second type of material (PXE-5) which permitted the evaluation of the influence of the piezoelectric properties in the transformation ratio (Figure 4.14).

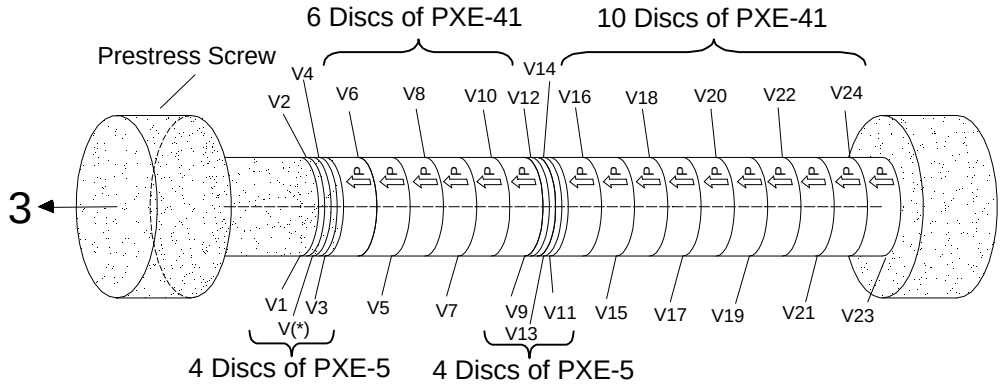

Figure 4.14. *The column was built with two types of piezoelectric materials disposed in 4 zones.*

Thus, PIEZOTRF1 was built by stacking 24 piezoelectric discs of two types of materials. 16 discs of PXE-41 of 10mm thickness and 25.4mm diameter were used to make the main body of the column and two groups of 4 discs of PXE-5 of 2mm thickness and 25.4mm diameter were strategically distributed in two regions of the column.

The disposition of the discs was divided in 4 zones, as illustrated Figure 4.14:

- A homogeneous zone with 10 discs of PXE-41
- A homogeneous column of 6 discs of PXE-41
- Two homogeneous columns of 4 discs of PXE-5

Definitive arrangement of the discs is displayed in Figure 4.15 where the two different materials used can be seen, the PXE41 in a dark colour and the PXE5 in light colour. Also, it is shown the two regions where the PXE5 discs were placed.

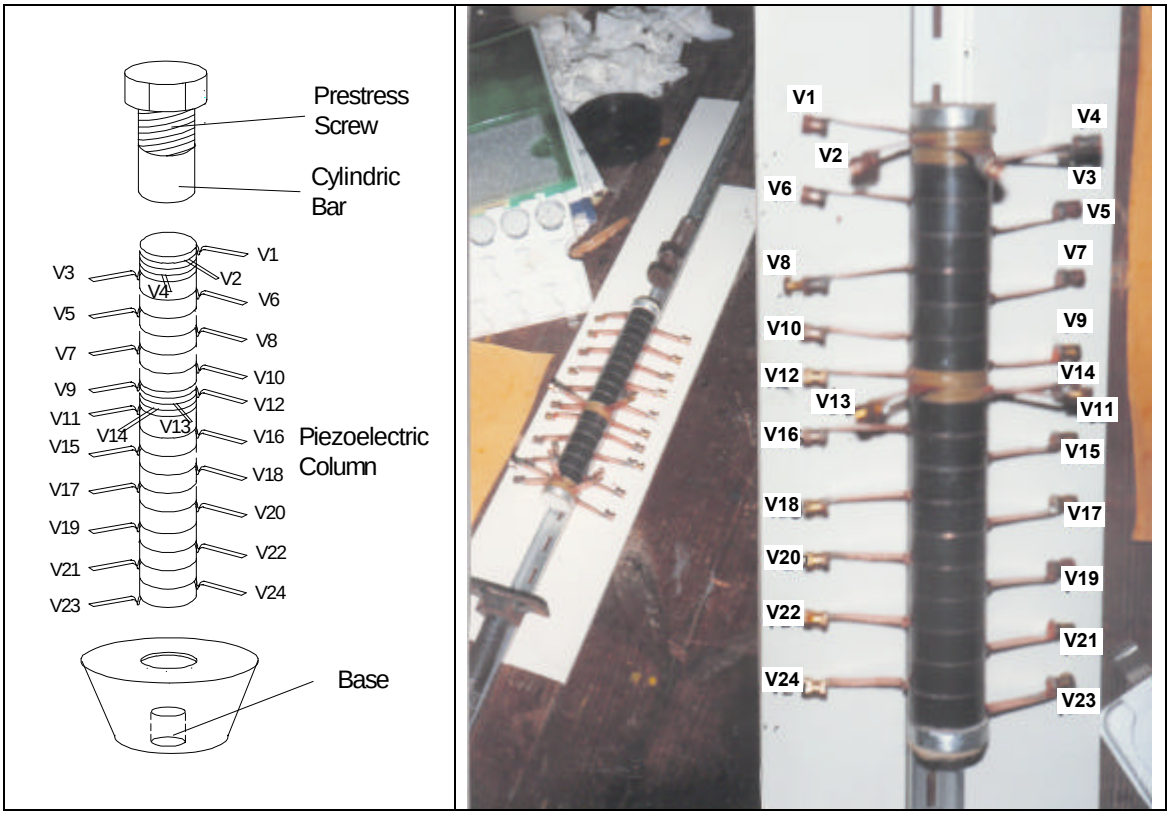

Figure 4.15. *Construction of the piezoelectric column. View of the two materials used.*

The discs were piled up by aligning the polarisation vector of each of them in the same direction. A thin sheet of cooper of 200μm thickness was intercalated between each disc to provide a complete versatility in the selection of the input and output configuration. Figure 4.15 shows a detail of the stacking process.

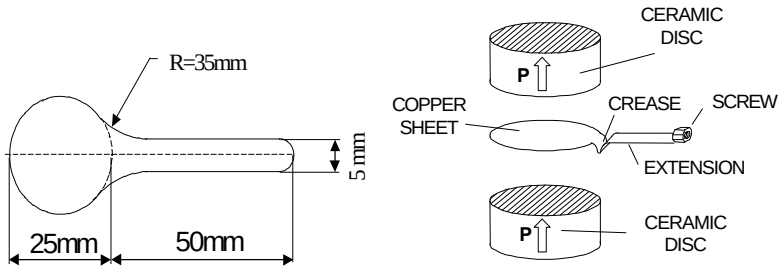

Figure 4.16. *Process of piling up the discs. Attention has to be paid to the polarisation vector.*

The column was recovered with a tape of fibre-glass and a silicone cushion to provide its dimensional stability (Figure 4.17).

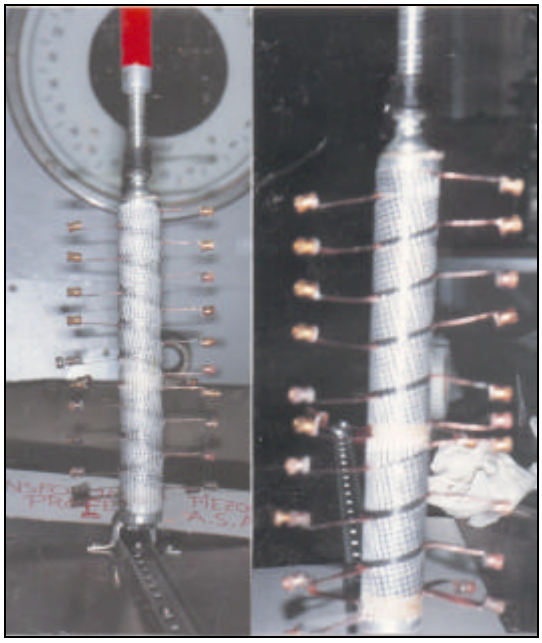

Figure 4.17. *View of the piezoelectric column prepared to be molded in epoxy.*

The column was subjected to a special treatment to provide it of an external dielectric housing of epoxy resin. Procedure consisted in the injection of a silica filled epoxy resin material in a special mould used in the construction of high voltage insulators. Once the resin is injected the mould is subjected to a thermal procedure rising the temperature until 150ºC. The molded process was carried out with the know-how of Laboratorio Electrotécnico, s.c.c.l., a qualified Spanish company having wide experience in the field of insulators and dry-type resin cast instrument transformers.

Figure 4.18 displays a view of the embodiment once the construction process finished. it is remarkable to indicate the existence of a preload screw in one of the ends of the column and the external electrodes for inputting and outputting the voltage.

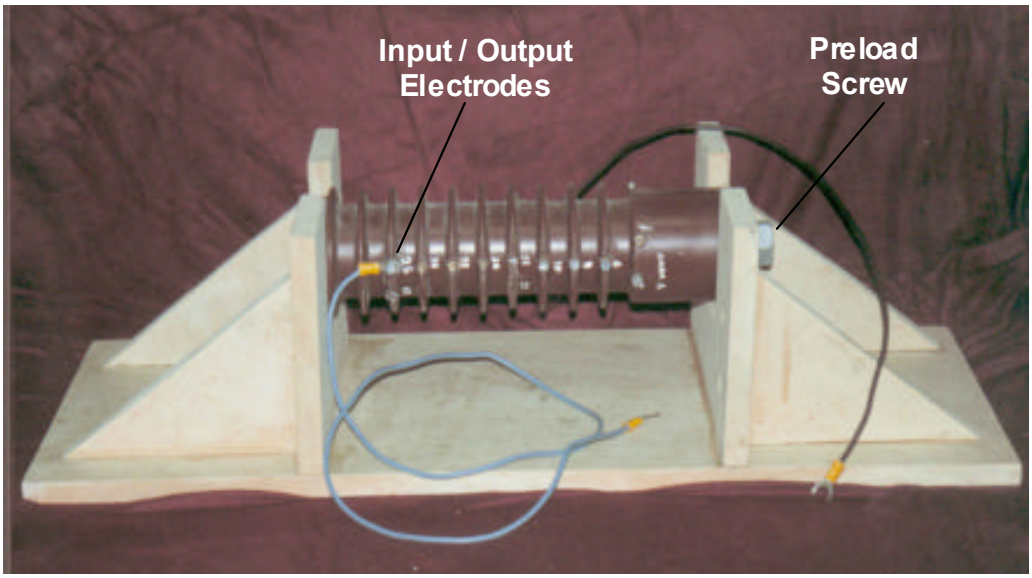

Figure 4.18. *A global view of the PIEZOTRF1 prototype*

4.5.3. Incidences and Experimental Set-up

After the construction process was done, some incidencies were detected in the prototype affecting some of the expected features of the device. The most important problem appeared in the preload screw and in some of the electrodes. Concretely, the prestress screw became useless because part of the epoxy used immobilised the screw.

As a consequence, the tests were performed without the possibility of prestressing the column. Accordingly to the electrodes, some of them were broken during the mounting, in particular V23, V22, V12, V11 and V4 remained useless. Nevertheless a R-X demonstrated that the internal structure of the piezoelectric column had not damage.

Under this circumstances, experimental tests were concentrated upon the determination of the transformation ratio of the piezoelectric transformer in the unknown level of stress. Figure 4.19 shows a view of the experimental test used to perform the transformer ratio measurements. A high voltage transformer up to 15kV was used to drive the input signal to the transformer.

The different output voltages were measured by using a high voltage Tektronix 1000:1 probe P6015. This probe also has a high input impedance of R_E=1000Ω ; C_E=2pF and a frequency bandwidth of 75MHz. The maximum input voltage is 20kV (DC+peak AC) or 40kV peak pulse. All the measurements were referred to ground and the voltage in each disc was obtained by subtraction.

The high input impedance of the probe allowed the measurements to be made under almost open circuit conditions.

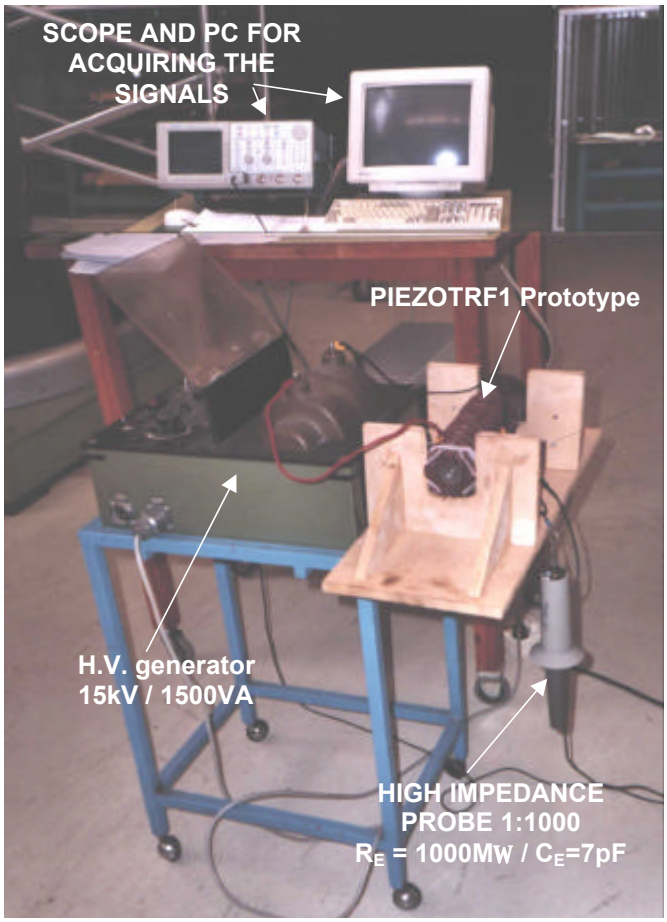

Figure 4.19. *Set-up used for measuring the transformer ratio in Prototype PIEZOTRF1.*

4.5.4. Results

Different configurations were experimentally tested by modifying the connection of the input and output electrodes. In brief, they can be considered in two groups:

- **All the column connected to the Vin**

Initially, the tests were carried out by applying the input voltage through all the piezoelectric column and measuring the partial voltages in every electrode (corresponding to one disc). The experimental tests demonstrated that the piezoelectric column excited like this had a behaviour similar to a capacitive transformer: The voltage in each disc was a portion of the total voltage which was depended of the thickness of the considered disc (considering all the disc with a similar capacitance).

$$V_{disc} = V_{total} \cdot \frac{C_{Total}}{C_{Disc}} = V_{total} \cdot \frac{t}{L} \qquad (4.22)$$

Hence, the voltage in the individual discs belonging to a piezoelectric column which is connected to a high voltage, will withstand a voltage proportional to their thickness. This is similar to say that the electric field is constant along the column.

- **The input voltage, V_{in}, is connected in only one portion of the total length of the column, leaving the other part without connection.**

A different result was found when it was connected only one part of the piezoelectric column to the high voltage and the rest of the column left free (as shown Figure 4.20). The discs belonging to the part of the column connected to high voltage shown a voltage proportional to its thickness (as a capacitive transformer), as above it has been described for the case that all the column is connected to V_{in}.

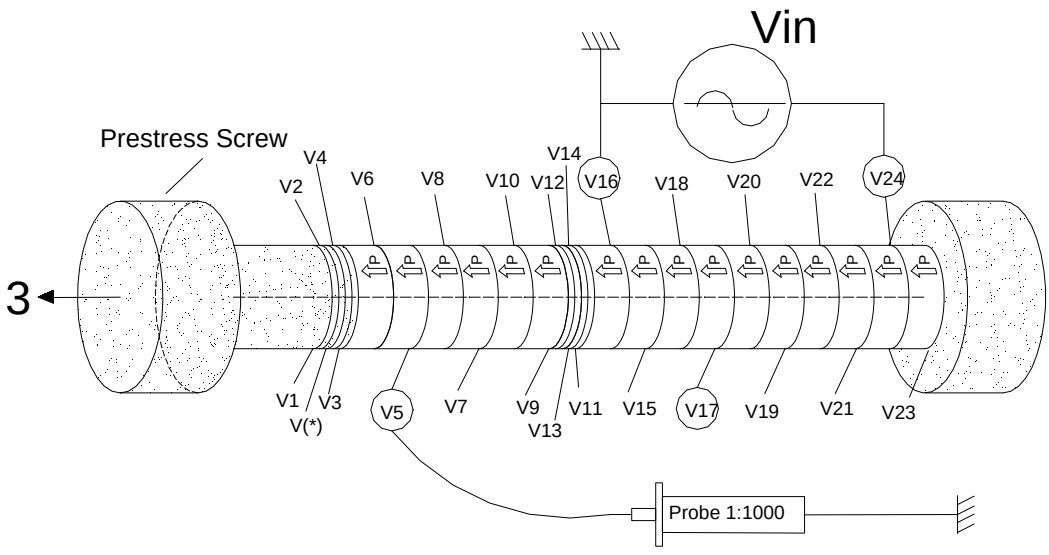

Figure 4.20. *The column is divided on two part: One part connected to the V_{in}, and a second part which is left free.*

On contrary, the discs no connected to V_{in} also shown a voltage. How is this possible?. The answer come from the piezoelectric theory. The vibration generated by the discs connected at the input voltage is transmitted to the rest of the column. In particular, this vibration arrives to

the piezoelectric placed in the second part of the column. In this way, this vibration excites the rest of the discs of the column, which actuates as a piezoelectric sensors. Hence, the force generated by the column connected to V_{in}, is converted to a proportional output voltage in the second part. The magnitude of the output voltage depend on the force transmitted and on the piezoelectric coefficient of the material, g_{33}, as indicated equation 4.23.

$$V_{out} = g_{33} \cdot \frac{t}{A} \cdot F_3 \tag{4.23}$$

Figure 4.21 illustrates one of the experimental tests performed, which summarises all the above discussion. The PIEZOTRF1 prototype is connected to a high voltage between the electrodes V24 (high voltage) and V16 (ground). The voltage referred to ground is measured for all the electrodes, both the electrodes belonging to the part connected to V_{in} and the electrodes no-connected to V_{in}.

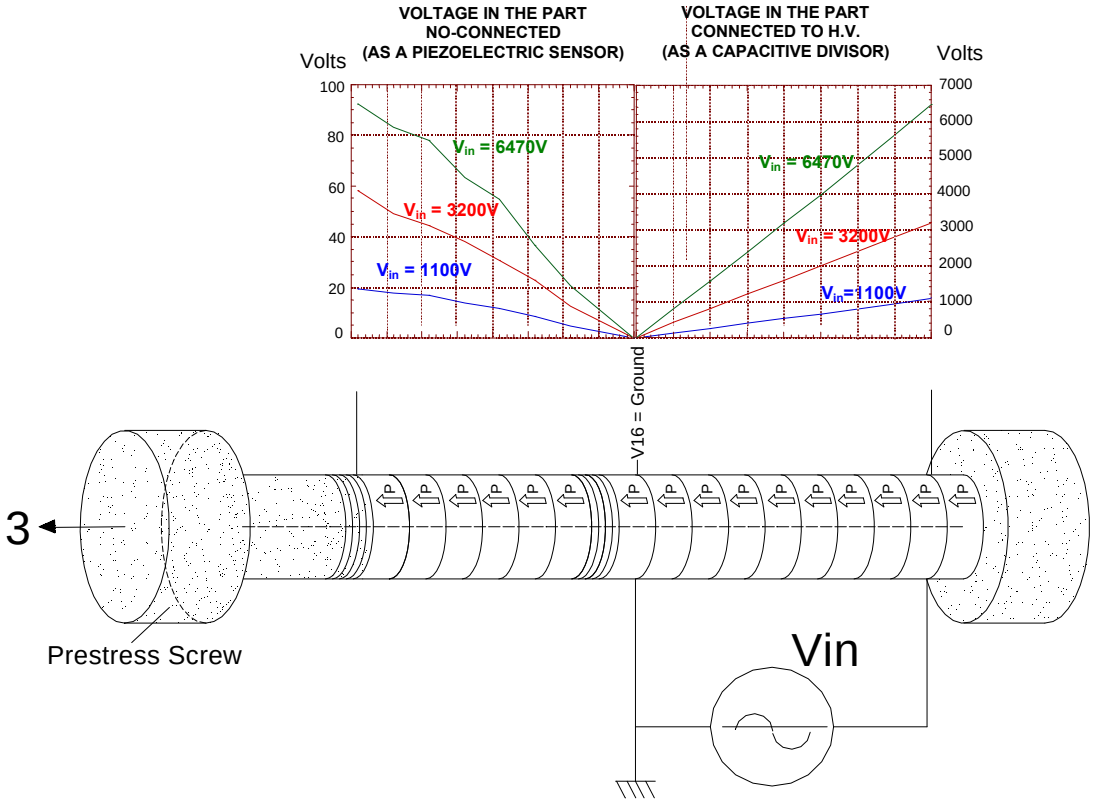

Figure 4.21. *Experimental results obtained with the PIEZOTRF1.*

Figure 4.21. shown the voltage measured for all the electrodes. The ratio transformer for the discs of the column connected to high voltage is similar to the case of a group of series capacitors (with the same capacitance) connected to the V_{in}:

$$\frac{V_{out}}{V_{in}} = \frac{t_{disc}}{L_{total}} = \frac{10mm}{80mm} = 0.125 \tag{4.24}$$

where t_{disc} is the thickness of the disc where the voltage is measured, and L_{total} is the total length were the V_{in} is applied.

With regard to the voltage measured in the free part, the ratio transformer is higher, and depending on the piezoelectric characteristic of the material and the force transmitted. Particularly, the force transmitted depend on the prestress applied. As previously it has been commented along this section, the prestress screw remained useless during the mounting process, and it was not possible to perform the evaluation of the effect of presstressing the column in their performances.

Figure 4.22 shows two samples of waves measured in the PIEZOTRF1 for both the part connected to V_{in} and the free part. It can be observed the linearity of the answer in both cases and the difference in the transformation ratio in one and another case.

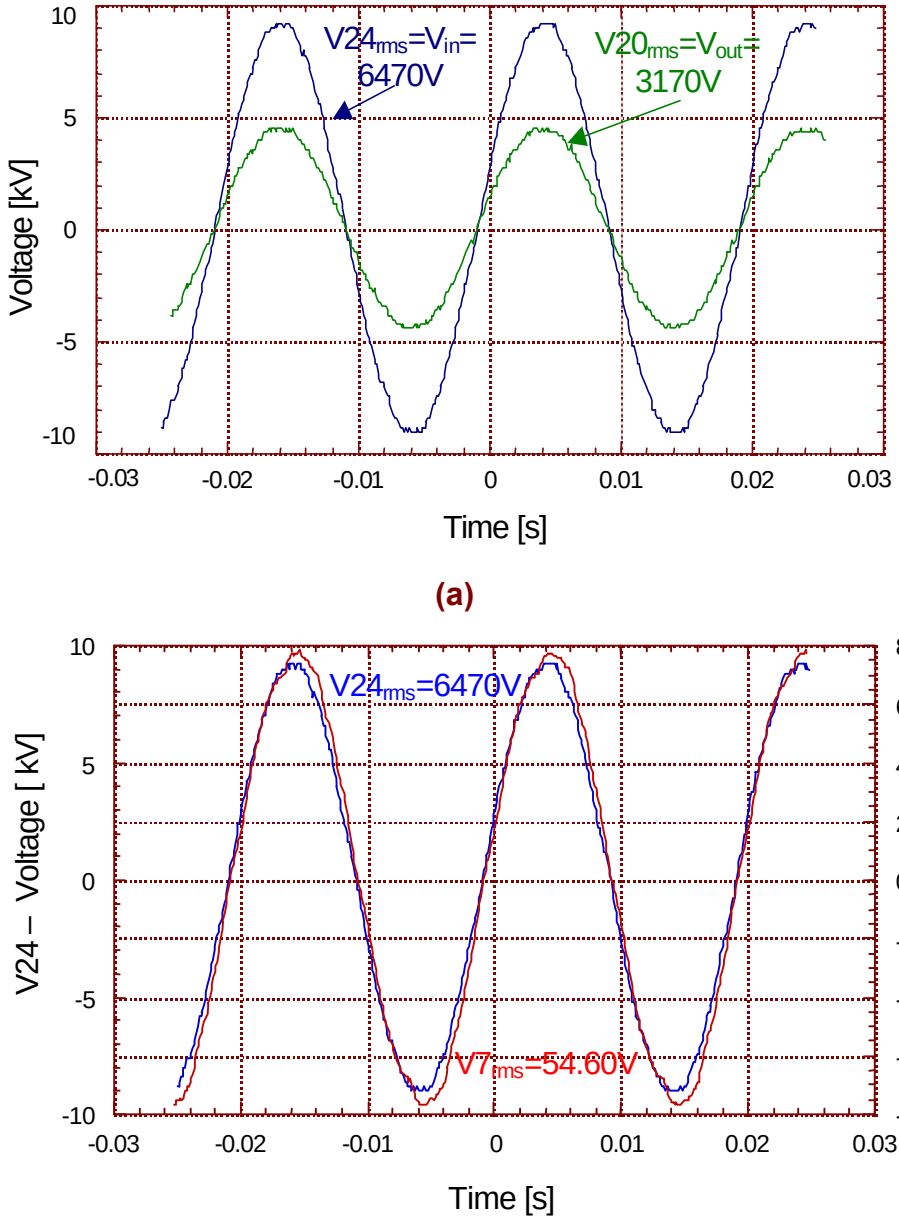

Figure 4.22. *Voltage measured under a V_{in} = 6470V referred to ground, (a) for the electrode V20 of the part connected to V_{in} ; (b) for the electrode V7 of the free part.*

4.5.5. Conclusions

Figure 4.23 illustrates the previous discussion with a model of piezoelectric transformer. The part of the piezoelectric column connected to V_{in} behaves as a column of capacitors which actuates as an ACTUATOR generating a mechanical force. The second part of the column has a piezoelectric SENSOR behaviour, and generates an electric voltage proportional to the force transmitted. As a result, this configuration will be named as ACTUATOR-SENSOR configuration or *Two-blocked columns configuration.*

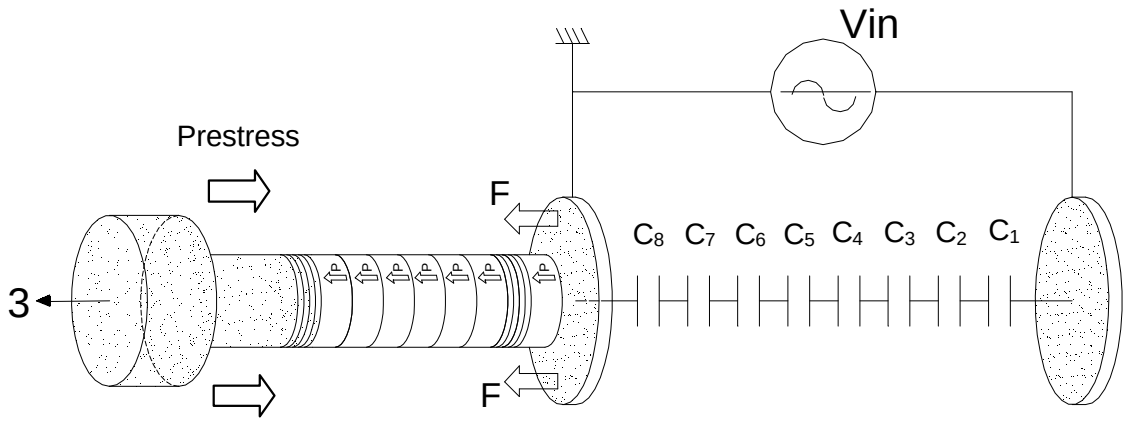

Figure 4.23. *Two-blocked columns configuration. Interpretation of the operation of the PIEZOTRF1.*

Hence, the configuration based in a Single Column of piezoelectric material connected totally to high voltage has not a significant applicability as instrument transformers because it behaves as a capacitor divisor. On contrary, the *Two column*s *configuration* has several characteristics which make it applicable as a instrument transformer:

1. The input voltage (high voltage) is sparated from the low voltage output. Thus, input and output are dielectrically separated, guaranteeing safety for the devices connected to the output.

2. The output voltage is depending on the force transmitted and on the characteristics of the piezoelectric material. Thus, it can be modified by an appropriate design and thus to obtain a high transformer ratio appropriate for electronic devices connected to the sensor.

The structure described below uses the longitudinal characteristics of the disc, other alternative structures are presented in the Figures 4.24 to 4.28. These structures are divided in two groups [6]:

- *Direct coupling structures*: In these structures the actuator and sensor columns are directly connected. Figure 4.24 shows an example of this type of structure.

- *Indirect coupling structures*: In these case, the transmission of the force between the actuator and the sensor is performed through a dielectric material in between. This material (i) increase the dielectric separation between the high and the low zones and (ii) allows the modification of the sensitivity of the sensor if is made as a parallel force path (see Appendix 2). The material used as coupling material require a similar stiffness to the ceramic to have a good mechanical transmission. Figure 4.25, 4.26 and 4.27 shown some examples. In particular, Figure 4.27 shows the case of a sensor using the transversal vibration generated for the column.

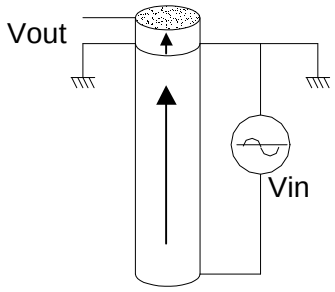

Figure 4.24. *Longitudinal actuator and sensor columns with direct coupling to be connected between phase and ground*

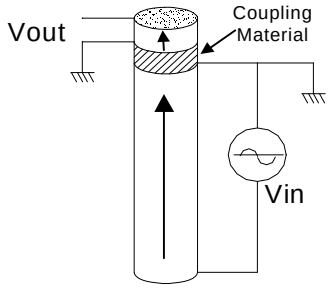

Figure 4.25. *Longitudinal actuator and sensor columns with a dielectric coupling material in between. It is connected between phase and ground.*

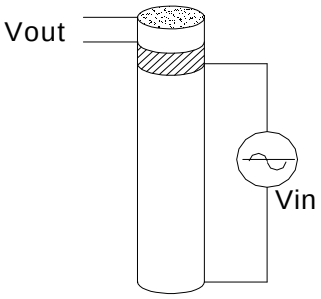

Figure 4.26. *Longitudinal actuator and sensor columns with a coupling material in between. It is connected between phase and phase.*

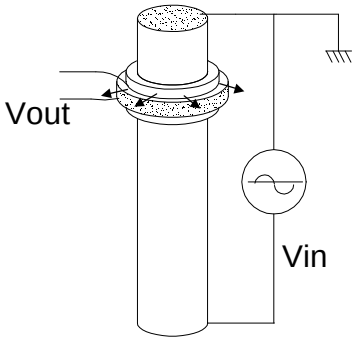

Figure 4.27. *Longitudinal actuator with a transversal sensor. The sensor have to be place very close to the ground of the actuator to avoid dielectric breakdown.*

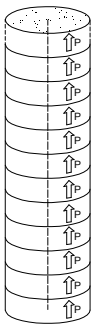

Figure 4.28. *The column is usually constructed by stacking single piezoelectric discs of lower thickness than the length total of the column*

The next chapter describes the construction and evaluation of a prototype based in the *Two columns* configuration. The new prototype will allow the measurement of the effects of the prestress in the behaviour of the transformer and to verify the characteristics of the output voltage depending on the materials used as sensor.

4.6. References

[1] A. Vázquez, *Desarrollo de un transformador piezoeléctrico. Análisis experimental de su aplicación para medida de alta tensión*. Proyecto Final de Carrera, ETSEI Barcelona, 1996.

[2] J. Álvarez Flórez, *Nuevas aportaciones al sistema de encendido de los MEP.* Tesis Doctoral Universidad Politécnica de Catalunya, ETSEI. Terrassa, 1990.

[3] Ramón pallás Areny, Sensores y Acondicionadores de Señal. Marcombo Boixareu Editores, Barcelona 1994.

[4] Manual on experimental stress analysis, Third Edition, Society for Experimental Stress Analysis, Westport, Ct., 1978.

[5] C.C.Perry and H.R.Lissner: The Strain Gage Primer, McGraw-Hill, Inc., New York, 1962.

[6] Oficina Española de Patentes ES2118042, Piezoelectric non resonant transformer to measure high voltages and its operation procedure, R.Bosch, J.Álvarez, A.Vázquez. U.P.C. Spain 01-Sep. 1998.

[7] R.Bosch, A.Vázquez, J.Álvarez, El transductor Piezoeléctrico. Un transductor viable para medida de tensiones. UPC, Ediciones CPDA, Enero 1997.

Chapter 5

Piezoelectric transformer of two blocked-columns. PIEZOTRF2 prototype

5 Piezoelectric transformer of two blocked-columns. PIEZOTRF2 prototype

5.1. Operation Principle

The *piezoelectric transformer of two blocked-columns* represents a novel idea in the operation of the instrument piezoelectric transformer, already presented in the Conclusions of Chapter 4. It divides the conversion process into two electrically separated but mechanically matched columns (see Chapter 4, cf. 4.5.5). The first column, which is connected to the high driving voltage, generates a mechanical vibration proportional to the voltage. The second column, mechanically matched to the previous one, receives the mechanical vibration and converts it back into an electrical signal.

In this way, the output of the transformer is electrically decoupled from the high voltage area guaranteeing safety for the protection and measuring systems of the secondary, which is one of the most important requirements for instrument transformers.

The first column operates as an actuator device (*converse piezoelectric effect*), and the second column operates as a sensor device (*direct piezoelectric effect*). Hereafter, the name of *actuator column* and *sensor column* will be used to refer the first and second column respectively. Also, actuator column can be thought of as the *primary* of a classical electric transformer, and the sensor will be thought of as the *secondary*.

The name of *two blocked columns* was used to reflect the existence of two different columns subjected to the same blocked state.

5.2. Configurations

In Chapter 4 different configurations of *Two Columns* piezoelectric transformer were proposed. In this chapter, only the longitudinal configuration is considered. For this type of transformer, two different structures were proposed [1,2]:

- *Direct coupling*: In this configuration the vibration generated by the actuator column is directly transmitted to the sensor without any mechanical coupling material in between. Accordingly, Figures 5.1 shows one possible embodiment.

- *Indirect coupling*: When between the actuator and the sensor columns a dielectric material is placed (Figures 5.2). In this kind of configuration the coupling material has to have acoustic properties similar to the ceramic materials to provide a good mechanical matching.

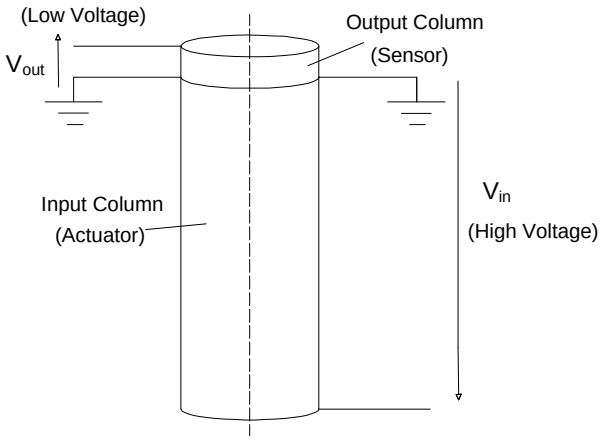

Figure 5.1. *Direct coupling configuration*

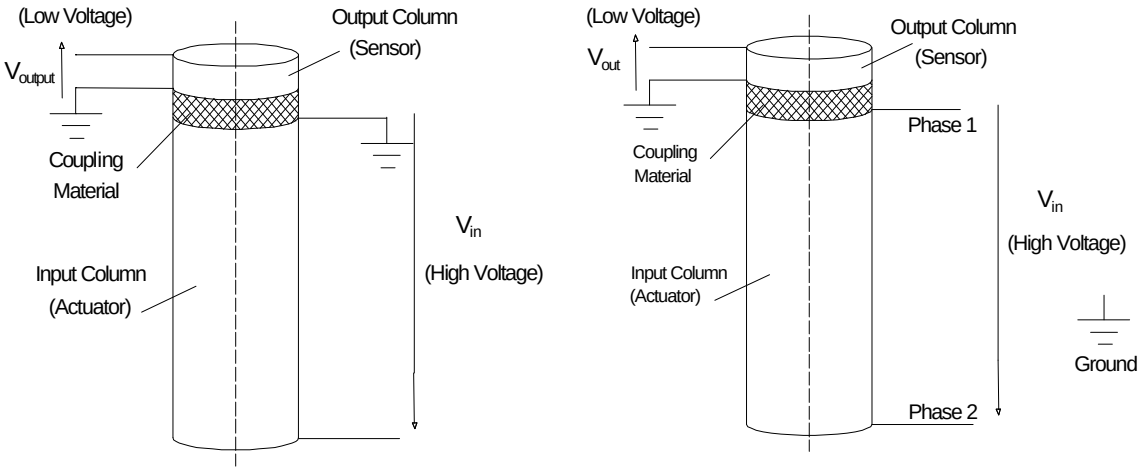

Figure 5.2. *Indirect coupling configuration*

• Ground Connection

In the previous prototypes it is important to observe the ground connection in the primary (actuator) and in the secondary (sensor) columns. The voltage of the sensor will always be referred to ground. Thus, the sensor of the embodiments of Figure 5.1 and 5.2 has an electrode connected to ground.

The voltage of the primary must be measured referred to ground or between two phases. If one uses the direct coupling, only measurements referred to ground are possible, so there is a electrode common for the sensor and the H.V. part which it must be connected to ground. On contrary, if the indirect coupling is used, it is possible to perform measurements between phases taking account of using a coupling material which separates dielectrically the H.V. from the low voltage.

5.3. Construction of the PIEZOTRF2

To overcome the problems appeared in the PIEZOTRF1 prototype after the moulding process, relating to the damage of both the prestress screw and electrodes, it was decide to simplify the construction process of the PIEZOTRF2. This was achieved by using a pre-constructed housing in order to avoid such incidences [4,5].

This pre-constructed housing was designed for accommodating both the piezoelectric actuator column and the piezoelectric sensor column. In order to do this, an internal hole for inserting both columns and a metallic base which operates as high voltage electrode, was arranged in the housing during the moulding process. One of the critical point during the insertion of the metallic base was to guarantee the perpendicularly of the plate of the base for resting the actuator column and the vertical axis of the column.

Figure 5.3 displays the housing used with both the actuator and the column sensor inside. The internal hole was make with enough tolerance (two times bigger) than the diameter of the piezoelectric actuator column to allow its easy installation and the subsequent incorporation of a dielectric material which dielectrically fills the cavity and gives dimensional stability to the actuator column.

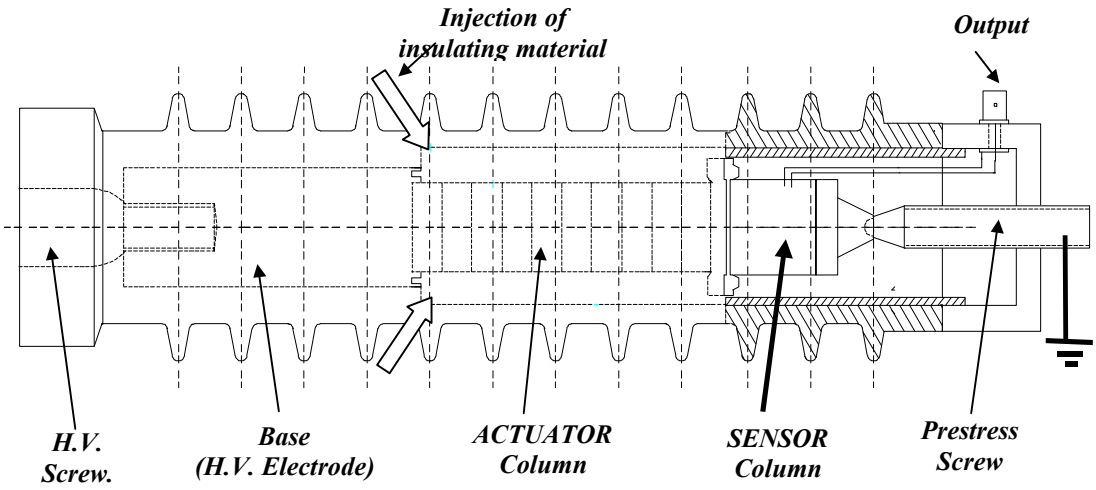

Figure 5.3. *View of the PIEZOTRF2 indicating the arrangement of both the actuator and the sensor columns*

Sensor and actuator columns were installed separately. The piezoelectric actuator column was constructed by piling up ceramic discs of PZT-8 from Morgan Matroc. This material has a higher depolarisation resistance than the PXE-41 (approximately 1500V/mm) which allows its length to be reduced to 144mm. In total, 12 discs of 12mm were used to construct the column.

The stacked column of discs was recovered by using a dielectric adhesive tape in order to give it dimensional stability as it has already been commented upon for the PIEZOTRF1. Once prepared, the actuator column was introduced in the cavity of the dielectric housing as is observed in the detail of Figure 5.4.(a).

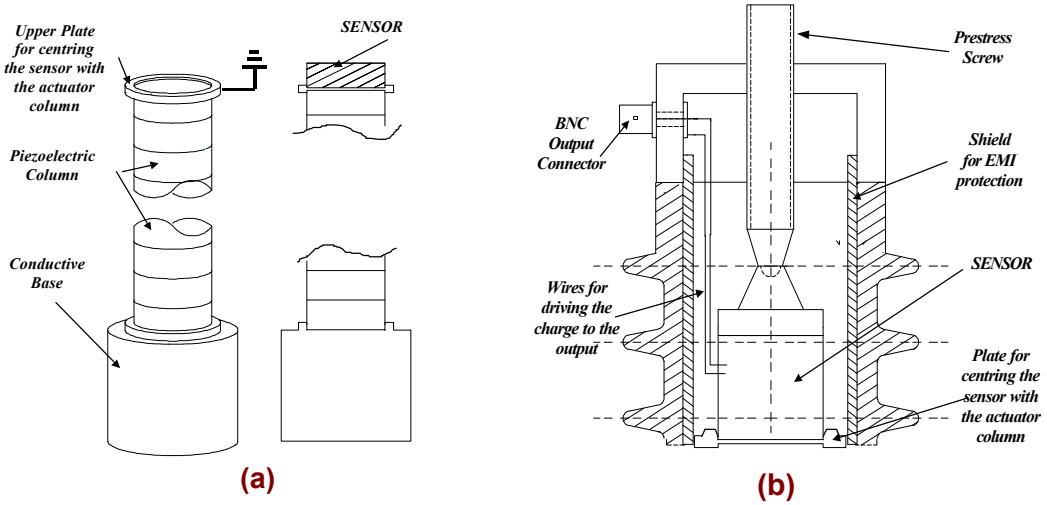

Figure 5.4. (a) *Details of the pieces for centring the actuator and sensor columns;* **(b)** *Faraday cage for protecting the sensor and view of the prestress screw.*

Once the actuator is centred inside the housing, an external prestress is apply to adjust all the disc. Following, the remained space of the cavity is sealing with dielectric silicone introduced by two lateral little holes wich permit the injection of the insulating material. Thus, the silicone covers the entire piezoelectric cylinder leaving free the upper electrode for making the coupling with the sensor.

When the silicone dries, a second centring plate is placed over the actuator column (Figure 5.4.a) which allows the arrangement of the sensor. Sensor column may be formed by an individual piezoelectric disc or a pile of discs connected in parallel to increase the charge generated and to reduce the output impedance.

To protect the sensor against electromagnetic interference, a metallic cylinder (Faraday cage) covers internally the housing. This Faraday housing is electrically connected to the metallic upper electrode (Figure 5.4.b). The upper electrode has a central screw to apply the necessary prestress to the piezoelectric column and a BNC connector to output the electric signal generated by the sensor. Furthermore, the upper electrode disposes of four M6 screws for fixing it to the epoxy housing. This allows the upper part to be removed when a different configuration or sensor materials wants to be tested.

Figure 5.5 shows an external view of the embodiment totally constructed and connected to high voltage.

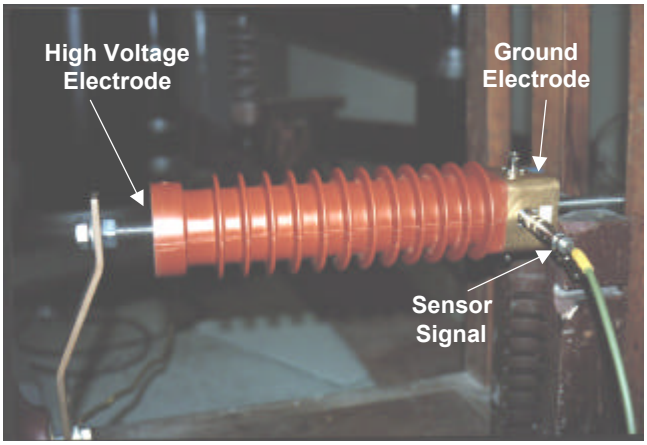

Figure 5.5. *PIEZOTRF2 prototype connected to high voltage.*

5.4. Experimental Tests

Two kinds of tests have been performed for analysing the behaviour of the piezoelectric transformer: (1) a test to evaluate the transformation ratio, and (2) a test to evaluate if the device can withstand dielectrically high electric fields.

• Dielectric Tests

Dielectric tests were carried out by applying a lightning 1.2/50μs pulse to the prototype until a voltage of 170kV. Shape of the pulse is normalised for the different standards and is displayed in Figure 5.6.

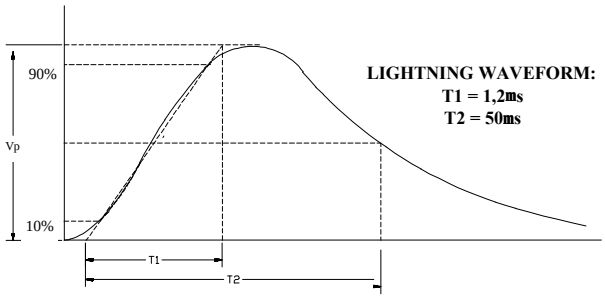

Figure 5.6. *Lightning pulse*

Negatives and positives pulses were applied verifying that the transformer withstand both polarities.

• Transformation Ratio

In order to characterise the transformation ratio of the transformer and to verify the influences of different piezoelectric materials used as sensor, several electrical test were performed. Four types of sensors were used: 2 discs of a hard ceramic material such as the PXE41 from Philips of 10mm and 15mm of thickness and 24 mm diameter, one disc of soft ceramic material, such as the PXE-5 from Philips of 2mm thickness and 24mm diameter, and finally a very low stiff material, such as the PVDF, of 100μm.

The experimental set-up is illustrated in Figures 5.7 and 5.8. A 220V/60kV power transformer was used as a voltage source for powering the prototype. The input voltage was controlled by using an autotransformer. In parallel to the prototype it was connected an electromagnetic voltage transformer in order to monitoring the signal arriving to the prototype.

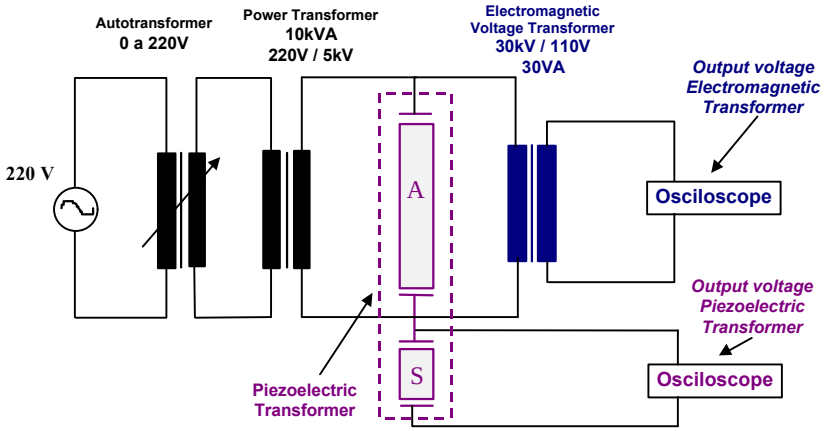

Figure 5.7. *Experimental set-up used for testing the PIEZOTRF2 prototype*

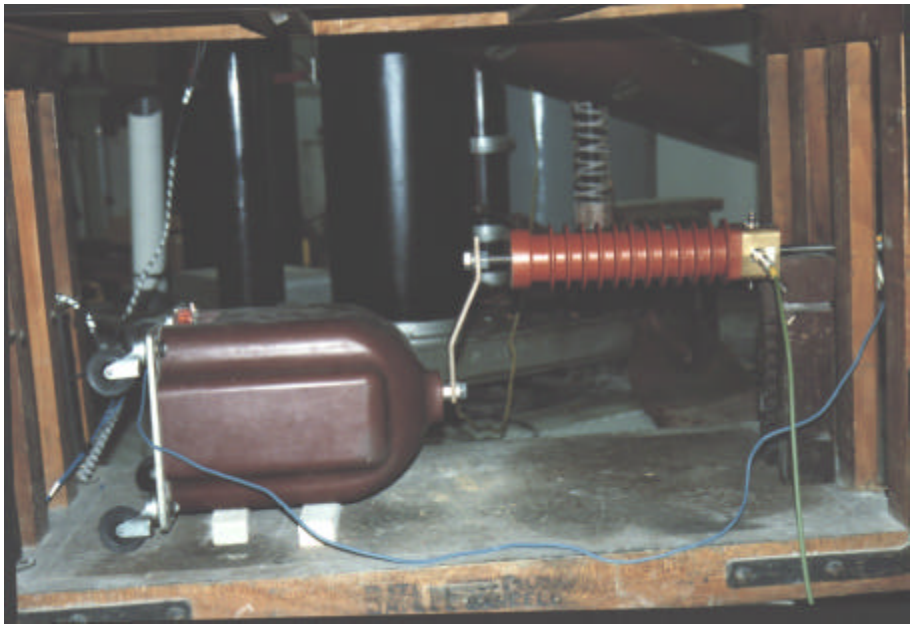

Figure 5.8. *Experimental test comparing the classical electromagnetic technology (left) with the novel piezoelectric technology (right).*

The tests were applied by placing each one of the different sensors in the prototype and measuring the output voltage when the input voltage was modify in a range between 0 to 60kV. The actuator column remained always the same, so the differences in the output signal came directly from the sensor.

The measurements were carried out by using the high voltage Tektronix probe P6015A with an input impedance of R_E=1000MΩ and C_E=2pF. In this way the measurements are very close to the open circuit conditions.

Figure 5.9 shows the experimental results obtained.

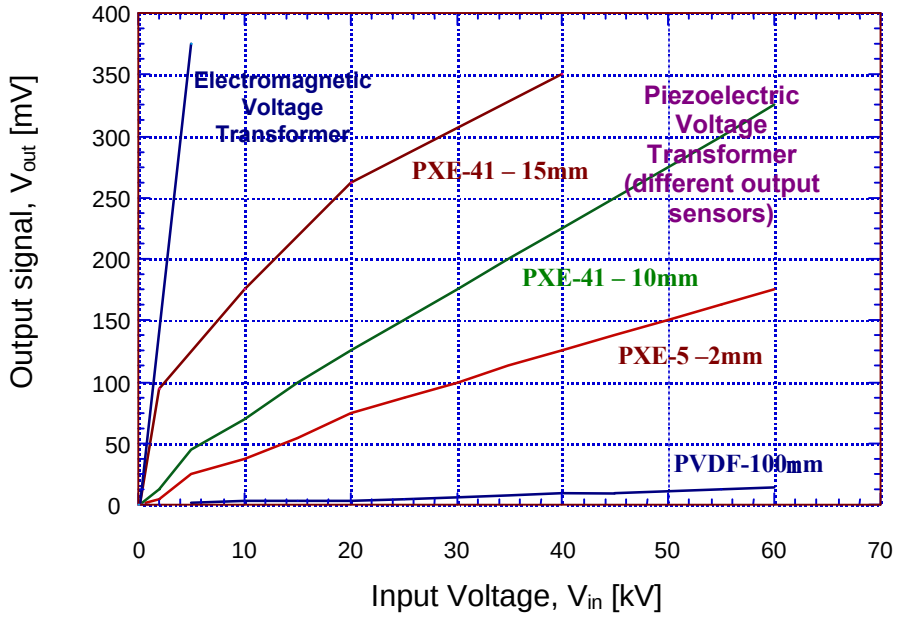

Figure 5.9. *Experimental measurements for the PIEZOTRF2 using different types of sensors.*

From Figure 5.9, the experimental transformation ratio for the different sensors used can be obtained as: $r_{t,PXE5\ (2mm)} = 266$; $r_{t,PXE\text{-}41\ (10mm)} = 172$; $r_{t,PXE\text{-}41\ (15mm)} = 115$; $r_{t,PVDF(100\mu m)} = 2500$

In all the tests the preload was apply by means of a screw. The strength of preload was applied up to obtain a signal of 'good quality' in the sensor. However, there are not experimental values about the concrete preload applied in each case. The reader will understand that in this stage of the research the most important variables were considered the input and output voltage and the material used in the secondary. The preload was considered a variable with a very little influence in the output voltage. In the following chapters, it will be seen that preload play a decisive role in the behaviour of the transformer.

In these conditions, the experimental values were compared with the expected theoretical values. The theoretical expression of the transformer ratio may be obtained from the transformer ratio calculation developed in Chapter 4 for the PIEZOTRF1 prototype, equations (4.16) and (4.17). Nevertheless, in the present case it is necessary to consider that the materials of the actuator column and the sensor column can be different. Equations (5.1) and (5.2) indicate the transformer ratio calculation.

$$V_{output}(t) = -\frac{d_{33,\,Actuator}}{s^{E}_{33,\,Actuator}} \cdot \frac{A_{Actuator}}{t_{Actuator}} \cdot \frac{t_{Sensor}}{A_{Sensor}} \cdot g_{33,Sensor} \cdot V_{input} \tag{5.1}$$

$$r_t = \frac{V_{input}(t)}{V_{output}(t)} = -\frac{s^{E}_{33,\,Actuator}}{d_{33,\,Actuator}} \cdot \frac{t_{Actuator}}{A_{Actuator}} \cdot \frac{A_{Sensor}}{t_{Sensor}} \cdot \frac{1}{g_{33,Sensor}} \tag{5.2}$$

where $A_{Actuator}$ is the actuator area, $t_{Actuator}$ is the length of the actuator column, A_{Sensor} is the sensor area, t_{Sensor} is the sensor thickness, $d_{33,Actuator}$ is the piezoelectric strain coefficient of the actuator, $g_{33,Sensor}$ is the piezoelectric voltage coefficient of the sensor and $s^{E}_{33,\,Actuator}$ is the compliance of the actuator.

Table 5.1 provides the different coefficients for the actuator and sensor column, for the different configuration experimentally tested.

Table 5.1. *Comparison of the properties of different configuration in order to evaluate the transformation ratio*

Actuator **Sensor**	Thickness (mm)	Area [mm^2]	Piezoelectric coefficient	Elastic compliance (m^2/N)
Actuator = PZT8 Sensor = PXE-41	$t_{Actuator}$ = 144 t_{Sensor} = 10	506,7	$d_{33,Actuator} = 225.10^{-12}$ C/N $g_{33,\,Sensor} = 30.10^{-3}$ V.m/N	$s_{33}{}^{E}{}_{Actuator} = 13{,}5.10^{-12}$
Actuator = PZT8 Sensor = PZT5	$t_{Actuator}$ = 144 t_{Sensor} = 2	506,7	$d_{33,Actuator} = 225.10^{-12}$ C/N $g_{33,\,Sensor} = 24.8.10^{-3}$ V.m/N	$s_{33}{}^{E}{}_{Actuator} = 13{,}5.10^{-12}$
Actuator = PZT8 Sensor = PXE-41	$t_{Actuator}$ = 144 t_{Sensor} = 15	506,7	$d_{33,Actuator} = 225.10^{-12}$ C/N $g_{33,\,Sensor} = 30{\cdot}10^{-3}$ V.m/N	$s_{33}{}^{E}{}_{Actuator} = 13{,}5.10^{-12}$
Actuator = PZT8 Sensor = PVDF	$t_{Actuator}$ = 144 t_{Sensor} = 0.100	506,7	$d_{33,Actuator} = 225.10^{-12}$ C/N $g_{33,\,Sensor} = -339.10^{-3}$ V.m/N	$s_{33}{}^{E}{}_{Actuator} = 13{,}5.10^{-12}$

Following the theoretical transformer ratio is calculated and the obtained value is used in Figure 5.10 to compare the obtained values with the experimentally measured.

Sensor: PZT-41 (15mm) $r_t = -\frac{13.5 \cdot 10^{-12}}{225 \cdot 10^{-12}} \cdot \frac{144 \cdot 10^{-3}}{15 \cdot 10^{-3}} \cdot \frac{1}{\left(30 \cdot 10^{-3}\right)} = -19.2$

Sensor: PZT-41 (10mm) $r_t = -\frac{13.5 \cdot 10^{-12}}{225 \cdot 10^{-12}} \cdot \frac{144 \cdot 10^{-3}}{10 \cdot 10^{-3}} \cdot \frac{1}{\left(30 \cdot 10^{-3}\right)} = -28.8$

Sensor: PZT-5 (2mm) $r_t = -\frac{13.5 \cdot 10^{-12}}{225 \cdot 10^{-12}} \cdot \frac{144 \cdot 10^{-3}}{2 \cdot 10^{-3}} \cdot \frac{1}{\left(24.8 \cdot 10^{-3}\right)} = -174.2$

Sensor: PVDF (100µm): $r_t = -\frac{13.5 \cdot 10^{-12}}{225 \cdot 10^{-12}} \cdot \frac{144 \cdot 10^{-3}}{0.0001 \cdot 10^{-3}} \cdot \frac{1}{\left(-339 \cdot 10^{-3}\right)} = 254867.2$

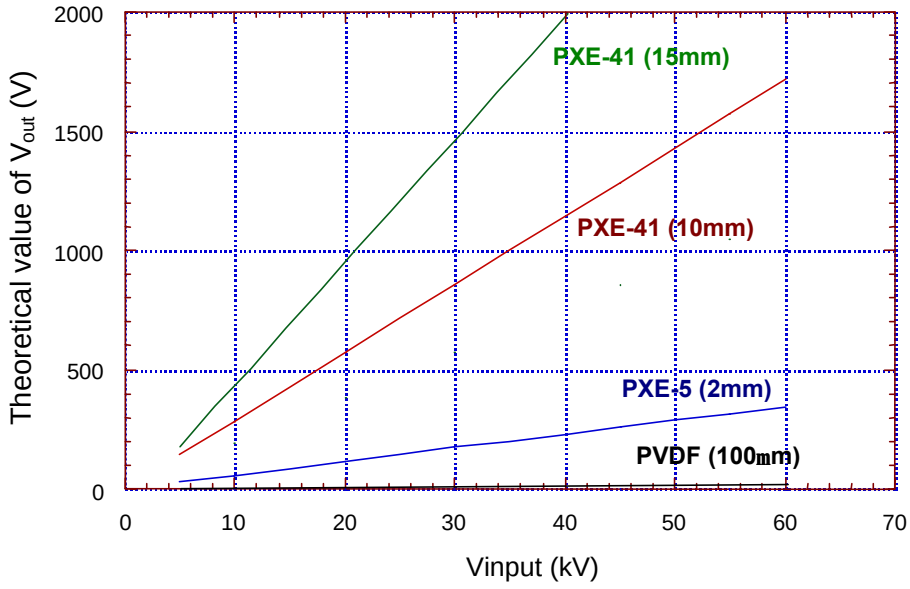

Figure 5.10. *Theoretical values for the PIEZOTRF2 using different kinds of sensors.*

5.7. Conclusions

An important difference is observed from the results of Figures 5.8 and 5.9. The evolution of the thesis will permit the reader, later on, to understand these differences. Nevertheless, it is convenient to mention them now:

- Mechanical considerations: The theoretical transformer ratio from equation (5.2) was obtained under the conditions of blocking force. This is the same that to calculate the maximum force that the actuator can generate and to transmit to the sensor when there is not deformations in the housing. Nevertheless, the big forces appeared in the column can deform easily the epoxy housing. In Chapter 7 and 8 a complete evaluation of the strength of this forces and the deformation generated in the housing is made.

Thus, due to the mechanical deformation appeared in the passive elements, the generated force is lower than the ideally expected. In order to improve the blocking state it is necessary to make a design which guarantees low deformation, and also, it is necessary to guarantee a certain preload in the actuator to be sure that always work under compression. In other case decoupling between discs could appear.

- Electrical considerations: In Appendix 1 a general review to conditioning circuit for piezoelectric sensors is given. In general is necessary to say that the output impedance of a piezoelectric material can be very high (several GΩ, depending on the geometry). Hence if one take the measure from a piezoelectric sensor and drive it to the readout, the lecture measured will be influence for the difference of the output impedance of the transducer and the input impedance of the scope.

Both considerations are treated with more detail in the following chapters. Firstly, Chapter 6 make a study of the experimental limitations of the piezoelectric ceramic materials. This will permit later, in Chapter 7, to apply the correct conditions for designing the PIEZOTRF3 prototype.

5.8. References

[1] Oficina Española de Patentes ES2118042, *Piezoelectric non resonant transformer to measure high voltages and its operation procedure*, R.Bosch, J.Álvarez, A.Vázquez. U.P.C. Spain 01-Sep. 1998.

[2] R.Bosch, A.Vázquez, J.Álvarez, El transformador piezoeléctrico. Un transductor viable para medida de altas tensiones. Ediciones CPDA, UPC-ETSEIB.

[3] A.Vázquez, R.Bosch, J.Álvarez, *Medida de Tensiones de Distribución en M.T. utilizando la Piezoelectricidad.* Revista Técnica ELECTRA, No. 83, pp. 19-24, June 1997.

[4] A.Vázquez, R.Bosch, *Transformador Piezoeléctrico para medida de A.T. Investigaciones en el seno de la UPC.* 5as Jornadas Hispano-Lusas de Ingeniería Eléctrica. Vol. 3, pp. 1607-13. Salamanca 1997.

[5] A.Vázquez, R.Bosch, *Transformador Piezoeléctrico para Medida de Altas Tensiones*, III Jornadas Latinoamericas en Alta Tensión y Aislamiento Eléctrico ALTAE'97, Vol. 1, pp. 175-179, October 1997.

Chapter 6

Characterisation and Selection of the Active Materials: Actuator & Sensor

6 Characterisation and Selection of the Active Materials: Actuator & Sensor

6.1. Introduction

The piezoelectric response of the materials used in the sensor and actuator columns of the piezoelectric transformer is dependent upon the external electrical and mechanical conditions, such as the amplitude and frequency of the external applied electrical field and the amplitude and frequency of the external stress.

Under extreme mechanical or electrical conditions, the traditional PZT ceramics often exhibit dispersion of piezoelectric coefficients with frequency, and unstable, non-linear and hysteretic response under external fields. For high precision measuring transformers the instabilities in piezoelectric response may be detrimental for the performance of the whole device.

For predicting and controlling the performance of devices based on piezoelectric ceramics, it is therefore essential, to understand the mechanisms behind the different processes that influence the properties of the materials. Particularly, the selection of material will depend upon certain characteristics such as *linearity*, *hysteresis*, *depolarisation*, behaviour under *static or alternative stress*, *ageing*, *thermal drift* and others.

Information contained within the manufacturer's data sheet is in general referred to *low signal behaviour* of piezoelectric materials and usually there is no information about the behaviour of the material under extreme conditions. Hence, there is a need to investigate the behaviour of the active materials under the special conditions that the instrument piezoelectric transformer will withstand and to determinate the *high-signal* coefficients for them.

In this chapter several piezoelectric ceramic materials, including different compositions of PZT from different manufacturers, are examined in detail and compared with each other. The chapter gathers results of personal experimental tests and a whole review of the state of the art of this field, providing information for evaluating the degradation of the features in such devices and a success selection of the materials. The final conclusions shows that it is possible to obtain a stable behaviour, independent of the frequency and magnitude of external driving field with proper modifications in the chemical composition of the ceramic.

The theoretical background and the experimental results shown in this section, were carried out in the Laboratory of Ceramics, Swiss Federal Institute of Technology, as a short-term research stay supported, in part by the Ministry of Education and Culture from Spain, and in part by the Swiss Federal Institute of Technology as a part of a FPI scholarship.

6.2. Non-linearities and Degradation in Piezoelectric Ceramics

Real materials involve mechanical and electrical dissipation. In addition, they may show strong non-linear behaviour, hysteresis effects, temporal instability (ageing), and a variety of magneto-mechano-electric interactions. Poled ferroelectric ceramics, because of the presence of ferroelectric domains, exhibit a variety of non-linearities and ageing effects which are not within the scope of the linear behaviour. In this chapter the concept of *non-linearity* is treated separately from the concept of *degradation*.

6.2.1. Non-linearities

Non-linearity is here associated to the variation of the response of the piezoelectric material in relation to its input for a low number of cycles. This response is mainly dependant upon the chemical composition of the material. For instance, in electrostrictive materials the response of the material will be quadratic related to the input. Also non-linearities are dependant upon the mechanic and electric field strength applied to the sample. High electric fields have influence in the second order coefficient of the material which are related to the electrostrictive behaviour of the material and, thus, related to nonlinear effects.

6.2.2. Degradation

Degradation is here used to describe the loss in performances with the natural time evolution, number of cycles evolution and/or stress of ferroelectric materials. Different mechanisms are usually considered together under the name of degradation to simply although it is convenient to have a clear knowledge of each of them particularly.

• Ageing (Natural time evolution)

The most fully understood form of degradation is *ageing*, where there is a spontaneous loss in the functional performance of the material with time. This is thought to be due to the progressive rearrangement of domains into more stable configurations. The loss in performance is usually logarithmic and manufacturers will quote ageing characteristics in terms of percentage loss per decade. Often piezoelectric measurements are performed 24 hours after poling, when the initial rapid rate of change in properties is reduced.

• Resistance degradation (Conductivity evolution)

Under a constant DC electric stress, the materials can undergo an increase in *conductivity* with time (termed *resistance degradation*). This leads eventually to dielectric breakdown, sometimes called time dependent dielectric breakdown. This phenomena is of most concern for reliability of multilayer ceramic capacitors. This concept will be not treated in this work but some references can be found elsewhere [1,2].

• Fatigue (number of cycles evolution)

Technical literature defines *fatigue* as a decay in the remanent polarisation and coercitive field associated with increasing electrical and/ or mechanical cycles.

The attempts made to explain the mechanisms for fatigue in piezoelectric materials have been based on intrinsic or extrinsic phenomena including 90º and 180º domain wall motion and/or domain switching, domain pinning via space charge effects, surface deterioration via electric discharge within pores and, ultimately, the generation of microcracks in response to the very large strain accumulation within pores and imperfections.

Many of the studies of ferroelectric fatigue are related to thin film memory applications, where the square hysteresis loop is used to good effect as a data storage device [3]. Here, the loss of switchable polarisation leads to the indistinguishability of the "on" and the "off" states.

Fatigue has also been used to describe the mechanical failure of piezoelectric materials, at loads below the failure strength, following the applications of cyclic mechanical loads, and also indirectly via cyclic electric loads. Many of the damage mechanics are similar to those found in mechanically cycling conventional ceramics, but there is the added complication that electrical fields can affect crack growth. The degradation is generally attributed to an accumulation of microcracks forming within the ceramic, and although domain reorientation occurs, this is not, however to microcrack evolution [4].

- **Depolarisation (High Electrical or/and Mechanical Stress)**

Most of the degradation phenomena discussed so far have been those that take decades of cycles or a long time to show significant change in properties. Piezoelectric ceramics are commonly poled polycrystalline devices, which can be readily depoled by applying a large electrical or mechanical stress, or by taking the material through its Curie temperature. Several workers have studied these effects of large mechanical stresses on typical piezoelectric ceramic materials [5].

- **Degradation quantification**

From all the previously comments, the degradation in a piezoelectric material may be simplified as the sum of two basic terms:

The *Natural Degradation*, relating to the loss of properties with time in not operating conditions.

The *Forced Degradation*, relating to the loss of properties caused by the operating conditions applied to the sample.

$$\text{Degradation} = \left\{ \underbrace{\text{Natural Degradation}}_{\text{Ageing}} \right\}_{\text{Depending on the time}} + \left\{ \underbrace{\text{Forced Degradation}}_{\text{Fatige} + \text{Depolarisation} + \text{Conductivity}} \right\}_{\substack{\text{Depending on:} \\ \text{- High Electric Field} \\ \text{- High Mechanical Stresses} \\ \text{- High Temperature} \\ \text{- Elevate Number of Operation Cycles}}}$$

6.2.3. Non-Linearity and Degradation Tests

Table 6.1 summarises the different tests to characterise the non-linearities and the degradation in a ferroelectric ceramic and the conditions normally used to perform the tests.

Table 6.1. *Non-linearity and experimental evaluation of the degradation. In brackets is indicated the section where the related subject is described.*

LINEAR BEHAVIOUR (6.3)	**Theoretical approach for low-signal applications**			**Measures of linear behaviour are indicated at the IEEE Standard on Piezoelectricity 176-1987 [6].**		**(6.3)**
NON-LINEARITIES (6.4)	**External ELECTRICAL Conditions (HYSTERESIS)**			**P-E S-E**	Soft: E_{max} =500V/mm Hard: E_{max} =1kV/mm	**(6.4.1)**
	External MECHANICAL Conditions		**Static Preload**	**Static piezoelectric effect which disappears in a short time.**		**(6.4.2)**
			Alternative Stress	**$d_{33} - T_3(t)$**	Preload = 18MPa $T_3(t)$ = 2MPa / 1Hz	**(6.4.2.2)**
			Effect of the static preload in the response for an Electrical input	**e - E tand - E**	Preload {0....5kN} E=300Vpp/mm f_1=100Hz f_2= 1kHz	**(6.4.2.3)**
	Frequency dependence			**$d_{33} - f$**	Preload = 18MPa T_3 (t) = 3MPa	**(6.4.3)**
	Thermal Dependence			**$d_{33} - T$**	**See Data Books [8-12]**	
DEGRADATION (6.5)	**NATURAL**		**Ageing (Time Evolution)**	**$d_{33} - t$**	Resonance measurements during time evolution	**(6.5.1)**
	FORCED	**ELECTRICAL DEGRADATION (amplitude and frequency of the externally applied electrical field)**	**(Conductivity Evolution)**	**(See [1,2])**		
			Fatigue (Number of cycles evolution)	**e - N_{cycles}**	500 Vpk-pk/mm f = 100Hz 10^4 cycles	**(6.5.2.1)**
			Electrical Depolarisation	**P-E**	f=10Hz Ramping at high voltages	**(6.5.3.1)**
		MECHANICAL DEGRADATION (amplitude and frequency of the external mechanical pressure)	**Fatigue (number of cycles evolution)**	**d_{33}-N_{cycles}**	Preload = 18MPa T_3 (t) = 3MPa f = 200Hz	**(6.5.2.2)**
			Mechanical Depolarisation	**$T_3 - S_3$**	Compressive test up to 400MPa	**(6.5.3.2)**
		THERMAL DEGRADATION (amplitude of the externally applied temperature)	**Thermal Depolarisation**			**(6.5.3.3)**

6.2.4. Types of Materials

Non-linearity and degradation in ferrolectric ceramics is dependent upon the chemical composition of the materials. In order to extract coherent conclusions when materials from different manufacturers are compared it is necessary to have a standard classification. Since in 1954 Bernard Jaffe discovered the PZT piezoelectric material, this one has been the most widely used material for piezoelectric applications in all their compositions. PZT manufacturing process and also the commercial name are protected under a patent which belongs at present to Morgan Matroc Ltd. However different companies manufacture piezoelectric materials based on the PZT procedures, but with different commercial names.

The DOD Standard 1376 [7] classifies the piezoelectric ceramic composed of Lead Zirconate Titanate (PZT) materials within 5 groups (Type I, Type II, Type III, Type V, and Type VI). These groups may also be joined in two primary groups:

Hard piezoelectric formulations: To this groups belongs the DOD Type I and III. The main characteristic of these materials is their capability to withstand high levels of electrical and mechanical excitations. They have a high depolarisation resistance (up to 1500kV/mm) and show hard stability and good linearity.

Soft piezoelectric materials, such as DOD Type II, V and VI have higher sensitivity and permeability, but higher dielectric loss factors, which can cause heating during high drive operating conditions. Also soft materials have low depolarisation resistance (approx. up to 500V/mm), are sensitive to fatigue and exhibit a significant level of hysteresis.

Table 6.2 provide a cross reference guide between different commercial piezoelectric materials with similar characteristics. The DOD Standard has been taken as the main reference.

Table 6.2. *Cross reference guide for different manufacturers of piezoelectric ceramics*

DOD 1376 Standard (*)	Morgan Matroc [9]	CeramTec [10]	Channel	EDO	Ferroperm [8]	Philips [11]	Sensor Technology [12]
Type-I (Hard)	**PZT-4**	SonoxP4	5400	EC-64	Pz26	*PXE41 PXE42*	BM400
Type-III (Very Hard)	**PZT-8**	SonoxP8	5800	EC-69	Pz28	*PXE43 PXE71*	BM800
Type-II (Soft)	**PZT-5A *PZT-5R***	*SonoxP5 SonoxP502*	5500	EC-65	Pz27	*PXE59*	BM500
Type-VI (Soft)	**PZT-5J**	*SonoxP51*	5600	EC-70	*Pz29*	*PXE5*	BM527
Type-V (Soft)	**PZT-5H**	*SonoxP53*	5700	EC-76	*Pz21*	*PXE52*	BM532

(*) *Type I,II...VI are so called Navy I, II,...VI respectively.*

6.3. Linearity. Small–signal parameters

Piezoelectric ceramics and ferroelectric crystals show linear relations, between components of stress and strain on the one hand and electric field and displacement on the other, only over limited ranges of the input signal. The limit of linear behaviour is related to the coercive force and varies widely with ceramic composition.

It is not possible to state concisely a specific set of conditions under which the definitions and equations of the linear theory apply. In many cases of practical interest mechanical dissipation is the most important limitation on the validity of an analysis carried out for an ideal piezoelectric material. In other cases non-linearities appear as consequence of high electric fields applied to the material.

Before starting the discussion about non-linearities it is convenient to know the coefficients relating to the *linear* response (low fields) of some commercially available hard and soft piezoelectric materials. Linear theory of piezoelectricity is briefly discussed in the chapter 2 and widely discussed somewhere else [6]. These *linear* coefficients are so-called *piezoelectric small-signal parameters*.

The most important small-signal parameters are:

- The *piezoelectric strain coefficient d*, which denotes the ratio between the relative mechanical expansion *S* and the applied field intensity *E* according to S=d.E
- The *piezoelectric voltage coefficient g,* which indicates the ratio between the electric field generated E to the mechanical stress T applied according to E=g·T
- The *relative permittivity* $\varepsilon/\varepsilon_0$.
- The *coupling factor k*, whose square k^2 is a measure of the conversion of electrical energy into mechanical energy
- The *dielectric loss factor*, *tan* δ, where δ denotes the real phase difference between the current and voltage (in an ideal dielectric $\delta=90º$)

Tables 6.3 and 6.4 show the small-signal parameters of some commercial hard and soft materials respectively. Parameters have been obtained from the respective manufacturer's data sheet.

Table 6.3. *Small-signal parameters for commercial 'hard-piezoelectric'*

Material (Lead Zirconate Titanate)		d_{33} (pC/N)	g_{33} (Vm/N)	e_{33}^T	tan d	k_{33}	s^E_{33} ($10^{-12}m^2/N$)	s^D_{33} ($10^{-12}m^2/N$)
Ferroperm [8]	**Pz24**	190	0.054	400	0.002	0.67	23	13
	Pz26	330	0.028	1300	0.003	0.68	20	11
	Pz28	320	0.034	1070	0.004	0.69	23	12
Morgan Matroc Limited [9]	**PZT-4D**	315	0.0246	1300	0.004	0.675	16.8	n/a
	PZT-8	225	0.0254	1100	0.002	0.640	13.5	8.5
	PZT-8S	-						
Ceramtech [10]	**Sonox P4**	310	0.0269	1300	0.003	0.68	18.1	n/a
	Sonox P8	240	0.0271	1000	0.002	0.68	13.7	n/a
	Sonox P88	325	0.029	1250	0.004	0.70	19.5	n/a
Philips Component [11]	**PXE41**	325	0.030	1225	0.0025	0.74	15	n/a
	PXE42	315	0.027	1325	0.0035	0.70	15	n/a
	PXE43	230	0.027	1000	0.0020	0.66	13	n/a

Table 6.4. *Small-signal parameters for commercial 'soft-piezoelectric'*

Material (Lead Zirconate Titanate)		d_{33} (pC/N)	g_{33} (Vm/N)	e_{33}^T	tan d	k_{33}	s^E_{33} ($10^{-12}m^2/N$)	s^D_{33} ($10^{-12}m^2/N$)
Ferroperm [8]	**Pz21**	540	0.016	3900	0.019	0.65	20	11
	Pz23	330	0.025	1500	0.013	0.65	19	11
	Pz27	425	0.027	1800	0.017	0.70	23	12
	Pz29	575	0.023	2900	0.019	0.75	23	10
Morgan Matroc Limited [9]	**PZT-5A**	374	0.0248	1700	0.020	0.710	18.8	9.4
	PZT-5J	500	0.0217	2600	0.020	0.690	22.7	n/a
	PZT-5H	593	0.0197	3400	0.025	0.750	20.8	9
	PZT-5R	450	0.025	1950	0.020	n/a	n/a	n/a
Ceramtech [10]	**Sonox P5**	450	0.0275	1850	0.020	0.73	19.0	n/a
	Sonox P502	440	0.0255	1850	0.0125	0.72	20.7	n/a
	Sonox P51	640	0.0200	3100	0.016	0.75	19.6	n/a
	Sonox P53	680	0.0190	3800	0.016	0.74	22.9	n/a
Philips Component [11]	**PXE 5**	500	0.024	2100	0.020	0.75	18	n/a
	PXE 52	700	0.020	3900	0.016	0.80	20	n/a
	PXE 59	460	0.028	1850	0.017	0.71	19	n/a
	PXE 21	450	0.025	2000	0.015	0.74	19	n/a

The bases of the linear theory are gathered in the IEEE Standard on Piezoelectricity 176-1987 and have been previously summarised in Chapter 2 of this thesis.

6.4. Non-linearities

6.4.1. External Electrical Conditions (Hysteresis)

The *expansion* of a ferroelectric ceramic is generally not proportional to the electric field *strength*. In a voltage/strain graph (*S-E* graph) this non-linear behaviour can be shown by a hysteresis curve. How much an actuator expands at a given voltage depends on whether it was previously operated at a higher or a lower voltage. The maximum width of the hysteresis loop is usually taken as a measure of the hysteresis of the material. This measurement depends on the maximum distance travelled, i.e., the maximum electric voltage applied to the actuator.

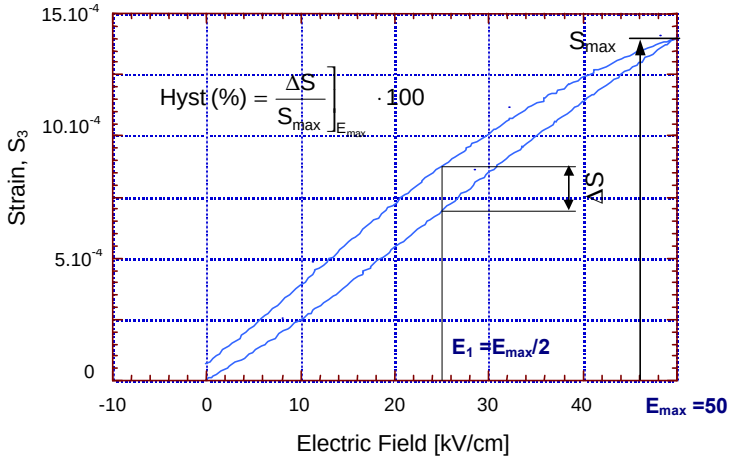

Figure 6.1. *Definition of the maximum strain and the degree of hysteresis*

Figure 6.1 shows the definition of the maximum strain S_{max}, and the degree of hysteresis $\Delta S/S_{max}(\%)$. The degree of hysteresis is calculated from the strain deviation during the rise and fall of the field ΔS at half of the maximum electric field divided by the maximum strain S_{max}.

$$\text{Hyst}(\%) = \left.\frac{\Delta S}{S_{max}}\right]_{E_{max}} \cdot 100 \qquad (6.1)$$

where S_{max} is measured at a maximum electric field, E_{max} , which has to be indicated.

Hysteresis is exhibited due to polarisation reorientation and is dependent upon the composition of the ferroelectric material. This is because a second interpretation of the hysteresis due to an electrical input can be made from the Polarisation – Electric Field graph. In this case hysteresis is measured as:

$$\text{Hyst}(\%) = \left.\frac{\Delta P}{P_{max}}\right]_{E_{max}} \cdot 100 \qquad (6.2)$$

Hard materials (materials with a coercitive field larger than 10 kV/cm) have a wide linear drive region, but relatively small strain magnitude. On the contrary, *soft materials*, with a coercive field between 1-10 kV/cm, have a large field induced strain, but relatively large hysteresis as will be displayed in the next sections.

• Experimental set-up for hysteresis measurements

(1) Set-up to measure the hysteresis from the P-E loop

To measure the hysteretic change in the *remanent polarisation* under *high electric field*, the Sawyer-Tower technique was used. This technique consists of measuring the polarisation in the piezoelectric sample against the electric field applied by means of a linear reference capacitor (Figure 6.2). All measurements were carried out at room temperature and with the sample maintained in a dielectric silicon oil bath to guarantee good dielectric conditions during the tests.

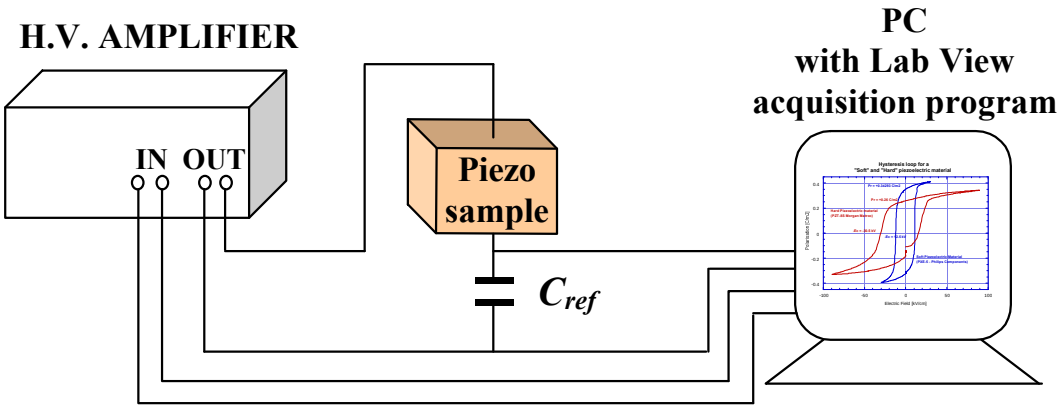

Figure 6.2. *Experimental set-up for measuring changes in the Polarisation.*

The piezoelectric sample was driven by a TREK RT6000HVA high voltage amplifier by ramping a maximum voltage up to +4kV and down to zero. The amount of the irreversible change in the remanent polarisation, DP_i, is equal to:

$$\Delta P_i = \frac{\Delta U_C \cdot C_{ref}}{A} \tag{6.3}$$

where DU_C is the residual voltage remaining on the capacitor C_{ref} after applying the electric field to the sample. The capacitor C_{ref} was chosen between a serial of 5 capacitors (10µF, 1µF, 100nf, 10nF, 1nF) to obtain a voltage DU_C in the range of 5V which was the maximum allowed for the acquisition card.

The output current in the TREK RT6000HVA high voltage amplifier is limited up to ± 20mA peak. This amplifier is configured as a non-inverting amplifier with a voltage gain of $1000V_{out}/V_{in}$. It has a solid-state four-quadrant, active output stage which sinks or sources current into reactive or resistive loads. The RT6000HVA is short circuit and overload protected and supplies a precision voltage monitor output which provides a low-voltage replica (in terms of voltage and phase) of the high voltage output. It has a small bandwidth of DC to 1 kHz (-3dB) and a large signal bandwidth of DC to 200 Hz. The DC gain accuracy is better than 0.1% over its full range. The experiments were controlled and monitored using LabView software.

It is important to note that Sawyer-Tower technique allows measuring only the change in the remanent polarisation but not the absolute value of the remanent polarisation.

(2) Set-up to measure the hysteresis from the S-E (Strain-Electric Field) loop

In order to measure the hysteresis behaviour of a piezoelectric material from the *S-E* loop, the same set-up may be used to drive the electric field to the sample. Nonetheless, the measurement of strain requires the use of a strain sensor. A photonic strain sensor MTI 2000 Fotonic Sensor (MTI Instrument Division, Latham, NY, USA) with a corresponding set of electronic equipment or a strain gauge attached to the disc may be used.

(3) Analogy between the S-E and the P-E (Polarization-Electric field) hysteresis measurements

Hysteresis measurement used to be made by measuring the function $S_3(E)$. However at voltages lower than the coercive field the relation between the polarisation and the strain is linear and hysteresis measured is equivalent if it is measured from the *S-E* curve or from the *P-E* curve [13].

The results shown here are regarding to the P-E hysteresis loop. Three different hard piezoelectric compositions, such as PZT-8S (Morgan Matroc) and Sonox P8 and P4 (from CeramTec), have been tested ramping a maximum electric field up to +1000V/mm and down it to zero. As for soft piezoelectric materials, the PXE-5 (Philips Components) and Pz21 and Pz29 (Ferroperm) were used. The voltage ramped in soft material was of only 500V/mm due to the lower depoling resistance of these type of materials. The frequency of the loops was 5Hz in both cases.

- **Experimental Results**

HARD MATERIALS (PZT-8S, Sonox P8, Sonox P4) (E_{max} = 1kV/mm)

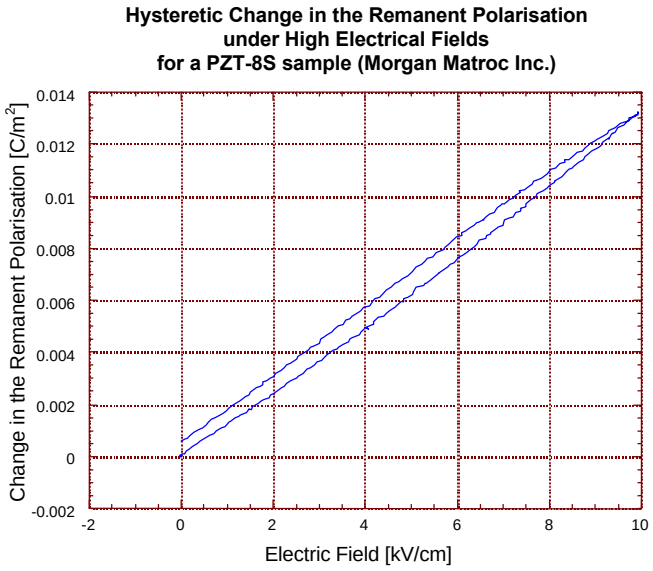

Figure 6.3. *Hysteresis loop exhibited for a sample of PZT-8S (Morgan Matroc Inc.)*

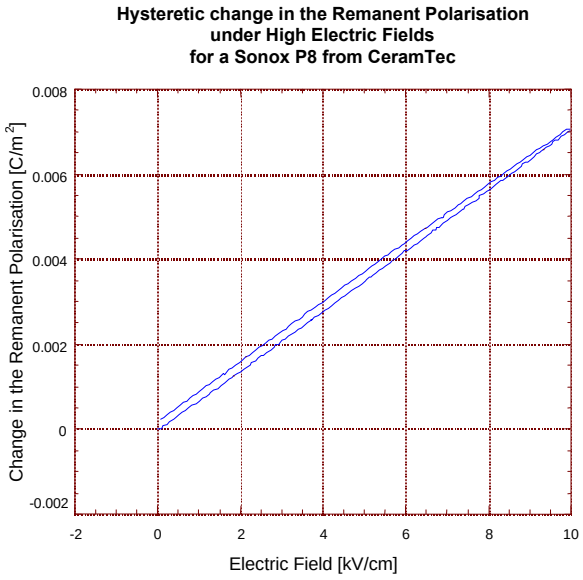

Figure 6.4. *Hysteresis loop exhibited for a Sonox P8 sample (CeramTec)*

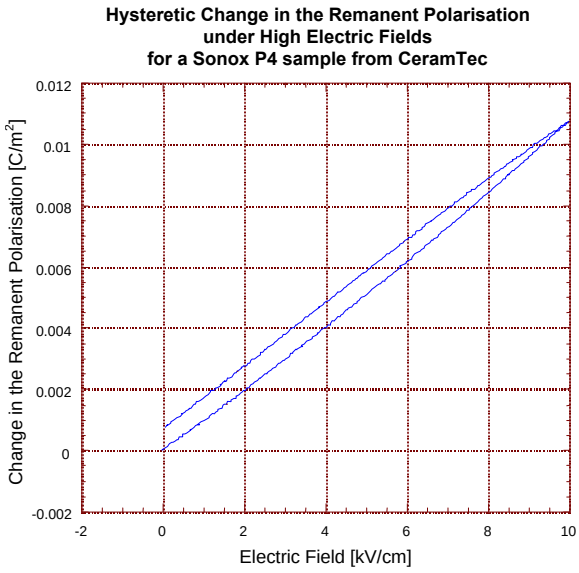

Figure 6.5. *Hysteresis loop exhibited for a Sonox P4 sample (CeramTec)*

SOFT MATERIALS (PXE-5, Pz21 and Pz29) (E_{max} = 500V/mm)

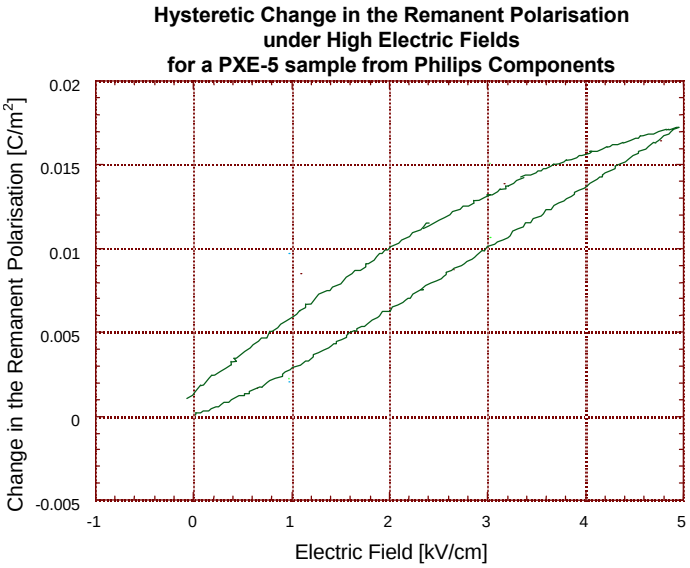

Figure 6.6. *Hysteresis loop exhibited for a PXE5 sample (Philips Component)*

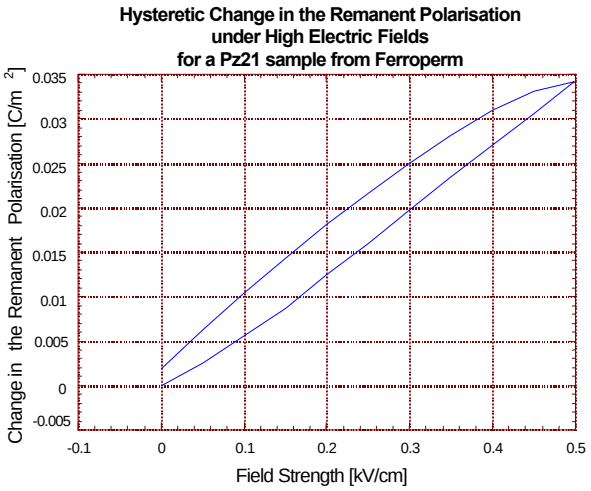

Figure 6.7. *Hysteresis loop exhibited for a Pz21 sample (Ferroperm)*

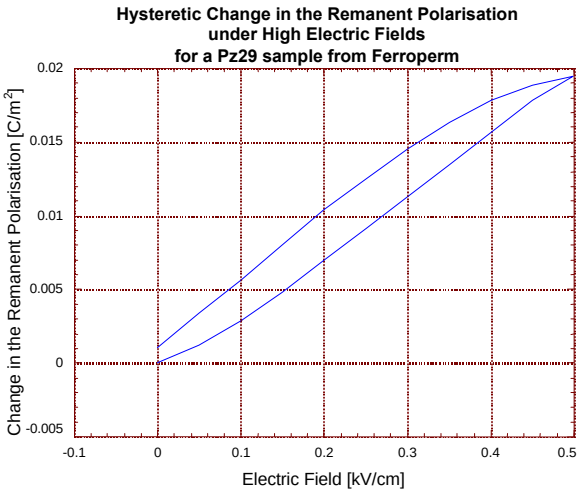

Figure 6.8. *Hysteresis loop exhibited for a Pz29 sample (Ferroperm)*

The next table summarises the results obtained in the previous results, which are compared with values of some manufacturers.

Table 6.5. *Typical Hysteresis valuse for commercial soft and hard piezoelectric ceramics*

Material (Lead Zirconate Titanate)			**Hysteresis**	
			DP/P_{max} (measured)	**DS/S_{max} (Data Sheets)**
Ferroperm [8]	**Soft**	Pz21	16.36%	25%
		Pz27		40%
		Pz29	17.22%	30%
	Hard	Pz26		40%
		Pz28		n/a
Morgan Matroc Limited [9]	**Soft**	PZT-5H		10-18
		PZT-5A		
		PZT-5J		
	Hard	PZT-4		6-10%
		PZT-8		3-6%
		PZT-8S	7.864%	
CeramTec [10]	**Soft**	Sonox P53		
		Sonox P5		
		Sonox P51		
	Hard	Sonox P4	6.838%	
		Sonox P8	3.052%	
Philips Component [11]	**Soft**	PXE52		
		PXE59		
		PXE5	31.670%	
	Hard	PXE41		
		PXE43		

Figure 6.9 compares in the same graph the previous experimental results from hard and soft piezoelectric materials. Hard materials show a hysteresis lower than 10% while in soft materials this value increases up to 35-40%. On contrary, the sensitivity (C/N) is higher in soft materials (higher slope angle).

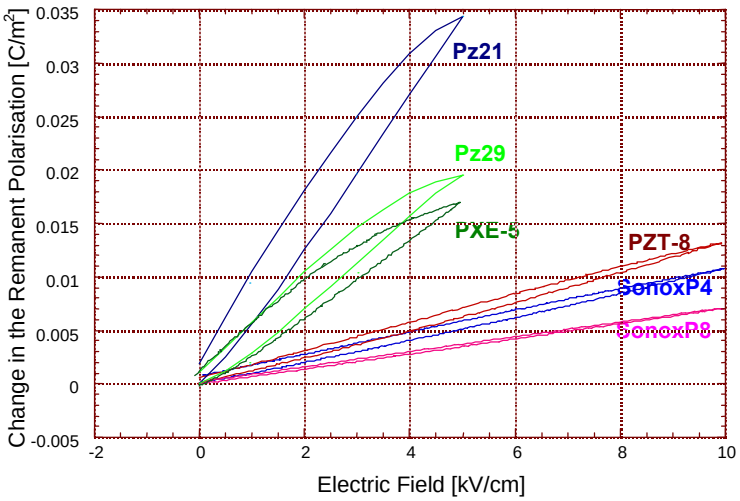

Figure 6.9. *Comparison of the hysteresis exhibited for different composition of soft and hard piezoelectric materials.*

6.4.2. External Mechanical Conditions

6.4.2.1. Static Stress in a Piezoelectric Material

Piezoelectric materials generate an electrostatic charge when forces are applied to or removed from them. However, even though the electrical insulation resistance is quite large, the electrostatic charge will eventually leak to zero through the lowest resistance path. In effect, if a static force is applied to a piezoelectric force sensor, the electrostatic charge output initially generated will eventually leak back to zero.

The rate at which the charge leaks back to zero is dependent on the lowest insulation resistance path in the sensor, cable and the electrical input resistance/capacitance of the amplifier used.

When leakage of a charge (or voltage) occurs in a resistive-capacitive circuit, the leakage follows an exponential decay. A piezoelectric force sensor system behaves similarly in that the leakage of the electrostatic charge through the lowest resistance also occurs at an exponential rate. The values of the electrical capacitance of the system (in farads), multiplied by the value of the lowest electrical resistance (in ohms) is called Discharge Time Constant (in seconds).

In this way, static stress has only a temporal piezoelectric response which disappears after some time. However, it will be shown later (cf. 6.4.2.3) that the strength of a static stress in the material may influence its piezoelectric behaviour.

6.4.2.2. Alternative Stress (with an initial Prestress)

If the mechanical stress is alternative, an electric alternative charge will appear which will be proportional to the strain piezoelectric coefficient given as:

$$Q_3(t) = d_{33} \cdot T_3(t) \tag{6.4}$$

Nevertheless, the piezoelectric coefficient may be higher or lower depending on the stress strength as it has been already found [14]. Here we introduce the experimental setup to carry out this kind of measurement and experimental results concerning to the behaviour of soft and hard materials.

- **Experimental Set-up**

In order to measure the dependence of d_{33} against T, $d_{33}(T)$, an uniaxial sinusoidal pressure of 2MPa and 1Hz is applied on the samples by using a stacked piezo actuator. The applied alternative stress is measured using a reference quartz sensor that is placed mechanically in series with the sample and the source of the alternating force. The piezoelectrically induced charges from the sample and the reference sensor were converted into voltage via charge amplifiers operating in virtual earth. The force and charge results may be digitised and collected using standard ADC techniques and the experiments controlled and monitoring using LabView software.

All measurements are performed under a static preload of 18MPa to ensure a good transfer of force between the source, the sample and the reference sensor. The static preload is measured using the 'LONG' integration time constant mode of the KYSTLER 5011 charge amplifier, and an oscilloscope operated in DC mode.

Figure 6. 10 offers a view of the used experimental setup.

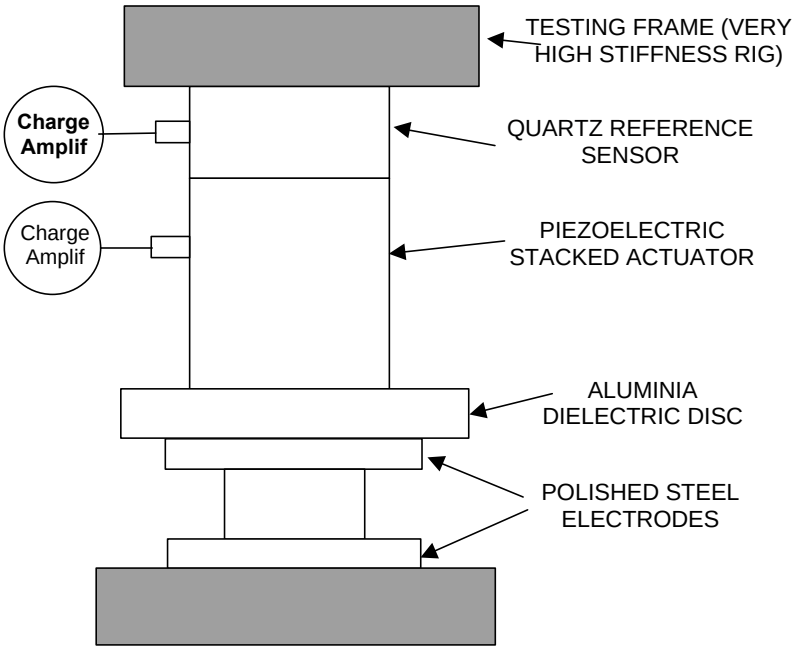

Figure 6.10. *Testing rig used to analyse the AC stress effect.*

- **Experimental Results**

The dependence of the coefficient d_{33} against an AC applied stress was measured for a soft sample of PZT-5A disc of 1mm thickness and 10mm diameter. The strain piezoelectric coefficient measured as function of applied AC stress is shown in Figure 6.11. It can be observed an increase of approximately 5% per each MPa .

This value is compared with the hard material behaviour, also shown in Figure 6.11. Hard materials have a higher stability against AC stress. In particular an increase of approx. 2% per 1MPa has been found for a similar PZT-8 sample.

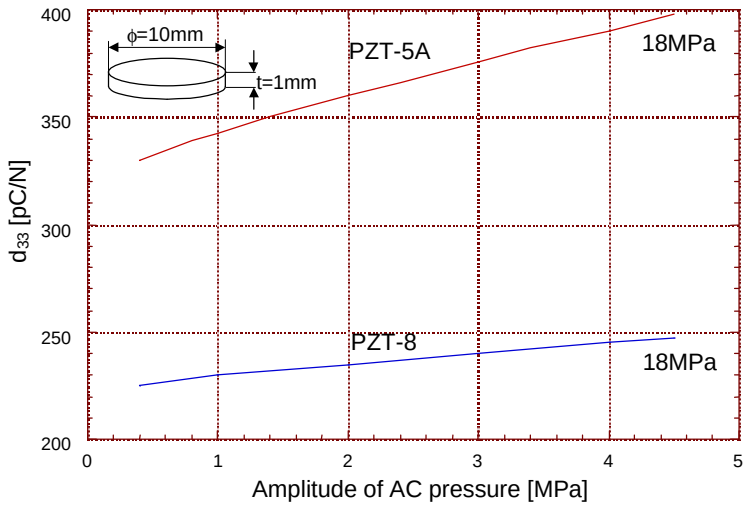

Figure 6.11. *Strain piezoelectric coefficient, d_{33} , as a function of the amplitude of AC pressure.*

6.4.2.3. Effect of the Static Prestress in the Response of a Piezoelectric material when is driven with an electrical signal

Effect of the static prestress has been analysed elsewhere [15,16,17,18] from the relative permittivity and the losses (*tan d*). In these studies, permittivity and loss are measured using an impedance analyser and associated high sensitivity dielectric interface unit. This system, is able to automatically measure the dielectric current, voltage and phase across the sample and compare this to the identical drive through either an internal or (in this case) an external standard reference capacitor.

- **Experimental Results**

The increase in permittivity and dielectric loss has been attributed to an increase in the extrinsic ferroelectric domain wall motion and domain switching at high applied fields. The measurement method ramped the applied electric field from a low signal response to values reaching approximately 300 $V_{pk\text{-}pk}$/mm. This value should be well below than the necessary for domain switching.

The graphs in Figure 6.12 (a,b) demonstrates the change in permittivity and loss for a hard material PZT-4 as a function of applied electric field and at various uniaxial static loads.

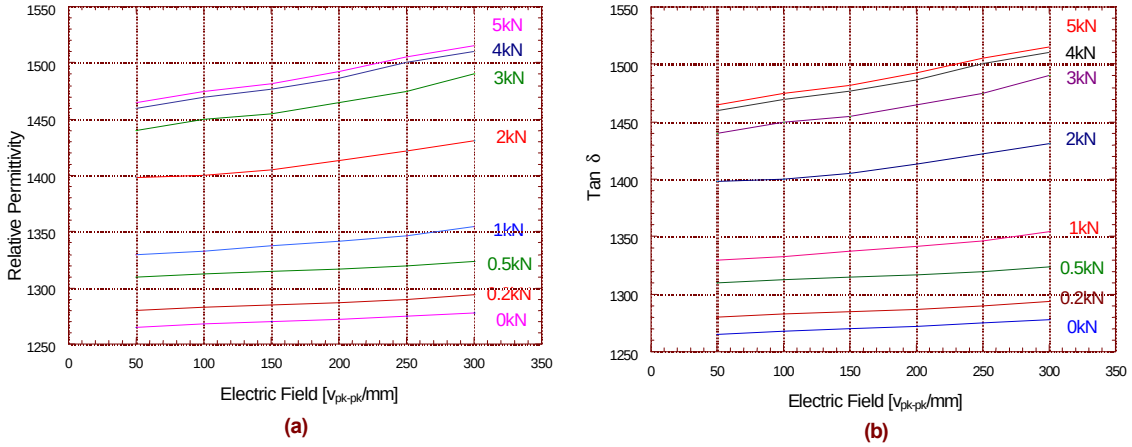

Figure 6.12. *(a) Permittivity and (b) losses as a function of static load and electric field for a PZT-4 hard material measured at 100Hz.*

The data for the PZT-4 material shows a large increase in permittivity with increasing uniaxial stress (approx. 16% for low signal response) and similarly a gradual increase in permittivity with electrical drive, as expected. In a similar fashion, the loss tangent increases with increasing electric field and static stress, Figure (6.12 b).

It is important to minimise any residual clamping at the ends of the sample, which have the effect of reducing the changes in permittivity with increasing stress. This may be accomplished through the use of polished end pieces, polished sample ends and by the use of a lubricant such as graphite powder applied between the mating surfaces. It is additionally important to ensure that the stress state present within the sample is as uniform as possible. This may be accomplished by ensuring that the diameter to thickness ratio exceeds 3:1 [16,19].

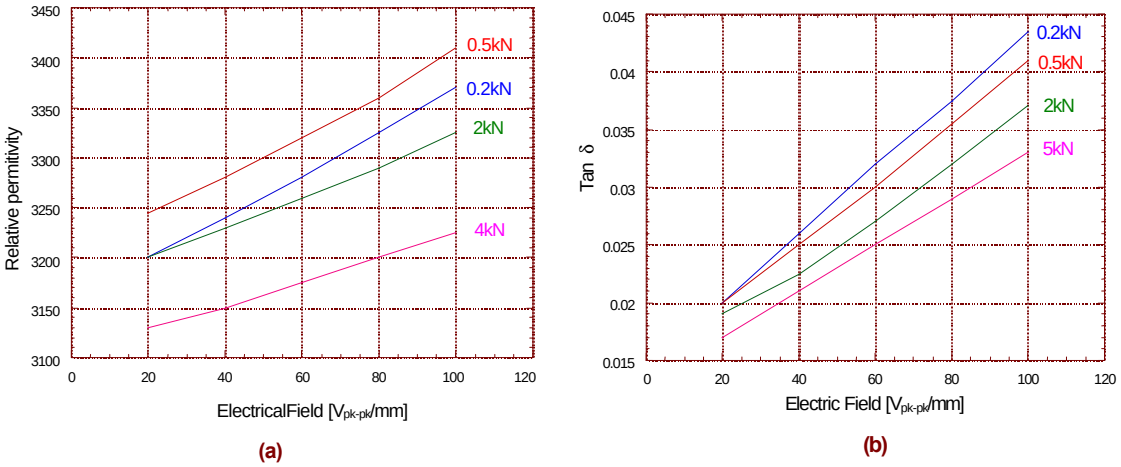

Figure 6.13. *(a) Permittivity and (b) losses as a function of static load and electric field for a PZT-5 soft material measured at 100Hz.*

The data obtained for the soft 5H material differs markedly from the results obtained with the harder material. In this case, the permittivity and loss tangent decrease with increasing static stress, whilst increasing with applied electric field, Figure 6.13(a,b) for 100Hz and 6.14(a,b) for 1kHz.

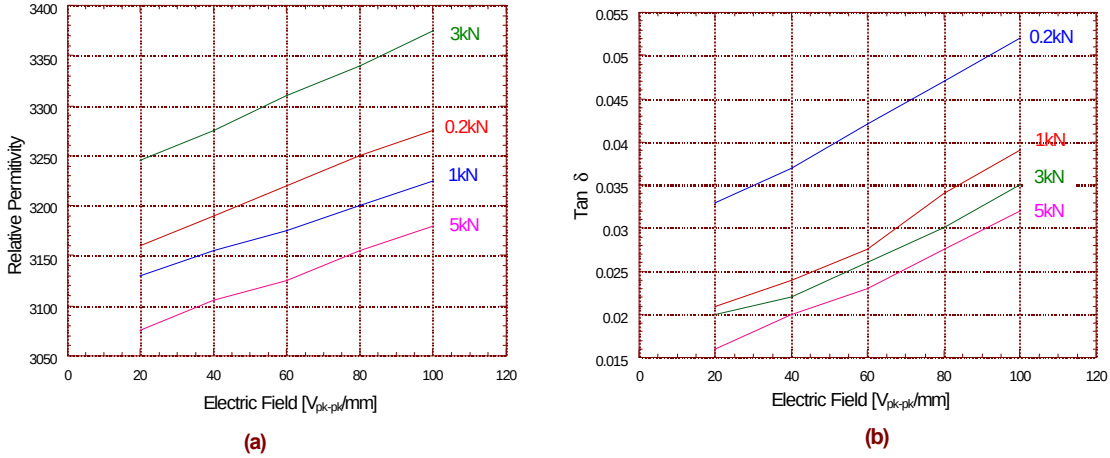

Figure 6.14. *(a) Permittivity and (b) losses as a function of static load and electric field for a PZT-5 soft material measured at 1000Hz.*

The increase in dielectric properties with increasing electric field is expected and has been widely reported, as having similar origins to the hard materials response, and linked to the irreversible domain wall motions [17]. It may be that with the softer materials stress clamping acts to hinder the generation of new domain walls which otherwise would have contributed to the permittivity and loss, evident in the harder materials. However, it is still not clear why the stress dependence of the dielectric properties of hard materials differ so dramatically compared with soft materials.

6.4.3. Frequency Dependence

Frequency dependence is measured with the same frame used to measure the dependence from the alternative stress (cf. 6.4.2.2). However, now an AC force is applied at different frequencies with the stacked piezo-actuator. The magnitude of the applied AC force was 3MPa. A static preload of 18MPa was applied to improve the mechanical transmission.

- **Experimental Results**

Measurements have been performed for soft and hard materials (Figure 6.15). In soft materials the piezoelectric coefficient, d_{33}, decreases with the logarithmic of the frequency as had been previously shown by different research groups [14,15,20].

This behaviour is compared with the data plotted for PZT-4 and PZT-8 hard materials. In both cases the behaviour does not exhibit the dispersive relationship that is found for the soft materials which indicates a better stability of this type of compositions.

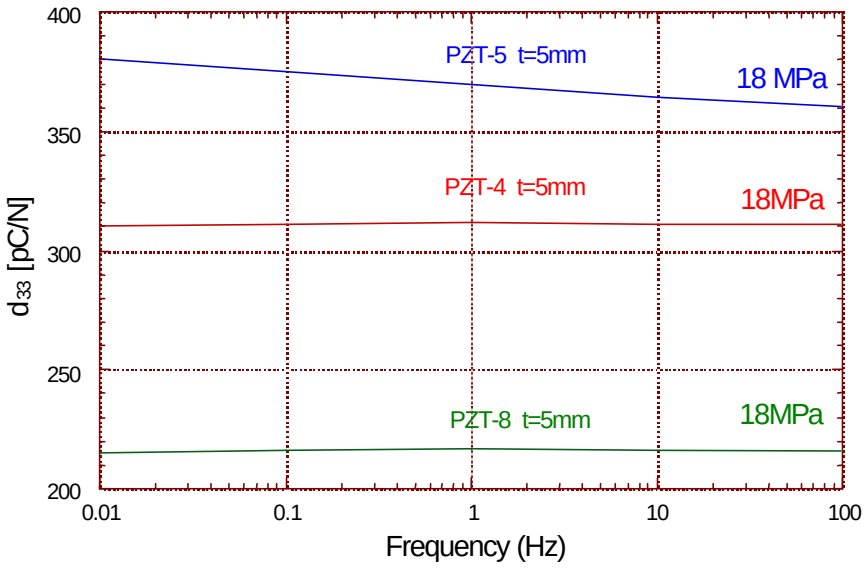

Figure 6.15. *Dependence of the d_{33} coefficient with the frequency for a soft (PZT-5) and hard materials (PZT-4 ; PZT-8)*

6.5. Degradation

6.5.1. Ageing (Natural Time Evolution)

Usually, properties in a piezoelectric material depend gradually on time. In general, this dependence may be explained by using a logarithmic function, which is called *Ageing Rate*.

$$\text{Ageing Rate} = \frac{1}{[\log t_2 - \log t_1]} \cdot \left[\frac{P_2 - P_1}{P_1}\right] \tag{6.5}$$

where:

- t_1 and t_2 are the numbers of days after the polarisation
- P_1 and P_2 represent the value of the parameter being studied

This evolution depends on the composition of the ceramic and on the processes following during their manufacturing. In particular, the evolution of the properties during the first moments after the poling is very unstable. In order to have a reference value for measuring the ageing, the time t_1 of equation (6.5) is taken as 24houres (1 day) after the polarisation, as is specified in reference [6].

Manufacturers provide the ageing rate in % of decay for the most characteristics parameters, as indicated equation (6.6).

$$\text{Ageing Rate} = \frac{\text{percent change}}{\text{decay of time}} = \frac{\%}{1 \text{ decay}} \tag{6.6}$$

Since this definition, $t_2 = 10 \cdot t_1$, and by using equation 5.5, it is possible to find the value of a certain magnitude after a decay of time may be expressed as:

$$P(t_2 = 10 \cdot t_1) = P(t_1) \cdot \left(1 + \frac{\text{Ageing Rate}}{100}\right) \tag{6.7}$$

The sign of the Ageing Rate will indicate weather the magnitude considered is increasing (+) or decreasing (-) with time.

Figure 6.16 shows the effect of ageing over three compositions of PZT materials. The soft PZT-5A has an initial d_{33} value of 374pC/N and an ageing rate of –2.9%/decay. The hard material PZT-4D has an initial d_{33} value of 315pC/N and an ageing rate of –3.4% and the PZT-8 has a d_{33} initial value of 225pC/N and an ageing rate of –6.3%.

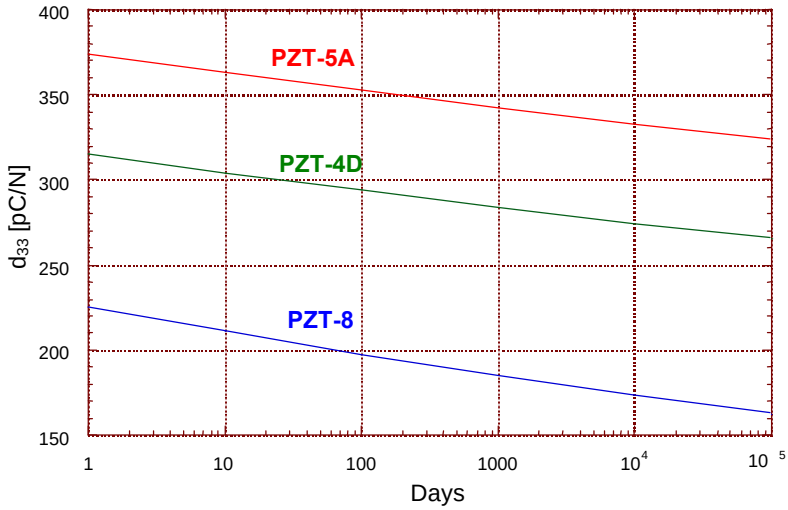

Figure 6.16. *Time Stability for d_{33} coefficient of soft and hard compositions.*

6.5.2. Fatigue

6.5.2.1. Electrical Fatigue (number of cycles evolution)

Electrical fatigue for hard and soft materials use to be measured using dielectric impedance methods and monitoring the degradation in electrical properties such as the permittivity.

The test may be carried out by using the same set-up used to measure the d_{33} evolution against the frequency and the AC stress. In previous work [20] permittivity was measured as a function of the time for a relatively short duration (approximately 10^4 cycles) with an applied electric field of $500V_{pk\text{-}pk}$/mm at a frequency of 100Hz. In the mentioned work [20] electrical fatigue in piezoelectric ceramics was manifest as degradation in polarisation and a corresponding increase in loss.

The degradation of dielectric properties with electrical cycling of a soft PZT-5H material is shown in Figure 6.17.(a), and for a hard PZT-4D material in Figure 6.17.(b). Both measurements correspond to a previous work [15].

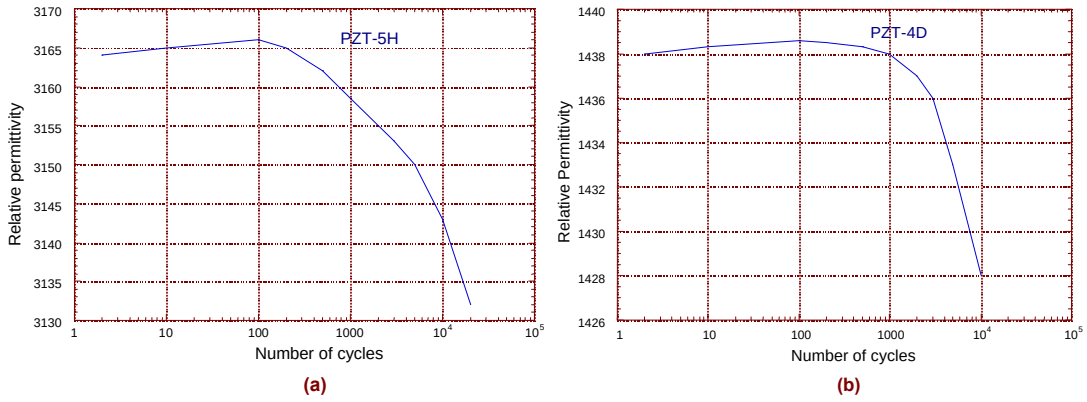

Figure 6.17. *Electrical fatigue for (a) a soft and (b) a hard material*

Figure 6.17 shows that the hard material is more stable against the electrical fatigue. Hard material requires 10^3 cycles to initiate the fatigue while soft material becomes fatigued with only 10^2 cycles. However, once the fatigue starts, the corresponding increase in loss was approximately 2.5% for soft material and practically 20% for the hard material.

6.5.2.2. Mechanical Fatigue (number of cycles evolution)

Mechanical fatigue in the d_{33} coefficient for a soft PZT-5 material is shown in Figure 6.18. The piezoelectric charge coefficient was measured as a function of cycles of an AC force of 3 MPa and 200 Hz. A static preload of 18 MPa is applied to guarantee a good mechanical transmission.

Figure 6.18 shows how the degradation arrives at 20% of the initial value of d_{33} after approximately 10^7 cycles.

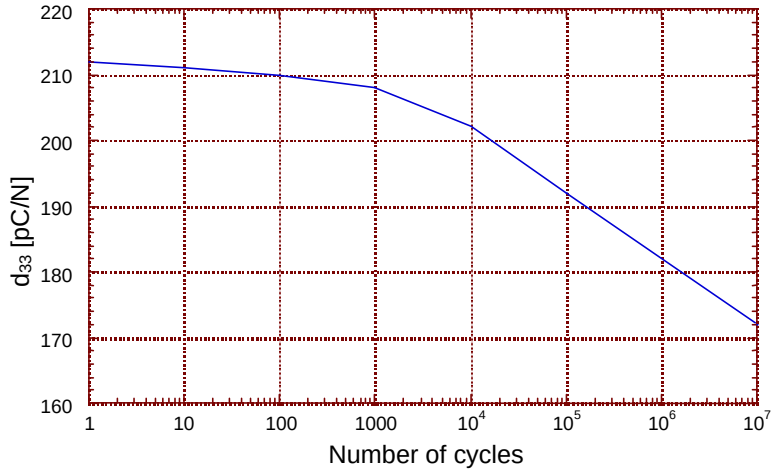

Figure 6.18. *Mechanical fatigue*

6.5.3. Depolarisation

6.5.3.1. Electrical Depolarisation

A very strong field opposite to the polarisation vector could lead to the reversal of the polarisation in the domains (*domain switching*). An evaluation of the resistance to domain switching could be made with the *coercive field strength* E_C, the strength of the field required to reduce the polarisation **P** to zero.

The experimental measurement of the resistance to domain switching was made by using the same set-up as was used for linearity measurement, i.e. the Sawyer-Tower technique. A pair of single triangular electric pulses having opposite polarities was delivered to the sample by means of an amplifier RT6000HVA already described. The frequency chosen for the triangular signal was 10Hz. The experiments were controlled and monitored using LabView software. The strength of the electric field applied to the sample was progressively increased until a complete change in the polarisation was observed. For soft material, as is shown in Figures 6.19 and 6.20, it is possible to obtain a complete polarisation loop because the strength necessary to turn the internal dipoles is low. However, when hard materials are tested (Figures 6.21 and 6.22) the field required to turn totally all the dipoles is very high and is only possible to obtain a complete loop if very thin samples are used. Also, problems of breakdown appear when this high voltage is applied.

Experimental tests were carried out with samples of SonoxP8, SonoxP4 and PZT-8 as hard materials, and a sample of PXE-5 as soft material. Dimensions and shapes are indicated in the graphs.

Figure 6.19 shows the polarisation loop for the PXE-5 sample. A coercive electric field was determined as approx. 12.5kV/mm while the shown remanent polarisation was 0.34C/m^2, which is consistent with result from similar experiments gathered in previous works [21].

It must be noted that the measurement performed correspond to the change in the remanent Polarisation. The value of P_r depends upon the poling conditions used. Standard poling conditions are used to apply a DC electric field of approx. 5kV/mm to the sample at 150ºC for 2 minutes under silicone oil.

In order to obtain the absolute value of the remanent polarisation (indicated as Pr=0.34293 in Figure 6.19) is necessary to apply a high voltage as close as possible to the poling voltage. For example, if an electric voltage of 15 kV/cm is applied, the P_r measured is less than 0.3C/m^2. If the voltage is increased up to 30kV/cm the polarisation increases up to 0.34. From this point an increase in the electric voltage provides practically the same value for *Pr*, which indicates that this is the maximum *Pr*.

Once the value of the remanent polarisation is known, it is possible to represent the polarisation loop against the electric loop for the absolute value of the polarisation (Figure 6.20).

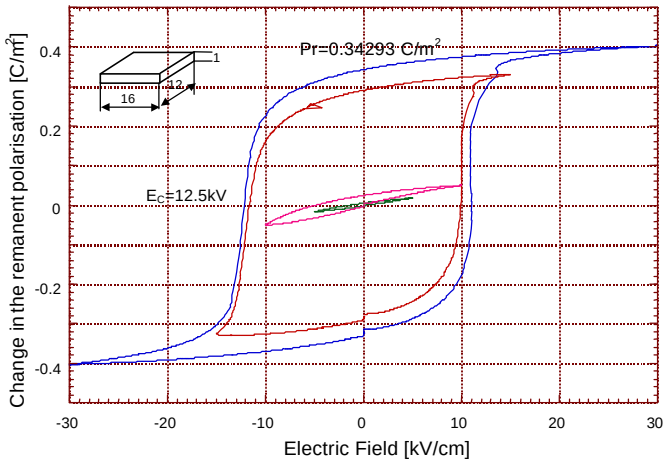

Figure 6.19. *Hysteresis loop for the Pxe-5 (Philips Component) piezoelectric material*

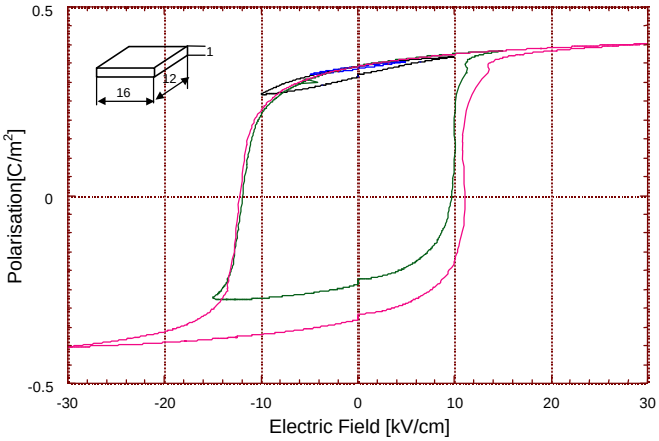

Figure 6.20. *Hysteresis loop for a PXE-5 sample (Philips Component) using the absolute polarisation to represent the loops*

Figure 6.21 shows the hysteresis loop of polarisation with an electric field for a sample of PZT-8S. The remanent polarisation P_r exhibited for the material was estimated as 0.30C/m^2 and the coercive field as E_C = 30.5kV/cm. The material can stand-up to fields higher than 15kV/cm before depolarisation.

It is interesting to note that before the 'first depolarisation' is achieved, the resistance of the material is harder (25kV/mm). Once the first complete loop is achieved the depolarisation resistance decreases (15kV/mm) because some of the dipoles remain partially switched. In order to obtain a more accurate result the sample should be repoled after each loop to start from the same initial properties.

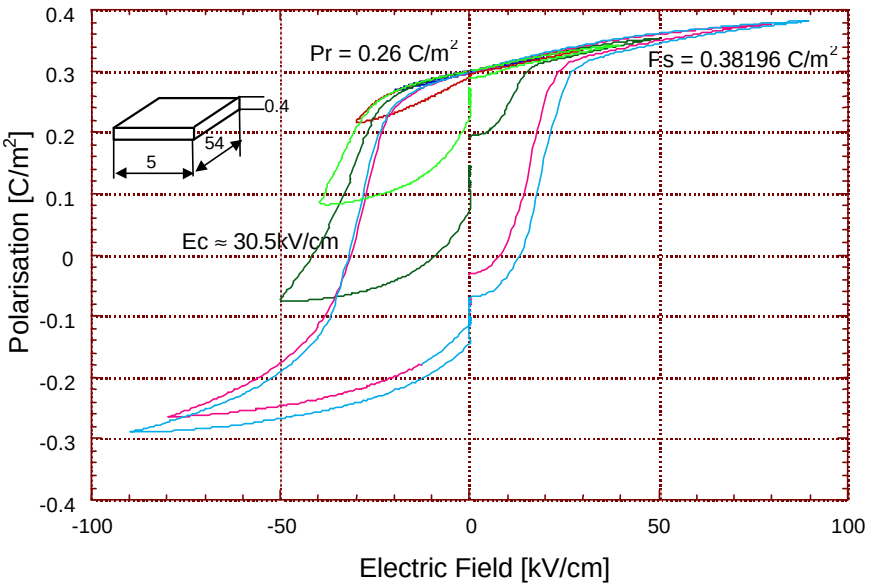

Figure 6.21. *Hysteresis loop for the PZT-8S (Morgan Matroc) piezoelectric material*

Figure 6.22 and 6.23 shows the analogous results for a sample of SonoxP8 and SonoxP4 from CeramTec.

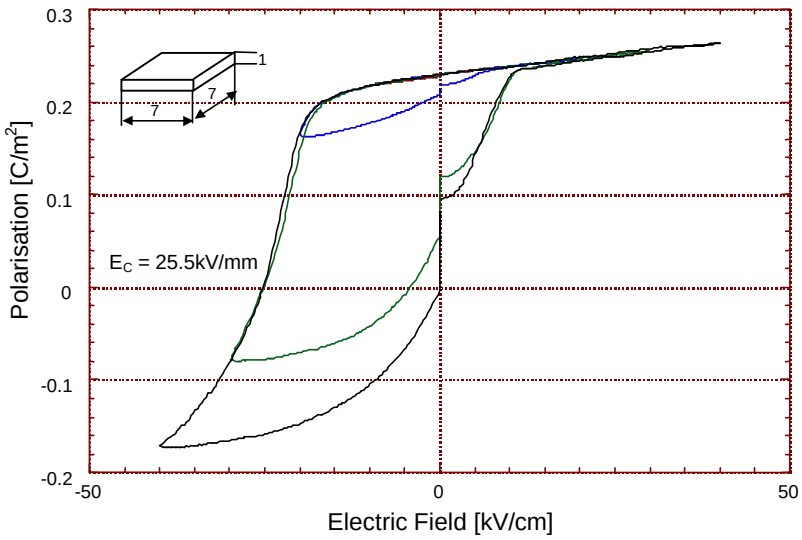

Figure 6.22. *Hysteresis loop for the SP8 (CeramTec)*

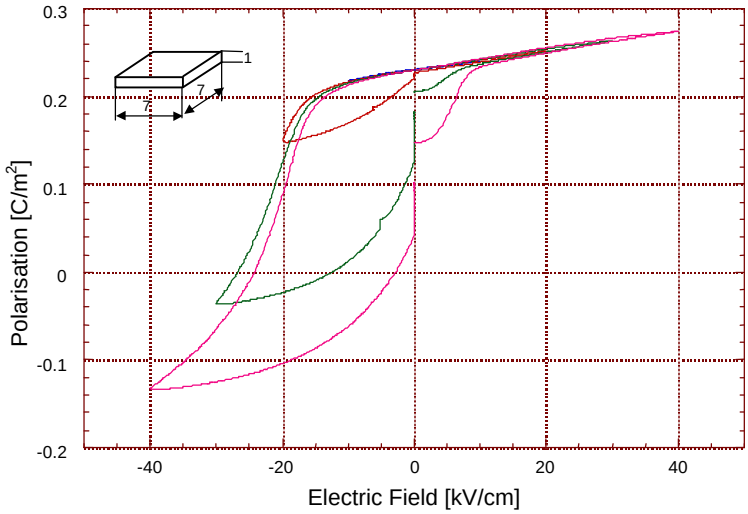

Figure 6.23. *Hysteresis loop for the SP4 (CeramTec)*

From the above results we obtain the values indicated at Table 6.6.

Table 6.6. *Depoling resistance of some commercial piezoelectric*

Material		Coercive Field Ec (kV/mm)
Morgan Matroc Limited [3]	**PZT-4D**	
	PZT-8	3.5
	PZT-8S	
Ceramtech [4]	**Sonox P4**	2.5
	Sonox P8	2.2
	Sonox P88	
Philips Component [5]	**PXE5**	1.1
	PXE41	
	PXE43	

Next figure 6.24 shows a comparison between the responses of the PZT-8S from Morgan Matroc and the SP8 from CeramTec when high electric alternative fields are applied.

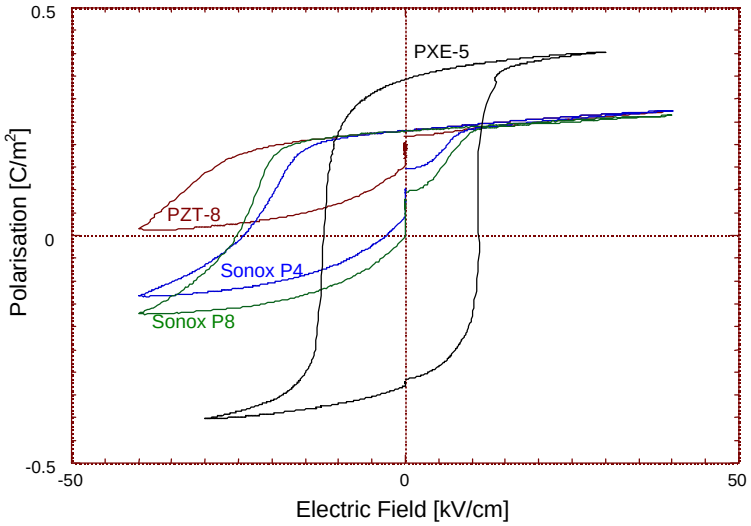

Figure 6.24. *Comparison between the depoling resistance of the PZT-8 and the Sonox P8*

6.5.3.2. Mechanical Depolarisation

Figure 6.25 shows the expected strain and depolarisation behaviour for a PZT-type material measured under uniaxial stress. In the initial linear region (A-B) the material behaves linearly, with the polar direction parallel to the applied stress. In the region C-D the domains start to switch, giving rise to non-linearity and it is only linear again in the region D-E, where the polar direction is now perpendicular to the applied stress. When the stress is removed (A-F) the material is left with a remnant strain and polarisation.

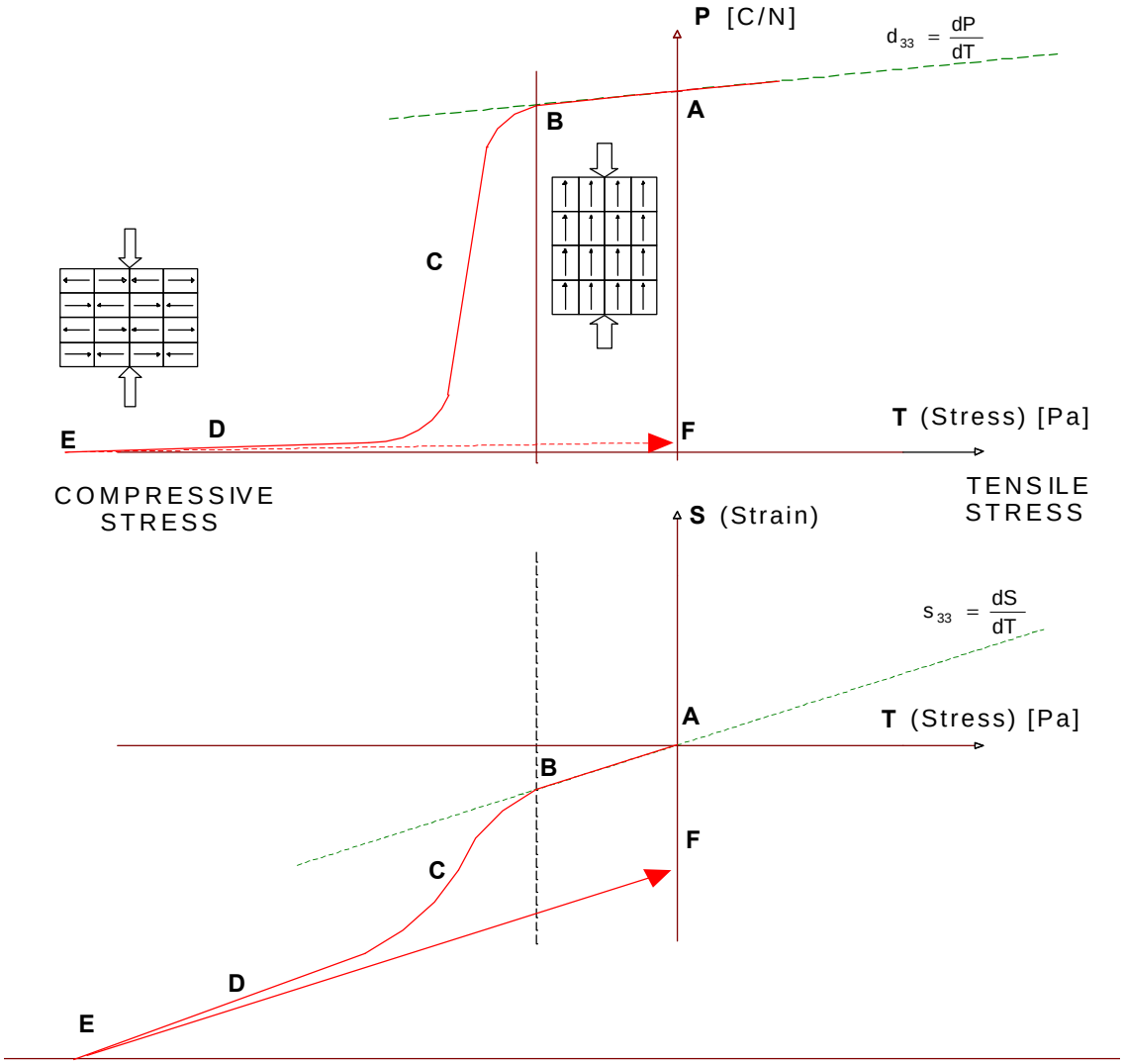

Figure 6.25. *Mechanical Depolarisation when a compressive force is applied*

In practice, the first linear region extends up to around 20 MPa for soft and 80 MPa for hard materials, with full depolarisation requiring up to 400 MPa stress levels. Clearly, 400 MPa is a large stress to apply to a piezo-ceramic. However, once the initial linear region is exceeded, there is always some remanent strain and polarisation. This may be accumulated by driving materials around this load cycle several times.

Philips Components provides a guide for the depoling limits as indicated in the following Table 6.7.

Table 6.7. *Depoling limits for a PXE materials (Philips Components)* [11]

PXE Composition	Electric Field Strength (V/mm)	Mechanical Pre-stress (MPa)
PXE59	350	5
PXE5	300	2.5
PXE52	100	-
PXE41	300	10
PXE42	400	25
PXE43	500	35

Recently a work regarding to the compressive behaviour of piezoelectrics has been carried out [22] where the behaviour of the compliance s_{33} of the material under stresses up to 400MPa is shown. Figures 6.26.(a) and 6.26.(b) illustrate the results obtained. Conclusions indicate that the mechanical stressing of PZT produces irreversible switching of 90º domains. This leads to highly anisotropic deformation behaviour for poled materials.

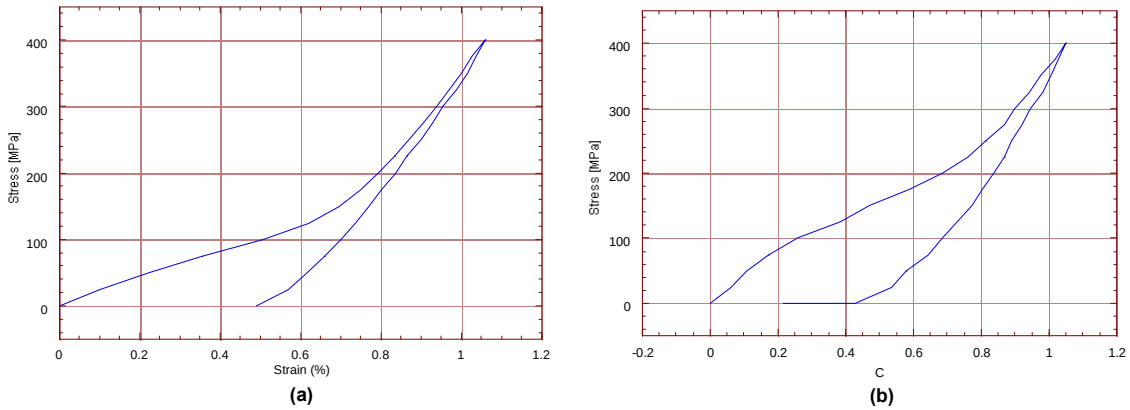

Figure 6.26. *Compression stress-strain test for (a) a PZT-5H soft material and (b) for a PZT-4D hard material.*

Figure 6.27 displays another interesting result according to the behaviour of the material under cyclic compressive stresses, 200, 300 and 400MPa. The cyclic loading initially produces a significant increment in the cumulative irreversible strain on each cycle before eventually saturating. These cyclic effects are much more significant for hard materials.

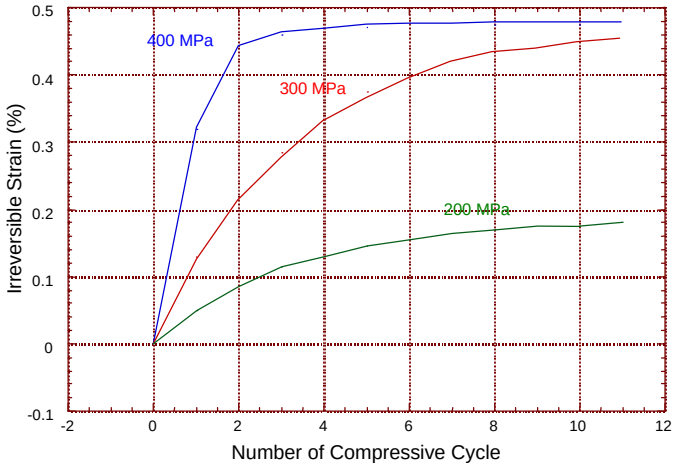

Figure 6.27. *Cumulative irreversible strain in constant stress amplitude cyclic compressive test*

The limit on the applied stress is also dependent on the duration of the applied stress. For dynamic stress (impact ignition) the limit is less severe; materials with higher energy output (high *g* constant) can be used. For impact applications, the material behaves quasistatically (non-linear) for pulse duration of a few milliseconds or more. When the pulse duration approaches a microsecond, the piezoelectric effect becomes linear, due to the short application time compared to the relaxation time of the domains

6.5.3.3. Thermal Depolarisation

If a piezoelectric element is heated to its Curie point, the domains become disordered and the material becomes completely depolarised. A piezoelectric element can therefore function for long period without marked depolarisation only at temperatures well below the Curie point. A safe operating temperature would normally be about half way between 0ºC and the Curie point. Following Table 6.8 gathers the Curie temperature of some commercial piezoelectric ceramics.

Table 6.8. *Curie temperature for some commercial piezoelectric ceramics*

Material			Curie Temperature [ºC]
Ferroperm [8]	**Soft**	Pz21	>180
		Pz27	>350
		Pz29	>235
	Hard	Pz26	>330
		Pz28	>330
Morgan Matroc Limited [9]	**Soft**	PZT-5H	195
		PZT-5A	365
		PZT-5J	250
	Hard	PZT-4D	320
		PZT-8	300
		PZT-8S	300
CeramTec [10]	**Soft**	Sonox P53	215
		Sonox P5	340
		Sonox P51	200
	Hard	Sonox P4	325
		Sonox P8	305
Philips Component [11]	**Soft**	PXE52	165
		PXE59	360
		PXE5	285
	Hard	PXE41	315
		PXE43	300

6.6. Conclusions

6.6.1. Introduction

The importance of the characteristics of the selected materials has been shown as determinant part for achieving high features in piezoelectric devices. In particular, this chapter has been concentrated upon ceramic piezoelectrics because these materials are commercially and widely available at low cost. The gathered results are for PZT soft and hard compositions.

Nonetheless, the non-linearity and degradation exhibited by PZT compositions limit their application in very accurate and feasible devices. This is the case of the instrument piezoelectric transformers considered in this thesis. Moreover, the ageing and fatigue displayed by PZT compositions clearly make them inadequate for a device which must operate constantly connected to the network at 50Hz.

As a result, there is a need to investigate and propose other ferroelectric ceramics as potential candidates for applications under extreme conditions and also to evaluate the possibility of using single crystals (such quartz) in our application.

6.6.2. Behaviour of PZT ceramics under extreme conditions

Here a brief review of the results obtained during this chapter relating to the limitations of the PZT compositions is provided.

Hysteresis was measured in hard materials and soft materials. A value lower than 10% was found for hard materials when the maximum ramping applied voltage was of 1kV/mm. In soft materials the hysteresis increased up to 20-30% for a driving voltage of 0.5kV/mm. On the contrary, the *sensitivity* displayed was higher in soft materials.

Electrical depolarisation in soft materials appears at voltages in the order of 500V/mm, while hard materials allow an alternative electric field higher than 1kV/mm without depoling. In particular PZT-8S have shown an electrical depolarisation resistance higher than 1.5kV/mm.

Mechanical depolarisation in a PZT-5H soft composition starts at around 20MPa while in a PZT-4D material this resistance go up to 80MPa. A field of 200MPa is required for the complete depolarisation of soft materials and 400MPa for hard materials.

According to the *thermal resistance*, which is dependent on the *Curie temperature*, this is higher in general for hard materials and with values of the order of 300-330ºC. Operation temperature must be kept bellow the Curie point, approximately at 150ºC for hard material and 90ºC-100ºC for soft materials.

Stability in front dynamic operation has also been measured. Under AC stress conditions, variations of approximately 5% of the initial value of the strain piezoelectric coefficient per MPa were measured for soft materials. This value was as lower as 2% per MPa for hard materials.

Dynamic electrical conditions under prestress displayed an increase in the permittivity and the losses of the material but not results about the evolution of the piezoelectric coefficients has been measured. These losses are more important in soft materials than in hard materials, which shown a harder stability to the external preloads.

Frequency dependence is also more important in the d_{33} coefficient of soft material, and remains practically stable when hard materials are considered.

Natural ageing is observed in all the piezoelectric ceramic materials and all their coefficients. Values of the ageing rate can oscillate between less than 1% up to 10% per decay. The variation is logarithmic and is very important during the firsts moments after poling. Later on the ageing is mot so aggressive.

Obviously, this ageing is increased according to the electrical or mechanical conditions at which the material is withstanding. Number of operating cycles affects importantly the properties of the ferroelectric materials. At the present this is an important research subject due to the ferroelectric memories application which requires materials with low loss after many operating cycles.

Electrical fatigue was measured by means of the change in the permittivity. Soft material become fatigued after 10^2 cycles ($V=500V_{pk-pk}$; f=500Hz) while soft materials require 10^3 cycles. Nonetheless, once the fatigue starts, the increase of loss is more significant and quicker in hard materials than in soft. Mechanical fatigue, measured directly over the d_{33} coefficient appeared after 10^3 cycles (AC stress 3MPa; f=200Hz) showing a degradation of 20% after 10^7 cycles.

6.6.3. Alternative materials

Recently, interest has been concentrated in the layered-perovskite phase of the bismuth as an alternative to the PZT material for applications where a high accuracy is demanded. The structure of bismuth layered compounds consist of layers of perovskite, infinite in two dimensions, separated from each other by a bismuth oxide layer. The perovskite layer can be one, two, three or more perovskite unit cells thick. Each of these thicknesses results in a separate structure type, but has the perovskite layer-bismuth oxide layer alternation, giving rise to the term bismuth *layered* compounds. Examples of ferroelectric bismuth layered compounds include bismuth titanate ($Bi_4Ti_3O_{12}$) and strontium bismuth tantale ($SrBi_2Ta_2O_9$), which is also known as SBT, as well as many others (Table 6.9).

Table 6.9. *Properties of some Bismuth layered compounds* [23,24,25]

	$Bi_2PbNb_2O_9$ **[PBN]**	$Bi_4Ti_3O_{12}$ **[BIT]**	$Bi_4PbTi_4O_{15}$ **[PBT]**	$Bi_4SrTi_4O_{15}$ **[SBT]**	$Bi_{4.5}Na_{0.5}Ti_4O_{15}$ **[NBT]**
T_{CURIE}	550ºC	675ºC	570ºC	420ºC	655ºC
Mechanical Q	2000	-	2700	7200	4200
$\varepsilon_{33}^T / \varepsilon_0$ (25ºC)	170	180	220	190	200
d_{33} (10^{-12} C/N)	15	20	23	15	10
d_{31} (10^{-12} C/N)	-0.9	-	-0.4	-2.5	-1.3
k_t (%)	17	-	7.2	22	15
k_p (%)	1.4	-	0.5	3.8	2.1
g_{31} (10^{-3} V.m/N)	-0.8	-	-0.3	-1.9	-1.1
s_{11}^E (10^{-12} m^2/N)	10.1	-	9.8	8.5	8.6
s_{12}^E (10^{-12} m^2/N)	-2.5	-	-2.7	-2.1	-2.0

SBT materials have been widely tested for non-volatile memories, due to its negligible fatigue from polarisation switching, low switching voltage, sufficiently large polarisation and minimal tendency to imprint (the tendency of one polarisation state to become more stable than the opposite state, manifested by a shift of the hysteresis curve along the voltage axis). The value of the longitudinal d_{33} coefficient in SBT is around 15pC/N and is independent of the frequency and amplitude of the applied A.C. stress.

For actuator applications, this material presents promising characteristics due to its low hysteresis under high electric fields. These characteristics make it also interesting for being applied in the construction of the actuator column of the instrument piezoelectric transformer.

Figure 6.28 and 6.29 present the comparison of the behaviour of the strain coefficient against the frequency and against the AC stress.

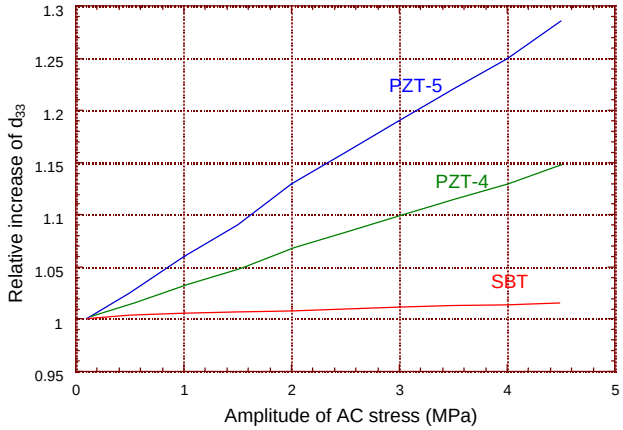

Figure 6.28. *Change in the d_{33} coefficient against the amplitude of an AC stress for soft and hard PZT compositions and SBT ceramics*

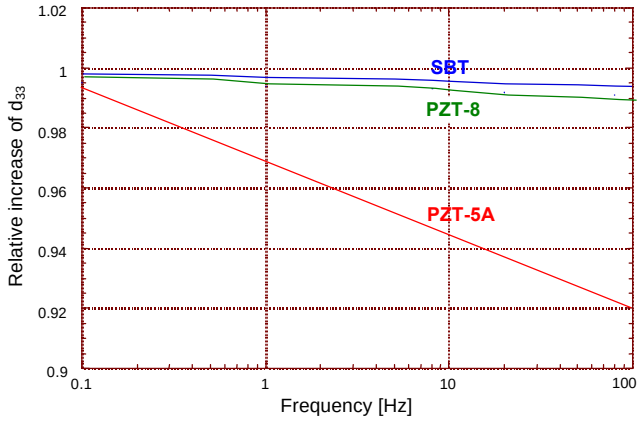

Figure 6.29. *Change in the d_{33} coefficient against the frequency for soft and hard PZT compositions and SBT ceramics*

A second alternative to a more reliable material than the PZT, is the use of some piezoelectric single crystal, as for instance the *quartz*. Since quartz is not ferroelectric the problem of the depolarisation is eliminated and also the thermal dependence, mechanical degradation, AC dependence, frequency stability, etc. This material has been successfully used for a long time in force sensor, but it has been never been applied as actuator, due to the low levels of blocking forces and displacement which generates.

However, in applications where the material must withstand hard electric fields, the intensity of the forces generated may be enough to transmit the force to a secondary sensor, as is the case of the application considered in this thesis. Moreover, if one reduce the levels of the forces generated the requirements of the external housing and preload will be lower, also reducing the fatigues of the materials.

Quartz could have other advantages. Manufacturing artificial methods for quartz allows growing crystals up to 15cm or more. This could permit the use of a whole piece of material to construct the actuator, eliminating the need to piling up discs. The stiffness of the material will be also increased and thus the blocking state could be perfectly kept.

The test of quartz as a possible material to build the actuator column of the instrument transformers remains as a future research task.

6.7. References

[1] Waser, R.M., Baiatu, T. and Hardtl K.H., *J. Am. Ceram. Soc*., 1990, **73**, 1645-1653.

[2] Warren W.L., Dimos D. and Waser, R.M., *M.R.S. Bulletin*, 1996, **21**, 40-45.

[3] Aoki, K. and Fukuda, K., *Jpn. J. Appl. Phys*., 1997, **36**, 1195-1197.

[4] Hill, M.D., White, G.S. and Hwang C.S., *J. Am. Ceram. Soc*., 1996, **79**, 1915-1920.

[5] Shaufele, A.B. and Hardtl, K.H., *J.Am. Ceram. Soc.,* 1996, **79**, 2637-2640.

[6] IEEE Standard on Piezoelectricity 176, 1987

[7] Ceramic Material and Measurements *Guidelines for Sonar Transducers*. Department of Defense, Military Standard: DOD-STD-1376B, 24 Feb. 1995, Philadelphia, USA.

[8] *Ferroperm Piezoceramics*. Industriselskabet Ferroperm A/S, Piezoelectric Ceramics Division, Denmark, July 1995.

[9] *Piezoelectric Ceramics Data Book for Designers*. Morgan Matroc Limited Transducers Products division. Thornhill, Southampton, England.

[10] *Piezoceramics*, CeramTec AG Piezo Applications Division, Germany.

[11] *Piezoelectric Ceramics*, Data Handbook MA03, Philips Components, The Netherlands, 1996.

[12] Sensor Technology Limited, http://www.sensortech.ca/

[13] Kugel, V.D. and Cross, L.E., *Behaviour of soft piezoelectric ceramic under high sinusoidal electric fields.* J. Appl. Phys., 1998, **84**, (5), 2815-2830.

[14] Damjanovic, D., Demartin, M., Shulman, H.S., Testorf, M., Setter, N., *Instabilities in the piezoelectric properties of ferroelectric ceramics.* Sensors and Actuators A, 1996, **53**, 353-360.

[15] *Electroactive materials under high stress or stress rate*, NPL Report CMMT (A)116, May 1998, Middlesex, U.K.

[16] Audigier, A. et al. Ferroelectrics, 1994, **154**, 219-224.

[17] Hall, D., J. Phys: Condens. Matter*,* 1998, **10**, 461-476.

[18] Robels, U. et al., Ferroelectrics, **133**, 163-168.

[19] Berlincourt, D.A., *J.Appl. Phys.*, 1959, **30** (11), 1804-1810

[20] Damjanovic, D., Demartin, M., Shulman, H. and Setter, N., *Instabilities in piezoelectric properties of ceramic sensors and actuators under extreme conditions*. Transducers'95-EurosensorsIX, Sweden, June 1995.

[21] Waanders, J.W., Piezoelectric Ceramics, properties and applications, Philips Components, 1991, Eindhoven.

[22] Calderon Moreno, J.M., Guiu, F., Meredith, M., Reece, J.M., Alford, N.McN. and Penn, S.J., Anisotropic and *Cyclic Mechanical properties of Piezoelectrics-Compression Testing.* Journal of the European Ceramic Society, **19** (1999), 1321-1324.

[23] Aurivilius, B., *Mixed Oxides with Layer Lattices*, Ark. Kemi, **1** [54] 499 (1950).

[24] Jaffe, B., Cook, W.R., Jaffe, H., Piezoelectric Ceramics, Academic Press Limited, Chapter 9, (1971)

[25] S.Ikegami, I.Ueda, "Piezoelectricity in Ceramics of Ferroelectric Bismuth Compound with Layer Structure", Japan. J. Appl. Phys., **13** [10], October 1974.

Chapter 7

Accurate instrument piezoelectric transformer prototype for being tested in Distribution Networks

7 Accurate instrument piezoelectric transformer prototype for being tested in Distribution Networks

7.1. Introduction

The experience accumulated since 1995 with the prototypes PIEZOTRF1 and PIEZOTRF2 demonstrated that the most important problems in the design of a instrument transformer come from mechanical aspects. In particular, the capacity of prestress of the set-up and its stiffness are significantly influent in the output response.

PIEZOTRF1 did not permit the measurement of the influence of the prestress due to the damage of the prestress screw during the construction of the prototype. PIEZOTRF2 solve this problem but only partially, since the designed prestress system was observed weakly to withstand the stress appeared in the column. Hence, a more reliable prestress system was concluded to be necessary in order to obtain a reliable prototype.

Together to this technical requirement, a new event increase the need of the construction of a very accurate prototype. At the end of 1997, the Electrical Spanish company *Hidroelèctrica de l'Empordà*, which operates in the province of Gerona (Spain), become interested in the project. The company proposed the installation of three piezoelectric voltage transformers to be tested under real conditions in the *Parc Eolic de Roses* (Girona, Spain), later described.

The purpose represented an important technical challenge in the evolution of the research. A test in real conditions represents the best demonstration of the actual behaviour of the device. Furthermore the mentioned installation has one of the higher average ratios of lightning fall of Catalunya (Spain). This factor represents a harder test for this type of devices. The response under lightning is one of the more rigorous requirements demanded by the instrument transformers.

As a consequence of both, the need to improve the technical features observed in the previous prototypes (in particular the prestress system) and, the need of obtaining a very accurate device which could pass successfully an experimental test under real conditions, a new prototype was designed.

The experience gathered in the previous works was used to develop a rigorous theoretical approach for the determination of the necessary requirements and selection of the involved materials.

This chapter describes the mentioned approach together with the process of design and construction of the prototype PIEZOTRF3. The work is particularly concentrated in the mechanical requirement of the different parts of the set-up in order to guarantee a behaviour as close as possible to the blocking state. An evaluation of the effect of the stiffness of the housing material in the decrease of the real value of the blocking force is made.

The description of the experimental test and results is reserved for the Chapter 8.

7.2. Description of the installation and basic requirements for the PIEZOTRF3 prototype

The *Parc Eolic de Roses* is a little Wind Power Station placed in the area of *Alt Empordà* (Girona,Spain). This area is considered as one of the most important in Spain in regard to its possibilities in wind power generation [1].

The *Parc Eolic de Roses* (Figure 7.1) was constructed in 1990 and consist of six aerogenerators, four of them of 110kW and the rest of 75kW. The aerogenerators are connected to the electrical network by means of a step-up electrical transformer of 1000kVA and nominal voltages of 380V (aerogenerators) and 25kV (electrical network).

The electrical connection of the Station is made by means of a general protection and measuring system, place inside a convenient protected building, *the control building*. In this building there are also all the power counters and security systems for disconnecting the aerogenerators and the monitoring equipment. All the control, protection and measuring systems are driven for the voltage or current to be monitored through a group of current and voltage electromagnetic instrument transformers.

Figure 7.1. *Parc Eolic de Roses. Courtesy of "Institut Català d'Energia" (http://www.icaen.es/icaendee/proj/ciprd.htm#eolica).*

The requirements for the voltage transformer to be installed were specified as:

- Nominal high voltage: 25kV
- Nominal low voltage: $\leq$ 110V

Taking account the standards on instrument transformers (see Table 1.5, Chapter 1), particularly the UNE 21088-2 (1995), such a transformer belong to the 36-type voltage transformer. The standard tests to be verified are:

- Lightning impulse voltage = 170kV_{peak}
- Power frequency withstand voltage = 70kV_{rms}

7.3. Active Material

7.3.1. ACTUATOR

• Type of Material

In Chapter 6 an evaluation of the different piezoelectric ceramic materials commercially available was discussed. Hard material demonstrated to have a better behaviour under hard electrical or mechanical conditions than soft material. Particularly, a PZT-8S composition, from Morgan Matroc [2], was chosen as the best hard material in order to withstand the expected very intenses mechanical and electrical conditions.

The PZT-8S composition displays a very high depolarisation resistance and a low hysteresis, which is a necessary requirement for accurate devices. Furthermore, this material was already used in the construction of the PIEZOTRF2 and was available to be used without waiting time delivery.

PZT-8S composition has a longitudinal d_{33} coefficient of $225 \cdot 10^{-12}$ C/N (measured 24 hours after poling), a compliance s_{33}^{E} of $13{,}5 \cdot 10^{-12}$ m^2/N and a Curie temperature of 300ºC. The maximum measured hysteresis in the *P-E* loop was of 7%, when the sample was driving at 1000V/mm.

It is also possible to use other alternatives hard compositions such as SonoxP8 (CeramTec [3]), PXE43 (Phillips [4]), Pzt28 (Ferroperm [5]) also analysed in Chapter 5.

• Dimensions of the actuator column

It has already been described (Chapter 4) the procedure for dimensioning the length of the actuator column. Two parameters must be taken into consideration: *the depolarisation resistance* of the used material, and the expected *maximum voltage* to be applied (lightning test).

The minimum length of the actuator column, *L*, may be obtained from:

$$L > \frac{V_{MAX}}{E_{depol}} \tag{7.1}$$

PIEZOTRF3 has been designed following the same criterion as for the two previous prototypes, that is, V_{MAX} = 170kV (lightning test for a 36kV voltage transformer). For the PZT-8 composition the depolarisation resistance is higher than 1500V/mm. Thus, the piezoelectric column length will be:

$$L > \frac{170\,\text{kV}}{1.5\,\text{kV/mm}} \approx 120\,\text{mm} \tag{7.2}$$

To provide dimensional stability to the stack and to reduce the coupling problems between discs, it is convenient to use fewer numbers of discs as possible. Discs of 12mm thickness were used which are the thickest commercially available from Morgan Matroc Inc. Another important parameter that guarantees dimensional stability is the ratio length to area. A long but thick column will be affected by bending stress. A diameter of 30mm was chosen to avoid bending effects.

The total number of discs finally used was 12, which represents a length of 144mm.

• Blocking force generated by the actuator

The maximum force developed by the column will appear in clamped conditions ($S_3 = 0$). This is the blocking force, and can be obtained by:

$$\frac{F_{bloq}}{V} = \frac{d_{33} \cdot A}{s_{33}^{E} \cdot L} = \frac{225 \cdot 10^{-12} \cdot 7{,}068 \cdot 10^{-4}}{13{,}5 \cdot 10^{-12} \cdot 144 \cdot 10^{-3}} = 8{,}181 \cdot 10^{-2}\ \text{N/V} \qquad (7.3)$$

Under nominal conditions, the piezoelectric transformer will be connected to $25kV_{rms}$. Hence, the maximum value of the force developed under these circumstances is given by:

$$F_{bloq\,(25kV)} = 8{,}1812 \cdot 10^{-2}\ \text{N/V} \cdot 25 \cdot 10^{3}\ \text{V} \cdot \sqrt{2} = 2892{,}5\ \text{N} \qquad (7.4)$$

The maximum value of the blocking force appears under the conditions of the lightning test. In this case, V_{peak} = 170kV and the force generated is:

$$F_{bloq\,(170kV)} = 8{,}1812 \cdot 10^{-2}\ \text{N/V} \cdot 170 \cdot 10^{3}\ \text{V} = 13{,}908\ \text{kN} \qquad (7.5)$$

This value determines the prestress conditions of the column and the mechanical strength of the housing.

• Static prestress of the actuator column

Mechanical depolarisation and fatigue in the material are very intense under tensile forces. In order to reduce these effects it is convenient that the column operates under compression. Moreover, when a stack of discs is used, it is necessary to guarantee contact between each disc throughout operation cycle. To do this, the column has to have an initial static compression higher than the maximum expected tensile force. Since the maximum force appearing during the lightning test is of 13,9kN the static prestress was estimated to be 15kN.

• Construction of the actuator column

Construction of the actuator column has been commented previously for prototype PIEZOTRF1 and PIEZOTRF2. Here below is a brief review.

Piezoelectric discs are stacked by aligning in the same direction the polarisation vector of each disc. Once the 12 discs are arranged, the stack is blocked in a press and held with a dielectric tape. An on-side adhesive paper tape from Tesa Tape Inc. was used during the holding and mounting process. After this process the column is perfectly compacted (see Figure 7.2).

A problem detected during the mounting and installation of the actuator column in previous prototypes was the fragility of the ceramic material during the construction and mounting process. As a consequence of this, fractures appeared in the ends of the stack because of the little impacts during the mounting process. These fractures caused loosening of small pieces of material which may cause problems if some of them remain between the column and the centred plate. Moreover this loosening of material, if important, can reduce the contact of the column with the electrodes, and thus to reduce the stability of the column.

This problem was solved by placing two metallic pieces at both ends of the column which were taped together with the stacked discs. In this way, the little impacts made during the mounting process did not affect the ceramic material.

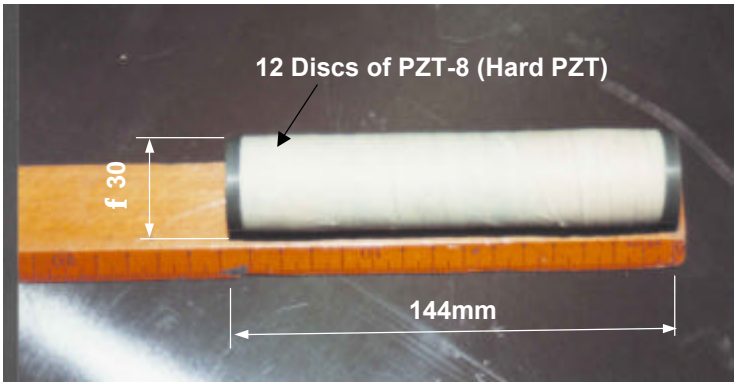

Figure 7.2. *Piezoelectric actuator column after the holding process with tape.*

7.3.2. SENSOR

• Material requirements

Several important considerations must be taken into account in the selection of the sensing device:

- The sensing characteristics of the material: *Piezoelectric sensitivity*
- The matching characteristic of the material: (1) *Electrical matching* (output impedance of the transducer, in particular, capacitance); (2) *Mechanical matching* (stiffness of the material and their capacity for measure force with a very little displacement).
- Other: Drifts (thermal, humidity), hysteresis, preload effects, ageing, frequency stability, etc.

Sensing Characteristics

For a force transducer it is defined the *piezoelectric sensitivity* as the characteristic which indicates the capacity of the material to generate an electrical charge (or voltage) when an external force is under the effect of an external force. The sensitivity depen on the properties of the material and on the mode in which the electrical charge generated is measured. There are two basic modes for measuring forces by using a piezoelectric sensor: *voltage mode* and *charge mode* (see Appendix 1).

In the *voltage mode* the measurement is performed in open circuit conditions. Thus, the voltage measured is depending on the piezoelectric coefficient g_{33} and on the geometry of the transducer. Thus, the sensitivity is expressed as:

$$S_v = \frac{V_{out}}{F} = -\frac{g_{33} \cdot t}{A} = \frac{d_{33}}{C_a} \tag{7.6}$$

In the *charge mode* the measurement is performed in short circuit conditions and the measured magnitude is the electrical charge generated owing to the application of the external force. Then, the charge Q depens on the piezoelectric coefficient d_{33}, but not from the geometry of the transducer, and the sensitivity is expressed as:

$$S_Q = \frac{Q}{F} = d_{33} \tag{7.7}$$

Electrical Matching Characteristics

A piezoelectric transducer requires a special electrical conditioning circuit. This circuit has the next functions:

- It permits an electrical coupling between the very high impedance of the transducer and the low input impedance of the readout system.

- It permits a reduction in the cut low frequency of the transducer for itself. This allows the quasi-static measurements.

Two basic conditioning circuits can be applied in piezoelectric transducers for conditioning. The *voltage amplifier* (or electrometer), applied in the voltage mode, and the *charge amplifier*, used in the charge mode measurements. (see Appendix 1).

In general, in both conditioning systems the sensitivity of the transducer is significantly affected owing to the impedance of cables and amplifier connected in parallel to the transducer. Voltage amplifier reduces the voltage sensitivity up to:

$$S_v = \frac{V}{F} = \frac{d_{33} \cdot G}{C_a + C_{cable} + C_E} \tag{7.8}$$

as for charge amplifier, the sensitivity is reduced to:

$$S_Q = \frac{Q}{F} = \frac{d_{33}}{C_f + \frac{(C_a + C_f)}{A}} \tag{7.9}$$

where, d_{33} is the charge piezoelectric coefficient, C_a is the capacitance of the transducer, C_{cable} is the capacitance of the connection cable, C_E is the input capacitance of the amplifier used, C_f the feedback capacitance, G is the close loop gain and A is the open loop gain. (see Appendix 1).

Mechanical Matching Characteristics

In order to have a good accuracy in the blocking force measurement, a very stiff material is necessary as a sensor. If the stiffness of the sensor is weak, the transducer will introduce deformation in the set-up to be measured an a fraction of the force will be expend in this deformation.

• Selection of the sensor material

The active elements of piezoelectric precision measuring cells consists very often of *quartz*, because this material is rather predestined for such applications thanks to its excellent mechanical (very high rigidity), thermal (stable in front the temperature) and electrical properties (very stable in frequency) (Table 7.1). Although quartz has a high piezoelectric field strength coefficient g_{11}, the relatively unfavourable data for d_{11} and ε_{11} restricts severely its application in miniature transducers.

Another group of piezoelectric transducer materials comprises of the numerous *ferroelectric ceramics* which, by definition, are all pyroelectric too. In this group, the potential advantage of the partly rather high longitudinal sensitivity is cancelled out by the pyroelectricity which moves in parallel with it. For the transverse piezoelectric effect, the conditions are even more unfavourable. Particularly serious disadvantages of ferroelectric ceramic are given by time-dependence and non-linearity of their properties, which exclude their application where high measuring precision is required. Moreover these materials depend on the static conditions

applied to them. If a prestress is applied to the material, as is the case for measuring blocking force, the piezoelectric coefficients change their value.

The application of the piezoelectric polymers for force measurement is excluded owing to its low stiffness, and thus the significant displacement which introduces.

One interesting family of piezoelectric ceramic material has already been described in chapter 6: The Bi-layered piezoelectric compounds (PBT, BIT, SBT, SBN, NBT). Although these materials show a low strain piezoelectric coefficient (d_{33}≈10÷20pC/N), they offer high time and frequency stability, low thermal dependence and low dependence to high external preloads.

Particularly, in the construction of the PIEZOTRF3 a disc of SBT composition has been used for sensing. The dimensions of the transducer were 10mm diameter and 2mm thickness. This sample was self-manufactured in laboratory.

Table 7.1. *Comparison of different piezoelectric materials used as sensor* [7,8,9]

		Material				
		PZT-5J (soft) (Morgan)	**PZT-8 (hard) (Morgan)**	**SBT ($SrBi_4Ti_4O_{15}$) (see Table 6.9)**	**Quartz (rhomboid)**	**PVDF (AMP)**
Transducer Voltage Sensitivity S_V = V/F	**d_{33} [pC/N]**	500	225	15	(d_{11}=2.3) (d_{14}=-0.7)	-33
Transducer Voltage Sensitivity S_Q = Q/F	**g_{33} [V.m/N]**	0.0217	0.0254	-	(g_{11}=-0.050)	-
Electrical Matching $C_a = \frac{e_0 \cdot e_{33} \cdot A}{t}$	e_{33}^T	1100	2600	150	(ε_{11}=4.5)	12-13
Mechanical Matching	c_{33}^E **[N/m^2]**	53·10^9	74·10^9	-	(c_{11}=86.7·10^9)	2-3·10^9
	Compression Strength [N/m^2]	>517MPa	>517MPa		2400MPa	-
	Maximum Static Compressive Stress (maintained) PARALLEL to polar axis	25MPa	82MPa	-	100MPa	-
Drifts	**Maximum Temperature Range (T_{Curie})**	300ºC	95ºC	550ºC	550ºC	-40 to 90º

7.4. Passive Materials

7.4.1. The Dielectric Housing

• Dielectric Specifications

Dielectric housing separates both electrodes connected to H.V. The dielectric strength of the material and its dimensions must guarantee that breakdown will not occur. This is specially important under lightning conditions (170kV$_{crest}$ for a 36kV-type voltage transformer).

In order to analyse the dielectric strength of the prototype it is necessary taken into consideration all the dielectric materials which are operating together (Figure 7.3). Combination of different dielectric materials may modify the strength of each material for itself.

1. The active piezoelectric material
2. The dielectric material between the active material and the dielectric housing (in the PIEZOTRF3 prototype was used atmospheric air).
3. The external atmospheric air.
4. The dielectric housing.

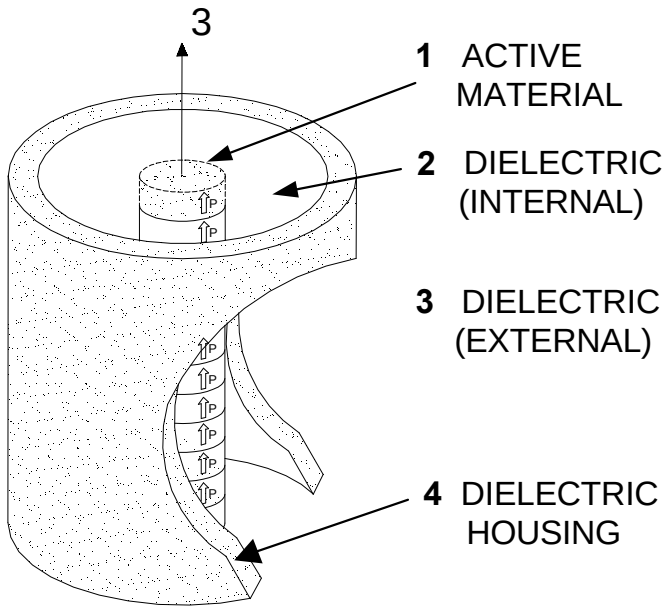

Figure 7.3. *Dielectric materials to be considered in the PIEZOTRF3 prototype.*

A first approach to the design of the dielectric housing would be consider that it can be analysed as the case of two electrodes (two parallels planes) without any insulator in between (Figure 7.4.b). However, it is well known from experimental tests that breakdown when a dielectric material is in between decreases up to 6 times or more in compare to the case without any insulation. The maximum decrease of breakdown voltage is observed when separation between the two electrodes is large, as illustrates in Figure 7.4.a.

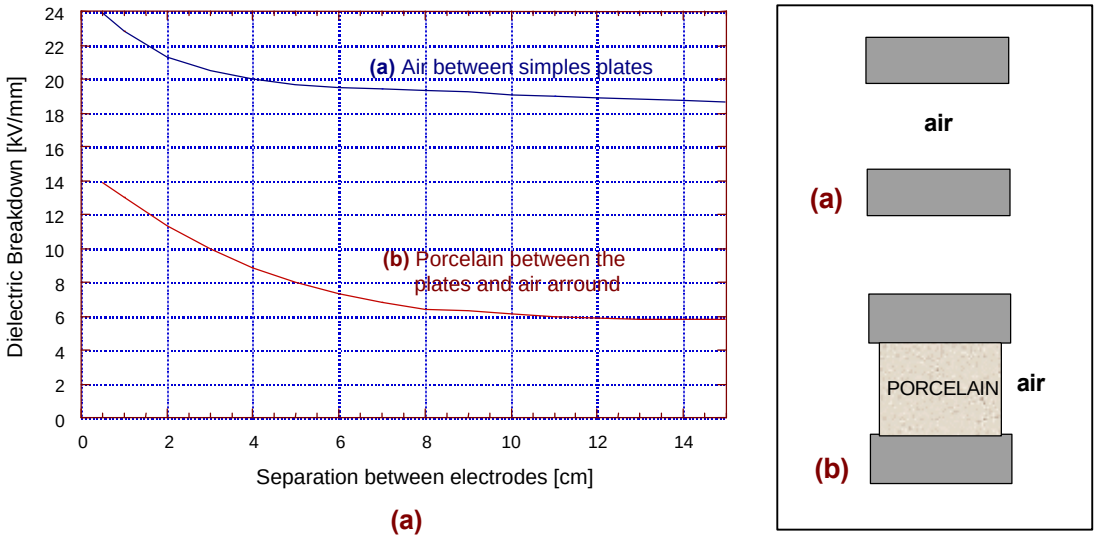

Figure 7.4. (a) *Graph of the breakdown voltage, between two plates, at 50Hz,* **(b)***when there is only air between the two plates* **(c)** *when a porcelain cylinder is place in between.*

This result is very surprising (although well know for high voltage experts) because of the significantly higher field strength of the porcelain (10 times dielectrically higher than the air). The cause of this surprising result it is not clear and it has been tried to be explained as due to some phenomenon relative to the surface [6,7]. Probably humidity, grease or acid sediments with a higher conductivity placed in some points of the surface may explain the reduction in the breakdown strength. In order to perform the design of the dielectric housing this fact has to be taken into account.

To consider the permissible field strength values verifying that the breakdown will not occur, many situations, materials, interfaces, etc. may be considered. Moreover, permissible field strength depends very much on the technology and the skill of a particular designer. The right thing, in order to obtain a general list of permissible field strength, is to collect the experience of many breakdown tests: each breakdown test yields a number of withstand values and one or two values of a breakdown field strength. Collecting this data through the years yields a valuable set of design values.

In the Table 7.2 an attempt has been made to collect such values. These values are on the safe side, sophisticated manufacturing techniques can easily push them upwards. A design based on these values might be too heavy, but it could be used as a first step in the procedure of designing.

The values indicated under A.C. voltage are given for a 24 hours period of testing at A.C. The related field strengths at nominal voltage are then 2.5 to 3 times lower. The values indicated under impulse voltage are given for 10 positive and 10 negative impulses according to I.E.C. and at operating temperature between 70ºC to 90ºC. Values for DC. voltage are not shown. In gases and liquids the A.C. value can be taken, multiplied by the shape factor 1.4. In solids at least twice the A.C. value can be taken.

Table 7.2. *Permissible field strengths* [7]

	At 24h. A.C. voltage kV/mm rms	At Impulse voltage kV/mm crest
VACUUM	15 to 30	25 to 45
AIR (dry)		
in free air, several cm's	1.5	2
interface with a solid	0.7	1
COMPRESSED AIR (5 bar)		
in free air, several cm's	6	12
interface with a solid	3	6
SF_6 – GAS (5 bar)		
in free gas, several cm's	10	25
interface with a solid	6	10
TRANSFORMER (CABLE) OIL		
between barriers	6	10
interface with a solid	3	5
PAPER, oil-impregnated		
perpendicular to the layers	12	50
parallel with the layers	2	7
PAPER, resin-impregnated		
perpendicular to the layers	10	25
parallel with the layers	2	5
EPOXY		
epoxy – SiO_2 (ε = 4)	10	25
epoxy – $BaTiO_3$ (ε = 10)	3	12
SYNTHETIC RUBBERS		
within the material	6	25
interface between solid and rubber under mechanical pressure	3	9
POLYETHYLENE		
extruded	20	50
hand applied and fused	5	25
PORCELAIN AND GLASS	>10	>25

With these basis in mind, dielectric housing was designed as a simple tube of dielectric material joined at both ends to the high voltage electrodes (Figure 7.3). A permissible field strength of 1kV/mm crest (dry air with interface with a solid) was considered for withstanding the lightning test at 170kV (which is the harder test). Under these conditions, the necessary length of the dielectric housing was determined given as:

$$L > \frac{V_{\text{lightning test}}}{E_{\substack{\text{breakdown} \\ \text{at impulse}}}} = \frac{170\text{kV}}{1\text{kV/mm}} = 170\text{mm} \qquad (7.10)$$

At this point, two considerations have to be made regarding possible future designs.

1. Permissible field strength in the external side of the housing may be easily increased by considering the following techniques:

   - Incorporating sheds
   - Using long creepage distances
   - Using synthetic materials joined to the surface of the housing increasing the dielectric strength

   This is especially important when it is necessary to withstand high voltage under external conditions such as rain, during fog, exposure to salt water spray (near the coast), under chemical pollution (in industrial areas), etc.

2. Field Strength in the internal side of the housing may be easily increased by using a compressed gas, such as air (5 bar) or SF_6 (5bar). In the first case, with air, the dielectric strength is increased in 6 times. With SF_6 the strength is increased in 10 times. Nevertheless, this option was rejected because the possibility of contamination of the piezoelectric material. Solid or liquid dielectric may also be possibly used.

• Mechanical Specifications

Apart of being used as a dielectric separation between both high voltage electrodes, the dielectric housing must be mechanically designed in order to:

1. Withstand the static prestress applied to the column.

2. Withstand the A.C. forces generated for the active column when the driving voltage is applied and also to withstand the forces appearing during the lightning test.

3. Have a very low deformation which guarantees the blocking state ($S_3 \approx 0$)

Maximum forces appearing

The maximum blocking force under lightning test has previously been calculated from equation (7.3) as 13.9kN. The necessary prestress to guarantee that the column will always operate in compression was also estimated as 15kN. This compression force creates a tensile force in the external housing which must be added to the tensile forces appearing during the operation of the device. Thus, when impulse is tested, the maximum tensile force to be withstood is of around 30kN. Next Figure 7.5 displays an interpretation of the forces actuating over the dielectric housing.

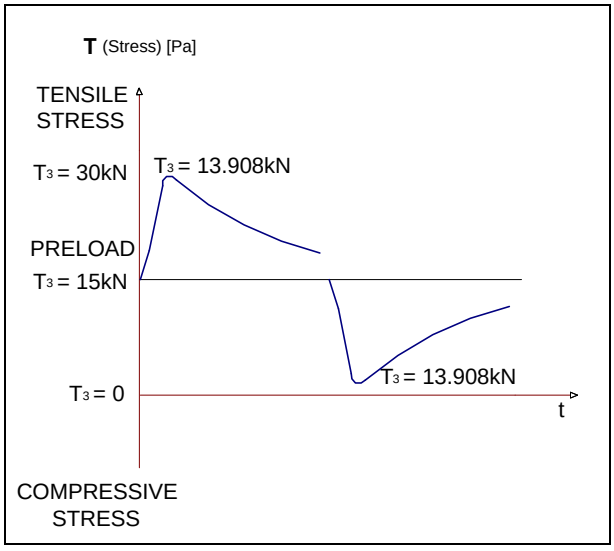

Figure 7.5. *Tensile forces which must withstand the dielectric housing*

Selection of the Housing Material

Dielectric materials with high rigidity have been used for long time in high voltage application for insulators and other applications in which (apart from the dielectric separation) the insulator is subjected to a mechanical stress. In general these types of materials belong to the family of ceramics, glasses and quartz. The next Table 7.3 gathers some mechanical and electrical properties for some of them. A special observation must be done regarding the properties of

these materials compare to the epoxy resin composition previously used in PIEZOTRAFO1 and PIEZOTRAFO2 construction, as is indicated in Table 7.3.

Table 7.3. *Ceramic and Glass Data Table*

		CERAMICS					QUARTZ	GLASS	RESIN
PROPERTIES		Hard Porcelain	Esteatita Isostea	Esteatita Rastea	Ceramic with a High level of Al_2O_3	Alumina (Al_2O_3)	Quartz Glass	Boron-Silicate Glass (Pyrex, Duraglass)	Epoxide Resin
PHYSICAL	Density [Kg/m^3]	2300 to 2500	2600 to 2800	2600 to 2800	2600 to 3300	3900	2000 to 2200	2200 to 2600	1600 to 1700
	Transmission - Visible light	-	-	-	-	-	-	Transpa-rent	-
MECHANICAL	Tensile strength, surface glazed [MPa]	30 to 50	60 to 95	60 to 100	-	-	-	-	-
	Tensile strength, not-glazed [MPa]	25 to 35	45 to 60	45-60	40-100	260	70 to 120	30 to 100	80 to 100
	Compressive strength, surface glazed [MPa]	450 - 550	850-950	900-1000	-	-	-	-	-
	Compressive strength, not-glazed [MPa]	400 to 450	850 to 950	900 to 1000	700 to 1500	2200 to 2600	1600 to 2000	500 to 1200	180 to 200
	Tensile Modulus [GPa]	55 - 80	80 - 110	110 - 130	100-110	330-400	60-90	60-90	12-13
THERMAL	Thermal Expansivity 20-1000^{0}C x10^{-6} K^{-1}	3.5 to 4.5	7 to 9	6 to 8	5 to 6	5 to 7	0.6	3 to 6	30 - 35
	Thermal Conductivity at 20ºC [W/m.K]	1 to 2	2 to 3	2 to 3	2 to 10	28 to 35			0.8 to 0.9
ELECTRICAL	Dielectric Strength [kV/mm]	30 to 35	20 to 30	30 to 45		10 to 35	20 to 40	10 to 20	n/a
	Dielectric Constant	≈ 6	≈ 6	≈ 6		9.0-10.1	≈ 4	4 to 6	n/a

Remarkable materials for both, mechanical and electrical properties, are the Alumina and the Sapphire. Sapphire is a transparent material commercially available as sheet (discs, squares,

rectangles, etc) but not as tubes because of the complication in treatment used to synthesise them.

Minerals containing Alumina represents some 15% of the earth's crust. It is therefore an abundant material and virtually inexhaustible, unlike raw materials for many alloys developed for special applications. This material combines high thermal conductivity, low thermal expansion, high compressive strength and good electrical insulation. Alumina has been used widely for furnace use as crucibles, tubes and thermocouple sheaths.

Another interesting material, of as not good electrical and mechanical properties as Alumina, is the Pyrex. Pyrex, as the Sapphire, is a transparent material and is widely use in a lot of commercial applications. It has good mechanical and thermal properties to make saucepans and laboratory devices. It is less expensive than Alumina and makes it a good choice for prototyping. This material also allows the observation of internal phenomenas due to its transparency.

Other materials commercially and widely available at a reasonable cost and similar in features to Pyrex are the Nuraceram, Firelite, Duraglas, etc.

For the construction of the PIEZOTRF3 prototype, Pyrex was chosen as dielectric material for the housing. A description of the calculation of the dimensions of the dielectric housing is described below.

• Dimensions of the dielectric housing

Table 7.4 displays the physical properties for a commercial Pyrex Glass.

Table 7.4. *Physical Properties for Pyrex Glass* [10]

Density	2230 Kg/m^3
Tensile Modulus	65 GPa
Poisson Coefficient	0.22
Tensile strength	15 MPa
Compressive strength	360 MPa

Since diameter of the piezoelectric discs was 30mm, an external diameter of around 60mm was chosen for the dielectric housing. The area of the housing was calculated by considering the maximum pressure it is able to withstand and the tensile strength of the Pyrex, as is indicated in equations 7.5 to 7.7.

$$A_{housing} = A_{ext} - A_{int} = \frac{p}{4} \cdot \left[f_{ext}^2 - f_{int}^2 \right] \tag{7.11}$$

$$P_{(170kV_{PEAK})} = \frac{30\,kN}{A} = \frac{30 \cdot 10^3}{\frac{\pi}{4} \cdot \left[\phi_{ext}^2 - \phi_{int}^2 \right]} < 15MPa \tag{7.12}$$

$$\phi_{ext}^2 - \phi_{int}^2 > \frac{30 \cdot 10^3\,N}{\frac{\pi}{4} \cdot 15 \cdot 10^6\,\frac{N}{m^2}} = 2.5463 \cdot 10^{-3}\,m^2 \tag{7.13}$$

where it is necessary that ϕ_{int} > 30mm, so this is the diameter of the piezoelectric discs. Table 7.5 shows the selection of the internal diameter which verify the previous conditions.

Table 7.5. *Selection of the Area of the Dielectric Housing*

ϕ_{ext} [mm]	ϕ_{int} [mm]	$f_{ext}^2 - f_{int}^2$ [m^2]	Thickness [mm]	Area [m^2]	
60	55	0.000575	2.5	$0.4516.10^{-3}$	$< 2.5463 \cdot 10^{-3}$
60	40	0.002	10	$1.5707.10^{-3}$	(no enough)
70	40	0.001575	15	$2.5918.10^{-3}$	$> 2.5463 \cdot 10^{-3}$ (enough)

From Table 7.5, it follows that at least a thickness of 7.5mm is necessary to guarantee the operation under lightning test. Nevertheless, in the construction of the PIEZOTRF3 a tube of Pyrex of 170mm length, ϕ_{ext}= 56mm and a thickness of 2.5mm was used due to commercial disposibility. Figure 7.6 displays a view of the dielectric housing once constructed.

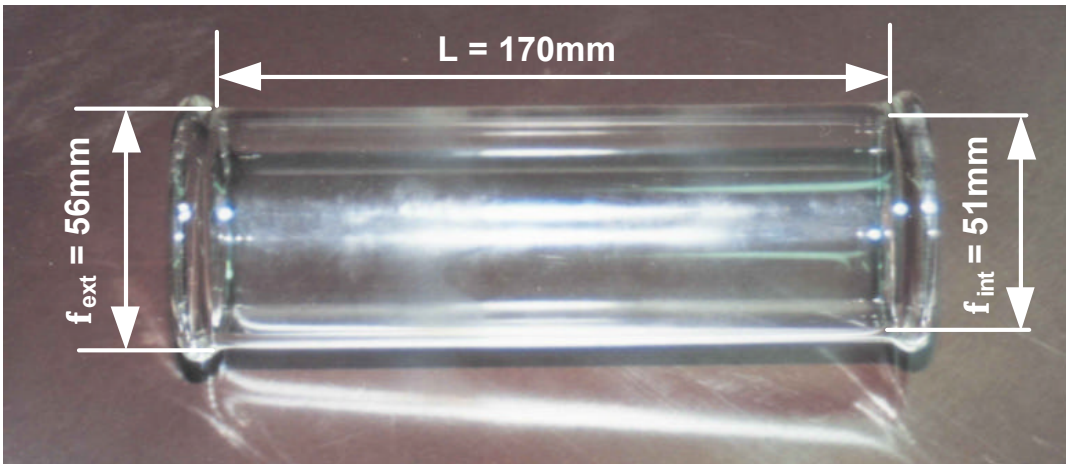

Figure 7.6. *Tube of Pyrex finally used as dielectric housing. The dimmensions used were forced by the commercial disposibility of Pyrex tubes.*

• Improvements for the fixation of the housing

In order to improve the fixation of the dielectric housing to the electrodes a special shape has been made at both ends of the Pyrex housing. This shape increases the area in contact with the electrode and strengthens the fixation. Figure 7.7 displays a detail of the shape.

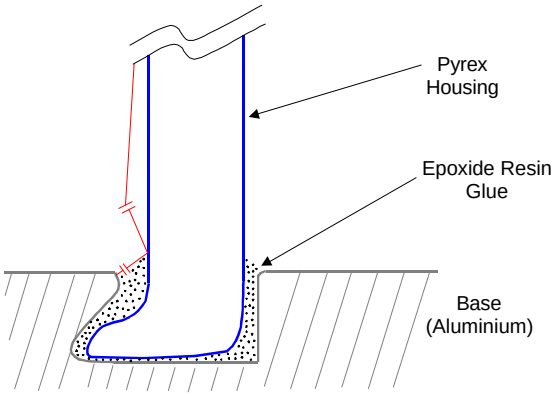

Figure 7.7. *Special shape at the end of the housing to improve the fixation*

A well known problem in high voltage technology appears when three or more different dielectrics have a shared interface. This is the case in the area of fixation of the housing to the electrode by using glue. Air, glue and Pyrex form a triple combination of dielectric. If the dielectric constants of the materials used are very different, important electric fields will appear in the higher dielectrically spoken material. This may provoke the appearance of discharges between the different points at the end of the housing, as was experimentally observed.

High voltage cables have similar problems and a solution has been found by using layers of semiconductive material to distribute homogeneously the electric field and avoid the gradients of field. A reliable material being used as semiconductive layer is the Graphite. This material was successfully applied during the test of the PIEZOTRF3 prototype. A thin layer of graphite was placed in the interface of the three dielectric materials. As a result, a total reduction of the observed discharges was achieved.

7.4.2. Electrodes and Other Pieces

- **Base of the column**

To achieve a good arrangement of the column, both sides of the electrodes in contact with the piezoelectric column must be perfectly flat and at right angles to each other. Moreover, it is necessary that the placement of the column is perfectly centred to guarantee a correct distribution of forces. Figure 7.8 displays a view of the piece used as base of the column.

Figure 7.8 illustrates the central plate for placing the piezoelectric column. A total depth of 2mm was made to allow the column to be centred. Furthermore, this plate made the installation process easier, guaranteeing a good operation. Externally, it can be shown a ring especially designed to fix the dielectric housing. The shape of this ring permits an increase in the fixation of the dielectric body as previously discussed.

The material used to construct the electrodes must be conductive and to have a high rigidity in order to guarantee the blocking state. Prototype PIEZOTRF3 was built by using Aluminium.

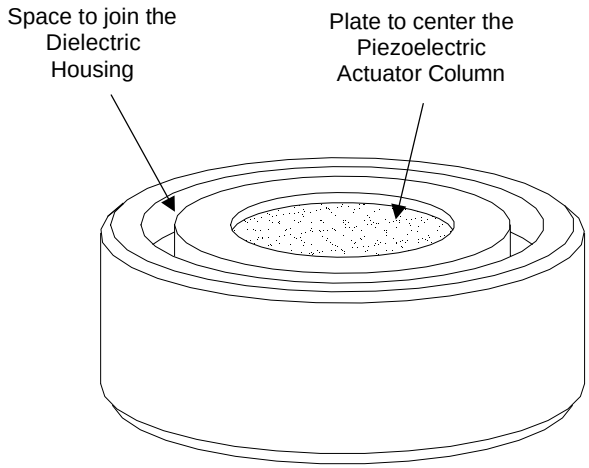

Figure 7.8. *Base of the piezoelectric transformer*

Aluminium is not the ideal material to construct the piezoelectric transformer because of its low tensile modulus. Nevertheless it is quite an accurate material for prototyping, reducing the cost and manufacturing time.

• Upper centred plate

Once the column is placed in the *base,* a special piece is place in the end which remains free. This piece is shown in Figure 7.9 and consists of a disc with two plates on both sides. The bottom plate allows the arrangement of the actuator at the end of the column. The top part will allow the sensor disc to be placed perfectly centred in relation to the actuator column.

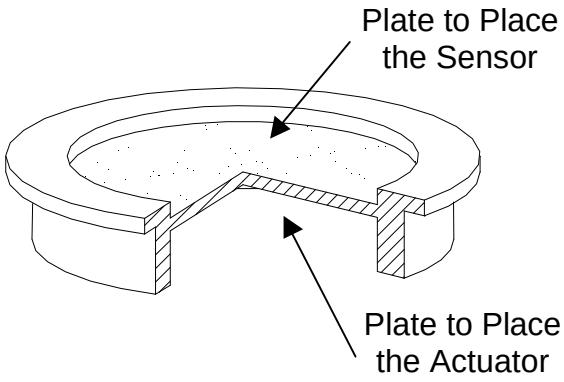

Figure 7.9. *Upper centred plate*

This piece permits: (i) a mechanical centred of the actuator and the sensor; (ii) a mechanical transmission of the forces from the actuator to the sensor; (iii) an electrical connection of the second end of the actuator to ground. Regarding the third point, the ground connection is made through this piece, the upper electrode and the prestressing piece, as will later be discussed. The prestress piece is mechanically and electrically connected with the Upper centred plate, transmitting the ground connection.

• Upper Electrode

The upper electrode is similar to the base electrode. It is fixed to the second end of the dielectric housing. It provides the second point of connection to high voltage. In this case, the upper electrode has an internal screw where the piece for preloading is placed to prestress the column.

Figure 7.10 displays a view of this piece. It can be seen the smooth shape of the borders to prevent gradients of electric field.

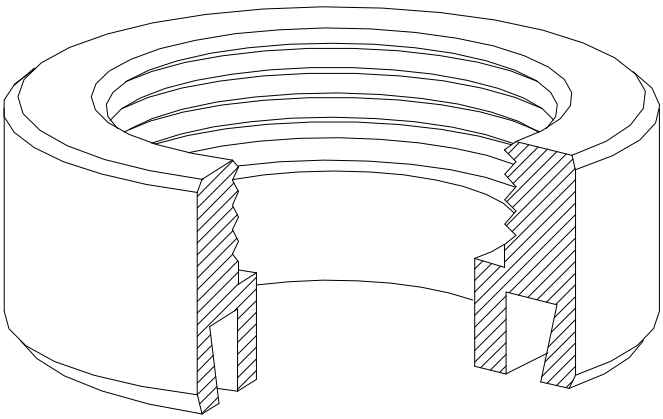

Figure 7.10. *Upper Electrode*

• Prestressing System

The prestressing system consists of two pieces which allow prestress to be applied to the piezoelectric column for guaranting that it will work under compression. Figure 7.11 shows the prestressing head for prestressing the actuator column. This piece has been designed with an internal hole which permits the mounting of the sensor once the column has an initial presstress. This facilitates the installation of the sensor and all the related electronics.

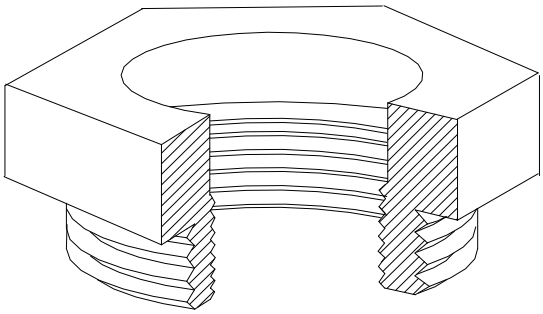

Figure 7.11. *Piece to prestress the actuator column*

The mentioned hole has an internal screw to lodge a second piece which prestresses the sensor and the column together, as is shown in Figure 7.12. This piece incorporates a BNC and forms a perfect Faraday cage to protect the sensor and the built-in electronic against the electromagnetic interference. Figure 7.13 displays a scheme of the extraction of the electrical signal from the piezoelectric sensor.

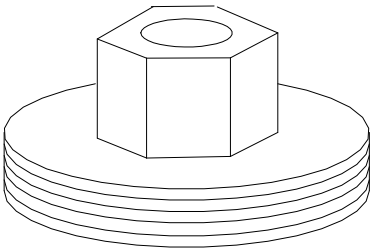

Figure 7.12. *Piece for prestressing the sensor*

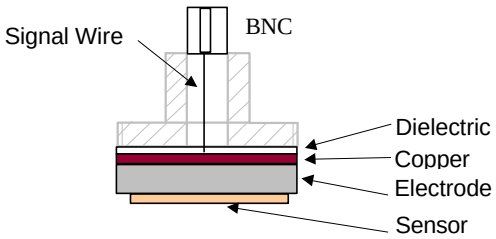

Figure 7.13. *Output of the signal from the sensor*

In the PIEZOTRF3 prototype, the prestressing pieces were constructed with screws which allowed the preload to increase or decrease. Nevertheless, significant deformation in the screw pitch was observed, as will be commented upon in Chapter 8. In order to solve this problem it is possible to eliminate the screw and to fix both pieces with epoxy resin. In this case, the prestress may be obtained from an external press. Furthermore, this solution makes easier a cheaper the manufacturing process. Nevertheless, screw solution has been kept because allows the material to be changed and also the modification of the preload strength altered during the test if necessary and allows the test of different configurations.

7.5. Prototype PIEZOTRF3

7.5.1. The mounting process

By mounting process is understood the procedure used to join the individuals pieces of the piezoelectric transformer. This process involves the join of both electrodes at the ends of the dielectric housing and the placement of the active columns (actuator and sensor) within the dielectric embodiment.

All the process is concentrated in to obtain a high parallelism between both electrodes to prevent the ceramic material to be broken during the prestress process and to guarantee a perfect distribution of the forces.

Figure 7.14 shows a scheme of the position of each one of the pieces of the transformer. During the mounting process the piezoelectric column is replaced by a stainless cylinder. This cylinder, which is very accurately constructed regarding to the parallelism of both ends, is used as reference guide during the mounting.

The mounting process starts by placing the stainless cylinder (2) at the base (1). Following the dielectric housing (3) is place inside the ring (1.2). Before joining the housing with the adhesive, it is necessary to guarantee the perfect alignment of the housing respect to the base. In order to achieve this, it is convenient to situate the upper electrode (4) with the pieces (5), (7) and (8) over the housing. In particular piece 5 permits the bottom and top parts to be centred thanks to the stainless cylinder guide.

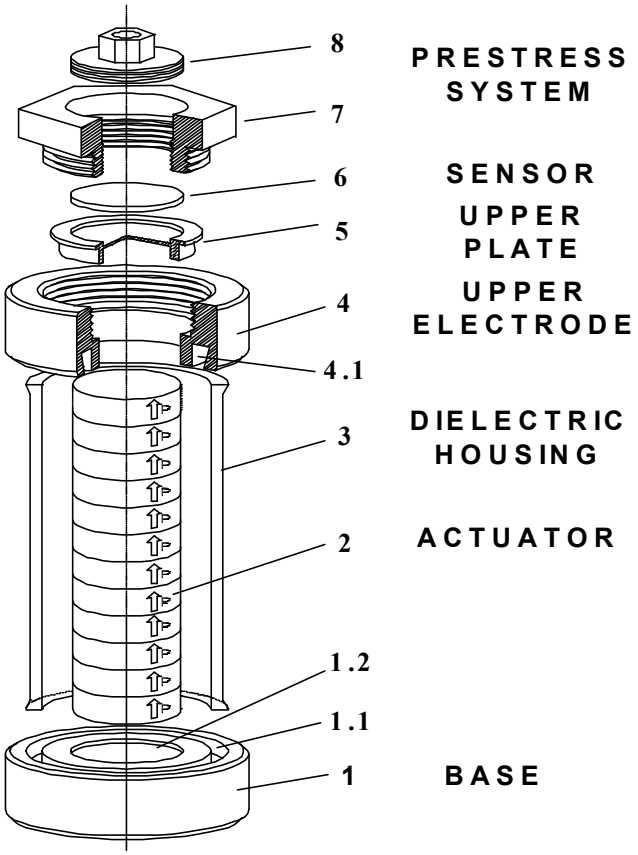

Figure 7.14. *Mounting of the PIEZOTRAF3 prototype*

The space for the placement of the dielectric housing (1.2 and 3.1) has been designed with longitudinal and transversal tolerance (see Figure 7.15) in order to avoid the Pyrex from getting into contact with the metallic electrodes. On the contrary, significant stress could appear in the contact points and, as a probably result, the mechanical breakdown of the Pyrex.

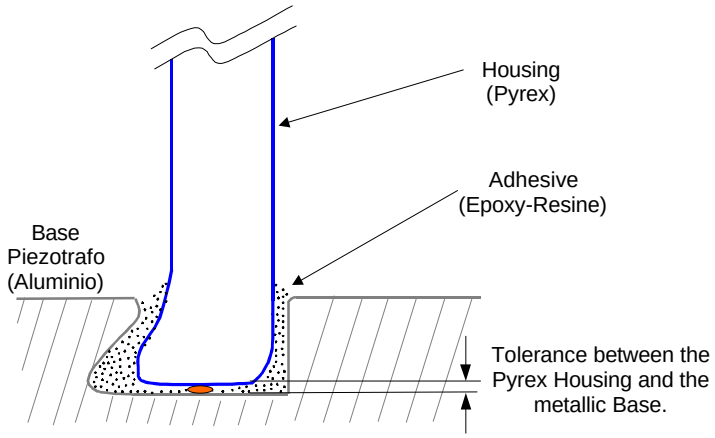

Figure 7.15. *During the mounting process it must avoid the Pyrex from getting into contact with the metallic electrodes.*

A good trick to make the process easier is to place glue at some points (1 o 2 mm thickness) previously in the base and to leave them dry. Thus, when later the Pyrex is place in the base, there are some points of glue where the Pyrex can rest keeping the convenient tolerance.

A Standard-type Araldite epoxide-adhesive was used to perform the fitting between the electrodes and the housing of Pyrex. It is convenient to start joining the base, and when it is dry, to join the upper part by rotating the prototype.

The curing of the epoxy glue was made in a furnace under a temperature between 90ºC – 100ºC during 8h. Figure 7.16 shows a final view of the prototype once mounted.

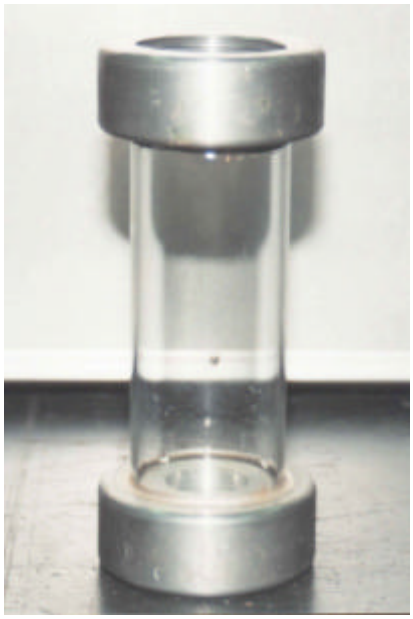

Figure 7.16. *View of the PIEZOTRF3*

7.6. Approach to the prototype operation

The previous theoretical discussion has been based on the supposition than the forces generated by the column were blocking force. This supposition means that the piezoelectric material is completely clamped. However, the real situation is different. The materials used in the prototype design have a certain deformation, and the 'quality' of the blocking state is lower than the ideal.

Thus, in order to determine the effect of the materials chosen in the blocking force, a theoretical attempt is below described by considering the equivalent static spring diagram (no-inertial effects) [11].

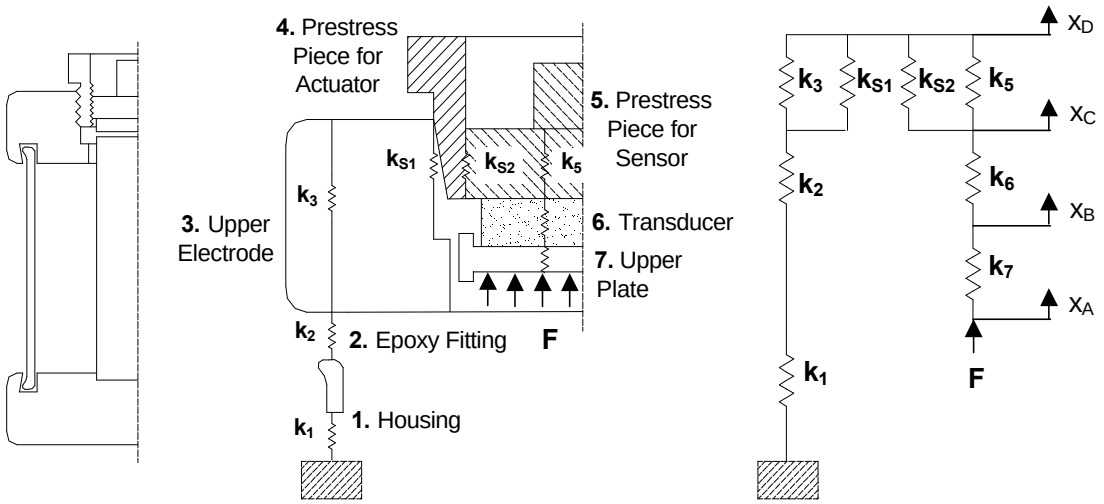

Figure 7.17. *Spring model for analysing the operation of the PIEZOTRF3 prototype*

The force, *F*, generated by the actuator is transmitted up to the housing following the series and parallel paths indicated in Figure 7.17.

$$F = k_7 \cdot (x_A - x_B) = k_6 \cdot (x_B - x_C) = k_{eq(1)} \cdot (x_C - x_D) = k_{eq(2)} \cdot x_D \tag{7.14}$$

$$k_{eq(1)} = k_{S2} + k_5 \tag{7.15}$$

$$k_{eq(2)} = \frac{k_1 \cdot k_2}{k_1 + k_2} + k_3 + k_{S1} \tag{7.16}$$

$$F = k_{eq(1)} \cdot \left(x_C - \frac{F}{k_{eq(2)}} \right) \Rightarrow F = \frac{k_{eq(1)} + k_{eq(2)}}{k_{eq(1)} \cdot k_{eq(2)}} \cdot x_C = \alpha \cdot x_C \tag{7.17}$$

The force measured under these conditions will be:

$$F = k_6 \cdot (x_B - x_C) = k_6 \cdot x_B - k_6 \cdot x_C = k_6 \cdot x_B - k_6 \cdot \frac{F}{a} \tag{7.18}$$

$$F = k_6 \cdot x_B \cdot \frac{a}{k_6 + a} \tag{7.19}$$

Under blocking conditions x_C=0 and the measured force will be $F=k_6 \cdot x_B$, from equation (7.18). Thus, owing to the deformation of the system the force measured is reduced compare to the ideal case of perfect blocking system. The coefficient of reduction is:

$$d = \frac{a}{k_6 + a} \tag{7.20}$$

where k_6 is the stiffness of the transducer and $a = \frac{k_{eq(1)} \cdot k_{eq(2)}}{k_{eq(1)} + k_{eq(2)}}$ is the equivalent of the stiffness of the housing and the prestressing system.

The spring constant of each part of the prototype may be calculated as:

$$k = \frac{Y_{material} \cdot A}{t}$$

where $Y_{material}$, is the Young's modulus of the considered material, A is the area of the material deformed, and t the thickness.

7.7. References

[1] ENERGIA demo, Parc Eòlic de Roses. *Planta d'aprofitament de l'energia eòlica*. nº 4. Institut Català d'Energia

[2] *Piezoelectric Ceramics Data Book for Designers*, Morgan Matroc Limited, Transducer Products Division, Hampshire, England.

[3] *Piezoceramics*, CeramTec AG Piezo Applications Division, Germany.

[4] *Piezoelectric Ceramics*, Data Handbook MA03, Philips Components, The Netherlands, 1996.

[5] *Ferroperm Piezoceramics*. Industriselskabet Ferroperm A/S, Piezoelectric Ceramics Division, Denmark, July 1995.

[6] F.H.Kreuger. Industrial High Voltage. 1.Fields. 2. Dielectrics. 3. Constructions. Delft University Press. The Netherlands, 1991.

[7] Arnold Roth. Técnica de la Alta Tensión. Editorial Labor S.A. Barcelona 1966.

[8] Goodfellow Catalogue 1998/99, Goodfellow Cambridge Limited, Cambridge, England.

[9] *High-Voltage Porcelain Insulators*, Siemens Catalogue, Germany, 1985

[10] *Vidrio Pyrex Plano Catálogo*, VitroTec, S.A, Barcelona, Spain, 1996

[11] *Measurement of Dynamic Forces*, Bulletin K20.220, Piezo Instrumentation KISTLER, Kistler Instrument Corporation, New York.

Chapter 8

Experimental Characterisation of the PIEZOTRF3 Prototype

8 Experimental Characterisation of the PIEZOTRF3 Prototype

8.1. Introduction

Experimental characterisation of PIEZOTRF3 prototype is gathered in this chapter. As previously commented in Chapter 7, PIEZOTRF3 was constructed with the aim of being tested in the *Parc Eolic de Roses*. However, an important fault caused for the fall of a lightning, motivated the cancellation of the project of installation. Hence, the experimental characterisation presented is regarding to experimental tests performed in laboratory conditions.

This chapter starts by presenting three different mechanical tests which provide information about:

1. The mechanical behaviour of the stacked column in comparison to a similar bulk material.
2. The mechanical strength of the prototypes and the mechanical breakdown limit.
3. The influence of the prestress in the behaviour of the prototype.

Following, several tests related to the dielectric strength of the housing are described. These tests were performed following the standards on high voltage and instrument transformers. The tests were carried out in a High Voltage testing platform by applying a lightning pulse (1.2/50μs).

Once the mechanical and dielectric strength of the actuator were tested, the tests were concentrated in the response characterisation of the device, in terms of linearity, frequency response and time dependence.

Tests related to the linearity and frequency response of the device were carried out in the Swiss Federal Institute of Technology by using an appropriate charge amplifier for the acquisition of the electrical signal from the sensor. This type of measurements made possible to determine accurately the electric charge generated by the sensor and thus the force developed by the actuator column. The experimental results were compared with the expected transformation ratio.

The time-dependence of the behaviour of the prototype was also measured in a special high voltage cell. The tests were carried out using a network analyser specially designed to offer very high input impedance for the sensor connection. The experimental data were collected daily over a months.

8.2. Mechanical Tests

8.2.1. Compression Test of the Actuator Column

The theoretical calculation of the transformer ratio made in Chapter 7, considered the actuator column as a bulk piece of piezoelectric ceramic. In this way, mechanical and piezoelectric coefficients were considered as the values indicated within the manufacturer's data sheet for bulk pieces.

Nevertheless, it has been previously described that the column was built by piling up single disc up to the required length. This configuration could have some influences in the coefficients used to make the theoretical attempt.

Particularly, one of the parameters which defines the expected transformer ratio under blocking force conditions is the compliance of the used material, as indicated equation (7.3). It is necessary, then, to verify if the compliance obtained for the stacked column behaves as in the case of a bulk material.

Compliance of the stacked column could be evaluated by means of a compressive test. The relation between the deformation of a material under the effect of a stress leads to the stiffness of the material being tested. In piezoelectric materials, the stiffness depens on the electrical conditions of the material during the test. One can apply the stress in open circuit conditions or in short circuit conditions. The test below presented is related to open circuit conditions, since this is the necessary coefficient for obtaining the blocking force generated by the actuator.

A second important information that one can obtain from a compression test is related to the existence of hysteric behaviour in the force-displacement curve due to non-linearities as it was discussed in Chapter 5. This is especially important in the present application where the column works under high static and alternative mechanical fields, and the cycle of 'up' and 'down' may be affected by the hysteresis.

• Experimental Set-up and Results

Experimental tests were performed in a compressive-press by monitoring the force-displacement curve. A stacked column of 12 individual discs of PZT-8S from Morgan Matroc of 12mm thickness and 30mm diameter were used to carry out the measurements.

The tests were made by applying a ramped compressive force up to $1.8 \cdot 10^3$ Kg which corresponds with a stress in the column of around 25MPa (see Figure 8.1). This value is lower than the depoling limit for hard materials as was described in Chapter 5 (Figure 5.26). Measurements were performed under short-circuit, E=0, and room temperature conditions. This corresponds to the so-called s_{33}^E coefficient. The selected velocity of the applied force was of 100Kg/min, which represents a quasi-static experiment and guarantees the redistribution of the electrical charges.

Figure 8.1 illustrates the results measured. Initially, when the value of the force is lower, the observed displacement is more important than in the case of high stresses. This behaviour is due to the lower compliance of the silver interface of the electrodes of each disc. This lower compliance affects the first range of measures. Once the force is higher than 200Kgf the compliance measured became totally linear and motivated exclusively for the deformation of the piezoelectric material, without influence of the interfaces of the discs.

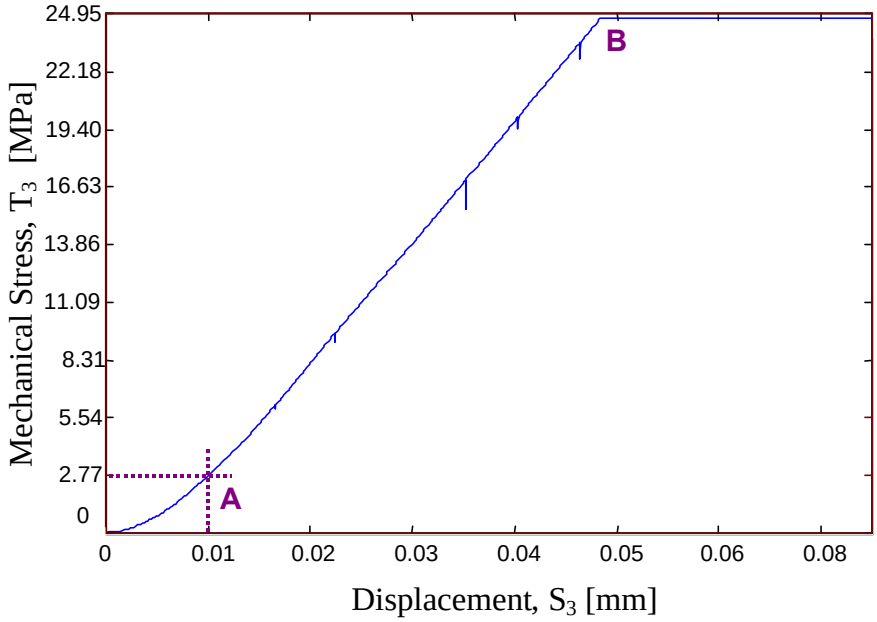

Figure 8.1. *Curve Displacement-Compressive Stress for a PZT-8S 12-discs stacked column.*

From Figure 8.1, one can calculate the experimental compliance of the stacked column, as is indicated in equation (8.1).

$$s_{33}^{E} = \frac{dS_3}{dT_3} = \frac{\Delta h_3 / L}{\Delta T_3} = \frac{(0.049 - 0.01)\cdot 10^{-3} / 144\cdot 10^{-3}}{22.043\cdot 10^{6}} = 12.363\cdot 10^{-12}\ m^2/N \qquad (8.1)$$

The previous calculation has been done considering the linear range (points A and B in Figure 8.1), where the coupling effects of the interfaces do not affect.

One can compare this value with the value provided in the Data Sheet of Morgan Matroc, s_{33}^{E} =13.5·10^{-12} m^2/N, which confirms that the mechanical behaviour of the stacked column is very close to the behaviour of a bulk piezoelectric material, and verifies the supposition used in Chapter 7 for determining the blocking force (equation 7.3).

8.2.2. Mechanical resistance of the housing to tensile forces

Once the mechanical behaviour of the active material (actuator column) has been tested and compared with the theoretical values used in Chapter 7, it is now necessary to verify the mechanical behaviour of the passive materials. Particularly the resistance of the dielectric housing under static compression.

- **Experimental Set-up**

In order to verify the resistance of the housing to external static loads, a pneumatic press has been used to perform the tests. This press has been re-adapted from a old welding by spot press SCIAKY (France) (Figure 8.2). This machine was used for SEAT, the Spanish car company, for welding components of the car body. In 1984, SEAT donated it to the *Universidad*

Politécnica de Catalunya, where rested without any particular service up to 1998, when was repaired for the present application.

The welding press working procedure consist of pressing the materials to be welded and applying a DC electric field which generates an important current. This important current results in a welding spot. The electrodes consist on a fixed plate, and a piston. The stress between both electrodes, during the welding process, can amount to 120Kg/cm^2. A pneumatic circuit activates the piston-electrode with compressed air up to 10Kg/cm^2. The internal structure of the compression chamber of the press, separated in two pistons, allows static preloads and dynamic preload to be applied. The external diameter of the piston is 10cm.

The operation of the machine depends on how the two piston are driven. There is a possibility of slow approximation, which permits apply a preload to the column, and a second faster course, which allows the application of alternative stresses. Both courses may be controlled independently with an external pneumatic circuit by using two valves of 5 vies-two positions and a manometer. The pneumatic pressure is inputted to the machine from an external pneumatic circuit which supplies pressures between 0 to 6Kg/cm^2.

This press thus obtained has a very significant stiffness, higher to similar commercial devices. Figure 8.2 shows an external view of the described press.

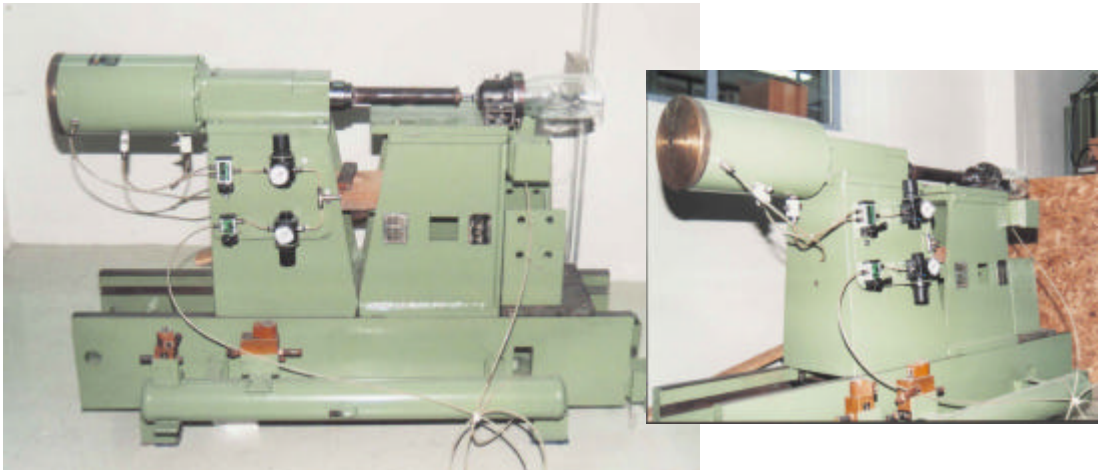

Figure 8.2. *SCIAKY pneumatic press used during the mechanical breakdown test.*

Before starting the experimental tests, a calibration of the press was performed. Figure 8.3 displays the calibration made to the press. The x-axis indicates the pneumatic pressure while the y-axis indicates the force obtained in the external, available for the tests. The maximum force available when a pneumatic pressure of 6 bar is applied can get up to approximately 1200kg.

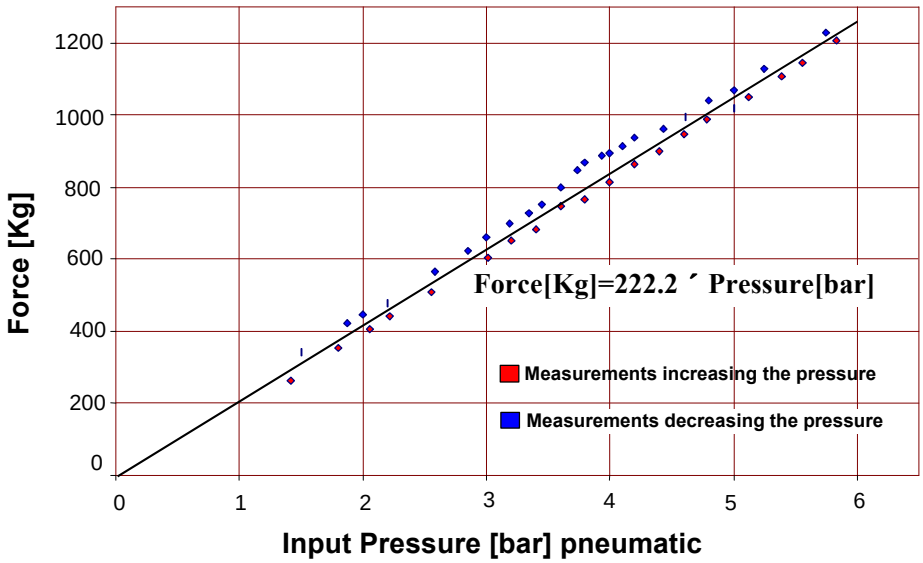

Figure 8.3. *Calibration of the pneumatic press.*

• Experimental considerations

Before starting the experimental evaluation it is convenient to establish the values of the expected maximum mechanical strength limit, from the manufacturer's information given in Table 7.4. In particular the tensile strength for Pyrex is 150bar.

The Area of the Pyrex housing is indicated in the next Figure 8.4.

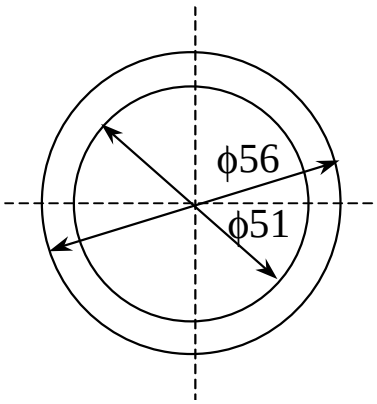

$A_{ext} = 2463mm^2$

$Aint = 2042.8mm^2$

$A_{eff} = A_{ext} - A_{int} = 420.188mm^2$

Figure 8.4. *Dimensions of the dielectric housing of Pyrex and indication of its effective Area.*

As stated in Chapter 7, the maximum tensile strength for the used Pyrex is 150bar (15MPa). One of the main interests of making a mechanical breakdown test, is to verify the quality of the fixation electrode-Pyrex, made with Araldit. In order to do that, it is necessary to verify if the fixation will break before or after the Pyrex. The expected strength limit of the Pyrex is found at:

$$F_{\substack{tensile \\ max}} = T_{\substack{tensile \\ strength}} \cdot A_{eff} = 1.5\ Kg/mm^2 \cdot 420.188\,mm^2 = 630.282\,Kgf \qquad (8.2)$$

This value is much lower than the maximum capacity of the press, as indicated equation (8.3), for a maximum input pressure of 6 bar from the external source (see Figure 8.3).

$$T_{\substack{tensile\\max}} = \frac{F_{\substack{tensile\\max}}}{A_{eff}} = \frac{1200Kg}{420.188mm^2} = 2.885\,Kg/mm^2 = 288.5\,bar \qquad (8.3)$$

Thus, with the pressure available from the pneumatic press is possible to overpass the breakdown expected value and verify the behaviour at very high stresses.

• Experimental Results and Conclusions

Stress was applied to the housing progressively by increasing the driving pressure of the pneumatic circuit in steps of 0.5bar. After each addition, the pressure was remained for a few minutes after passing to the next one. The tests were carried on up to the mechanical breakdown appeared at a force of 834 Kg (Figure 8.5). This leads to a stress in the housing of:

$$T_{\substack{tensile\\max}} = \frac{F_{\substack{tensile\\max}}}{A_{eff}} = \frac{834Kg}{420.188mm^2} = 1.985\,Kg/mm^2 = 198.5\,bar \qquad (8.4)$$

This value is about a 30% higher that the limit recommended by the manufacturer (150bar).

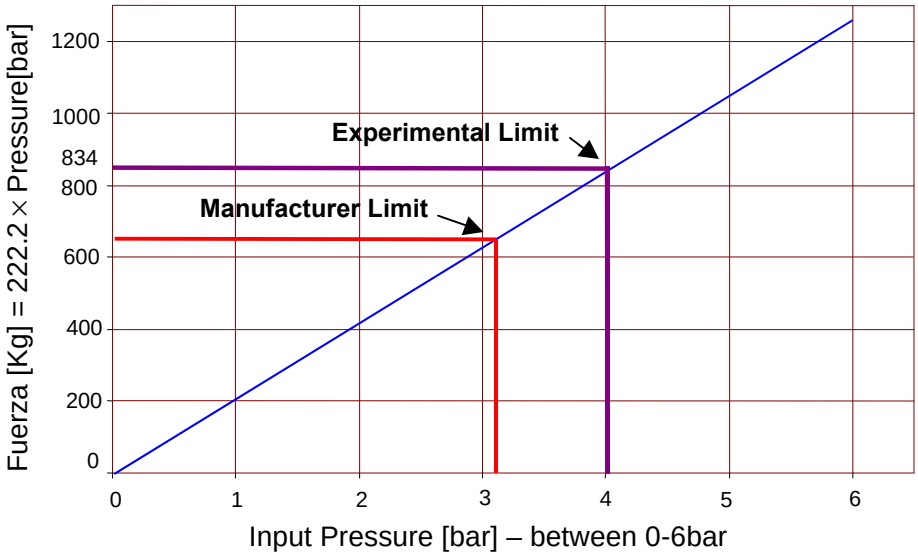

Figure 8.5. *Mechanical breakdown test.*

It is important to analyse the shape of the failure, illustrated in Figure 8.6. From the shape is clear that the breakdown was caused for the concentration of forces in the join of the metallic electrode with the Pyrex. This concentration of forces could be caused for the different special shape make to improve the electrodes fixation. A probable reduction in the area due to the hand-make system used in the elaboration of this shape is though as the cause of the breakdown. Figure 8.7 give a visual interpretation of the phenomenon.

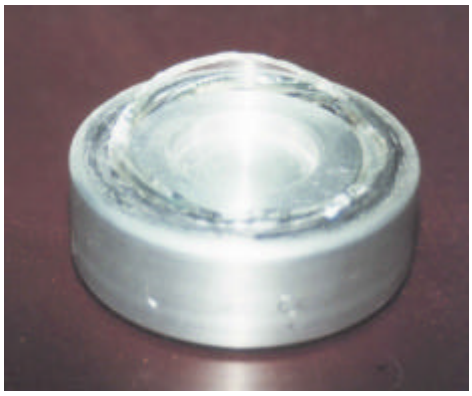

Figure 8.6. *Appearance of the bottom electrode after the mechanical breakdown.*

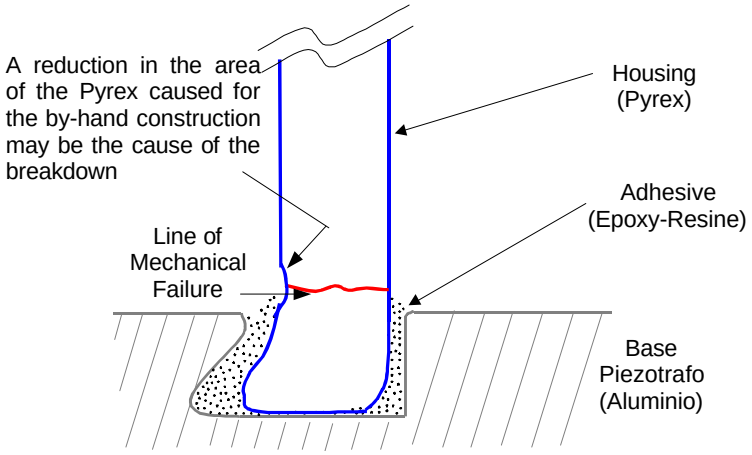

Figure 8.7. *Schematic of the breakdown line.*

8.2.3. Prestress Measurements

The importance of prestressing the piezoelectric column in order to reduce mechanical depolarisation effects, has been commented upon previously (chapter 5). The significant forces appearing in the piezoelectric column require also of an important prestress which guarantees the perfect contact at the interface of the discs. On the contrary decoupling could appear.

A test to verify the behaviour of the piezoelectric column under greater or lower prestress was performed. A pneumatic cylinder-press with capacity up to 10 bar was used to apply static preloads of different strengths and to measure the modification of the external voltage output. Nevertheless the maximum available pressure was only of 6 bar, so the cylinder was driven from a external pneumatic compressor with capacity of 6.5 bar.

The measurements were made by driving the external electrical signal from the sensor to a YOKOGAWA DL1200 4-channel digital oscilloscope. The input impedance of the oscilloscope was R_E=1MΩ / C_E=27pF.

The voltage measured with this system depens upon the input characteristics of the oscilloscope (see Appendix 1) but since these characteristics are constant during the tests, differences observed in the measured signal will be caused for the preload influence.

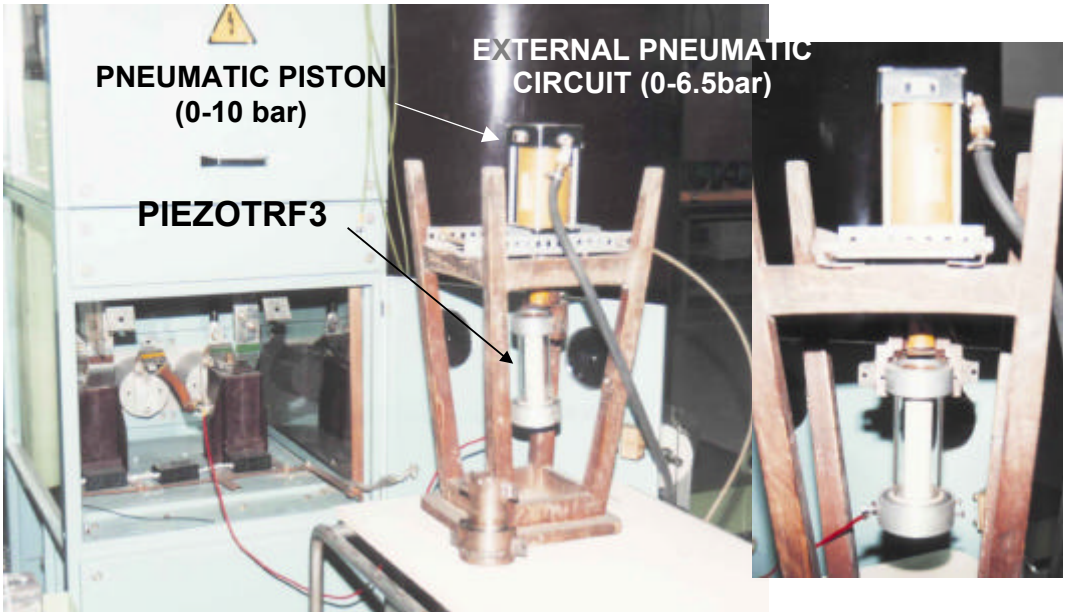

Figure 8.8. *Set-up for prestress measurements. A 10bar pneumatic piston has been used*

Table 8.1 offers the relation between the external pressure applied to the piston and the pressure in the piezoelectric column.

Table 8.1. *Pressure relation between the input pneumatic pressure and the preload in the actuator column.*

Pressure of the External Pneumatic Circuit [bar]	Preload in the Piezoelectric column [MPa]
1	0.71
1.5	1.07
2	1.42
2.5	1.78
3	2.13
3.5	2.49
4	2.84
4.5	3.20
5	3.56
5.5	3.91
6	4.27

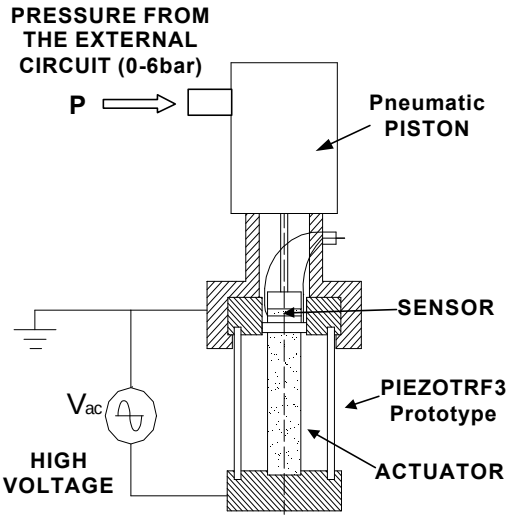

Figure 8.9. *Schematic of the used experimental set-up.*

Figure 8.9 shows, more clearly, the operation followed during the test. The piezoelectric internal actuator and sensor columns were prestress with a mechanical stress coming from a pneumatic piston. Once the required pressure was applied, an electrical high voltage was applied into the column. The modification of the sensor response was then measured by using the YOKOGAWA digital oscilloscope.

Figure 8.10 gathers the experimental results obtained. The x-axis indicates the input voltage applied and the y-axis indicate the output voltage measured in the sensor. The used sensor was a piezoelectric disc of PZT-8 material, with 24mm of diameter and 2 mm of thickness. The sensor and the output signal were perfectly shielded to avoid any electromagnetic interference.

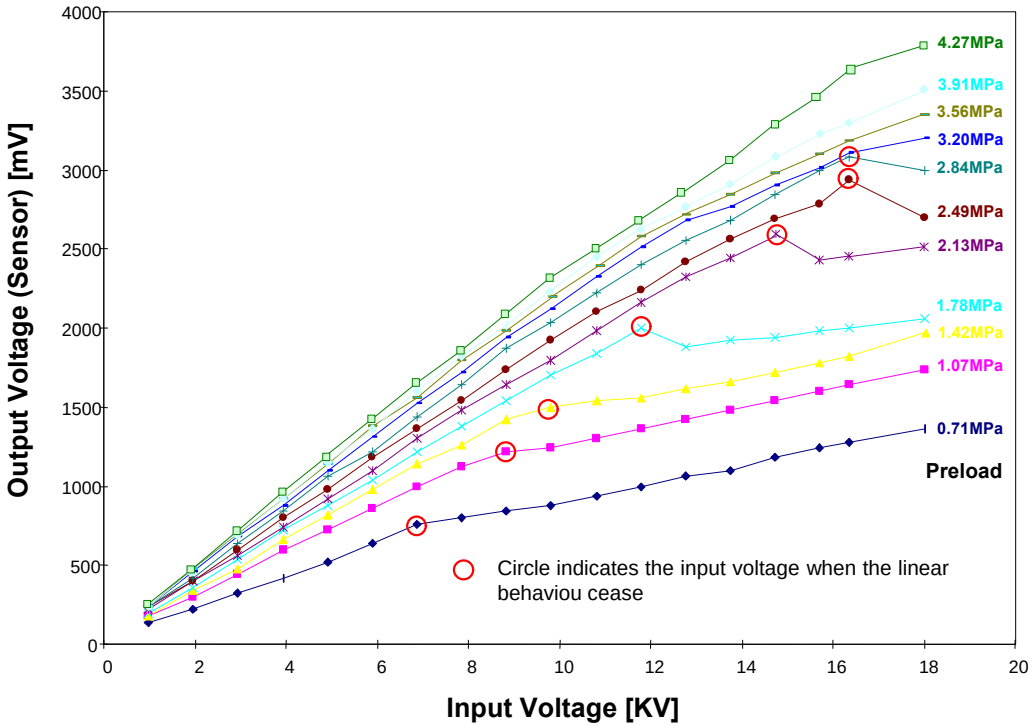

Figure 8.10. *Influence of the prestress in the behaviour of the piezoelectric transformer.*

Points inside a circle indicate the voltage values when the response of the transformer ceases of being linear. A comparison between the preload existing in these points and the blocking force generated by the actuator in such circumstances is indicated in Table 8.2. From this values is clear than linearity cease when the force generated by the actuator reaches a value similar to the preload applied. Hence, decoupling of the stacked discs is indicated as the main cause of the loss of linearity when the voltage is increased over a certain value.

Moreover, deformation of material has significant influence in the loss of the linearity. This is especially important with very high preload.

Table 8.2. *Expected blocking force and preload values when the linearity in the response of the transformer ceases*

Preload applied when linearity is not followed [MPa]	**Theoretical Blocking Stress in the moment when linearity ceases [MPa]** $\frac{T_{bloq}}{V} = \frac{d_{33}}{s_{33}^{E} \cdot L} = \frac{225 \cdot 10^{-12}}{13.5 \cdot 10^{-12} \cdot 144 \cdot 10^{-3}} = 115\ Pa/V$
0.71	(linearity ceases at 7kV) → 0.805MPa
1.07	9kV → 1.03MPa
1.42	10kV → 1.15MPa
1.78	12kV → 1.380MPa
2.13	15kV → 1.725MPa
2.49	17kV→ 2.185MPa
2.84	17kV→ 2.185MPa
3.20	-
3.56	-
3.91	-
4.27	-

8.3. Dielectric Tests

8.3.1. Dielectric Housing

The insulators must be able to withstand three types of conditions:

(1) Alternating voltages at 50Hz

(2) 1.2/50 μs lightning impulse voltage, and

(3) 250/2500μs switching impulse voltage (outdoor insulators also in the presence of rain) which are far above the normal operating stresses. The safety factors are laid down in CEI 186 Standard for instrument transformers.

In this section, the results of the electric tests carried out to the dielectric housing of the instrument transformer are gathered. Tests were performed without the active material to verify the behaviour of the dielectric material itself. Important results were found relating to the join of the Pyrex with the electrodes. Due to the different permittivity of the epoxy, Pyrex and air, the join became a *triple* point. The electric field may increase considerably at that point and partial discharge may appear, as it was effectively observed. A technique consisted of placing a carbon semiconductive layer between the epoxy and the air, allows to make homogeneous the electric field in that area and to reduce to zero the partial discharge as will be shown in the next results.

• Power-frequency withstand voltage

Power-frequency test withstand voltage is the 50Hz alternating voltage at which the instrument transformer must not suffer flashover or puncture. The value of the voltage applied during this test use to be approximately twice the operating voltage. In electromagnetic transformer this test is especially important because it permits one to verify the behaviour of the insulator which covers the wires. This test is performed during 1 minute. In particular for a 36kV-type instrument transformer the required test is up to 70kV.

An important level of partial discharge was detected in the fixing point of Pyrex and the metallic electrodes. In one of the two prototypes tested a semiconductive layer of graphite was applied in the join to reduce the discharges, verifying a complete reduction for all the voltages tested, as previously expected.

• Lightning Test (170kV; 1.2/50 ms)

The lightning test belongs to the category of dielectric tests because it permits one to verify the dielectric behaviour of a device under extreme conditions. In real situations, these conditions usually are related to atmospheric or internal overvoltages. Atmospheric overvoltages appear when atmospheric discharge falls over the network, while internal overvoltages are caused by switching operation. Both conditions are clearly different due to the energy applied to the device in one or another case. Atmospheric overvoltages are tested as a very fast phenomenon (impulse of 1.2/50 μs) while switching overvoltages are tested with an impulse of 250/2500 μs.

The dielectric tests applied to the piezoelectric transformer were limited to the atmospheric test. This switching test is not required for the Standards for transformers of 36kV. The procedure followed was according to the CEI standards for high voltage measurements in instrument transformers (CEI 186).

A high voltage HAEFELY platform with capability up to 1MV impulse test was used to carry out the tests. Voltage applied was measured by using a high voltage spintherometer (ball spark gap) and monitored with a 4 channel YOKOGAWA DL1200 digital oscilloscope.

Figure 8.11 displays the calibration of the platform to a voltage of 140kV before starting the tests.

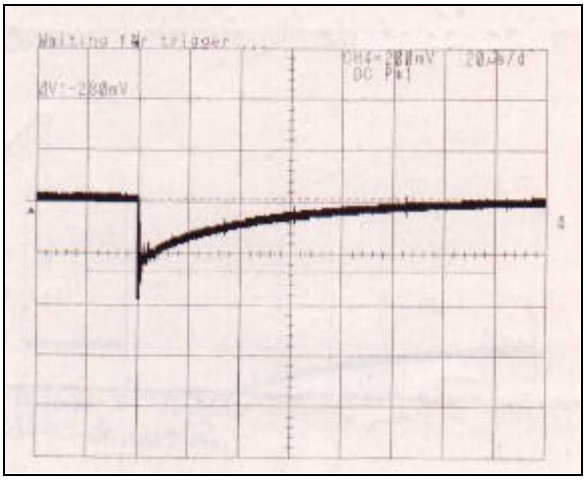

Figure 8.11. *Calibration of the H.V. platform.*

The signal (Figure 8.11) corresponds to a double exponential with a rise time of 1.2μs and a down time of 50μs. Peak voltage is also determined by standards and is related to the nominal voltage of the considered instrument transformer. Particularly, for a 36kV-type instrument transformer a lightning test up to 170kV$_{crest}$ is required. The aim of this section is to verify the maximum peak voltage that the prototype could withstand.

Experimental tests were performed over two similar housing constructed by Pyrex but one with a layer of semiconductive graphite. In both prototypes, the dielectric distance between electrodes was the same, 125mm. The tests were started at 140kV and were increased until the partial discharge or breakdown appeared. Figures 8.12.a and 8.12.b show the response of both prototypes to a voltage of 140kV without breakdown.

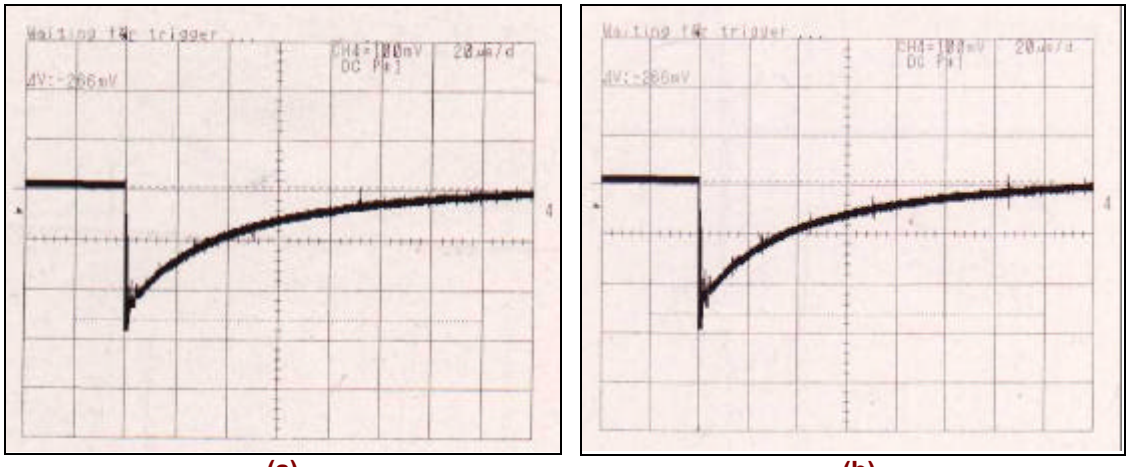

(a) **(b)**

Figure 8.12. *Impulse test to 140kV (a) only Araldite, (b) with a semiconductive layer*

Following Figures 8.13.a and 8.13.b indicate the response of both prototypes under a voltage of 155kV. The test was repeated five times without appearance of breakdown. Nevertheless, the partial discharges in the prototype without semiconductive layer were very important and visual. On the contrary, in the prototype with semiconductive layer did not appear partial discharges.

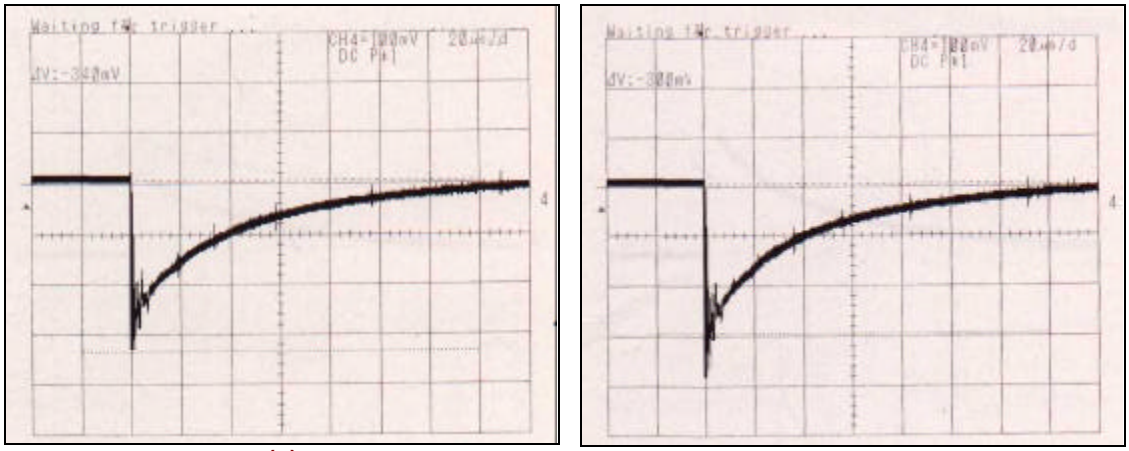

(a) (b)

Figure 8.13. *Maximum voltage before breakdown (a) only Araldite, (b) with a semiconductive layer*

The voltage was increased until the breakdown, as it is displayed in Figures 8.14.a and 8.14.b for both prototypes. In the prototype without semiconductive layer the breakdown appeared at 160kV, while in the case of the graphite prototype the first breakdown appeared at 170kV. This small difference observed might be explained due to the higher level of partial discharge in the prototype without semiconductive layer, which makes the breakdown easier. Nevertheless, it may be also explained due to statistic reasons (pollution, humidity, etc) which reduce the breakdown slightly in the prototype without the semiconductive layer.

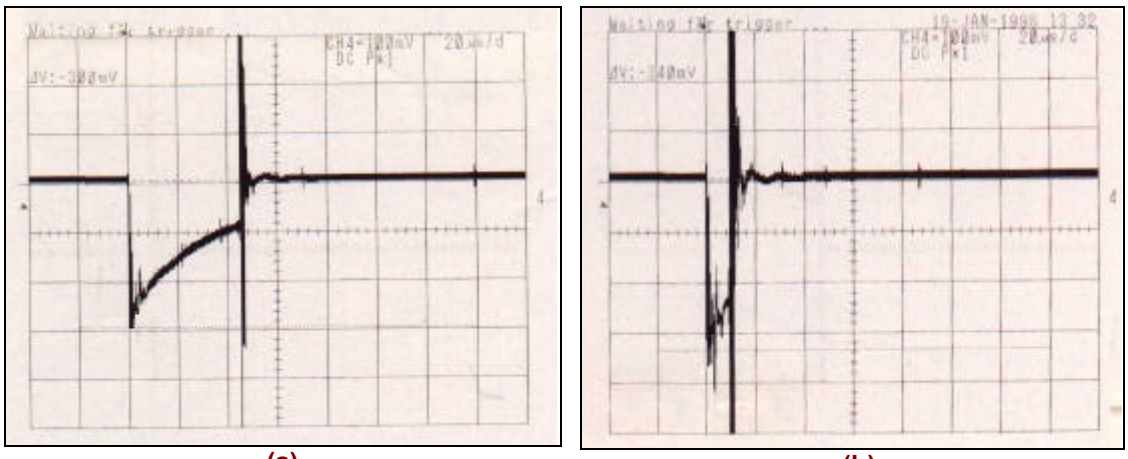

(a) (b)

Figure 8.14. *Breakdown (a) Araldite prototype; (b) Prototype with semiconductive layer*

With the data obtained, it seems clear that the actual design is not dielectrically enough to pass the lightning test. An increase in the creepage distance is necessary to increase its dielectric resistance. It is interesting to note that in both cases breakdown occurred inside the dielectric housing (it was visual thanks to the transparence of the prototype).

In order to reduce internal discharge, a simple solution may consist of fill the internal cavity of the housing with some dielectric gas, as air under pressure or, even, dielectric liquid as oil. Externally, if necessary, the breakdown resistance may be increased by using a shed profile for the housing.

8.4. Electrical behaviour of the prototype under H.V.

In order to verify the behaviour of the transformer in similar conditions to a real operation, a test was considered under a continuous AC voltage of $20kV_{eff}$ over a month. To carry out this test a specific H.V. cell was especially readapted which allowed the prototype to be left working at H.V. continuously and without risk for the rest staff in the laboratory.

The cell is divided at the following three zones, as can be appreciated from Figure 8.15:

1. The *high voltage zone*, where there is placed the power transformer for driving the high voltage to the prototype. This transformer elevates the network voltage from 110V (using a previous transformer to reduce from 220V to 110V) up to 36kV. A high voltage electromagnetic transformer of 30VA was used. Although the power drive for this type of transformer is very low compared with a power transformer it is enough to drive the voltage to the piezoelectric transformer. Furthermore, the precision achieved is better than for a power transformer.

2. The *control, protection and monitoring zone*, which allows the input and output voltage signals to be monitored. Also protect the cell against overvoltages or overcurrents. The control of the voltage is made by using an autotransformer which regulates the voltage arriving at the input of the power transformer and then the voltage arriving to the prototype.

3. A third *testing zone*, which is used to place and testing the prototype. This area is protected by a transparent dielectric material permitting the visual control of the prototype.

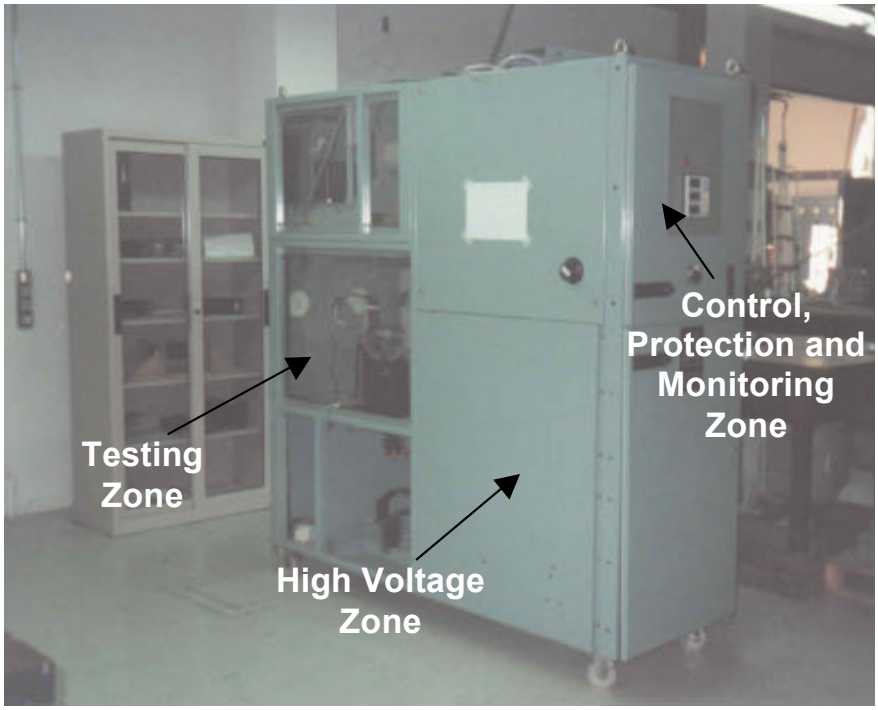

Figure 8.15. *General view of the H.V. cell used during the electric tests.*

Figure 8.16 shows the electric diagram of the different elements of the cell.

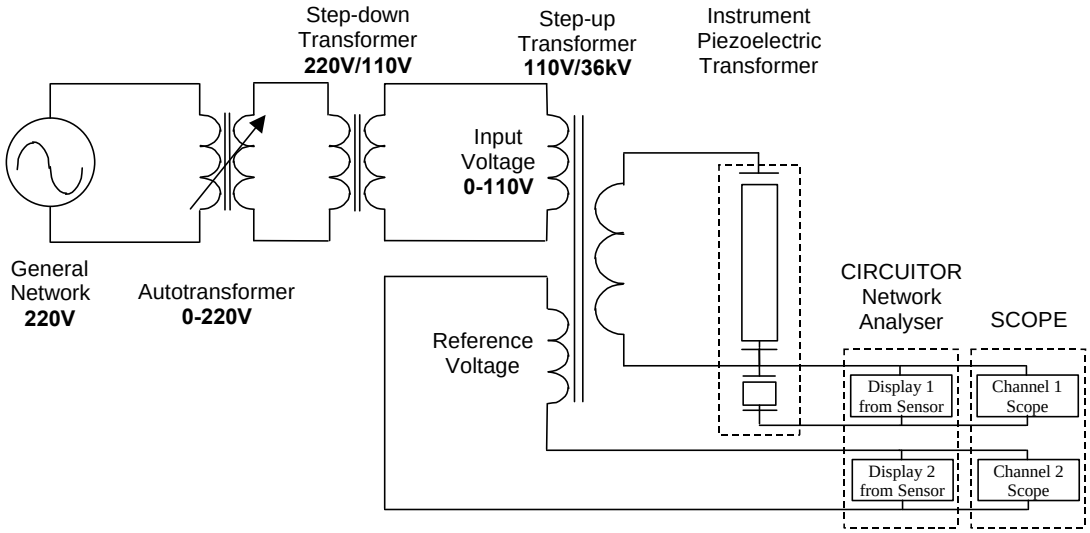

Figure 8.16. *Electric diagram of the H.V. cell*

Connection of the prototype was carried out between phase and ground Figure 8.17 displays a detail of the connection of the device.

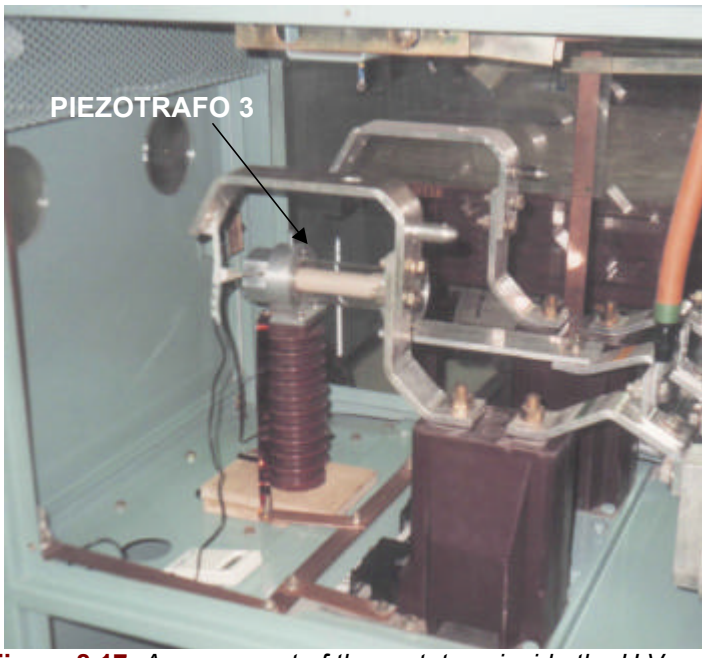

Figure 8.17. *Arrangement of the prototype inside the H.V. cell*

Monitoring of the signal was carried out using a digital compact network analyser equipment from CIRCUITOR. This type of device allows the measurement of 6 electrical signals, 3 voltages and 3 currents, which is sufficient to characterise the rest of magnitude of the three-phase network. The device requires an independent supply to 220V for powering the internal electronics.

Externally the network analyser has three displays and a controlling menu to select the appropriate magnitude to be shown. Two of these displays were used for continuously monitoring the voltage in the input and output of the piezoelectric transformer. Furthermore, the input voltage shape was monitored with an oscilloscope.

Since temperature is an important factor which may affect the behaviour of the transformer, an exact control of temperature in the prototype and in the surrounding area was also measured. Figure 8.18 displays the results of the data collected during a month of testing.

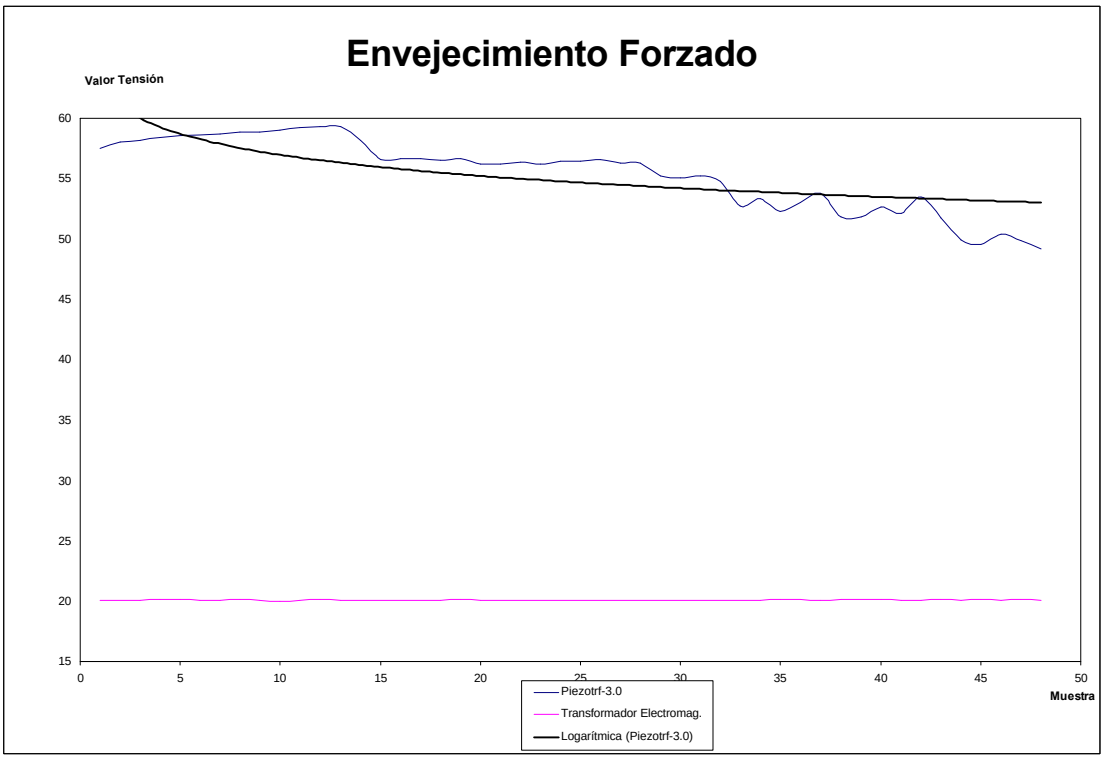

Figure 8.18. *Experimental results obtained during a month of testing.*

A very irregular behaviour has been observed. Different factors may have provoked this type of behaviour:

1. Modifications in the properties of the piezoelectric materials (as has been analysed in chapter 6) may be important when high alternative electrical or mechanical fields are acting. Nevertheless this behaviour is expected to actuate progressively in the response of the device.

2. Relaxation of the preload screw due to the alternative electrical and mechanical cycles. This possibility was considered to be the most probable since the preload applied was not high enough to withstand the compressive forces. Preload was applied by hand and without measurement. An estimation of the value applied is around 0.5MPa which is very low in comparison to the 2.3MPa (approx.) appearing in the column when 20kV were applied. Thus decoupling of discs could have happened and continuos shocks against the screw occurred. This could affect seriously the mechanical resistance of the screw.

A minimum preload of about 5MPa was demonstrated as being necessary during prestress measurements in order to obtain a good behaviour under a voltage of 20kV.

8.5. Linearity

Linearity determination involves the measurement of the correlation between the input and the output signal of the piezoelectric transformer in magnitude and phase and shape. The response of the device during this test depen on the conditions of the input signal, in particular on its shape, frequency and strength. Moreover parameters such as the preload applied to the material may affect the measurements obtained (as previously it has been experimentally observed in 8.2.3)

In order to take account the most varied conditions, the experimental characterisation was carried out with sinus and triangular shaped input signals. In each case the frequency of the signal was varied between 10Hz up to 500Hz and three different levels of preloads were tested: 0.46MPa, 0.92MPa and 1.10MPa.

A TREK RT6000HVA high voltage amplifier was used for driving the input signal up to 3kV. This amplifier, as previously commented, has a small signal band width of DC to 1kHz (-3dB) and a large signal bandwidth of DC to 200Hz. To exploit the maximum performances of the amplifier, the tests were limited to 500Hz.

The output charge generated from the sensor was measured by using a KISTLER 5011 charge amplifier connected to the piezoelectric output sensor. Since the strain piezoelectric coefficient of the SBT material used as sensor has a value of d_{33} = 15pC/N, and the parameters of the charge amplifier were established as T.S = $1 \cdot 10^{-1} \cdot 1 \cdot 10^{-2}$ pC/V, the force measured may be obtained from the output voltage from the charge amplifier as:

$$F_{\text{sensor}} = \frac{\text{Parameters Charge Amplifier}}{\text{Strain Piezoelectric Coefficient Sensor}} = \frac{T \cdot S}{d_{33}} = \frac{10 \frac{pC}{V}}{15.5 \frac{pC}{N}} = 0.645 \frac{N}{V} \qquad (8.5)$$

The mentioned parameter T.S of the charge amplifier depends upon the internal resistance and capacitance used in the charge amplifier to integrate the signal.

The preload was measured by using a KISTLER 5011 charge amplifier operated at ‘long’ mode (quasi-static measurements) and measuring the charge generated in the output sensor.

All the following test were performed in the laboratories of the Swiss Federal Institute of Technology.

8.5.1. Response under sine waveform signals

Figures 8.19, (a),(b) and (c) indicate the behaviour of the piezoelectric transformer under ‘low’ voltage in input and modification of the preload applied to the actuator. The measurements were carried out at different frequencies and preloads in order to evaluate the influence of this variables. Preloads tested were 0.46MPa, 0.92MPa and 1.10MPa. The frequencies chosen were 10Hz, 20Hz, 50Hz, 100Hz and 500Hz.

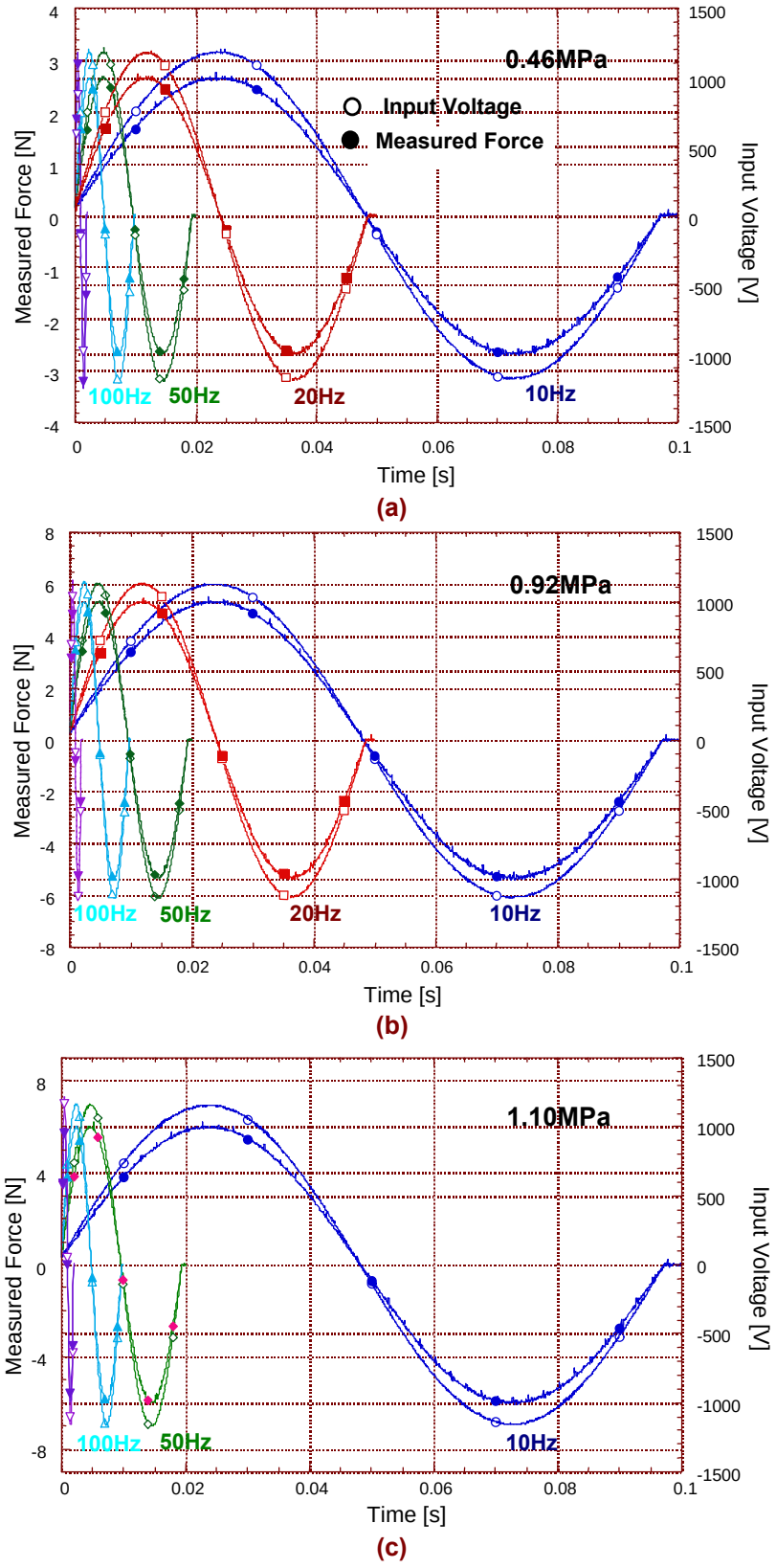

Figure 8.19. *Response of the transformer under an input voltage of 1000V and different preloads: (a) 0.46MPa, (b) 0.92MPa and (c) 1.10MPa.*

The previous results show a linear behaviour in magnitude and phase for the tested frequencies. The transformer ratio was observed to depend on the preload applied, as previously it was observed from the prestress experiments.

The maximum force measured was 6.5N when the input voltage was of $1000V_{max}$ and the preload of 1.10MPa. The theoretical expected blocking force under these conditions was of 81.81N. Difference between these values is related to the compliance of the material, as is indicated in Figure 8.20.

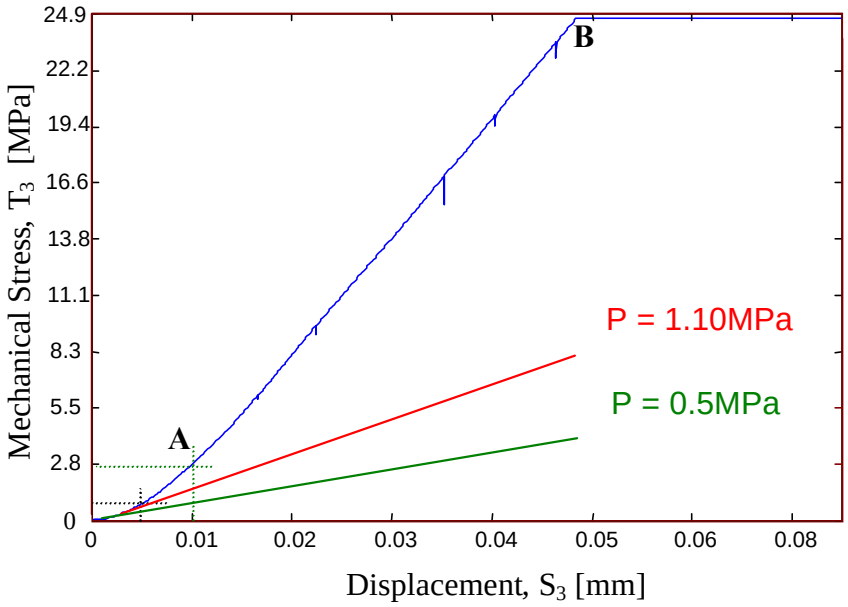

Figure 8.20. *Force-displacement curve.*

As Figure 8.20 displays, when the compression in the material is lower than 2.8MPa the behaviour of the material is softer. When the prestress is increased the material become stiffer and the stiffness become linear (with an approximate value of $12.363 \cdot 10^{-12}$ m^2/N).

This dependence of the stiffness with the prestress affects the force measurement which is dependent on the value of the stiffness. In particular estimating as $40 \cdot 10^{-12} m^2/N$ the value of the stiffness when the compression is only of 1.1MPa (see Figure 8.19), the blocking force generated will be:

$$\frac{F_{bloq}}{V}(P = 1.1\ MPa) = \frac{d_{33} \cdot A}{s_{33}^{E}(P) \cdot L} = \frac{225 \cdot 10^{-12} \cdot 7.068 \cdot 10^{-4}}{40 \cdot 10^{-12} \cdot 144 \cdot 10^{-3}} = 2.2 \cdot 10^{-2}\ N/V \qquad (8.6)$$

Which indicates than the expected value for an input voltage of 1000V is 22N, which is closer to the 7N measured.

Another source that may explain the difference is the dependence of the coefficient d_{33} with the preload. There are no experimental data available relating to this, not even in literature, and is being proposed as a task for future work.

In conclusion, it is clear that the necessary preload for the actuator column, in order to work in the linear range of the stiffness, must be higher than 2.8MPa.

The same experiments were carried out with a voltage of 2kV as is displayed in Figure 8.21.(a), (b) and (c). The maximum force measured under 1.1MPa was 13N while the theoretical

expected force was of 44N. Again, the dependence of the stiffness with the prestress is affecting the measurements.

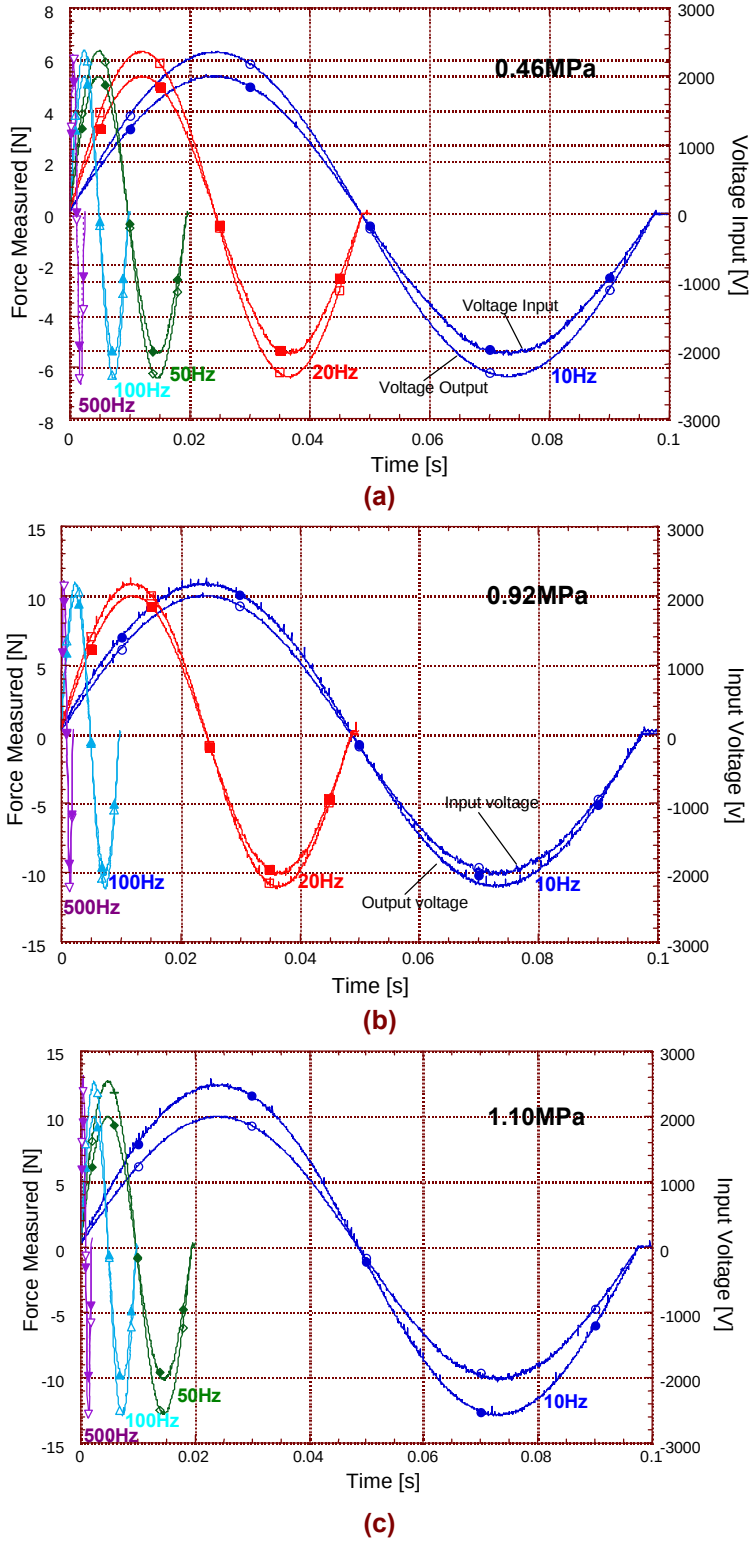

Figure 8.21. *Response of the transformer under an input voltage of 2000V and different reloads: (a) 0.46MPa, (b) 0.92MPa and (c) 1.10MPa.*

The previous results for the response under a sine waveform signal are gathered in a graph voltage input-voltage output in order to display more clearly the linearity. Figure 8.22 displays the force measured against the input signal for the three different values of prestress frequency.

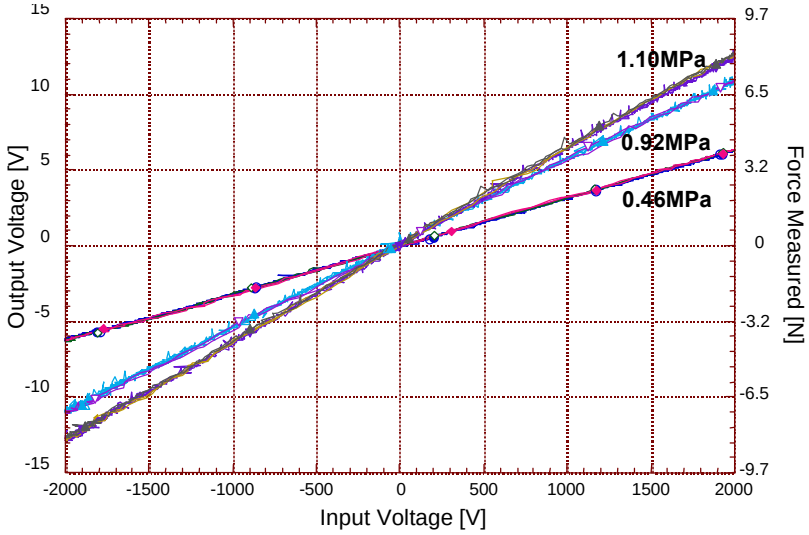

Figure 8.22. *Response of the PIEZOTRF3 prototype under sinewave signals.*

8.5.2. Response under triangular wave signals

Similar tests were performed by inputting a triangular wave signal to the transformer. Figures 8.23 (a), (b) and (c) show the results obtained when the amplitude of the input signal was of 2000V. Three levels of preload were testes, 0.46MPa, 0.92MPa and 1.10MPa. The frequency of the input signal was chosen as 10Hz, 20Hz, 50Hz, 100Hz and 500Hz.

Figure 8.24 gathers all the results in a graph were the linearity demostrated.

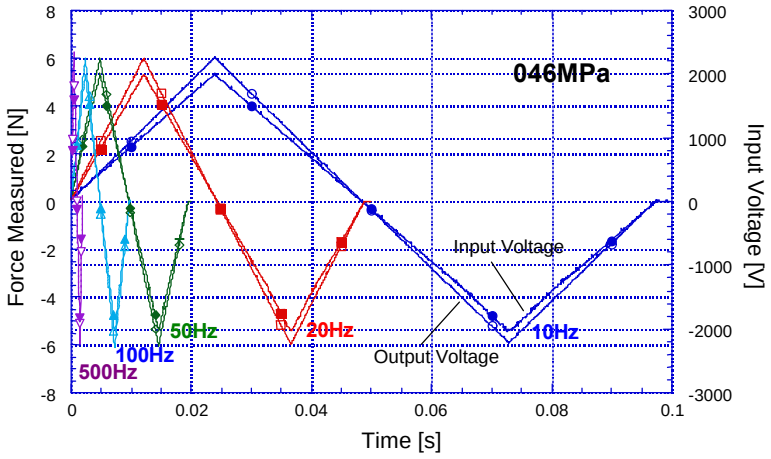

(a)

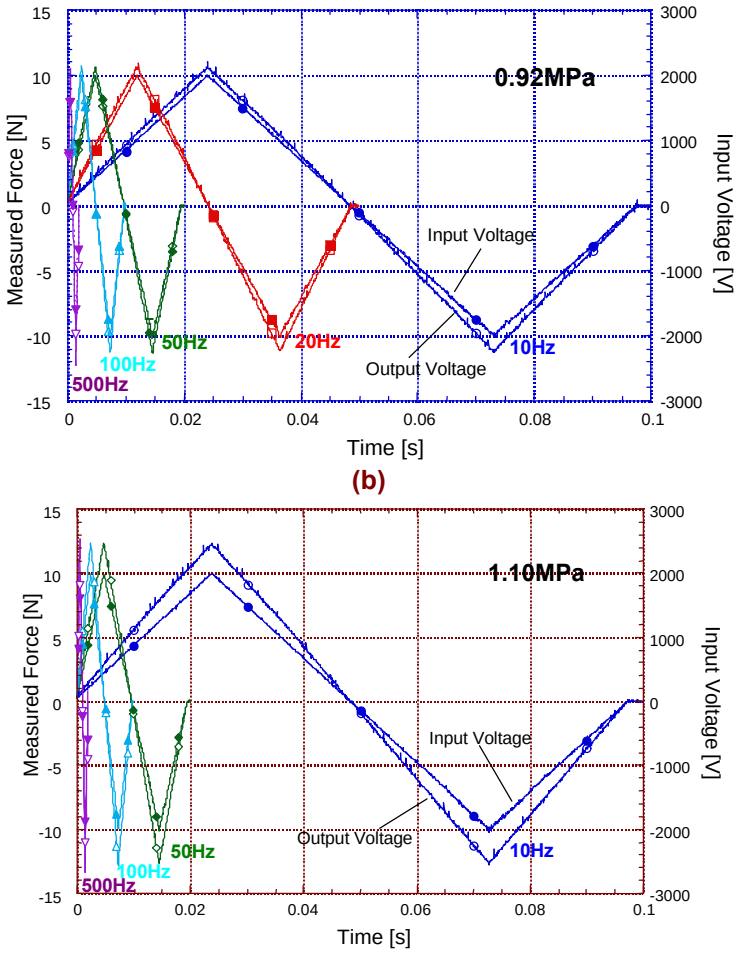

Figure 8.23. *Response of the piezoelectric transformer under an input voltage of 2000V and different preloads: (a) 0.46MPa, (b) 0.92MPa, (c) 1.10MPa*

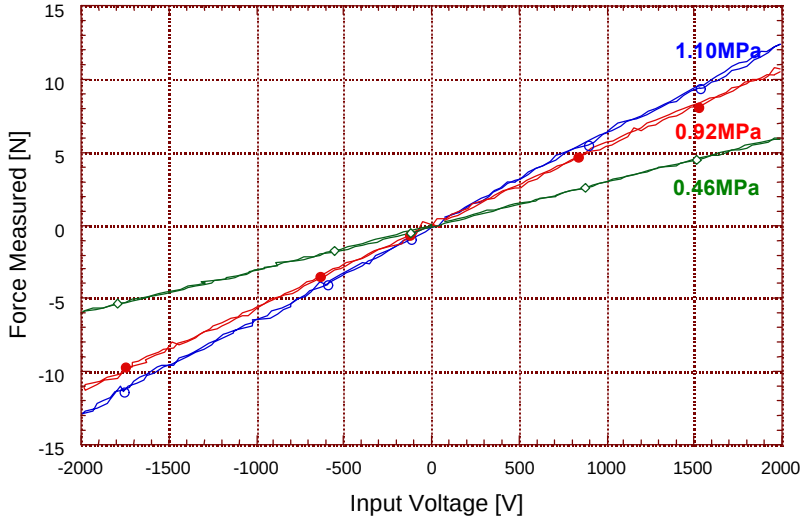

Figure 8.24. *Response of the PIEZOTRF3 prototype under triangular wave signals.*

8.6. Frequency response of the device

In section 8.5 linearity has been experimentally verified in the frequency range between 10Hz to 500Hz. These results are now represented in a frequency spectrum in Figure 8.25 for a sinus waveform signal, and in Figure 8.26 for a triangular waveform signal.

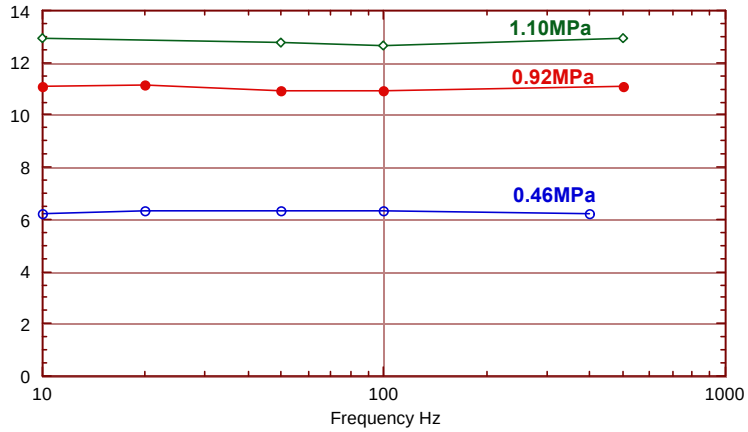

Figure 8.25. *Frequency behaviour under a sinus wave of 2kV with different preloads.*

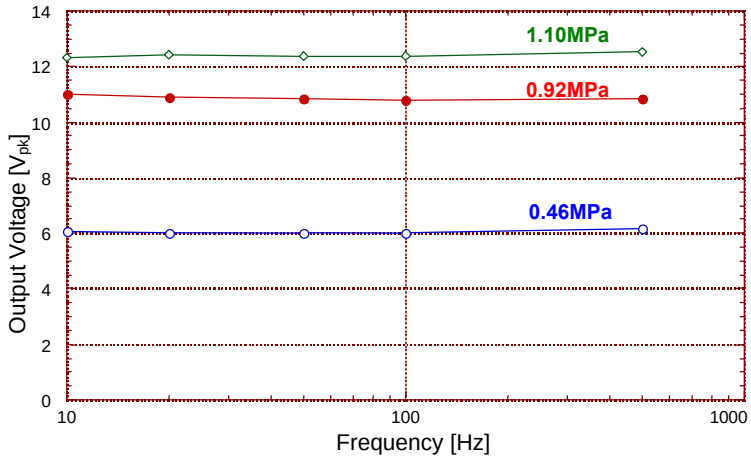

Figure 8.26. *Frequency behaviour under a triangular wave of 2kV with different preloads.*

Figures 8.25 and 8.26 show the stability of the piezoelectric transformer against the frequency. Test were carried for frequencies up to 1000Hz. Moreover, it is possible observe that the output voltlage increase with the pressure applied, as is expected, since the blocking situation is closer.

Let we characterise now the response of the transformer for higher frequencies, a spectrum analyser HP 8568A has been used. The spectrum analyser provides a measurement of the impedance spectrum in magnitude and phase (*Z(w)*). This allows one to obtain the resonance of the system, and thus its frequency spectrum.

In order to verify the behaviour of the transformer, a first test was made with a simple disc of PZT-8 of 12mm thickness and 30mm diameter. The results are shown in Figures 8.27 in a range between 100Hz to 300kHz.

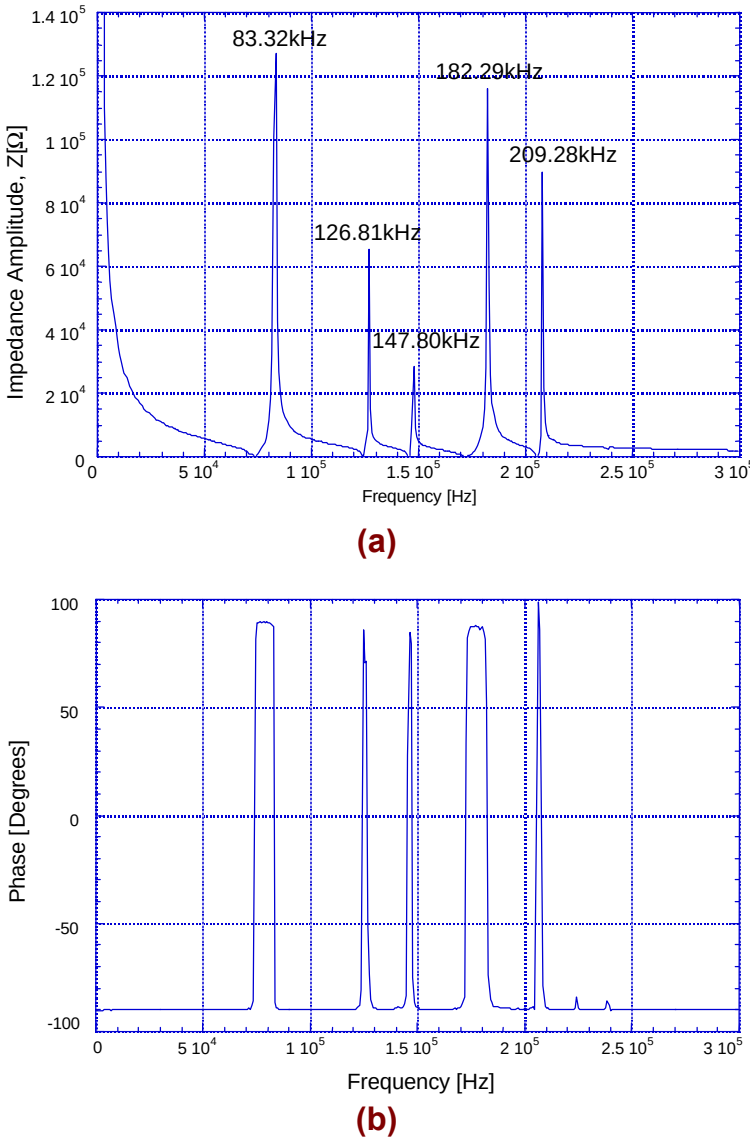

Figure 8.27. *(a) Impedance Amplitude, Z(w) and (b) Impedance Phase, for a simple PZT-8S disc of 30mm diameter and 12mm thickness.*

The first resonance peak, at 83.32kHz, corresponds to the radial mode of vibration (axis 3). It is possible to compare this value with the information within the Data Book of Morgan Matroc by using the N_p coefficient for the PZT-8, as shown equation (8.7). The second big peak, at 182.28kHz corresponds with the longitudinal mode of vibration, as can be obtained from the N_{33} information (8.8).

$$f_{r,radial} = \frac{N_p}{d} = \frac{2300}{0.030} = 76.66kHz \tag{8.7}$$

$$f_{r,longitudinal} = \frac{N_{33}}{L} = \frac{2070}{0.012} = 172.5kHz \tag{8.8}$$

The frequency characterisation of the instrument piezoelectric transformer was made in a similar manner by connecting the spectrum analyser in the input of the transformer. The measured spectrum is displayed in Figure 8.28 up to a frequency of 100kHz. The tests were performed under a prestress in the actuator column of 1.10MPa.

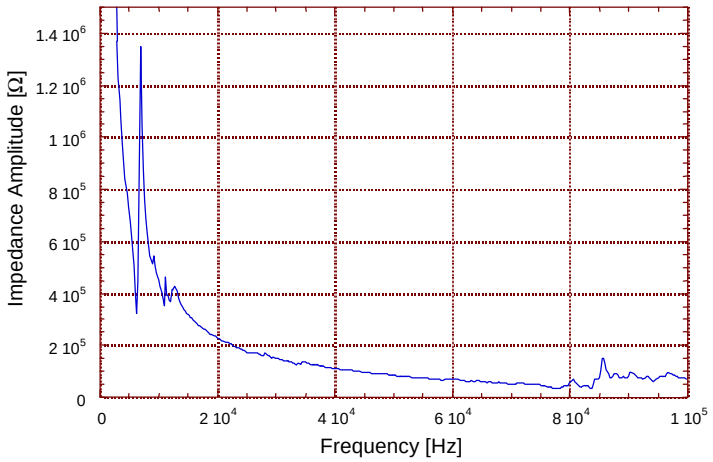

Figure 8.28. *Spectrum for the PIEZOTRF3 prototype in the range up to 100KHz*

The next figure provides a zoom of the first resonance,

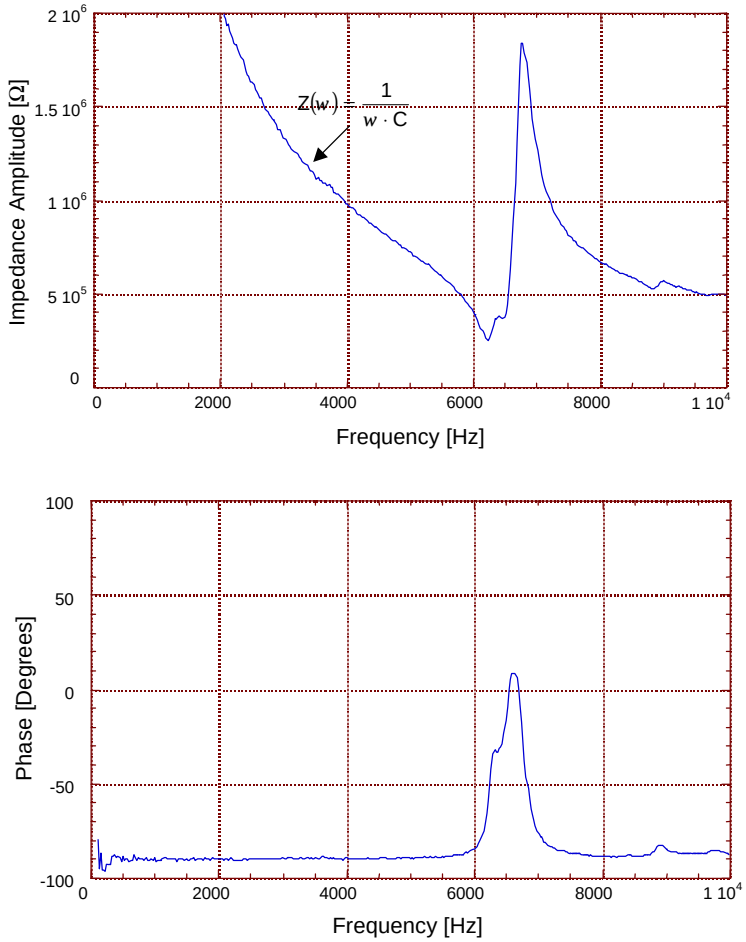

Figure 8.29. *First resonance in the PIEZOTRF3 prototype.*

From the previous results, a first resonance peak at 6.5kHz is observed, which limits the linear operation range at 6kHz. For safety it is recommended to limit the operation range to half part the first resonance, i.e. 3kHz. It can be noted in previous figures, regarding to the impedance magnitude, that the curve shown indicates the frequency evolution of a capacitive circuit.

8.7. Characterisation by using impulse waveform signals

8.7.1. Measurement Method and Signal Processing

The technique for the laboratory measurement of the instrument transformer frequency response is based on injecting a signal into the input terminals of the instrument transformer under test. The input and output waveforms are recorded. Then, the frequency response is computed using averaging Fourier transform techniques.

Many types of inputs were considered initially: step functions, impulse functions, swept sine wave, and white noise. The final selection was based on the following criteria:

- Feasibility of producing the waveform
- Sufficient energy distributed over the frequency range of interest.
- If the signal is a pulse, it must have minimal overshoot and high damping.
- The amplitude level of the input waveform must be near the nominal rating of the tested instrument transformer.

As a best compromise, an *impulse-type double-exponential input* signal was selected which can be easily generated from the high voltage platform available at the laboratory.

The input and output signals thus resulting were recorder in a digital Tektronix TDS520 scope. The digital information was sent to a computer where was mathematically evaluated by using a Matlab software. Then, the transfer function is computed as the ratio of the output Fourier transform over the input waveform Fourier transform.

Like this, the *transfer function* of the device (including the effect of the load) may be found as [8,9,10]:

$$H(w) = \frac{V_{out}(w)}{V_{in}(w)} \tag{8.9}$$

where $V_{in}(w)$ and $V_{out}(w)$ are the Fourier transforms of the input and output waveforms, respectively. In practice the measured signals ($\tilde{v}_{out}(t), \tilde{v}_{in}(t)$, the symbol ~ denotes measured data) contain added noise so that:

$$\begin{aligned} \tilde{v}_{in}(t) &= v_{in}(t) + x_{in}(t) \\ \tilde{v}_{out}(t) &= v_{out}(t) + x_{out}(t) \end{aligned} \tag{8.10}$$

where x_{in} and x_{out} are uncorrelated noise signals added to the exact input and output waveform functions.

By performing N series of measurements of $\tilde{v}_{in}(t)$ and $\tilde{v}_{out}(t)$, a good approximation of the instrument transformer transfer function can be obtained as follows:

$$\tilde{H}(w) = \frac{\sum_{k=1}^{N} \tilde{V}_{out}(w) \cdot \tilde{V}_{in}^{*}(w)}{\sum_{k=1}^{N} V_{in}(w) \cdot \tilde{V}_{in}^{*}(w)} \tag{8.11}$$

where the summation index *k* indicates the measurement number, and * denotes complex conjugation.

The module of *H(w)* provides the spectrum of the module of the transfer function, while the angle of *H(w)* indicates the difference of phase between the output and the input.

8.7.2. Experimental Set-up

In order to apply the impulse waveform technique to the characterisation of the PIEZOTRF3 prototype, the tests were carried out in the high voltage platform of the Department of Electrical Engineering of the ETSEI.Barcelona (Figure 8.30). An impulse waveform signal with a rise time of 2.14μs and a fall time of 60μs (half of the maximum peak) was chosen to perform the characterisation. The peak value was taken as 32kV in order to avoid dielectric problems, such as partial discharges or breakdown.

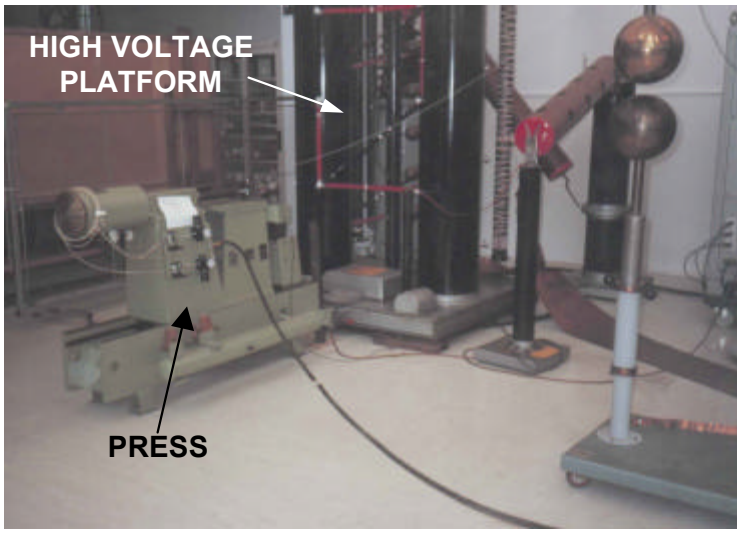

Figure 8.30. *Experimental set-up used testing the prototypes to the impulse, under static prestress*

Together with the response of the prototype to an impulse signal, it was decide to take advantage of the test for characterising, at the same time, the influence of the prestress of the column in the output signal of the transformer. In order to achieve this, the SCIAKY press was used to subject the prototype to different levels of preloads (Figure 8.30). The press was driven from an external pneumatic circuit. The preload in the column was applied through a piston which prestressed both, the actuator and the sensor column. The static stress was applied by using the pneumatic press previously described in this chapter. The tests were carried out under static preloads of 3.17MPa, 4.23MPa, 5.28MPa and 7.40MPa.

A PZT-8 piezoelectric disc of 25mm diameter and 2 mm thickness was used as force sensor. The disc was perfectly situated in plate to maintain it centred with respect to the actuator. The sensor was shielded to avoid any external electromagnetic interference, and the output was directly inputted to the scope by using a coaxial cable. The input impedance of the used scope was of R_E = 1MΩ and C_E = 2pF.

The lightning wave was also captured for with the second channel of the scope by means of a resistive divisor. In this way, both signals, input and output responses were available to analyse the frequency response of the prototype by using the previously described Fourier techniques. The number of acquisition point was N=500. Figure 8.31, display the lightning waveform obtaining during the calibration of the high voltage platform.

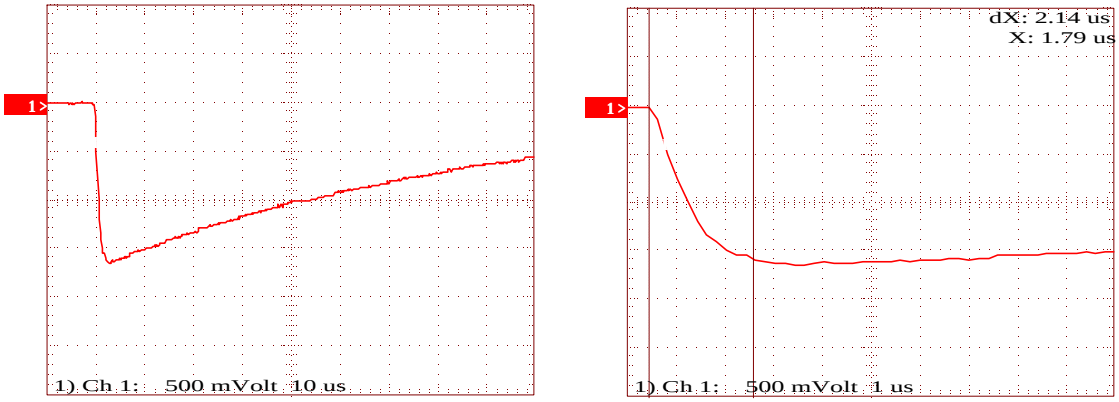

Figure 8.31. *Impulse-type signal (32kV$_{crest}$ used for the characterisation of the PIEZOTRF3 prototype*

In figures 8.32 to 8.35 are represented the temporal input and output waveforms obtaining in the prototype after applying the impulse test.

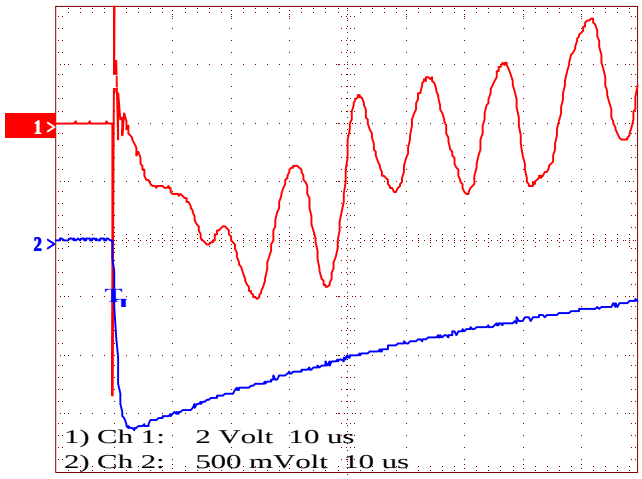

Figure 8.32. *Channel 1 indicates the output from the sensor when a preload of 3.17MPa is applied to the prototype. Channel 2 indicates the input voltage applied*

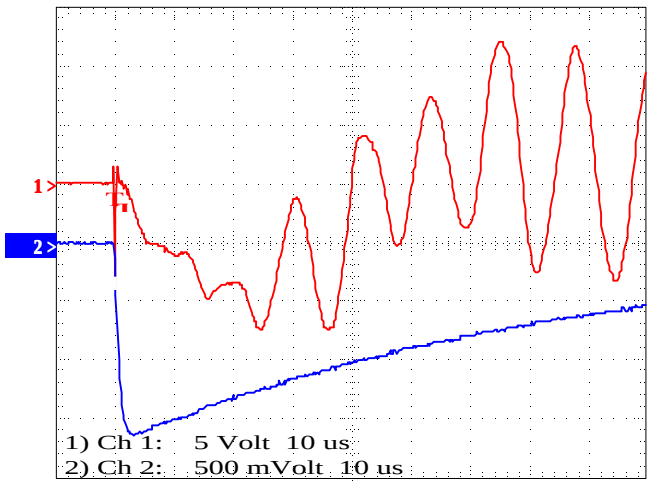

Figure 8.33. *Channel 1 indicates the output from the sensor when a preload of 4.23MPa is applied to the prototype. Channel 2 indicates the input voltage applied.*

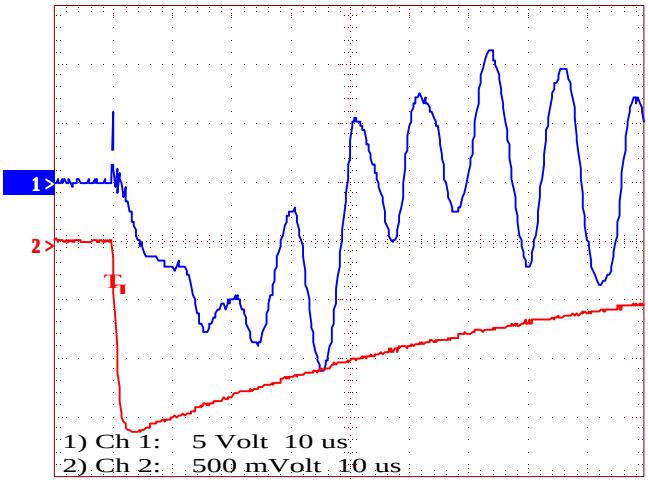

Figure 8.34. *Channel 1 indicates the output from the sensor when a preload of 5.28MPa is applied to the pototype. Channel 2 indicates the input voltage applied.*

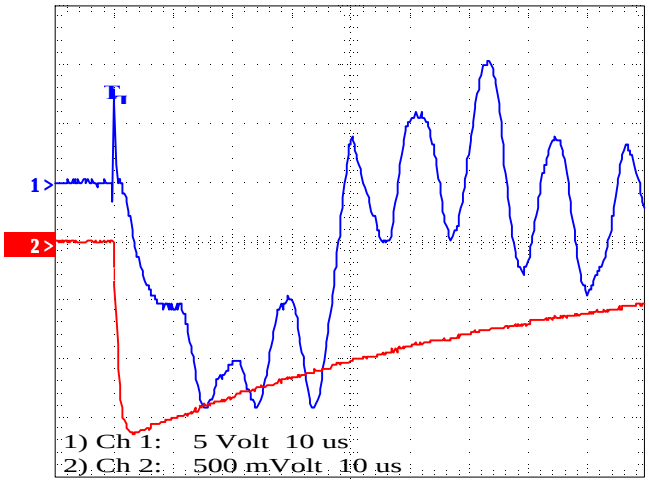

Figure 8.35. *Channel 1 indicates the output from the sensor when a preload of 7.40MPa is applied to the prototype. Channel 2 indicates the input voltage applied.*

From the visual observation of the results, it is noted that:

- The output voltage peak increases when the preload is increased. This has already been observed (cf. 8.2.3) in the evaluation of the prestress influence with a 50Hz electrical input.
- A improvement in the frequency response of the prototype is observed when the static preload is increased. This is consisted when the blocking state principle. The reduction of the inertial effect of the system (by increasing the preload and thus the blocking state) increase the frequency wide band response of the device.

8.7.3. Frequency Response of the PIEZOTRF3

The evaluation of the frequency response of the prototype has been done by considering the input and output signal from Figure 8.34, corresponding with a preload of 7.40MPa. Input and output time signals are evaluated in frequency by using the Fourier transform techniques. Then the evaluation of the transfer function of the system is obtained by applying equation (8.9).

Figure 8.36 illustrates the frequency response of the prototype in a frequency range up to 1MHz. The y-axis denotes the evolution of the magnitude of the transfer function. In Figure 8.37 the corresponding evolution of the phase difference between input and output signals is shown.

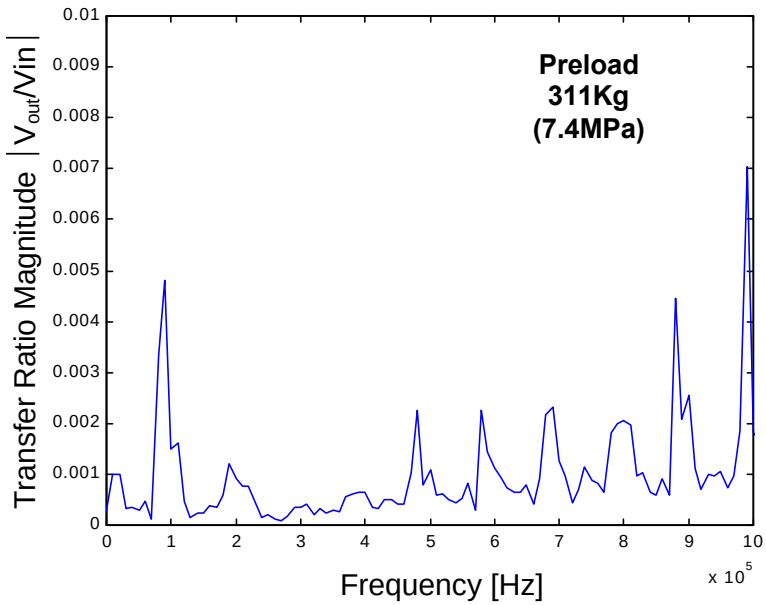

Figure 8.36. *Dependence of the magnitude of the transformer ratio with the frequency of the input signal.*

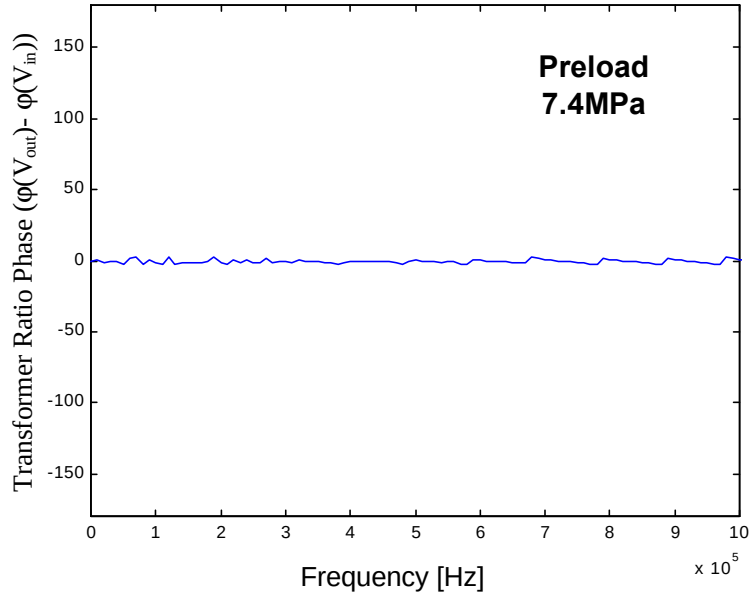

Figure 8.37. *Dependence of the phase of the transformer ratio with the frequency of the input signal.*

In order to compare the previous results with similar studies made in electromagnetic transformers [1,2,4] is convenient to consider the frequency band of 1kHz and 10kHz. Figures 8.38 displays the magnitude of the transfer function in a range of 0 to 1kHz, while Figure 8.39 illustrates the case for a range between 0 to 10kHz. In both cases the phase was shown practically zero in all the frequency range.

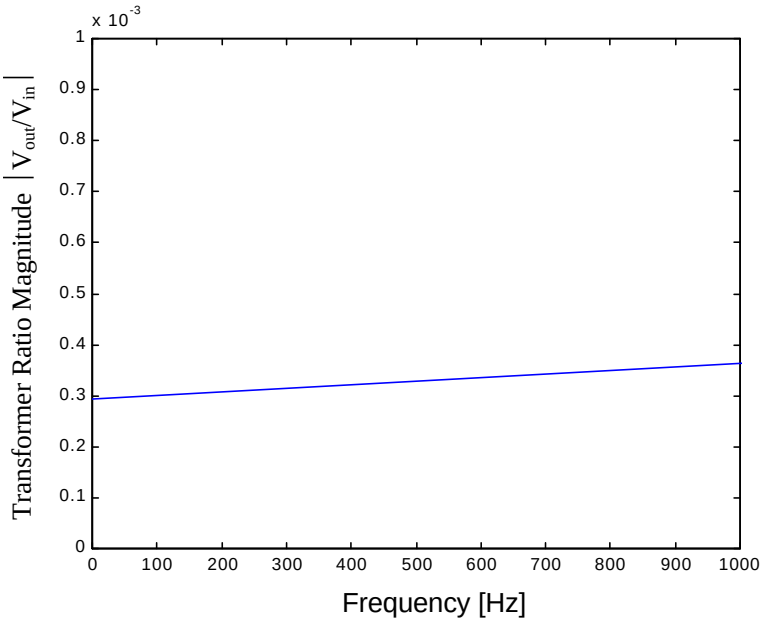

Figure 8.38. *Transformer ratio in a range from 0 to 1kHz.*

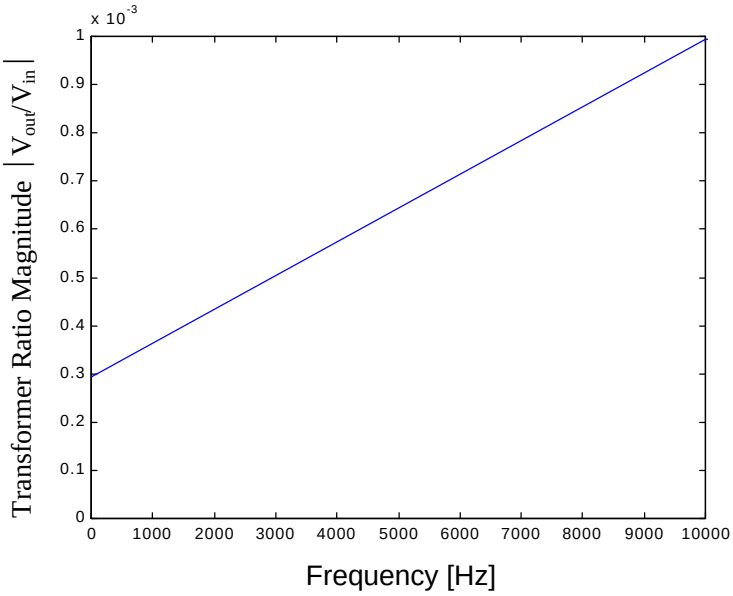

Figure 8.39. *Transformer ratio in a range from 0 to 10kHz*

In conclusion, the transfer function of the piezoelectric transformer has been evaluated in magnitude and phase in a wide frequency range. From the results obtaining, after applying the FFT transformer, transformer ratio shows a very stable behaviour at low frequency (up to 1kHz) and a increased linear evolution for a longer range. The first important resonance was observed at 10kHz, which confirm the measures performed with the spectrum analyser at low voltage (see cf. 8.6). An improvement in the acquisition set-up, and the accuracy of the obtained data will pass by increasing the number of acquire samples, *N*.

8.9. References

[1] M.I.Samesima,J.C. de Oliveira, E.M.Dias. *Frequency response analysis and modeling of measurement transformers under distorted current and voltage supply*. IEEE Trans. on Power Delivery, Vol. 6, No. 4, October 1991, pp. 1762-1768.

[2] A.P.Sakis Melipoulos, Fan Zhang, S.Zelingher, G.Stillman, G.J.Cokkinides., *Transmission level instrument transformers and transient event recorders characterisation for harmonic measurements*. IEEE Trans. on Power Delivery, Vol. 8, No. 3, July 1993, pp. 1507-1517.

[3] G.J.Cokkinides, L.E.Banta, and A.P.Meliopoulos., *Transducer Performances for Power System Harmonic Measurements*, Proceedings of the International Conference on Harmonics, Worcester, Massachusetts, pp. 225-228, October 1984.

[4] D.A.Douglas, *Potential Transformer Accuracy at 60Hz Voltages Above and Below rating and at Frequencies Above 60Hz*, IEEE Transactions on Power Apparatus and Systems, Vol. 100, No.3, pp. 1370-1375, March 1981.

[5] D.A.Bradley, P.S.Bodger, P.R.Hyland, *Harmonic response Tests on Voltage Transducers for the New Zealand Power System*, IEEE Transaction on Power Apparatus and System, Vol. PAS-104, No. 7, July 1985, pp. 1750-1756.

[6] Julios Barrios Guadalupe, Victor M. Moreno Saiz, Tomas Cora de la Cavada, *Sistema para la Caracterización Frecuencial de Transformadores de Tensión y Corriente*, 5as Jornadas Hispano-Lusas de Ingeniería Eléctrica, Tomo III, 1997, Salamanca.

[7] R.Malewski, *Digital Techniques in High Voltage Measurements*, IEEE Transaction on Power Apparatus and Systems, Vol. PAS-101, No. 12, December 1982, pp. 4508-4517.

[8] R.Malewski, G.R.Nourse, *Transient Measurement Techniques in EHV Systems*, IEEE Transactions on Power Apparatus and Systems, Vol. PAS-97, No. 3, May – June 1978, pp. 893-902.

[9] G.S.Hope, *Transfer Function Measurement Under Normal Operating Conditions Using pseudorandom Binary Input Signal*, IEEE Transactions on Power Apparatus and Systems, November – December 1977, pp. 1798-1808.

[10] R.W.Ramirez, *The FFT, Fundamentals and Concepts*, Prentice-Hall, INC, Englewood Cliffs, N.J., 1985.

[11] R.Malewski, B.Poulin, *Impulse Testing of Power Transformers Using the transfer Function Method*, IEEE Transaction on Power Delivery, Vol. PWRD-3, No. 2, April 1988, pp. 476-489.

[12] N.H.Younan, A.B.Kopp, D.B.Miller, and C.D.Taylor, *On correcting HV Impulse Measurements by Means of Adaptive Filtering and Deconvolution*, IEEE Transaction on Power Delivery, Vol. 6, No. 2, pp. 501-506, April 1991.

[13] M.Kezunovic, E.Soljanin, B.Perunicic, and S.Levi, *New Approach to the design of Digital Algorithms for Electric Power Measurements*, IEEE Transactions on Power Delivery, Vol. 6, No. 2, pp. 517-523, April 1991.

THIRD PART:

CURRENT TRANSDUCERS

Chapter 9

Piezoelectric Transducers for Measuring Current. Possibilities

9 Piezoelectric Transducers for Measuring Current. Possibilities

9.1. Introduction

An accurate electric current transducer is one of the key components in power system instrumentation. It provides the current signal source for the revenue metering, control and relaying apparatus.

Conventionally, wound type current transformers (CTs) have been widely used in power system to measure the conductors current. The secondary of these transformers is connected to meters and protective devices. As previously was commented in Chapter 1, the evolution in the protection and measuring system connected toward the digital and microprocessor technology demands new requirements for the instrument transformers. To this natural evolution of the technologies, evolution in instrument transformers come also from other technical aspects, described below:

1. For high-voltage applications, porcelain insulators and oil-impregnated materials have been used to provide insulation between the primary bus and the secondary windings. The insulation structure requires to be designed carefully to avoid electric field stresses which could eventually cause insulation breakdowns. The electric current path of the primary bus has to be designed properly to minimise the mechanical forces on the primary conductors for through faults. With the short circuit capacities of power systems getting larger, and the voltage levels going higher, the conventional CT becomes more and more *bulky and costly*. Although the introduction of SF_6 insulated CTs in recent years has improved reliability, it has not reduced the cost of this type of CT.

2. Moreover, numerous faults in these oil-insulated current transformers – with devastating consequences – have questioned the reliability of conventional high-voltage CTs by engineers at several utility companies. This is the case of Tennessee Valley Authority [1] and BC Hydro [2] who have experienced *violent destructive failures* of these CTs which caused fires and impact damage to adjacent apparatus in the switch yard, electric damage to relays, and power service disruptions.

3. In addition to the concerns mentioned above, other performance limitations of the conventional CT have raised more concerns [3,4]. The *saturation* of the iron core under fault current –large current- of the conventional CT make it difficult to obtain accurate current signals under power system transient conditions. This is specially so for those currents with transient DC components, which aid a remanent flux condition in the core and may cause inappropriate functioning of relays. The saturation of the iron core also reduces the dynamic range of the CT. In power systems, the electric current is much smaller (<1KA) under normal operating conditions than under fault conditions (>10KA). Because of the small dynamic range of conventional CTs, more than one CT is needed at one location to cover the requirement of metering and relaying.

4. Another aspect that affects the response under transient conditions is the *low frequency* response of the conventional. Moreover this aspect become, at present, more and more significant due to the increase of harmonic level in the networks.

5. With computer control techniques and digital protection devices being introduced into power systems, conventional CTs have caused further difficulties:

   5.1. Although secondary current is 5A, during a short circuit fault on the power system, the current magnitude increases from several times to ten times. This large current may *cause electro-magnetic interference* through the ground loop into the digital systems. This has required the use of an auxiliary CT or optical isolator to avoid such problems.

   5.2. The standard 5A low burden secondary configuration is not compatible with the new technology which uses analog to digital convertors requiring low voltage input at the front end.

The above mentioned limitations of the conventional CTs have increased the motivation for finding alternative ways of performing current measurements as is the case of the optical technology [5-10], already commented in Chapter 1.

The present chapter describes the development and experimental results obtained with some piezoelectric transducers for measuring current.

9.2. Electromagnetic-Piezoelectric Transducer

An electromagnetic-piezoelectric transducer measures the magnetic force created by means of the magnetic field existing in the gap of a electromagnet and which tend to close it. The magnetic field appears when an electrical current is driven in a winding placed through the core of the electromagnet, as is illustrated in Figure 9.1.

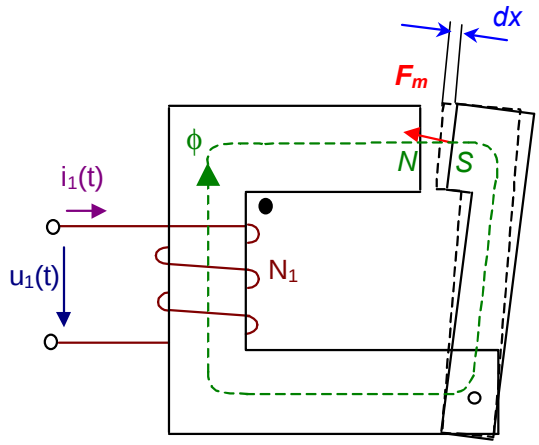

Figure 9.1. *Magnetic force appeared in the gap of an electromagnet*

9.2.1. Magnetic force appeared in the gap of an electromagnet

The determination of the magnetic field in the gap is calculated applying the Ampere Law to the magnetic circuit of the electromagnet, considering the different reluctance of the core and the gap.

$$N \cdot I = H_{core} \cdot \ell_{core} + H_{gap} \cdot \ell_{gap} \qquad (9.1)$$

where:

- N = number of turns of the winding
- I = current to be measured [A]
- H_{core} = magnetic field intensity in the core [A/m]
- H_{core} = magnetic field intensity in the gap [A/m]
- ℓ_{core} = longitude of the magnetic core
- ℓ_{gop} = longitude of the gap

The total flux of the magnetic field, B, that goes out through a general close surface must be cero. This is because $\nabla B = 0$, one of the Maxwell's equations. Thus, considering the leaks negligibled, the magnetic flux of B, F, must have the same value in all the sections of the magnetic circuit and:

$$B_{core} \cdot S_{core} = B_{gap} \cdot S_{gap} \tag{9.2}$$

where S_{core} and S_{gap} are the transversal sections of the magnetic core and of the gap.

Combining the equations (9.1) and (9.2), it is obtained the following relationship:

$$B_{gap} \cdot S_{gap} \cdot \left[\frac{\ell_{core}}{m_{core} \cdot S_{core}} + \frac{\ell_{gap}}{m_{gap} \cdot S_{gap}} \right] = N \cdot I \tag{9.3}$$

and the magnetic flux will be:

$$\Phi = B_{gap} \cdot S_{gap} = \frac{N \cdot I}{\frac{\ell_{core}}{m_{core} \cdot S_{core}} + \frac{\ell_{gap}}{m_{gap} \cdot S_{gap}}} \tag{9.4}$$

Since the gap used to be a non-ferromagnetic material with a permeability very low compare to the permeability of the core, $\mu_{gap} << \mu_{core}$, the equation (9.4) may be expressed as:

$$\Phi = B_{gap} \cdot S_{gap} \approx \frac{N \cdot I \cdot m_{gap} \cdot S_{gap}}{\ell_{gap}} \tag{9.5}$$

This equation has been obtained considering that the magnetic flux leakage is zero. This supposition is closer to the actual value when low gaps are considered. In all case, this equation will give the higher limit of the flux F in the considered conditions. There are empirical equations for estimating the leakage factors for magnetic circuits [11].

Once the flux in the electromagnet is known, one can calculate the magnetic force which appears in the gap. Considering the Energy Conservation Law in a low time interval, it is obtained the following relationship:

$$U \cdot i \cdot dt = i^2 \cdot r \cdot dt + dW_{mag} + F_{mag} \cdot dx \tag{9.6}$$

where r expresses the resistance of the winding, and $i^2 \cdot r \cdot dt$ are the Joule losses.

The two last terms of the equation (9.6) express the variation of energy in the magnetic system. This variation must be the same that the variation of the magnetic flux F, as indicated equation (9.7):

$$i \cdot d\Phi = dW_{mag} + F_{mag} \cdot dx \tag{9.7}$$

However, the variation of the magnetic flux (if leaks are negligible) is zero, and thus equation (9.7) become:

$$F_{mag} = -\frac{dW_{mag}}{dx} \tag{9.8}$$

The variation of the magnetic field energy may be obtained considering an increase d*x* in the separation of the gap. This increase causes an increase in the volume where is place the magnetic field, as: d*V* = *S*.d*x*, where *S* is the transversal section of the gap. Thus:

$$dW_{mag} = W_{mag} \cdot dV = \frac{B \cdot H}{2} \cdot S \cdot dx \tag{9.9}$$

From equations (9.8) and (9.9) one obtains:

$$F_{mag} = \frac{B \cdot H \cdot S_{gap}}{2} = \frac{B^2 \cdot S_{gap}}{2 \cdot m_{gap}} = \frac{\Phi^2}{2 \cdot m_{gap} \cdot S_{gap}} \tag{9.10}$$

Finally, the magnetic force in the gap is expressed by equation (9.11) as function of the current to be measured by substituting in equation (9.10) the equation (9.5):

$$F_{mag} = \frac{\Phi^2}{2 \cdot m_{gap} \cdot S_{gap}} = \frac{N^2 \cdot I^2}{2 \cdot \ell_{gap}} \tag{9.11}$$

Thus, the magnetic force created in the gap of an electromagnet is quadratically proportional to the current to be measured and inversely proportional to the gap separation.

9.2.2. Electromagnetic-Piezoelectric Current Sensor

The above calculated magnetic force can be measured if a piezoelectric sensor is placed in the gap of the electromagnet. If the piezoelectric effect is considered in the same direction as the magnetic force (3-axis), the electric charge generated is given by equation (9.12):

$$Q = -d_{33} \cdot F_{mag} \tag{9.12}$$

and substituting the result obtained in equation (9.11), the transformation ratio will be:

$$Q = -d_{33} \cdot F_{mag} = -d_{33} \cdot \frac{N^2 \cdot I^2}{2 \cdot \ell_{gap}} \tag{9.13}$$

If the applied current is a sine waveform signal, the generated charge will be a temporal expression indicated by equation (9.14):

$$Q(t) = -d_{33} \cdot \frac{N^2 \cdot I_{max}^2 \cdot \sin^2(w \cdot t)}{2 \cdot \ell_{gap}} \tag{9.14}$$

Equation 9.14 shows the transformation ratio of the generated charge, when measurements are performed by using charge amplifiers.

On contrary, if the measurements are carried out under open circuit conditions, the open circuit voltage measured is given by equation (9.15):

$$U_3(t) = -g_{33} \cdot \ell_{gap} \cdot T_{mag} = -g_{33} \cdot \frac{N^2 \cdot I_{max}^2 \cdot \sin^2(w \cdot t)}{2 \cdot S_{sensor}} \qquad (9.15)$$

where T_{mag} is the stress corresponding with the magnetic force in the gap.

9.3. Construction of an Electromagnetic-Piezoelectric Current Sensor

9.3.1. Prototype construction

Figure 9.2 illustrates a schematic of the prototype developed for testing the electromagnetic piezoelectric current sensor.

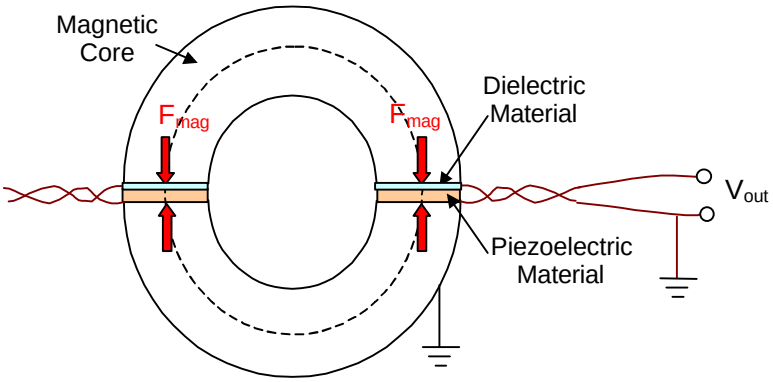

Figure 9.2. *Prototype of Electromagnetic-Piezoelectric Current Sensor*

This prototype consists of a magnetic core where a wire is winded. The current to be measured is driven through the winding. A piezoelectric sensor is placed in the gap of the electromagnet and all the system is prestressed to allow a good mechanical matching.

When the current to be measured is applied to the winding, the generated force tends to close the both parts of the core of the electromagnet, and thus a compression force appears in the gap. Since the force is quadratic respect to the current, a compression force will always appear in the gap. The frequency of the measured force is twice the frequency of the primary current and so, the generated voltage will be quadratic respect the current, as it was indicated in equation (9.15).

The magnetic core was made from two half rings of stainless steel. The area was of square shape and of 10x10mm^2. The total length of the core (without gaps) was of 180mm. Two disc of PXE-5 from Philips Components of 20mm diameter and 1mm thickness, were placed in the two gaps of the core in order to measure the force. The g_{33} coefficient of this piezoelectric soft material was 0.0242 Vm/N. In order to avoid a short-circuit through the core between both sides of the piezoelectric material, one of the sides is protected with a dielectric material, such as paper, and the other side is connected to ground as is shown in Figure 9.2.

Figure 9.3 illustrates the experimental set-up used to carry out the experimental characterisation of the prototype. A current transformer of 300A/5A and 40VA has been used as a current source in order to generate the primary current for testing the prototype. The secondary of the transformer was driven by an autotransformer inputting a current between 0 to 5A. The primary was in shortcircuit to obtain a current in the range of 0 to 300A. The current in the sensor was monitored by using an electromagnetic current transformer (300A/5A) and a shunt (10A/60mV) to drive the signal to the digital scope. The input current from the autotransformer was also controlled by an current probe for guaranteeing that the current does not pass 5A. Moreover, a voltmeter measures the voltage input in the current transformer in order to keep the maximum input power lower than 40VA.

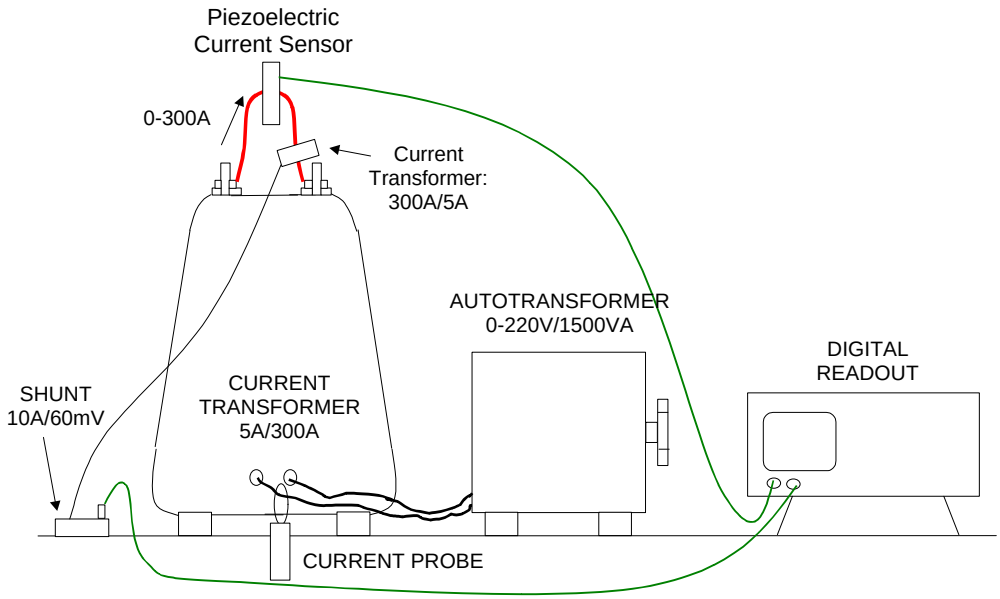

Figure 9.3. *Experimental set-up used for testing the Electromagnetic Piezoelectric current sensor.*

Next Figure 9.4 shows the response of one of the piezoelectric sensors when an input current of 330A was driven. The scope shows the signal from the shunt with a characteristic frequency of 50Hz, and the wave signal from the force sensor with a typical frequency of 100Hz.

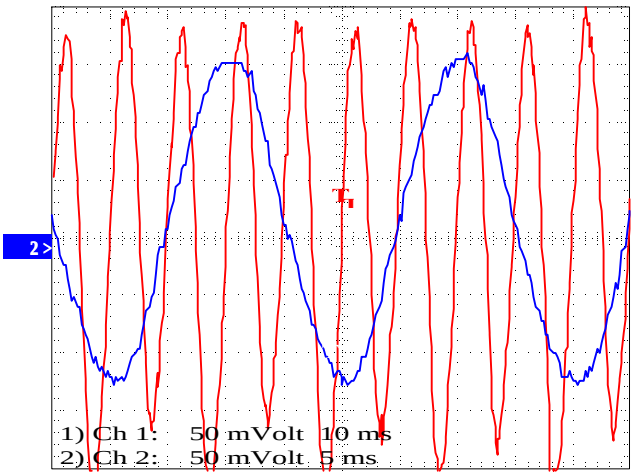

Figure 9.4. *Experimental results obtained in the Electromagnetic-Piezoelectric current sensor under a primary current of 330A*

Some fluctuations can be observed in the signal from the sensor. The explanation to this fluctuations come from the operating cycle of the sensor. During the compression cycle, firstly the material compresses itself and later on it relaxes the compression again the applied preload. In this way, the mechanical conditions of the piezoelectric material can be different and some fluctuations can appear during the decompression time. The fluctuations are completally eliminated by using a totally blocked structure.

9.3.2 Features and Limitations

In spite of this system presents an interesting alternative for current measurement, their application is limited due to similar problems as the conventional current instrument transformer. This is due to the existence of the magnetic core which can be saturated when falls appear. Nevertheless the existence of the gap increase importantly the limit of the saturation and then the working limit of the transformer compared to the classical transformer, where there is not gap.

Regarding to the power required from the source, this might significantly be reduced because power is not necessary for driving the secondary. The output signal in the secondary may drive directly digital electronic as a result of its low power.

The cost and weight of the system is importantly reduces due the no existence of secondary winding. Nevertheless the weight of the core, and their dimensions are similar to the electromagnetic current transformer. A most reliable alternative which reduce totally the use of magnetic material (and thus which overcomes the problems of hysteresis, weight and dimensions) is presented below.

9.4. Two-wires Piezoelectric Transducer

The two-wires Piezoelectric Transducer is a second alternative proposed for the current measure. It consist of using the well known property of the creation of a magnetic force when a current is driven for two parallels wires when the distance between them is little.

If the current in both conductors is driven in the same direction, the appeared force will tend to approach the conductors. On contrary, if the current in one conductor is opposite to the current in the other one, the force will tend to separate both conductors. Figure (9.5) shows a schematic of the first case.

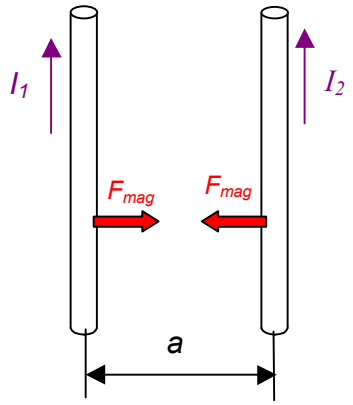

Figure 9.5. *Force appearing when a current is driven in two parallel conductors*

The magnitude of the force created under these conditions is found elsewhere [12,13], and here is expressed in the equation (9.16).

$$F_{mag} = \frac{m_0 \cdot I_1 \cdot I_2 \cdot \ell}{2 \cdot p \cdot a} \tag{9.16}$$

where ℓ is the length of the parallel conductors.

Particularly if the current in both wires is the same (half of the main current), the open circuit voltage is obtained from equation (9.17) as:

$$U_3(t) = -g_{33} \cdot \ell \cdot T_3 = -g_{33} \cdot \frac{m_0 \cdot I^2 \cdot \ell^2}{8 \cdot p \cdot a \cdot S_{\mathbf{sen}\ sor}} \tag{9.17}$$

9.4.1. Measure of the force using a piezoelectric sensor

In order to measure the force between the two wires, a piezoelectric sensor is placed in between both wires. If the output of the piezoelectric sensor is driven to a charge amplifier, the magnitude measured will be the generated charge, as indicated by equation (9.18).

$$Q = -d_{33} \cdot F_{mag} = -d_{33} \cdot \frac{m_0 \cdot I_1 \cdot I_2 \cdot \ell}{2 \cdot p \cdot a} \tag{9.18}$$

On contrary, if the measure is carried out under open-circuit conditions, the open voltage measured will be expressed from the following equation (9.19):

$$U_3(t) = -g_{33} \cdot \ell \cdot T_{mag} = -g_{33} \cdot \frac{m_0 \cdot I_1 \cdot I_2 \cdot \ell^2}{2 \cdot p \cdot a \cdot S_{\mathbf{sen}\ sor}} \tag{9.19}$$

9.5. Prototype of a Two-Wires Piezoelectric Current Sensor

9.5.1. Prototype construction

Two types of construction were evaluated, depending if both currents were driven in the same sense or on contrary senses. In the first case, the appeared forces are always in compression, while in the second case the forces will be tensile. Here it is discussed a prototype with compressive forces. This type of device has the advantage in front the tensile-type that the decoupling between piezoelectric discs and the conductors does not occur and the mechanical requirements are lower.

Prototype with two parallel currents

The prototype, shown in Figure 9.6, consists of two piezoelectric rings of PZT-5 connected in parallel. The current arrives to the sensor and is divided in an upper and a lower cooper electrode. In this way two parallel current appear in both sides of the piezoelectric sensor and so a compressive force. The path of the current is closed in the opposite end. The external electrodes of the sandwich are connected to ground and the middle electrode provides the

generated output voltage. Both copper electrodes were constructed to provide a necessary stiffness to the sandwich (quasi-blocking measurement). The sensor was finally fixed together with the electrodes by using a screw passing through the internal hole.

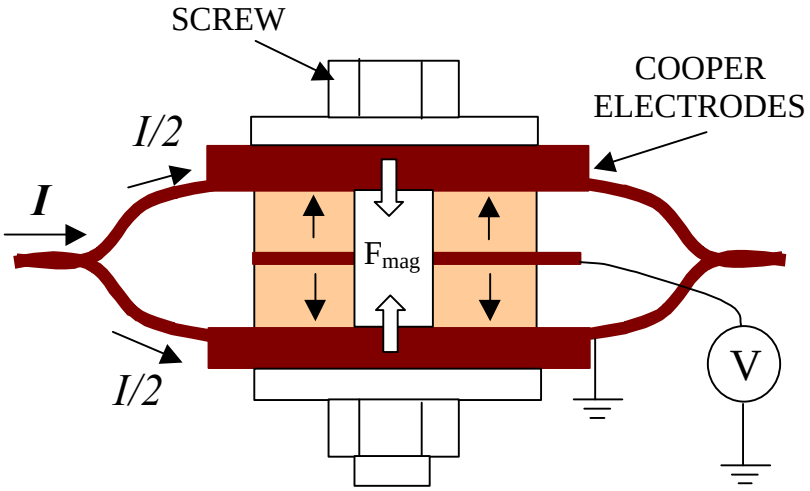

Figure 9.6. *Two-wires Piezoelectric Current Sensor*

Figure 9.7 shows the experimental set-up used for testing the prototype, similar to the described previously for the characterisation of the Electromagnetic piezoelectric current transducer.

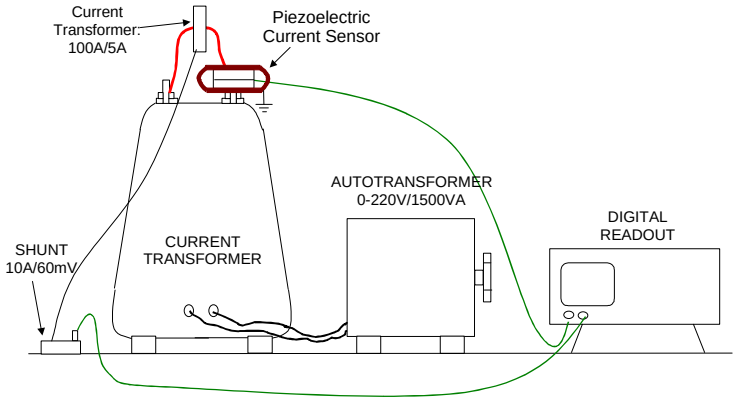

Figure 9.7. *Experimental set-up used for testing the Two-Wires Current Sensor*

Figure 9.8 illustrates the measured force in the piezoelectric sensor when an input current of 125A is driven. The input signal is noted because their frequency is half the frequency of the signal measured by the transducer.

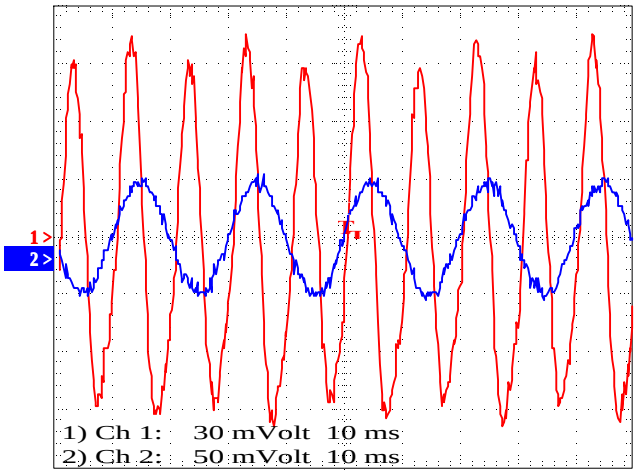

Figure 9.8. *Response of the piezoelectric sensor (CH1) under an electrical current of 125A*

During the tests, the preload was modified in order to verify the effects of the mechanical blocking state in the response of the transducer. Figure 9.9, shows the response obtained when the preload was reduced. In this case the fluctuations observed are very significant.

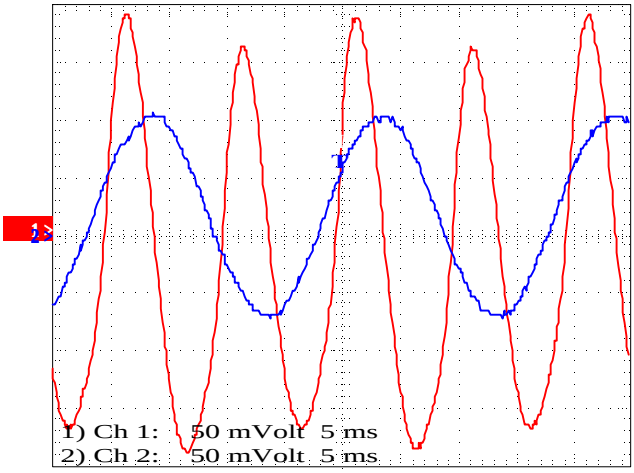

Figure 9.9. *Response of the piezoelectric sensor (CH1) under an electrical current of 211A.*

9.6. Conclusions

Two configurations of piezoelectric current transformers has been successfully designed and tested in this chapter. The *Electromagnetic-Piezoelectric Transducer* configuration has similar technical problems, due to the use of a magnetic core for generating the electrical signal. In particular, they weight is not significantly reduced compare to the electromagnetic transformers, they can saturate, in spite of the gap used for the sensor placement and hysteresis may appear.

On the other hand, the *Two Wires prototype* is presented as a more reliable alternative for measuring current. It reduces in a 100% the magnetic core use, and so all the associated problems with it.

The prototypes presented represent only the first successful step in the research in the field of piezoelectric current transducer. In the future, it is necessary to analyse the mechanical structure that guarantees a very stable operation.

Another important effect to be analysed corresponds to the effects of the temperature in the measurements. Ceramic materials are pyroelectrics and then they stability in front the temperature is very low. The temperature reached by the wire when currents of the order of 100A or more is driven can be very important and thus the effect in the behaviour of the sensor. A countermeasure to this consists in the use of piezoelectric materials with a good thermal stability, such as the quartz.

9.7 References

[1] J.R.Boyle, et al, *The Tennessee Valley Authority's (TVA's) experience and action plans with freestanding oil-filled current transformers (CTs)*, IEEE Trans., Vol PWRD-3, No. 4, October 1988, pp 1769-1775.

[2] B.C.Hydro, *Optical fiber optical current transducer*, CEA 189 T 353, July 1990.

[3] IEEE power system relay committee, *Gapped core current transformer characteristics and performance*, IEEE Trans., Vol. PWRD-5, No . 4, November 1990, pp 1732-1740.

[4] IEEE power system relay committee, *Relay performance considerations with low ratio CTs and high fault current*, IEEE Trans., Vol. PWRD-8, No. 3, July 1990, pp 884-897.

[5] M.Kanoi, et al*., Optical voltage and current measuring system for electric power systems*, IEEE Trans., Vol. PWRD-1, No. 1, January 1986, pp 91-97

[6] T. Mitsui, et al., *Development of fiber-optic voltage sensor and magnetic field sensors*, IEEE Trans., Vol PWRD-2, No. 1, January 1987, pp 87-93

[7] G.W.Day, et al., *Limits to the precision of electro-optic and magneto-optic sensors*, NBS Technical Note 1307, March 1987.

[8] H.Schwarz, M.Hudasch, "Optical current transformers-successful first field test in a 380kV system", ABB Review, March 1994, pp 12-18.

[9] T.D.Maffetone, et al., *345kV substation optical current measurement system for revenue metering and protective relaying*, IEEE Trans., Vol. PWRD-6, No. 4, October 1991, pp 1430-1437.

[10] S.Kobayashi, et al., *Development and field test evaluations of optical current and voltage transformers for gas insulated switchgear*, IEEE Trans. Vol. PWRD-7, No. 2, April 1992, pp 815-821

[11] R.K.Tenzer, *Estimating Leakage Factors for magnetic Circuits by a Simple Method,* Electrical Manufacturing, February 1957.

[12] P.Lorrain and D.R.Corson, Campos y Ondas Electromagnéticos*,* Selecciones Científicas, 1990, Madrid.

[13] F.E.Evdokímov, Fundamentos Teóricos de la Electrotecnia*,* Editorial Mir Moscu

FOURTH PART:

CONCLUSIONS

Chapter 10

Contributions, Conclusions and Suggestions for future work

10 Contributions, Conclusions and Suggestions for future work

The research work presented in this thesis is based on the development of novel piezoelectric transducers for high voltage measurements. The work has particularly been concentrated on the development of a voltage transducer for operating in the environment of electrical networks up to 36kV, but it has also extended to some proposals for the current measurement.

Voltage transformers has been developed by using *non-resonant piezoelectric structures* working under *blocking conditions*, due to their most reliable characteristics in front other evaluated configurations. Their operation principle is based on piezoelectric materials (active materials) which generate a mechanical perturbation under the application of an electric field. This mechanical perturbation can be measured as a force or acceleration by using a *piezoelectric sensor*. Thus, the sensor converts back the mechanical perturbation into an electrical signal and the process of electrical to electrical conversion is completed. The output voltage from the sensor has been found (theoretically and experimentally) depending on the piezoelectric characteristics of the active material, the conditioning circuit for driving the signal and the mechanical characteristics of the housing system. Particularly, the preload of the mechanical column and the deformation of the passive materials (the housing) have a significant influence in the 'quality' of the blocking conditions, and hence, in the output signal.

Current transformer has also been developed with non-resonant structures. The operation principle of the current transformer is a few different from the voltage transformer. In the voltage transformer a double conversion from electrical to mechanical and from mechanical to electrical energy was used. However, in the case of the current transformers, the force is directly generated by a magnetic field and measured from a piezoelectric sensor, for obtaining a proportional output voltage. Thus only a mechanical to electrical conversion is used. The output signal depend also on the piezoelectric characteristics of the used sensor and the mechanical conditions of the housing.

In both cases, the electrical signal obtained in the output is proportional to the force measured. In voltage transformer input and output voltage have a linear relationship while in current transformer there is a quadratic relationship between the input current and the output voltage, so the magnetic force is quadratic with respect to the current which generates it. The transformer ratio can be modified by taking an appropriate sensor material with a convenient voltage sensitivity (S_V=V/F).

All the developed structures gathered in this thesis are originally designed by the author in the context of the research work and great part of them are protected under a specific patent.

Contributions of the thesis

Voltage transformers

- Development of three different original *non-resonant* configurations of transducers for measuring high voltage. The configurations were implemented in the range up to 36kV:

    - *Single column with free displacement*. A piezoelectric column (actuator) fixed in only one end produces a mechanical free-vibration when is connected to high voltage. The secondary sensor measures either the displacement of the free end of the column or its acceleration, and converts it back into an electrical signal. The output voltage depends on the displacement (or acceleration) generated and the piezoelectric sensitivity of the sensor. Thus this configuration operates as a real piezoelectric transformer devices.

    - *Single blocking column*. A piezoelectric column (actuator) is totally fixed (blocked) between two electrodes and connected to high voltage. Thus a force is generated in the column but there is not displacement under ideal suppositions. The secondary sensor is taken as a part of the actuator column. The output voltage is a fraction of the input voltage and only depending on the relationship between the total length of the actuator and the length of the part used as a sensor. Hence, the transformer operates as a capacitor divisor, and the modification of the piezoelectric properties of the sensor does not affect the output voltage.

    - *Two-blocked columns*. This configuration consists of two mechanically matched columns (an actuator and a sensor column). Both columns are fixed together under blocking conditions. The actuator column is then connected to an electrical voltage and a force is generated in the column. This force is mechanically transmitted and piezoelectrically measured by the sensor column. The output electric voltage depends on the force generated by the actuator column and on the piezoelectric properties of the sensor material. Hence, this configuration operates as a real piezoelectric transformer.

- Development of an original procedure for dimensioning and choosing the active materials, i.e. the corresponding to the actuator and the sensor columns which is based on:

    - Determination of the different limitations in the operation of piezoelectric ceramics, particularly under conditions where non-linearities can appear. Hysteresis level, depoling characteristics and expected ageing in natural of forced conditions must be considered in the selection of the material.

    - Determination of the necessary *length* of the actuator column in function of the electrical depoling characteristics (extracted for the previous step) of the chosen material and on the maximum applied voltage.

    - Determination of the necessary preload to be applied to the column to keep it operating under prestress. This is necessary to guaranty the coupling between discs and the matching between sensor and actuator. Also prestress has been determined necessary to reduce the ageing effects in the material, higher under tensile forces.

- Determination of the theoretical transformer ratio under blocking conditions and their dependence from the piezoelectric coefficients.

- Development of the high voltage passive components required for the whole transducer. In particular, development of three different passive embodiment as a housing:

  - A dielectric *cast resin housing*. The housing is obtained by casting the active material in epoxy resin. Thus, all the active material remain totally fixed by the epoxy. Externally the preload in the active material could be fixed by a screw and the cavity is filled with silicone or another dielectric material.

  - A dielectric *epoxy-based housing*, consisted in a epoxy dielectric with a special cavity for placing the active material. The active material is fixed and prestress by an external preload screw.

  - A dielectric *Pyrex-based housing*, which consist of a Pyrex cylinder fitted to two metallic electrodes by using an epoxy adhesive.

- Construction of three prototypes of voltage transformer based on the blocking force state, and using the three different developed housing mentioned.

- Experimental verification of the response of three prototypes of voltage transformer to different electrical and mechanical tests, such as:

  - Electrical tests under 50Hz conditions.

  - Electrical tests under lightning conditions for evaluating the dielectric behaviour of the housings.

  - Mechanical tests to analyse the dependence of the output voltage from the pressure.

  - Mechanical tests for analysing the breakdown of the passive housing.

  - Verification of the frequency stability from the study of the resonance of the active column

  - Verification of the frequency behaviour of the transformer from the lightning test and their behaviour under different preload conditions.

  - Experimental analysis of linearity.

  - Experimental analysis of ageing.

- Experimental evaluation of different piezoelectric materials as sensor material, such as perovskite ceramics (PZT family) and Bi-layer compounds (PBT, SBT).

Current transformers

- Development of two different configurations of piezoelectric transducer for measuring high currents:

  - *Electromagnetic-Piezoelectric transducer.* Current transformer based on the magnetic force appeared in the gap of an electromagnet.

  - *Two-wires current piezoelectric transducer*. Current transformer based on the magnetic force appeared between two wires driven for the same current.

- Establishment of the theoretical transformer ratio for the proposed prototypes.

- Experimental verification of the response of the prototypes based on test under 50Hz conditions.

Conclusions

Voltage transformers

- The three different prototypes of voltage transformers have been successfully tested under 50Hz - high voltage conditions. The transformer ratio in such conditions has been observed depending on the preload conditions and the electrical load. A conditioning amplifier is required for standardise the application of the transducer to whatever load.

- Selection of *active material* must be considered separately for the actuator and sensor columns:

  Actuator:

  - Very high stiffness
  - Low hysteresis (<7%)
  - High depoling resistance (>1000V/mm)
  - Commercially PZT-type piezoelectric ceramics to be used as actuator are: PZT-8 and PZT-4 from Morgan Matroc, PXE41 and PXE-43 from Philips, Sonox P4 and Sonox P8 from CeramTec and Pz26 and Pz28 from Ferroperm

  Sensor:

  - Very high stiffness
  - High sensitivity
  - High stability in frequency and temperature
  - The best material as a sensor, for their stability and linearity, is the quartz. Nevertheless, PZT ceramic material offers higher sensitivity and cost features (but lower stability and linearity). A good alternative is the novel SBT compositions.

- Mechanical design of the *passive components* of the prototype has been observed as the more important parameter to obtain a very reliable device. The dimensioning of the housing has to withstand very high levels of mechanical forces due to:

  - The stresses generated for the ceramic piezoelectric column are very high in blocking conditions.
  - It is necessary to apply a preload as higher as the maximum expected tensile stress.
  - When the column works under tensile operation conditions, the sum of the preload and the maximum piezoelectric compression generated produces a tensile force which is twice the maximum compression.

  Particularly, in the case of the hard ceramic material used, PZT-8 from Morgan Matroc, the blocking forces appeared under the lightning test were calculated as approximately 14MPa, so the necessary preload was taken in the order of 15MPa, for security reasons. When the polarity of lightning test generates a tensile stress, the total stress in the housing, will be the sum of the preload stress (15MPa) and the piezoelectric tensile (14MPa), which results in 30MPa.

- The characterisation of the prototype under lightning test provided important information relative to the accuracy and stability of the transformer in frequency.

  - The transfer function, as it was previously supposed, is depending on the preload characteristics, so the blocking state is modified with the preload. Increasing the preload the sensitivity of the sensor increase because the transmitted force is higher.

- The transformer ratio has been observed significantly dependant on the readout (or corresponding load) due to the electrical impedance matching. This dependence made necessary to use conditioning amplifiers such as voltage amplifier or charge amplifier, depending on the variable to be measured.

- The frequency behaviour has also been observed depended on the preload conditions. Higher preloads improve the behaviour of the transformer since they reduce the 'mobility' of the mass of the system and then the existence of inertial forces. The maximum preload applied was limited by the mechanical breakdown of the transformer. Future research has to improve the capacity of the housing for withstanding high preload in order to improve the frequency response.

- In particular, the frequency response of the PIEZOTRF3 prototype under a preload of 7.40MPA was analysed. The behaviour of the transformation ratio in a range of 10000Hz was observed very stable, without any resonance peak. Nevertheless a progressive increase in the magnitude of the transformer ratio was observed.

Current transformers

- Successful tests under 50Hz conditions has been made with two different prototype configurations, showing that effectively the force measured had a quadratic relationship with the current to be measured.

- In spite of both prototypes show a similar behaviour under the level of currents applied (up to 300A), the Electromagnetic prototype has been concluded less suitable for current measures, because it incorporates a magnetic core. Better perspectives have the two wires transducer, a current transducer completely made in piezoelectric technology.

Suggestions for future work

Voltage transformers

The electrical response of the voltage transformer has successfully been tested under 50Hz conditions. Nevertheless, when the input frequency or the electrical voltage are higher, as is the case of the lightning test, the behaviour is influenced by the inertia of the masses of the system. These forces are caused for the high mechanical stresses generated by the actuator, which deforms easily the housing and produce deformations and accelerations with significant associated inertial forces.

In order to overcome this problem different suggestions for future work are purposed:

- *Improvement of the housing:* To increase the stiffness and strength of the passive material in order to withstand with a very low deformation the forces appeared (30MPa). Ceramic housing of higher strength and higher stiffness could keep much better the blocking conditions.

- *Modification of the geometrical dimensions of the active column:* To reduce the area of the active column. The blocking force is proportional to the area, thus a reduction in twice of the diameter will reduce the forces in 4 times. Nevertheless, a reduction of the area may affect the dimensional stability of the column, and this point must be evaluated to determine the best geometrical relation between the area and the length of the column.

- *To modify the active material used:* To modify the active material in order to reduce the produced stresses and so the requirements of the passive housing and preload system. This countermeasure offers some interesting advantages and permits an important reduction in manufacturing and engineering cost.

  A concrete purpose related to this countermeasure is following evaluated below. By considering the blocking force equation, one can to analyse the different variables to be modified in order to reduce the stresses generated:

$$\frac{F_{bloq}}{V} = \frac{d_{33} \cdot A}{s_{33}^{E} \cdot L}$$

  The compliance coefficient s_{33}^{E} must be as low as possible to obtain a very stiff piezoelectric column. PZT-ceramics and single crystals have similar values, although in general single crystals offer higher stiffness (lower value of s_{33}^{E}). Nevertheless, the differences from these values in different 'good' material does not represent a significant difference in the blocking force.

  On contrary, the coefficient d_{33} may be chosen in a very wide range. In particular in PZT-ceramics this value is in the order of 200-500, while in a single crystal such as quartz is 2.3. The reduction of the piezoelectric coefficient in two orders, will reduce the forces generated from 30MPa to 0.3MPa, much lower and easier for dimensioning the passive housing.

  Geometrically, the use of single crystal may offer other characteristics. A single crystal such as quartz can be grown in bulk column of length up to 15cm (at the present this value is higher). This type of material does not need polarisation and so it can be used as a bulk material to built the column. Moreover quartz is very stable in front the temperature, has not depoling effect and a very stable response in frequency.

  Furthermore, if a bulk piece of quartz was used (as actuator) the diameter of the column could be reduced to 10mm or less, so the stability is guaranteed because it is a bulk column. In this way, a new reduction in the appearing forces may be obtaining up to 50kPa (with PZT8 it reach 30 MPa). This allows making a mechanical structure for working under blocking conditions without to very high mechanical requirements.

  As there is not stacked single discs, the column will have not problems of decoupling. So the only required prestress will be related to guarantee the matching between sensor and actuator columns.

  The time stability of a such bulk column and the related passive housing will also be lower so the forces are reduced. Also the frequency behaviour will improve so the inertial force can be easily controlled.

  Certainly, the reduction of the d_{33} coefficient will be limited by the output signal generated by the sensor, drifts, etc. A very low force in the actuator will produce a very low output voltage in the sensor part, and probably some problems for driving the external load. Thus, it is a compromise to decide the best value of force generated by the actuator and the external voltage for driving the load. At the present, electronic loads permits to be driven with very low voltages. This would permit to reduce the d_{33} coefficient of the actuator in several values without very big problems.

FIFTH PART:

APPENDIXES

A1 Conditioning and Transmitting the signal from a Piezoelectric Sensor

A1.1. Introduction

The electrical signal generated by a piezoelectric sensor (in form of electrical charge) needs to be converted into a 'standard' electrical magnitude (voltage or current) in order to activate measurement devices. It is also a general need, to send this low electrical signal to long distance, where the measurement devices are placed.

In general this signal is currently transmitted by using shielded wire or coaxial, for avoiding the interference in the signal being transmitted caused by the external electromagnetic influences. When the signal is received by the measured device it is not possible a direct connection of the cables to the measuring device, due to the high output impedance of the piezoelectric transducers. As a result, it is necessary to place a preamplifier which converts the high impedance of the transducer in a lower impedance for being matched with the measuring devices. This problem is higher in low frequency measurement due to the capacitive behaviour of the piezoelectric for quasi-static signals. Two type of amplifiers are used: *electrometer amplifiers* and *charge amplifiers*.

When the transmission distance is important, it is necessary the incorporation of *bulk-inside amplifiers* in the sensor to drive the signal. These amplifiers require an excitation power and cable for driving the signal. This is because different alternatives are purposed for reducing the number of cables and the possibility of electromagnetic interference during the transmission.

A novel transmitting signal, very well adapted for long distances transmission and very critical environment (with high level of EMI interference) consist on using *optical transmission* system. This type of solution converts the electrical signal generated for the piezoelectric sensor in a optical signal which is used during the transmission.

In this chapter an overview to the different conditioning and transmitting systems for the signal generated from a piezoelectric sensor is gathered.

A1.2. Piezoelectric Sensor

A piezoelectric transducer (force or acceleration sensor) is an *active charge* sensor that generates an electrical magnitude when withstands a mechanical magnitude. The name of *active* sensor comes from the fact that this type of sensor does not need an external power supply to operate. The name of charge sensor comes from the electrical charge which is generated under mechanical forces or accelerations.

A piezoelectric sensor may be represented as an elastic system with an electrical equivalent circuit displayed in Figure A1.1. In this circuit, the voltage $V_o(t)$ is proportional to the mechanical magnitude actuating in the transducer. The capacitor C_1 is inversely proportional to the transducer elasticity, while L_1 represents the seismic mass M. The capacitor C_0 is the static capacitance of the transducer, which result from a seismic mass infinitely big ($M \rightarrow \infty \Rightarrow L_1 \rightarrow \infty$).

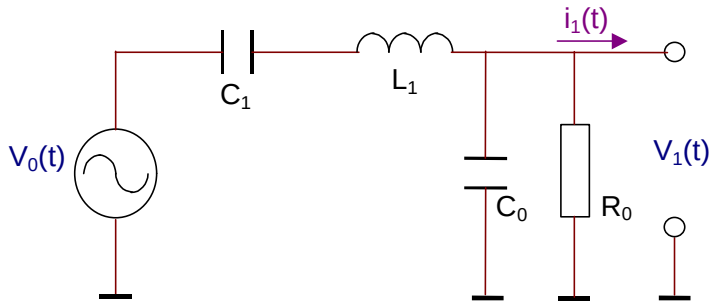

Figure A1.1. *Equivalent circuit diagram of a piezoelectric transducer*

The equivalent circuit of Figure A1.1 evaluates the response of a piezoelectric sensor in dynamic conditions. In the particular case of an exciting signal (force acceleration) with frequencies far below the system resonant frequency, the previous circuit can be simplified. This is due to the effect of L_1 can be neglected. In this case, the sensor is represented by the static capacitance C_0 and the capacitance relative to the elasticity (mechanical capacitance), as is shown in Figures A1.2 and A1.3 for the equivalent circuits with voltage or current source, respectively. For a finite value of M (seismic mass), the capacitance of the transducer far below the resonance is :

$$C_a = C_0 + C_1 \qquad \text{(A1.1)}$$

The value of C_a can easily be calculated by considering the transducer as a capacitor of parallel surfaces. In this case the capacitance of the sensor disc at low frequency is given by:

$$C_a = \frac{e_0 \cdot e_r \cdot A}{t} \qquad \text{(A1.2)}$$

where A is the surface area [m^2], t is the thickness of the piezoelectric material [m], and e_0 and e_r are the permtivity of the vacuum and the relative permitivity of the piezoelectric material. If the shape of the transducer is complicate this value must be measured.

The value of R_0 makes reference to the insulation resistance (resistance between signal and ground) of the transducer element itself. The value of R_0 in dry and clean conditions is assumed to be very large (>$10^{12}\Omega$) and sometimes is neglected in the equivalent circuit. The value of R_0 may be obtained from the value of the resistivity, r [Ω·m], of the material, form $R_0[\Omega] = r \cdot \frac{t}{A}$.

Typical values for the resistivity are in the order of 10^{10} Ω·m.

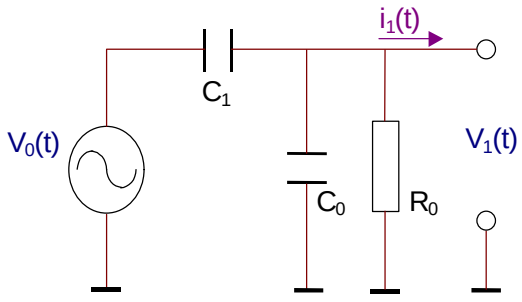

Figure A1.2. *Simplified equivalent circuit (voltage source), for frequencies far below the first resonance of the transducer.*

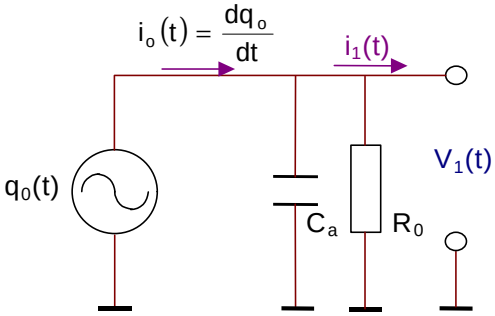

Figure A1.3. *Simplified equivalent circuit (current source), for frequencies far below the first resonance of the transducer.*

A1.2.1. Characteristics of the output of a *charge* sensor

Due to their low conductivity and capacitive behaviour, piezoelectric sensor have a very high impedance output signal. As a result, this type of sensor has a special characteristics in their output signal.

1. Due to the high output impedance, the output generated is extremely sensitive to corruption from various environmental factors. Low noise cabling must be used to reduce radio frequency interference (RFI) and electromagnetic interference (EMI). The use of tie wraps or tape reduces triboelectric (motion-induced) noise. A high insulation resistance of the sensor and cabling should be maintained to avoid drift and ensure repeatable results.

2. To properly analyse the signal from piezoelectric transducers, the high impedance output must normally be converted to a low impedance voltage signal. This can be done directly by the input of the readout device or by in-line voltage and charge amplifier.

    - Direct connection to the readout device: Certain piezoelectric sensors exhibit exceptionally high values of internal source capacitance and can be plugged directly into high impedance (>1MΩ) readout devices such as oscilloscopes and analyzers.

    - In line conditioning: On contrary, piezoelectric sensors with a low internal source capacitance may require in-line signal conditioning such as voltage amplifiers (electrometric amplifiers) or charge amplifiers.

3. Low frequency and DC response: The charge generated in a piezoelectric sensor only appears when there is a change in the applied force. After this, the charge will leak across the input resistance of the instrument used to measure the signal and the resistance of the piezoelectric sensor itself. The discharge time constant characteristic of the sensor is depending on both its capacitance and its conductivity. Because of this, it is not possible to use piezoelectric sensor to measure directly a static force or pressure. Nevertheless, some signal conditioners devices allow improving the low frequency response of the sensors up to almost-static values, as is the case of the charge amplifier.

The above mentioned characteristics indicate the need to use a signal conditioning in order to properly analyse the signal.

A1.2.1. Output Modes for measuring

There are two main output conditions which are used to performed the measurement with piezoelectric transducers:

• Open circuit conditions

If an axial force parallel to the poling direction (named as 3) is applied to a piezoelectric transducer, a change in both the remanent polarisation and the remanent charge in the material Q_b will happen. In open circuit conditions the free charge Q_f does not change. Then, the resulting surface charge $Q_r = |Q_b - Q_f|$ produces an electric field E and, as a result, a current density which neutralise completely Q_r and make the electric field E again zero.

Nevertheless, due to the material conductivity is extremely low, only a little current pass through the material and the equilibrium need a long time to be established again. In general this

dynamic process is considered negligible (if not static events want to be measured) and the current of neutralisation is considered zero.

Thus, in the condition of *open circuit*, a electric voltage $V_o(t)$ appears between the metallic surfaces of the transducer, which is proportional to the applied force F. In this conditions the electrical displacement, D, is zero, and equation A1.3 is obtained.

$$E_3 = -g_{33} \cdot T_3 + \frac{D_3}{e_{33}^T} \quad \rightarrow \quad V_0 = E_3\big]_{D=0} \cdot t = -g_{33} \cdot t \cdot \frac{F_3}{A} \qquad \text{(A1.3)}$$

In order to reduce the matching impedance effects of the piezoelectric transducer when open circuit measurement want to be achieved, it is necessary to adapted an conditioning electronic circuit in the transducer output is required.

- **Short-circuit conditions**

If the piezoelectric crystal is short-circuited, the polarisation and charge Q_b will also vary under the influence of an external force. When Q_b changes, an instantaneous change in the free charge Q_f which compensate the change in Q_b will appear. As a result of this, the relation $Q_f = -Q_b$ is always kept. An electrical displacement current will then appear through the shortcircuit wire, with a density as $j = \frac{dD}{dt}$.

The integration respect to the time of the displacement current $j(t)$ leads to the variation of the free charge, ΔQ_f, which corresponds to the displacement D. The function $\Delta Q_f(t)$ is proportional to the force $F(t)$. The intensity of field E in the condition of short-circuit is zero.

By using the piezoelectric constitutive equations one can express this function as:

$$D_3 = d_{33} \cdot T_3 + e_{33}^T \cdot E_3 \quad \rightarrow \quad D_3\big]_{E=0} = d_{33} \cdot T \qquad Q_3 = d_{33} \cdot F \qquad \text{(A1.4)}$$

Short circuit conditions may be achieved by short-circuiting the electrodes of the transducer and measuring the current fluxing by using a current probe. Nevertheless this type of solution require of current probe which capacity to measure very low current (pic-ampers or lower).

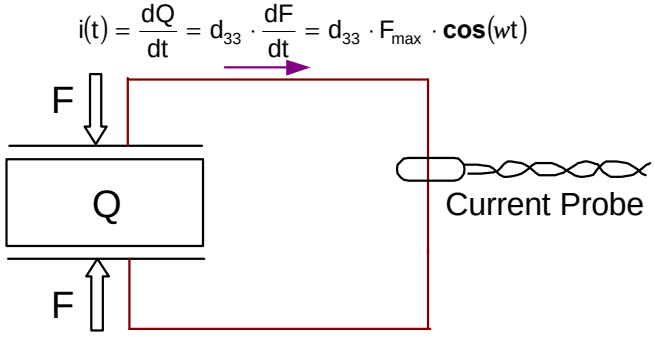

Figure A1.4. *Short-circuit condition current measurement*

A more widely used solution consists in integrated the generated current by using an electronic circuit which kept the condition of short-circuit. To do this, charge amplifiers are used.

A1.2.2. Signal Conditioning Alternatives

There are different techniques for acquiring the signal from a piezoelectric sensor. Next Table A1.1 indicate briefly the different possibilities and conditions where are applied.

Table A1.1. *Techniques for conditioning the signal from a piezoelectric sensor*

Mode of Connection		When is applied	Output Conditions used
DIRECT CONNECTION	Direct connection to a high input impedance readout instrument (oscilloscope and analyzer)	Transducers with very *high internal source capacitance*, and short cable length required. $C_{sensor} \uparrow\uparrow$	Open circuit conditions (D=0) $V_0 = Q/C_{sensor}$
EXTERNAL AMPLIFIER	Connection with wires to an external *Voltage Amplifier*	Transducer with low internal source capacitance $C_{sensor} \downarrow\downarrow$	Open circuit conditions (D=0)
	Connection with wires to an external *Charge Amplifier*		Short Circuit Conditions (E=0)
BUILT-IN AMPLIFIER	Built-in an internal *Voltage Amplifier*	Transducer with low internal source capacitance $C_{sensor} \downarrow\downarrow$	Open circuit conditions (D=0)
	Built-in an internal *Charge Amplifier*	Long Distance to transmit the signal. Hard environment conditions.	Short Circuit Conditions (E=0)

A1.3. Measurements in open circuit

A1.3.1. Conditions to be achieved

The open circuit conditions are applied if the voltage $V_1(t)$ of a transducer matched with a external device with impedance (R_E, C_E) is practically the same as should appear with the electrodes in open circuit conditions. This corresponds to a negligible output current.

In order to achieve these conditions, the load impedance has to verify:

$$C_E << C_a$$

$$R_E >> \frac{1}{w \cdot (C_a + C_E)} \approx \frac{1}{w \cdot C_a} \qquad \text{(A1.5)}$$

within the operation frequencies established. If these conditions are verified, the operation zone will be far below of the first resonance of the transducer, depending on the load and defining as:

$$f_r = \frac{1}{2p \cdot R_E \cdot (C_a + C_E)} \qquad \text{(A1.6)}$$

In general a modification in the response of 3dB appears when the frequency is: $f_{limit} = \frac{1}{2} \cdot f_r$

If the required input impedance is very high, there are two ways to prevent the cut off frequency from rising:

- use a parallel capacitor (C_p) externally coupled to the piezoelectric sensor.
- use a stack of discs in parallel (stack), and thus the total capacitance will be higher and lower the required input impedance.The capacitance of a parallel stack increase proportionally to the number of stacked discs, as indicated in the following equation:

$$C_{stack} = N_{disc} \cdot C_a \qquad \text{(A1.7)}$$

Nevertheless this increase in capacitance reduces the open-circuit sensitivity of the transducer, and the output voltage is depending on the capacitance of the external cables and conditions of different loads.

In order to find a more stable solution a voltage amplifier is used as is described below.

A1.3.2. Voltage Amplifier (Electrometric Amplifier)

The Electrometric Amplifier amplifies the voltage in the electrodes of the transducer by using a very high input impedance amplifier. The configuration of the amplifier must guarantee the open circuit condition, i.e. a negligible current flux from the transducer.

Figure A1.5 displays the equivalent circuit of a electrometric amplifier, where the transducer and cable connection are also illustrated.

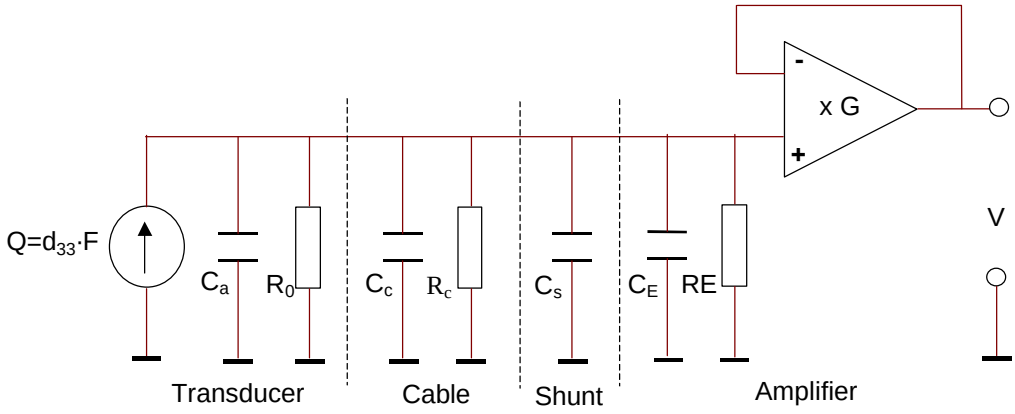

Figure A1.5. *Equivalent circuit of a piezoelectric transducer operating in voltage mode*

Applying a force to the piezoelectric transducer produces electrostatic charge *Q* across the transducer internal capacity C_a. The voltage at the transducer connector is:

$$V = \frac{Q}{C_a} = \frac{d_{33} \cdot F}{C_a} \qquad \text{(A1.8)}$$

The internal impedance of the transducer is typically $10^9\ \Omega$ or more. The value $\frac{V}{F} = \frac{d_{33}}{C_a}$ is known as the *charge sensitivity of the transducer itself*.

The voltage developed at the end of a coaxial cable with a capacitance C_c attached to the transducer is:

$$V = \frac{Q}{C_a + C_c} \tag{A1.9}$$

An average value for the cable capacitance can be taken as 75pF per 1m of length.

If the anticipated full scale level on the transducer is high, an additional shunt capacity C_s may be added giving the attenuated voltage:

$$V = \frac{Q}{C_a + C_{cable} + C_{shunt}} \tag{A1.10}$$

If the low voltage is low due to low signal level or high cable capacity an amplifier provides the needed voltage gain, introducing the amplifier input capacity C_E and amplifier gain G. This is usually an electrometer tube or emitter follower in the amplifier input. The value of this impedance varies from 10^9 to $10^{14}\Omega$ depending upon the low frequency response required and piezoelectric material used. Special attention is necessary to ensure that all components and connections in the input circuit are shielded from electromagnetic radiation.

$$V = \frac{Q}{C_a + C_{cable} + C_E} \cdot G = \frac{d_{33} \cdot F \cdot G}{C_a + C_{cable} + C_E} \tag{A1.11}$$

The value V/F in the previous equation is known as the *overall system sensitivity* measured at the output of the voltage amplifier which is reduce compare to the basic charge sensitivity of the transducer for itself.

Equation A1.11 has not considered the effect of the different leakage resistance. This resistance affects the frequency response of the system, as indicated in equation A1.12.

$$\frac{V(s)}{F(s)} = \frac{d_{33}}{C} \cdot \frac{R \cdot C \cdot s}{1 + R \cdot C \cdot s} \tag{A1.12}$$

where $C=C_a+C_{cable}+C_E$ and $R=R_0||R_{cable}||R_E$.

From equation A1.12 one can extract several conclusions:

• Conclusions

1. The transducer sensitivity (V/F) is reduced in a magnitude depending on the cable used and the amplifier chosen. Thus, the system scale factor or calibration depends upon the various circuit parallel capacities as well as the amplifier gain stability. This explains why the voltage mode sensitivity of high impedance type piezoelectric sensors is measured and specified with a given cable capacitance. If the cable length and/or type is changed, the system must be recalibrated.

2. The frequency response is as high pass filter, with a cutting frequency depending both on the cable length and on its insulation (capacitance to ground). This may be also depending on external conditions such as temperature and humidity. For example, excessive moisture or other contamination in the input circuit provides a low resistance to ground resulting in additional possible signal instability.

3. Voltage mode system is capable of linear operation at high frequencies. Certain instrumentation has a frequency limit exceeding 1MHz, making it useful for detecting shock waves with a fraction of a microsecond rise time. However, care must be taken as large capacitive cable loads may act as a filter and reduce this upper operating frequency range.

- **Possible improvements**

1. If a very high capacitor is placed in parallel with the input of the amplifier, an independence from the variations of the other capacities is achieved. However, an important loss of sensibility will appear. In practice the calibration is reasonably stable providing the amplifier gain is not adjusted after calibration and, additionally, that the input coaxial cables are not interchanged.

2. The influence of the cable capacitance may also be reduced using an active shield. However, this leads to a complication because a three-axial cable is needed (a guard shield and other for the ground of the transducer).

3. Ultra low noise coaxial cables minimise the electrostatic charge generated by the primary insulation rubbing against the shielding braid. This is accomplished by the use of oil or Teflon lubrication in the cable.

- **Typical application**

1. According to the equations A1.10 and A1.11, sensing elements with a low capacitance will have high voltage sensitivity. This explains why low capacitance quartz sensors are used predominantly in voltage systems.

A.1.4. Measurements in short-circuit

A1.4.1. Conditions to be achieved

The short circuit conditions are applied if the output current fluxing through the electrodes of the external capacitance C_E of the external measuring devices is approximately like the short-circuit current. This means that the output voltage $V_1(t)$ from the transducer is negligible.

In order to achieve these conditions, the load impedance has to verify:

$$C_E >> C_a$$

$$R_E >> \frac{1}{w \cdot (C_a + C_E)} \approx \frac{1}{w \cdot C_E} \qquad \text{(A1.13)}$$

within the operation frequencies established.

In order to obtain the needed very high external capacitance, C_E, a capacitive feedback is used in an operational amplifier (Miller effect). Thus, C_E may be calculated from:

$$C_E = C_f \cdot (1 + A) \qquad \text{(A1.14)}$$

where A is the amplification factor. This kind of amplifier structure is known under the name of charge amplifier.

A1.4.1. Charge Amplifiers

Figure A1.6 shows a commercially available measuring assembly consisting of a piezoelectric transducer on which the forces *F* act, and the collector electrodes 2 and 3 connected to ground and to direct-current amplifier. This amplifier constitutes a charge amplifier with negative feedback capacitance C_f and input impedance of $10^{14}\Omega$.

The charge amplifier is based on the principle of integrating which is also known as Miller integrator. Compared with the usual Miller integrators, however, it is distinguished by high input impedance and high gain. The principle of these amplifiers consists of transferring the electric charge from the transducer (in parallel with the cable and the input of the amplifier), toward the feedback capacitor, very well known. The voltage in the feedback capacitor is then measured with an amplifier with electrometric characteristics.

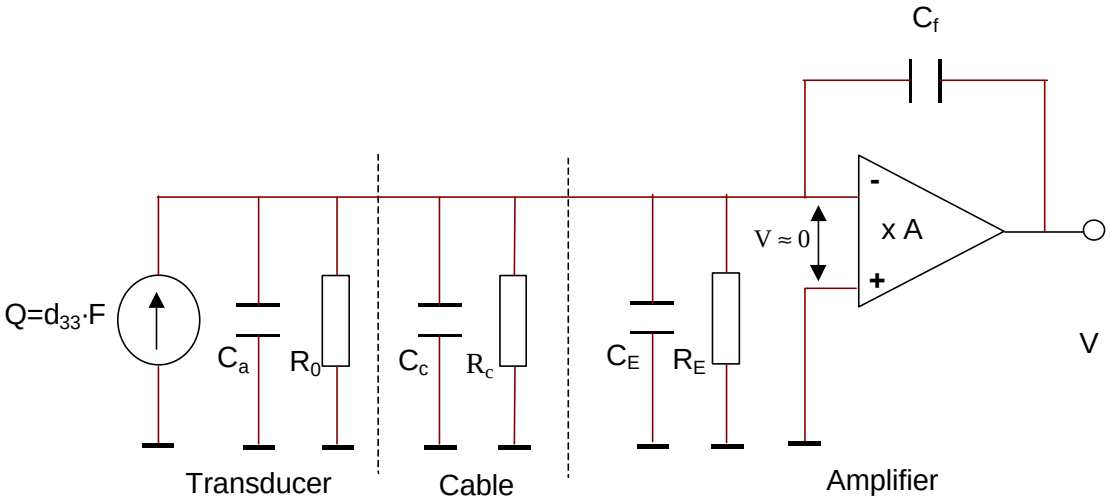

Figure A1.6. *Equivalent circuit of a piezoelectric transducer operating in charge mode*

In a first approximation, considering only the capacitance of the transducer and the feedback capacitance, the output voltage will be:

$$V = \frac{-Q}{C_f + \frac{(C_a + C_f)}{A}} \tag{A1.15}$$

where *A* is the amplifier open loop gain. Open loop gain, *A*, is typically 3000 to 10000 (A>>1). Thus the previous expression can be simplified as:

$$V = \frac{-Q}{C_f + \frac{(C_a + C_f)}{A}} \approx \frac{-Q}{C_f} \tag{A1.16}$$

This expression has ignored the leakage resistance of the transducer, the cable and the input of the amplifier. A more accurate expression is the next:

$$\frac{V(s)}{F(s)} = -\frac{d_{33}}{C_a} \cdot A \cdot \frac{R \cdot C_a \cdot s}{1 + R \cdot [C + (1 + A) \cdot C_a] \cdot s} \tag{A1.17}$$

where $C=C_a+C_{cable}+C_{in}$ and $R=R_0||R_{cable}||R_{in}$

Thus, the sensibility has a high pass behaviour, as in the electrometer amplifier. This means than static phenomenon can not be measured. Nevertheless, the cut frequency in this case is much lower as a result that C_a is multiplied by A.

A feedback resistance in parallel with C_f is also necessary since the operational amplifier requires a DC path from each input to common (for bias current flow). In the absence of this resistor R_f the capacitors will build up a DC charge until reaches saturation. This resistor limits the lower cutoff frequency of the charge amplifier. Its effective value is divided by 1+A and appears in parallel with R. Furthermore, its presence affects the contribution of V_0 and I_0 in the output. The analysis of these contributions may be done considering the equivalent circuit of the amplifier (Figure A1.7). Thus, the output voltage caused exclusively to the unbalanced voltage and current are:

$$v_0\big]_{unbalanced} = V_0 \cdot \left(1 + \frac{R_f}{R}\right) - I_0 R_f \qquad \text{(A1.18)}$$

where R_p is supposed chosen in order to that the polarisation current affect to the output only through their difference, i.e., $R_p = R \,||\, R_f$.

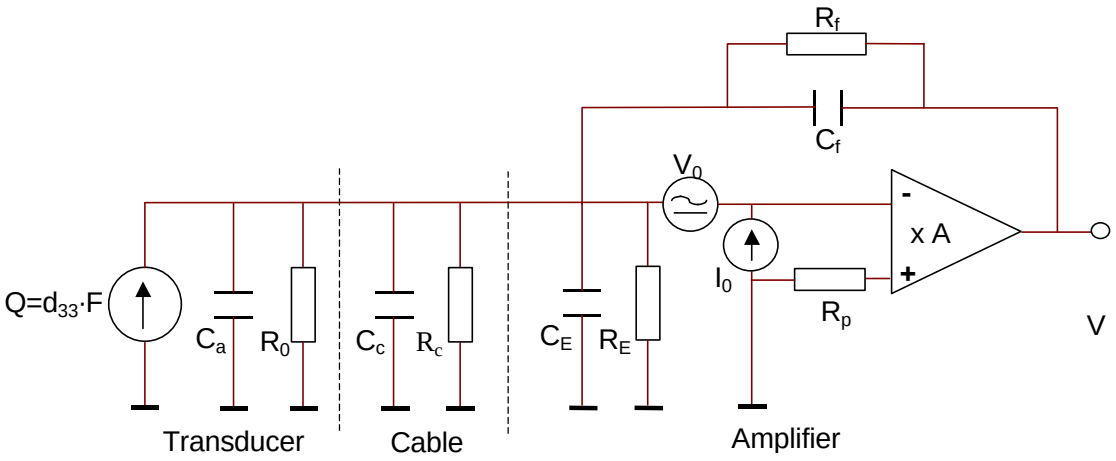

Figure A1.7. *Equivalent circuit for analysing the effect of the feedback resistor R_0*

From the previous equation is clear that a value of R_f as low as possible is convenient, within the range of frequencies for being measured. Thus R_f is to be fixed for the lower cutoff frequency to be measured:

$$f_{cutoff} = \frac{1}{2p \cdot (R_f C_f)} \quad \rightarrow \quad R_f = \frac{1}{2p \cdot C_f \cdot f_{cutoff}} \qquad \text{(A1.19)}$$

For stabilisation purposes, and sometimes for protection of the amplifier input stage, it is also desirable to insert the series resistor R_1 (Figure A1.8). This resistor limits the upper response frequency.

$$f_{upper} = \frac{1}{2p \cdot (R_1 C)} \rightarrow \qquad R_1 = \frac{1}{2p \cdot C \cdot f_{upper}}$$

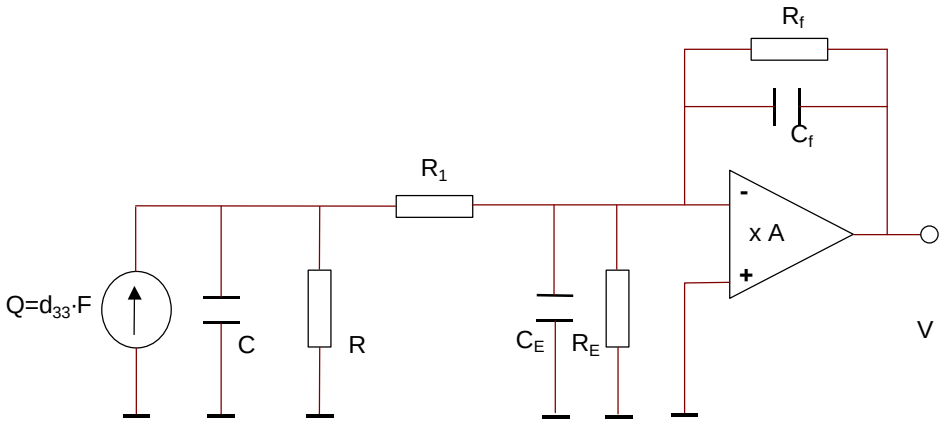

Figure A1.8. *A resistor R_1 could be used to limit the high frequency response of the amplifier.*

• Comments

1. The high level voltage feedback across the amplifier keeps the input circuit at or near zero volts (Figure A1.6). This virtually eliminates the effects of all shunt capacities in the input circuit. Thus, the same quantity of electrostatic charge *Q* developed in the transducer is found in the feedback capacitor. The voltage across this capacitor is the output voltage of the Charge Amplifier.

2. The sensibility scale factor is now dependent upon but two stable elements, a good quality Piezoelectric Crystal and a precision feedback capacitor.

3. The output voltage is virtually independent of the amplifier gain and input cable length. Vibration and Shock Transducer with varying capacities can be used interchangeably as long as the charge sensitivity is known. Accumulated errors should not exceed 2-4% of full scale.

• Limitations

There is, as in the case of the voltage amplifier, serious limitations, especially in field environments or when driving long cables between the sensor and the amplifier:

1. The electrical noise at the output of a charge amplifier is directly related to the ratio of total system capacitance, *C*, to the feedback capacitance, C_f. Attenuation may be expected when the input capacity, C, approach 100 times the feedback capacity. This may be observed in the equation A1.16, where if A.C_f approaches 100 times C_a, the simplified expression is no longer valid and attenuation is experienced. Because of this, *cable length* should be limited as was the case in the voltage mode system.

2. Moreover, very long cables produce additional problems. A large proportion of capacity outside the feedback loop reduces an inherent attenuating effect on noise and increases noise and system resolving level appreciably. Also, “ground loops” are commonly experienced with long cables whereby the amplifier ground is at a different level than the case –grounded transducer. Isolation studs inserted between the transducer and the surface upon which it is mounted to eliminate “ground loops” commonly introduce compliant elements to the transducer that lowers the effective resonant frequency.

3. Because the sensor output signal is of a high impedance type, special low-noise cable must be used to reduce charge generated by cable motion (triboelectric effect) and noise caused by excessive RFI and EMI.

4. While many of the performance characteristics are advantageous as compared to voltage mode systems, the per-channel cost of charge amplified instrumentation is typically very high. It is also impractical to use charge amplifier systems above 50 to 100kHz as the feedback capacitor exhibits filtering characteristics above this range.

A1.4.2. Charge Amplifier Circuits

• Zero Shift

The failure of the acceleration vs. time trace to return to zero is called zero shift. This may be caused electronically by overload, rectification or in some cases by insufficient low frequency response related to RC time constant. These conditions are best handled with the correct choice of measuring equipment.

A mechanical translation or shift of the piezoelectric crystal in its mount causes another type of zero shift. This phenomenon is generally noted during measurements in high frequency, high amplitude shock environments. Mechanical and electrical filtering have proved effective in eliminating this zero shift phenomenon in certain models of low output impedance piezoelectric accelerometer.

In particular, a large quantity of such devices has been successfully employed in conjunction with associated integrators for ground motion surveys (velocity profiles). Obviously any zero shift of the primary sensor during these field blast measurements would be grossly exaggerated by the integrating process involved and would distort, if not completely mask, the desired velocity data.

• Arrangements for zeroing the amplifier

A fundamental problem occurring in metrology and control engineering is the amplification of a very small electrical variable into one that can be exploited for measuring, recording and control purposes and in this regard various types of measuring amplifier are employed. As an important secondary function in such operation, every measuring amplifier must be adjusted to a certain value at the beginning of a measurement, usually zero if the measured value at the transducer is zero.

Only after this is done, the phenomenon to be measured commences. Upon its completion, when the measured value is zero again for example, the measuring amplifier is set to the initial value of zero once more and kept there until a new measuring operation is initiated. In most cases, the measuring amplifier delivers a voltage as an output signal, usually of the order of 0 to +10V.

With such measuring amplifier, therefore, before starting a measuring operation the amplifier output must be adjusted to 0 V by means of a switching operation known as zeroing or resetting.

Further consideration here will be directed mainly to an electrometer and charge amplifiers as are used in piezoelectric metrology to convert relatively weak signals from piezoelectric transducers into proportional measuring and control voltage. For initiating reset, mechanical relays are employed in such transducers. In this case the switchover is performed by means of mechanically operated conductors, which are moved by building-up removing magnetic or electric fields, with attendant disadvantages and undesirable side effects.

In the first place these zeroing operations take a relatively long time. Secondly there are always disturbing charges in the proximity of these relays, which are located on the glass surfaces near to the melted-in contacts and cannot be led off again. After a “zeroing” of this kind the result is a residual voltage set up by static induction, which cannot be removed even by repeated

resetting. While a variety of proposals have been made for overcoming this difficulty, no satisfactory solution has emerged.

Considerable difficulties are experienced in the design of miniature amplifier owing to the mechanical variable and the need to operate the relays mechanically. When such miniature amplifier is to be combined with piezoelectric transducers to form a unit, however, the problems become almost insurmountable. For the industrial application of piezoelectric transducers in particular, the miniature amplifier has to be located in the immediate proximity of the transducer, so that the signal leads to the evaluating instruments may consist of simple, uncritical cable connections involving no particularly stringent requirements in the way of insulation

In view of all these problems, present solutions adopt a new approach, eliminating the use of mechanically operated relays or switches for zeroing miniature amplifiers. Instead, controllable semiconductor elements are employed, controlled not by the magnetic action of a current, but by a voltage, for instance. By eliminating all mechanically moved elements, all static induction is prevented, and the energy required for resetting is incomparably smaller. In particular, however, the time taken is shortened by orders of magnitude. Entirely new possibilities are opened up by this, especially where the circuitry has to be accommodated in a miniature amplifier which is to be fitted in the immediate proximity of the transducer or actually inside it. In one major embodiment of the invention, the current supply, signal transmission and triggering of a reset can be transmitted via a lead of the cable, allowing a simple plug-and-socket and cable connection to be used

An important advantage of the zeroing device using a semiconductor is that the semiconductor protects the input transistor, which is usually a field effect transistor with insulated control electrode, against overvoltages. Because the inputs of electrometer and charge amplifiers have input impedance of the order of 10^{14} Ω, the electrostatic charges caused by friction are enough to set up voltages of several hundred volts at the input of such amplifiers, leading to a breakdown of the insulation in the input transistor and a destruction of it.

The semiconductor in the zeroing circuit is also exposed to this static charge, and if the voltage at this element exceeds a certain limiting or breakdown voltage it becomes conductive, leading the static charge away without being destroyed by it if a suitable current limiting resistor is included. Semiconductor elements can be found for the zeroing device having a breakdown voltage below the destruction voltage of the input transistor, so that the latter is protected.

Figure A1.9 shown the basic configuration of a charge amplifier in conjunction with a piezoelectric transducer. Usual capacitance of the negative feedback capacitor lie between 10pF and 0.1μF. To obtain a large time constant $\tau = R \cdot C$ of, for example, 1000s with almost static measurements, in the case of the 10pF capacitor the total effective insulation resistance, represented by resistance R_f, must amount to at least 10^{14} Ω.

Before starting a measurement, the negative feedback capacitor is discharged by closing a parallel switch, for which the switch is set briefly to the reset position. For the measurement that follows, the switch remains open, i.e., in operation. It will be apparent from the mode of operation that switch must have very high insulation.

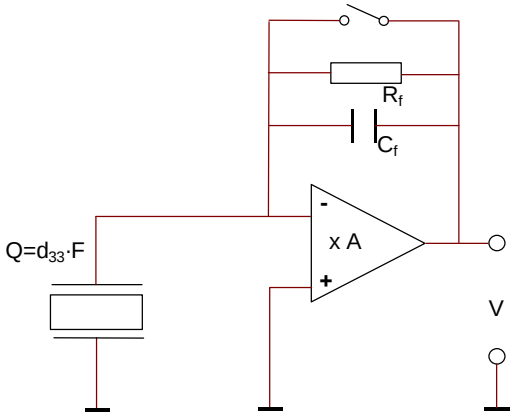

Figure A1.9. *Basic configuration of a charge amplifier*

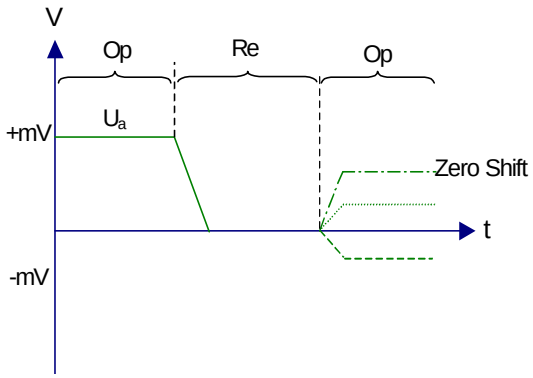

Figure A1.10. *Zeroing operation when very low frequency measurements are performed*

Figure A1.10 displays a zeroing operation plotted against the time scale as may be recorded with an oscillograph. The initial signal U_a, drops to zero during the zeroing phase when the switching is short-circuited, i.e., switched to Reset position. Upon switching-back, i.e., opening to the operating position, the *zero shift* takes place with a partly irregular and partly reproducible value, which may be positive or negative. The measurement which now follows is in error by this initial error, which in the case of small measured variables often leads to unsatisfactory measuring results.

The mechanical switches or relays usually employed for this purpose are mostly of the reed relay type on account of the high insulation resistances demanded. These relays incorporate reeds melted into glass, which are actuated by an externally applied magnetic field. These relays correspond to the latest state of the art and give high insulation values and relatively short switching times. Nevertheless, however, they have a number of major disadvantages for this application. For example, the magnetic field needed to trigger them requires a relatively large amount of energy, while on the other hand it gives rise to undesirable induction effects and disturbing charges. Upon resetting relays for operation, these disturbances cause the notorious zero shift, which is irregular and may have positive or negative voltages. The main cause of these disturbances is charges on the inside wall of the glass tubes of the reed relays customary in the trade. Owing to these disturbing charges, the desired starting position at the commencement of measuring, i.e., voltage at the negative feedback capacitor equal to zero and thus, in the case of an ideal amplifier the initial amplifier voltage, 0V, is in error by an amount corresponding to a few 0.1pC at the input. Since the charges on the inside of the glass wall of the reed relay which cause the zero shift in the manner described are variable compensation by appropriate zero displacement in the amplifier, for example is ruled out in practice.

Controllable semiconductor elements have been used to replace the mechanical relays in order to eliminate the cause of these difficulties. These semiconductors do not require magnetic fields and can be actuated much more rapidly and with much less energy expenditure due to the elimination of all mechanical contacting. Interruption is less abrupt, minimising the errors caused by noise. Similarly, eliminated are errors caused by frictional and thermoelectric voltages.

Moreover, the much smaller dimensions of the semiconductor element in the piezoelectric transducer and amplifier system according to the invention make it possible to construct miniaturised amplifiers on both the charge amplifier and the electrometer amplifier principles. The piezoelectric transducer and amplifier system may be accommodated in a single housing, or else in two housing joined by a cable suited for the arduous temperature and vibration conditions under which the transducer must operate.

Figure A1.11 illustrates the idea of a controllable semiconductor element for zeroing the charge amplifier. The amplifier is equipped with a negative feedback capacitor, which is short-circuited

with the controllable semiconductor element or is opened. The control impulse for opening (Op) or closing (Re) is given to the semiconductor by a control signal. As with the reed relay, the semiconductor element requires very high insulation of the order of $10^{13}\Omega$, at least; this is technically achievable with field effect transistors.

Of paramount importance, however, is the fact that the zero shifts with the semiconductor elements are absolutely reproducible and therefore is possible to compensate it. This can be accomplished by feeding in an appropriate compensation signal.

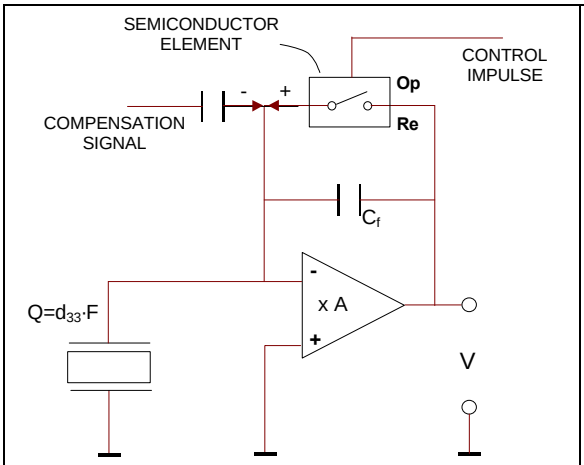

Figure A1.11. *Controllable semiconductor element for zeroing the charge amplifier*

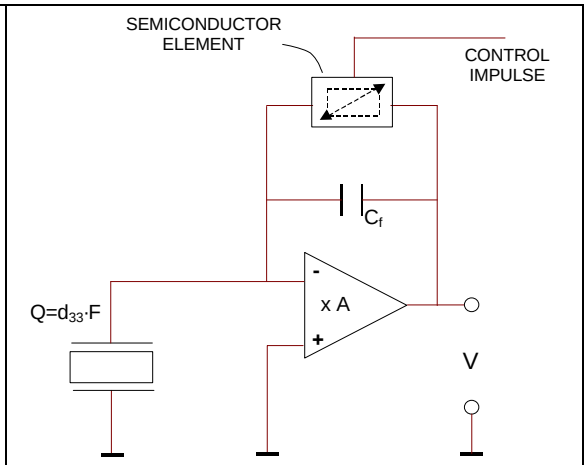

Figure A1.12. *Zeroing semiconductor with different intermediate stages between short circuit and maximum resistance.*

In Figure A1.12 instead of a semiconductor element operated as a switch, one is used which can be adjusted to any intermediate stages between short circuit and maximum resistance, e.g. 10^8, 10^9, 10^{10}, 10^{11}, $10^{13}\Omega$. The magnitude of the effective resistance can be regulated by the control signal. With dynamic measurements, this possibility is exploited to determine the lower frequency limit.

Figure A1.13 shows another alternative piezoelectric transducer and amplifier system. Instead of a controllable semiconductor element, an optic-electronic switching element is used here, for complete or partial short-circuiting of the negative feedback capacitor. This switching element consists of two photodiodes in opposition, which can be illuminated by one or two light-emitting diode via the control signal.

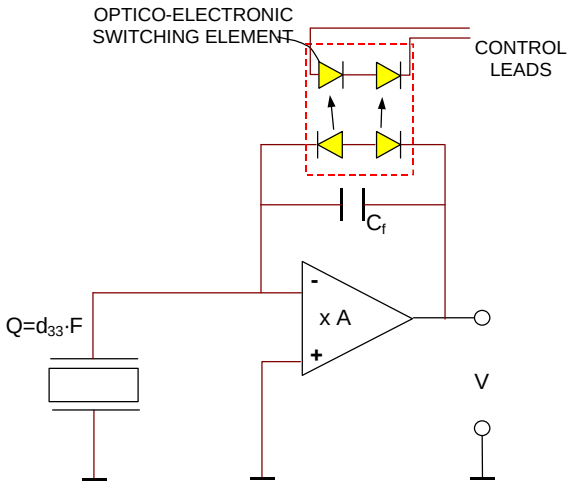

Figure A1.13. *Zeroing semiconductor of optic-electronic technology.*

A1.5. Bulk-in Amplifier for Conditioning Piezoelectric Sensors

A1.5.1. Low Output Impedance Piezoelectric Transducer

With the advent of contemporary solid state technology a rugged miniature field effect transistor circuit was incorporated within the transducer case. The impedance matching function was thus accomplished internally while retaining most of the desirable features of the crystal transducer, i.e. ruggedness, small size, and high speed.

Powered by constant current signal conditioners of this built-in amplifier result is an easy-to-operate, low impedance, two-wires system. In addition to ease-of-use and simplicity, built in sensor offer many advantages over traditional charge mode sensors, including:

1. Fixed input sensitivity independent of cable length or capacitance.
2. Low input impedance (<100Ω) allows signals to be transmitted over long cables through harsh environments with virtually no loss in signal quality.
3. Two-wires system accommodates standard low cost coaxial or other two conductor cable.
4. High quality, voltage output compatible with standard readout, recording or acquisition instruments.
5. Intrinsic sensor self-test feature by monitoring sensor output bias voltage.
6. Low per channel cost as sensors require only low cost constant current signal conditioners.
7. Reduced system maintenance.
8. Direction operation into readout and data acquisition instruments which incorporate power for use with the transducer.

Two types of integrated circuits are generally used in built-in amplifiers: voltage and charge amplifiers. Low capacitance quartz sensing elements exhibit a very high voltage output (according to V=q/C) and are typically used with MOSFET voltage amplifiers. Ceramic sensing elements, which exhibit a very high charge output, are normally coupled to charge amplifiers.

A1.5.2. Solutions Based on Electrometric Amplifiers

Figure A1.14 shows an electrometer amplifier circuit suitable for combination with the piezoelectric transducer in miniature design. This would include all components inside the amplifier unit. The matching electronics with power supply and signal evaluation output U_a are shown inside the matching unit, while in between there is a coaxial transmission line. The piezoelectric transducer is shown in parallel with a capacitance *Cpz*. In certain cases this will consist merely of the inherent capacitance of the transducer and its parts.

The metal oxide semiconductor field effect transistor, *Q*, serves as impedance converter, and the switch for the short-circuiting the capacitance *Cpz* on the piezoelectric transducer directly. This ensures that no residual charges from previous measurements are added to the new measurement at the commencement of measuring. If displacements from zero due to other influences become noticeable, such as major temperature variations, these can be easily eliminated if the measurement is interrupted briefly by switching-off the switch *Sw*. For the measurement that follows, the switch remains open. It will be apparent from the mode of operation that this switch must have high insulation.

The mechanical switches or relays usually employed for this purpose are mostly of the reed relay type on account of the high insulation resistance demanded. These relays incorporate reeds melted into glass, which are actuated by an externally applied magnetic field. These reed

relays correspond to the latest state of the art and give high insulation values and relatively short switching times; nevertheless, however, they have a number of major disadvantages for this application. For example, the magnetic field needed to trigger them requires a relatively large amount of energy, while on the other hand it gives rise to undesirable induction effects and disturbing charges. Upon resetting the relay for operation, these disturbances cause the notorious zero jump, which is irregular and may have positive or negative voltages. The main cause of these disturbances is charges on the inside wall of the glass tubes of the reed relays customary in the trade. Owing to these disturbing charges, the desired starting position at the commencement of measuring, i.e., voltage at the capacitor *Cpz* = 0 and thus, is in error by an amount corresponding a few 0.1pC at the input. Since the charges on the inside of the glass wall of the reed relay which cause the zero jump in the manner described are variable compensation by appropriate zero displacement in the amplifier, for example is ruled in practice.

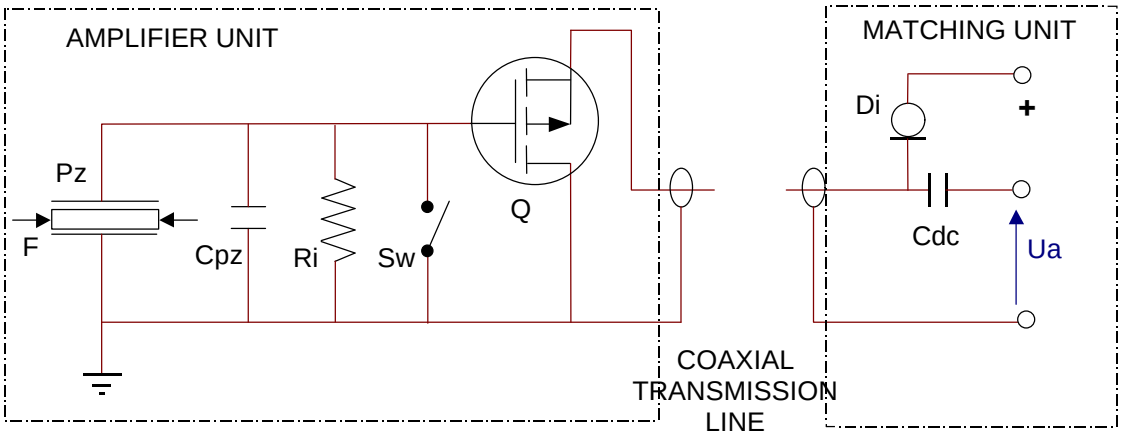

Figure A.14. *Electrometer amplifier circuit using a switch for zeroing*

Instead of the relay use to zeroing the amplifier, one may use a controllable semiconductor element. Figure A1.15 shown a p-channel field effect transistor Q2 for short-circuiting the capacitance *Cpz* or the piezoelectric transducer directly. The field effect transistor is controlled by switching the supply voltage on and off via the coaxial transmission line from the matching and power supply unit. The field effect transistor is thus arranged so that when the power unit is switched off any charges that might arise due to the action of force on the piezoelectric transducer are short-circuited constantly. Only upon switching-on is the FET transistor blocked by the voltage. If necessary, this opening can be delayed by the capacitance C_D until the metal oxide semiconductor field effect transistor is in full action.

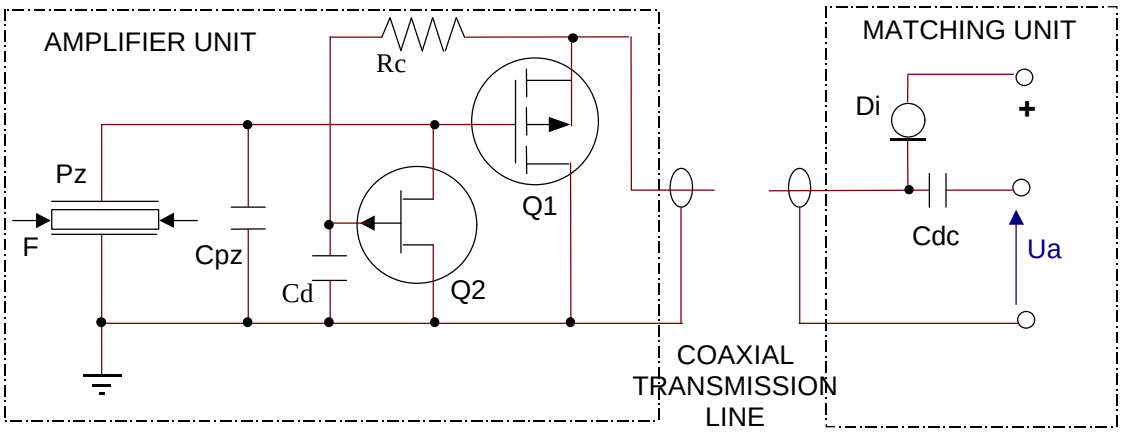

Figure A.15. *Electrometer amplifier circuit using a transistor for zeroing*

Instead of the switched field effect transistor operated as a switch, one may be used which can be adjusted to any intermediate stages between short circuit and maximum resistance, e.g., 10^8, 10^9, 10^{10} to $10^{13}\Omega$ in the blocked state. The magnitude of the effective resistance can be regulated by a control signal. For certain changes this enables disturbances due to temperature variations to be corrected automatically, especially with dynamic measurements. Such solution is shown at Figure A1.16 similar to Figure A1.15, differing in the use of an assembly of two diodes in opposition and controlled by the light source from a LED, instead of the controllable semiconductor element.

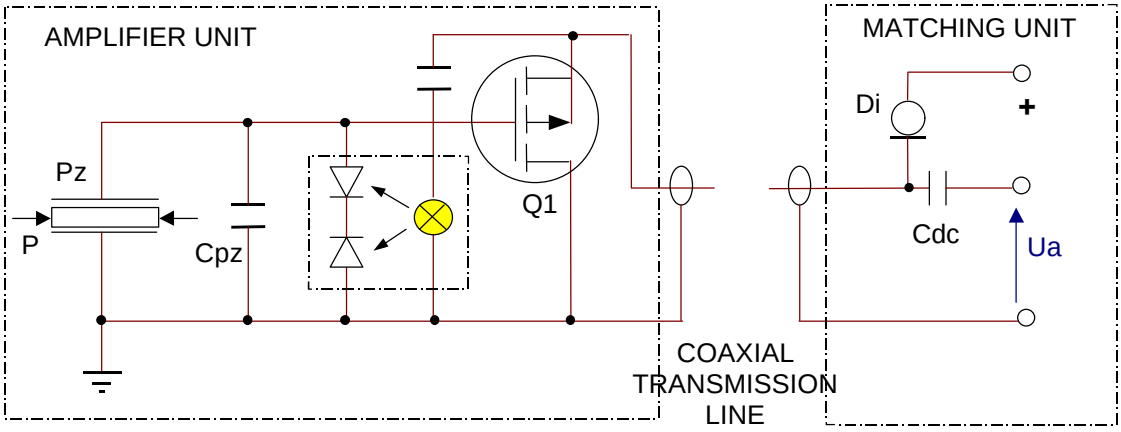

Figure A.16. *Electrometer amplifier circuit using an optic device for zeroing*

Figure A1.17 shows other variant of the previous designs. This circuitry employs a miniature MOSFET input stage followed by a bipolar transistor stage and operates as a source follower (unity gain). A monolithic integrated circuit is utilised which incorporates these circuit elements. This circuit has very high input impedance ($10^{14}\Omega$) and low output impedance (100Ω) which allows the charge generated by the quartz element to be converted into a usable voltage. Power to the circuit is provided by a power supply which supplies a source current (2-18mA) and energising voltage (20-30VDC).

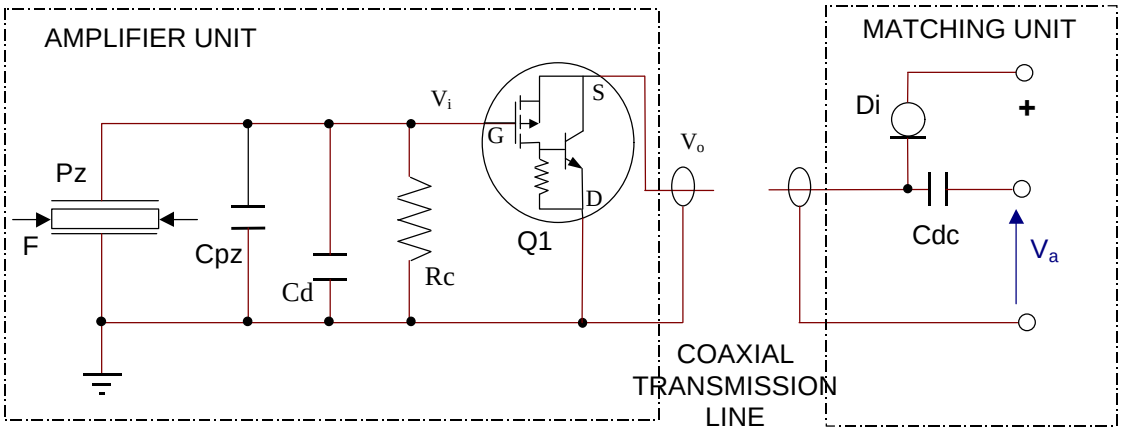

Figure A1.17. *Electrometer amplifier circuit using a special semiconductor for driving the charge from the transducer.*

A1.5.3. Solutions Based on Charge Amplifiers

Figure A1.18 shows a configuration operating on the charge amplifier principle. The operational amplifier is connected to the piezoelectric transducer and is powered via two leads. To short-circuit the negative feedback capacitor the n-channel field effect transistor is employed, which blocks when the supply voltage is switched on and thus brings the operational amplifier into action. Resistance R_T serves to protects the field effect transistor.

The measuring signal is tapped via other two different leads. On account of this system requires a four-core connection between the transducer and the matching electronics not shown. In many cases, especially for industrial applications, the dimensions of the transducer, plug and cable are so large that four-core transmission lines present no particular problems.

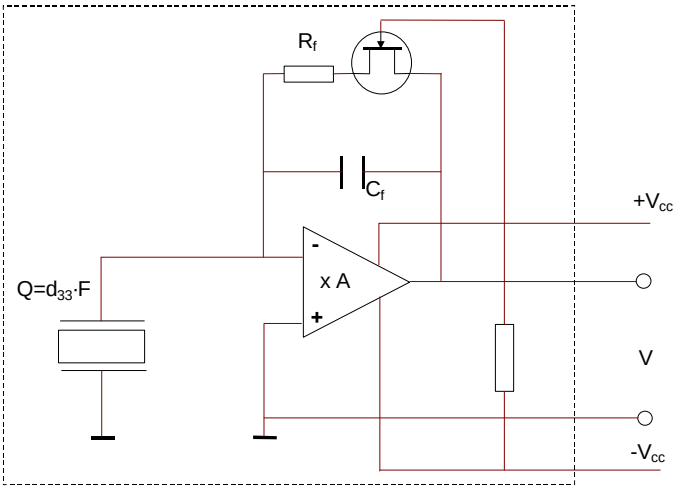

Figure A1.18. *Four leads built-in charge amplifier*

Figure A1.19 shows a variant of Figure A.18 in which the charge amplifier circuitry is used once more but a two-core or coaxial transmission line is employed. A configuration of this king will admit a higher degree of miniaturisation, though a somewhat greater outlay is required. The piezoelectric transducer has a direct connection with the operational amplifier and an indirect connection via the Zener diode. In another variant, however, it can be connected direct to the + and – input of the operational amplifier as well.

The discharge of the negative feedback capacitor is controlled in turn by the p-field effect transistor, which can be operated with a time lag via the capacitor C_D. By switching-on the current supply via the leads of the transmission line, field effect transistor is blocked, bringing the operational amplifier into action. The signal from the piezoelectric transducer is superimposed upon the constant feed current supplied via the transmission leads. The signal is then separated from the feed current in the signal processing unit.

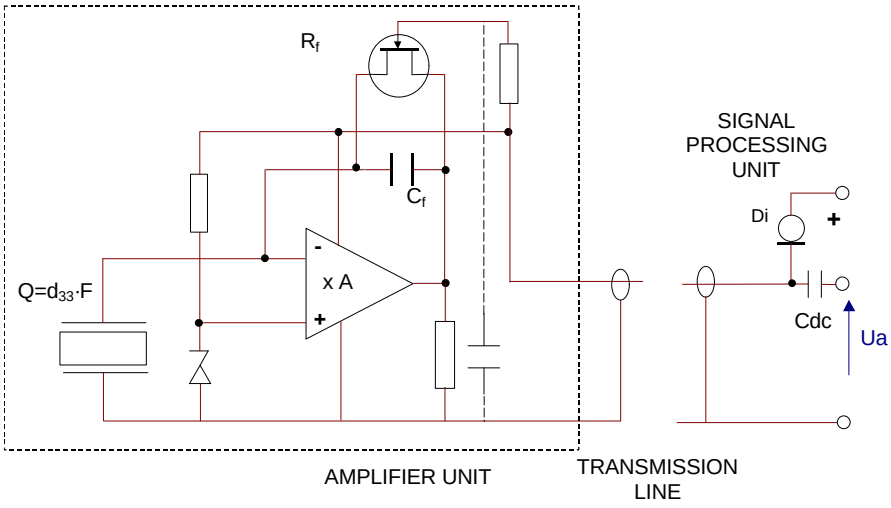

Figure A1.19. *Two leads built-in charge amplifier*

Figure A1.20 shows a variant of Figure A1.19, differing in that the field effect transistor is replaced by the optic-electronic circuit, in which two light-controlled diodes are arranged in opposition so that they release the negative feedback capacitor when the feed current is switched on. The signal is evaluated as in Figure A.19, converting the variation of the feed current into a voltage variation by means of an operational amplifier.

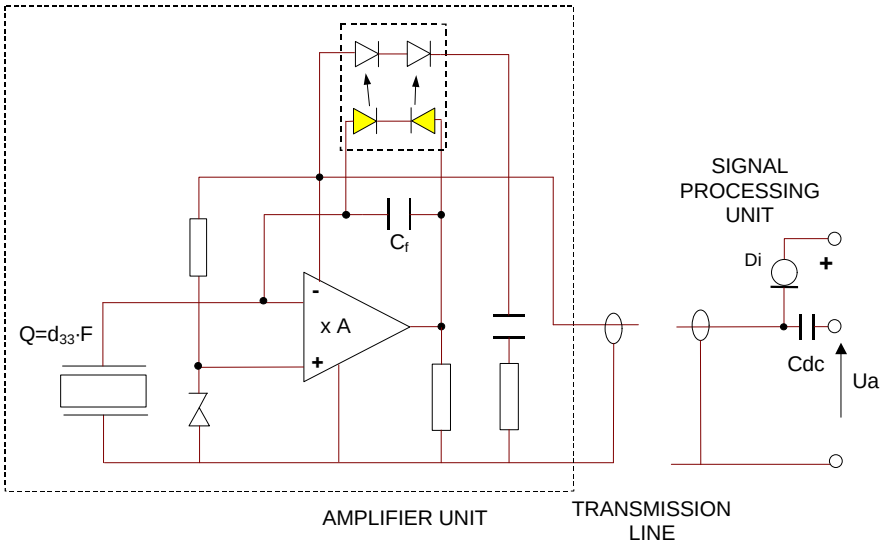

Figure A1.20. *Two leads built-in charge amplifier with an optical semiconductor*

A1.6. Optical Transmission System

Recently, an alternative solution for the signal transmission from piezoelectric sensor has been developed [9]. This solution is based on converting the electrical signal generated by the piezoelectric transducer into an optical signal for being transmitted.

In this type of devices, the electrical signal from the piezoelectric sensor is driven to the electrodes of an electro-optical material. This electro-optical material is part of an optical circuit and through of it a polarised beam of light is drived. The voltage generated by the piezoelectric sensor produces, by Pockel's effect, a mechanical deformation of the electro-optical material (due to the inverse piezoelectric effect). This mechanical deformation produces both a modification of the structure of the electro-optical material and, by Kerr effect, an effect of piezopermitivity causing a modification of the dielectric constant leads to a modification of the refraction index of the electro-optical material. As a result, the output optical signal from the electro-optical material is influenced by the electrical voltage coming from the sensor. (Figure A1.21)

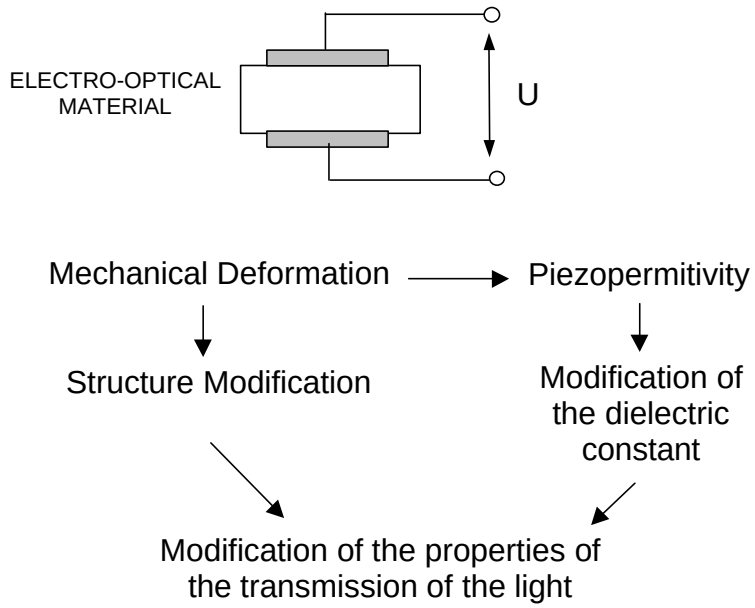

Figure A1.21. *Behaviour of an electro-optical material under an electric field.*

The electro-optical effect is found in ferroelectric materials both single or polycristalines and in the liquide crystals. This effect is characterised by a constant describing the dependence of the index of refraction from the electric field applied. Some materials used in electro-optical applications are: $LiNbO_3$, KH_2PO_4, $BaTiO_3$, ZnO, CdS, $AgGaSe_2$, and other.

Figure A1.22 illustrates an application of this transmitting method. It consists of a piezoelectric accelerometer where the electrodes are connecting to the Pockel's sensor. The properties of light transmission are modified proportionally to the voltage generated by the piezoelectric sensor.

This system has the advantage of permiting the transmission of the signal by means of a light beam using optical fibre. This type of transmission is not affected for the length of the cable or the electromagnetic interference of the environment. Also, it does not require power with voltage or current any internal electronic, as is the case of the built-in amplifiers. Moreover, the technology used has been also implemented in the electro-optical transformer (Chapter 1), making easier the implementation in this kind of sensors.

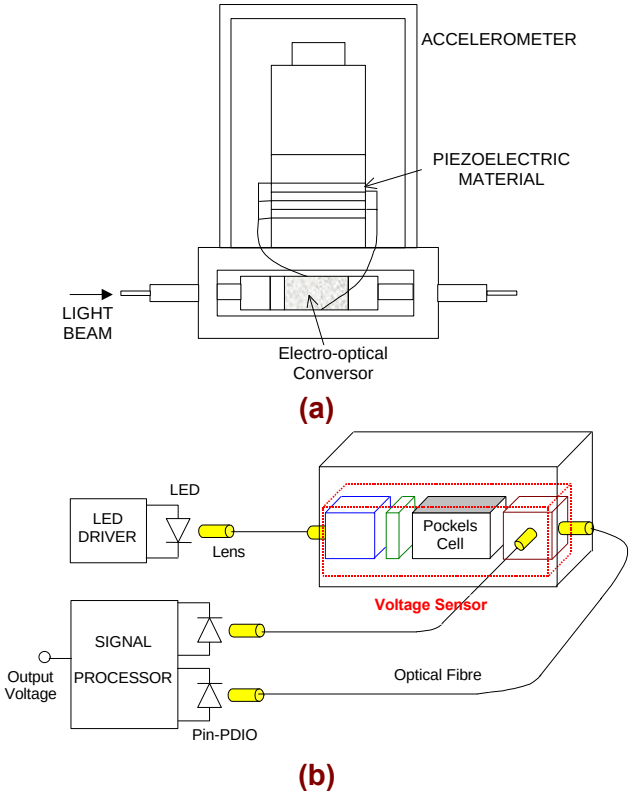

Figure A1.22. *(a) Acceleration Sensor with electro-optical system. (b)Voltage Sensor used*

References

[1] *Electronics for Piezoelectric Sensors*, PCB Piezotronics, 1994

[2] *Piezoelectric Measuring instruments and their Applications*, R. Kail, W.Mahr, Kistler Instrumente AG, Winterthur, Switzerland.

[3] *A case for low impedance*, M.Bennett, Kistler Instrument Corporation, USA.

[4] U.S. Patent US4009447, *Amplifier arrangement with zeroing device for piezoelectric transducers*, Inventors: W. Hans-Joachim, M.Franz, B. Hans Ulrich, Solicited by: Kistler Instrumente AG, 22-February-1977.

[5] U.S. Patent US4546658, *Piezoelectric force/pressure sensor*, Inventors: Rocha Henry, A.F., Harnden, J.R.John, Solicited by: General Electric (U.S), 15-Ocober-1985.

[6] U.S. Patent US4256987, *Constant current electrical circuit for driving piezoelectric transducer*, Inventors: Akihiro Takeuchi, Kiyokazu Asai, Solicited by: Kabushiki Kaisha Toyota Chuo Kenkyusho, Nagoya, Japan, 17-March-1981.

[7] U.S. Patent US4760345, *Charge amplifier circuit*, Inventors: Buesser Bruno, Amstutz Leo, Solicited by: Kistler Instrumente AG (C.H), 26-Juliol-1988.

[8] U.S. Patent US5339285, *Monolithic low noise preamplifier for piezoelectric sensors*, Inventors: Straw Timothy B, Solicited by: U.S. Army (US), 16-August-1994.

A2 Sensing mechanical signals with piezoelectric transducers

A2.1. Introduction

The aim of this chapter is to give a general overview to measurement technique of mechanical magnitudes. In general a mechanical vibration may be measured from the acceleration which generates or from the force which generates. Both concepts are different and the result of the measurement, measure technique, devices to use, influence in the vibration to measure, etc must to be perfectly well know.

A2.2. Accelerometers

Accelerometers have a wide range of application, including *sound* and *vibration monitoring*, and the detection and measurement of *velocity changes*. Hence a great many accelerometer sensor types have been devised, developed and made commercially available.

Each type of accelerometer has characteristics that make it more or less suitable for a particular application. For example, geophones are highly sensitive at very low frequencies; hence they are excellent for monitoring earthquakes. Conversely, miniature solid-state accelerometers are very cheap, quick, and easy to use. While they have very poor sensitivity, they fit the needs of sensors for triggering air bags.

The broadest commercial class of accelerometers is the *longitudinal type*. This type fills the requirements falling between the above extremes. Longitudinal type accelerometers have good sensitivity over a wide frequency band, and are rugged enough for general purpose industrial use. Longitudinal type accelerometers are the key component for most machinery diagnostic equipment, inclinometers, and vibration monitoring. There are many major manufacturers of this type of accelerometer, such as the PCB (registered trademark) piezoelectric accelerometers by Piezotronics Co. and by Wilcoxon Research, of Rockville Md.

A2.2.1. Basic Operation Principle

Conventional piezoelectric accelerometers have a seismic mass, *M*, supported by a piezoelectric element with electrodes. When the accelerometer is subjected to acceleration, inertial forces introduce strains in the piezoelectric element which produce electrical outputs by virtue of the piezoelectric effect. At frequencies much below than the natural resonant frequency of the total accelerometer system, the seismic mass is forced to follow the vibrations thereby acting on the piezoelectric element with a force which is proportional to the seismic mass and the acceleration, as indicated in equation (A2.1):

$$F = M \cdot a \tag{A2.1}$$

The mechanical stress T in the piezoelectric support is given by:

$$T = -a \cdot \frac{M}{A} \qquad \text{(A2.2)}$$

where the stress is considered positive is applied as a compression over the piezoelectric.

Under such a stress, the piezoelectric element delivers a charge or voltage to the electrodes which is proportional to the stress. Hence the output charge or voltage is proportional to the acceleration of the system.

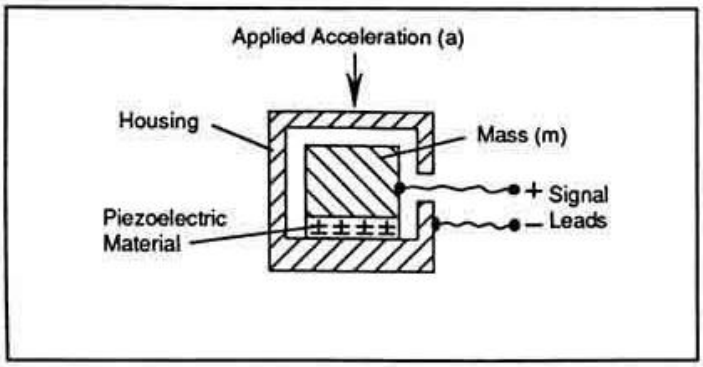

Figure A2.1. *Basic Accelerometer*

The ***Sensibility*** of the accelerometer is defined as the quotient of the output charge or voltage generated and the acceleration, i.e:

Charge sensibility: $S_Q = \frac{Q}{a}$ (A2.3)

Voltage sensibility: $S_U = \frac{U}{a}$ (A2.4)

A2.2.2. Classification

When the piezoelectric element is subjected to compression forces during vibration, the accelerometer is of the *compression type*, and when the piezoelectric element is subjected to shear forces during vibration, the accelerometer is of the *shear type*.

A compression type accelerometer (Figures A2.3 to A2.5) is the most simple in its construction, but it is rather sensitive to temperature transients since the ceramic piezoelectric material is pyroelectric in the axis of polarisation. In contrast to the compression type accelerometers, the shear type accelerometers (Figure A2.2), for which type of accelerometers the electrical signal is developed on surfaces parallel to the axis of polarisation, have a low dynamic temperature sensitivity.

It is known that a higher sensitivity can be obtained by an accelerometer of the *bender* type. In such an accelerometer, the force from the seismic mass acts to bend a so-called "bender element", which has a layer of an electric conductive material sandwiched between two layers of piezoelectric material being polarised in their direction of thickness. Thus, when the element is bent in a plane perpendicular to the longitudinal axis of the element, stresses of compression are generated in one of the two layers and stresses of tension are generated in the remaining layer. When the length of the bender element is considerable larger than the thickness of the element, the electrical charges generated on each of the two layers will be larger than the charges obtained if the same seismic mass is operating directly for the purpose of compression or shear of the piezoelectric material.

However, a disadvantage of the bender element is that it is pyroelectric, since the electrodes are arranged on surfaces which are perpendicular to the axis of polarisation. Another disadvantage of the bender element is that the piezoelectric material constitutes a major part of the mechanical construction which causes some problems when trying to optimise this construction.

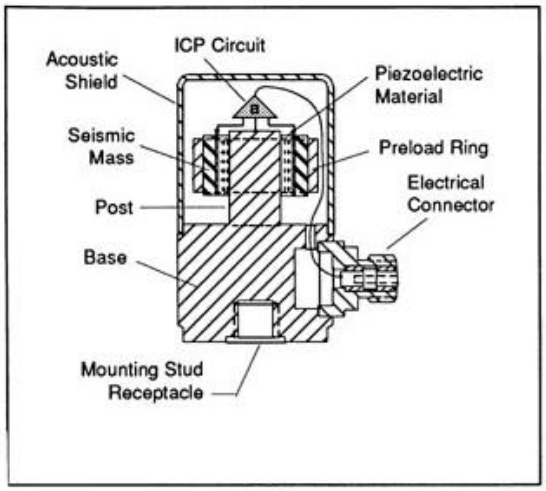

Figure A2.2. *Shear mode (Courtesy PCB accelerometers)*

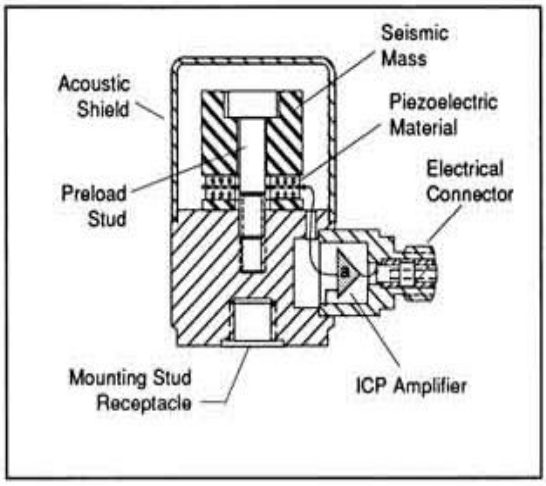

Figure A2.3. *Upright Compression (Courtesy PCB accelerometers)*

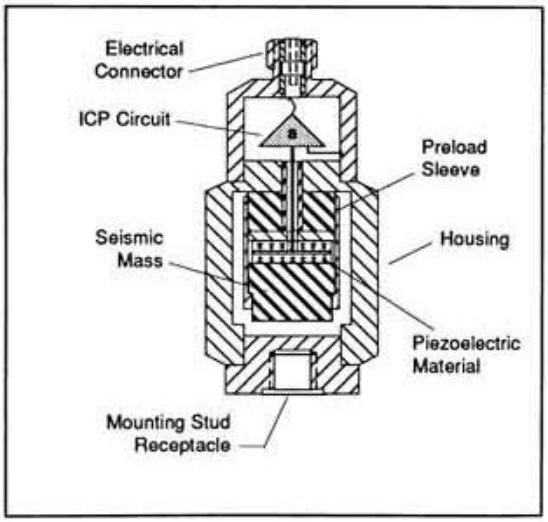

Figure A2.4. *Inverted Compression (Courtesy PCB accelerometers)*

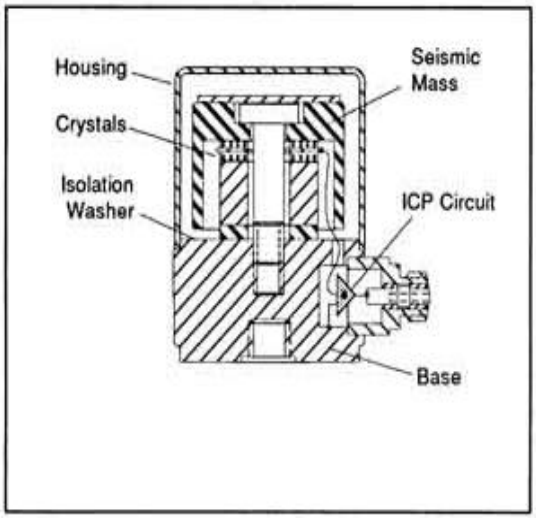

Figure A2.5. *Isolated Compression (Courtesy PCB accelerometers)*

A2.2.3. Operation Modes

As all the charge sensors, the piezoelectric sensor requires a special output conditioning for driving the output signal. This output conditioning determines the type of magnitude and sensibility of the output signal. There are two types of output modes (Appendix 1):

• Open Circuit Mode

Sensitivity of the transducer itself

In this case, the electrical current (o charge) driving from the sensor is very close to zero, D=0. Under this conditions the measured magnitude is the open circuit voltage determined as:

$$E = -g_{33} \cdot T + \frac{D}{e^T} \qquad \rightarrow \qquad E\big]_{D=0} = -g_{33} \cdot T \tag{A2.5}$$

For a compressive accelerometer:

1. If the seismic mass M is much larger than the mass m of the transducer, the mechanical stress in the transducer is obtained as:

$$T(t) = -\frac{F(t) \cdot M}{A} \qquad \text{(compression)} \tag{A2.6}$$

The sensibility of the accelerometer under a perfect open circuit ($R_E \rightarrow \infty$; $C_E \rightarrow 0$) is then:

$$S_V(0)\Big|_{\substack{M>>m \\ R_E \rightarrow \infty \\ C_E \rightarrow 0}} = \frac{V}{F} = g_{33} \cdot \frac{t}{A} \cdot M \tag{A2.7}$$

2. If the transducer mass *m* is not negligible compared with *M*, then M must be replaced by $(M+\frac{1}{2}m)$ in the equation A2.6, as indicated equation A2.8:

$$S_V(0)\Big|_{\substack{M\approx m \\ R_E \rightarrow \infty \\ C_E \rightarrow 0}} = \frac{V}{F} = g_{33} \cdot \frac{t}{A} \cdot \left(M + \frac{1}{2}m\right) \tag{A2.8}$$

3. In the limit case where there is no seismic mass, M=0, the sensibility is calculated as:

$$S_V(0)\Big|_{\substack{M\approx m \\ R_E \rightarrow \infty \\ C_E \rightarrow 0}} = \frac{V}{F} = g_{33} \cdot \frac{t}{A} \cdot \frac{m}{2} = \frac{1}{2} \cdot r \cdot g_{33} \cdot t^2 \tag{A2.9}$$

Sensitivity of the transducer connected with the electronic circuit

As described in Appendix 1, when the transducer is connected to a voltage amplifier (open circuit mode), the input impedance of the readout device (R_E and C_E) must be considered. Under these circumstances, the *voltage sensibility of the accelerometer* is:

1. If $R_E >> \frac{1}{w \cdot (C_a + C_E)}$ the influence of R_E is negligible and the sensibility is expressed by:

$$S_V(E)\Big|_{R_E, C_E} = S_V(0) \cdot \frac{1}{1+\frac{C_E}{C_a}} \tag{A2.10}$$

C_a describes the transducer capacitance calculated as: $C_a = \frac{e_0 \cdot e_r \cdot A}{t}$. Thus, due to the influence of the readout device, the sensibility in open circuit is reduced in the factor: $\frac{1}{1+\frac{C_E}{C_a}}$.

2. If R_E is not negligible, the general expression of the sensibility will be:

$$S_V(E)\Big|_{R_E,C_E} = S_V(0) \cdot \frac{1}{1+\frac{C_E}{C_a}} \cdot \frac{1}{\sqrt{1+\frac{1}{w^2 R_E (C_a + C_E)^2}}} \qquad \text{(A2.11)}$$

• Short-circuit mode

In this case, the electrical voltage through the sensor is very close to zero, E=0. Under this conditions the measured magnitude is the open circuit voltage determined as:

$$D = d_{33} \cdot T + e^T E \qquad \rightarrow \qquad D\big]_{E=0} = d_{33} \cdot T \qquad \text{(A2.12)}$$

For a compressive accelerometer:

1. If the seismic mass M is much larger than the mass m of the transducer, the mechanical stress in the transducer is obtained as:

$$T(t) = -\frac{F(t) \cdot M}{A} \qquad \text{(compression)} \qquad \text{(A2.13)}$$

The sensibility of the accelerometer under a perfect open circuit ($R_E \rightarrow \infty$; $C_E \rightarrow 0$) is then:

$$S_Q(0)\Big|_{\substack{M>>m \\ R_E \rightarrow \infty \\ C_E \rightarrow 0}} = \frac{Q}{F} = d_{33} \cdot \frac{t}{A} \cdot M \qquad \text{(A2.14)}$$

2. If the transducer mass *m* is not negligible compared with *M*, then M must be replaced by $(M+\frac{1}{2}m)$ in the equation A2.6, as indicated equation A2.8:

$$S_Q(0)\Big|_{\substack{M \approx m \\ R_E \rightarrow \infty \\ C_E \rightarrow 0}} = \frac{Q}{F} = d_{33} \cdot \frac{t}{A} \cdot \left(M + \frac{1}{2}m\right) \qquad \text{(A2.15)}$$

3. In the limit case where there is no seismic mass, M=0, the sensibility is calculated as:

$$S_Q(0)\Big|_{\substack{M \approx m \\ R_E \rightarrow \infty \\ C_E \rightarrow 0}} = \frac{Q}{F} = d_{33} \cdot \frac{t}{A} \cdot \frac{m}{2} = \frac{1}{2} \cdot r \cdot d_{33} \cdot t^2 \qquad \text{(A2.16)}$$

Sensitivity of the transducer connected with the electronic circuit

As described in Appendix 1, when the transducer is connected to a voltage amplifier (open circuit mode), the input impedance of the readout device (R_E and C_E) must be considered. Under these circumstances, the *current sensibility of the accelerometer* is:

1. If $R_E >> \frac{1}{w \cdot (C_a + C_E)}$ the influence of R_E is negligible and the sensibility is expressed by:

$$S_Q(Q)\big|_{C_E} = S_Q(0) \cdot \frac{1}{1 + \frac{C_E}{C_a}} \qquad \text{(A2.17)}$$

C_a describes the transducer capacitance calculated as: $C_a = \frac{e_0 \cdot e_r \cdot A}{t}$. Thus, due to the influence of the readout device, the sensibility in open circuit is reduced in the factor: $\frac{1}{1 + \frac{C_E}{C_a}}$.

2. If R_E is not negligible, the general expression of the sensibility will be:

$$S_Q(E)\big|_{R_E, C_E} = S_Q(0) \cdot \frac{1}{1 + \frac{C_E}{C_a}} \cdot \frac{1}{\sqrt{1 + \frac{1}{w^2 R_E (C_a + C_E)^2}}} \qquad \text{(A2.18)}$$

- **Comments**

If the voltage sensitivity of a piezoelectric transducer is known, the charge sensitivity may be easily obtained.

$$S_Q(0) = \frac{Q}{F} = S_V(0) \cdot C_a \qquad \text{(A2.19)}$$

A2.2.4. Frequency application

The application limit of the accelerometer can be obtained from its resonance frequency. In a compressive accelerometer (with an axial vibration), the piezoelectric material form the elastic part of a vibrant system. It elastic constant may be calculated as.

$$C = \frac{F}{\Delta h} = \frac{1}{s} \cdot \frac{A}{h} \qquad \text{(A2.20)}$$

s is the elasticity of the piezoelectric material. The value of *s* depends on the operation mode: open circuit, s_{33}^E, or short-circuit conditions, s_{33}^Q.

$$s_{33}^D = \left(1 - k_{33}^2\right) \cdot s_{33}^E \qquad \text{(A2.21)}$$

k_{33} is the coupling factor of the piezoelectric material. k_{33} of the order of 0.7 for ceramic and k_{33}=0.09.

From a mechanical point of view, the resonance frequency of a vertical bar fixed in one of its end and with a mass M fixed in its free end, which is vibrating longitudinally is equal to:

$$f_r = \frac{1}{2p} \cdot \sqrt{\frac{C}{M + \frac{1}{3} \cdot m}} \qquad \text{(A2.22)}$$

As a general rule, the response increase in +3dB for a frequency is taken as the frequency limit of the accelerometer. This frequency is equal to:

$$f_{limit} = \frac{1}{2} \cdot f_r \qquad \text{(A2.23)}$$

A2.2.5. Review Accelerometers

Table A2.1. *Review about accelerometers characteristics*

Material	**Quartz Accelerometers**	**Ceramic Accelerometers**
Relative Permitivity e_{33}^r	4.5	1800
Coupling factor k_{33}	0.09	0.7
d_{33} [C/N]	$2.0 \cdot 10^{-12}$	$300 \cdot 10^{-12} - 500 \cdot 10^{-12}$
g_{33} [Vm/N]	-50	20 - 25
Sensitivity S_V ($C_E << C_a$)	$S_V(E)\Big\vert_{\substack{R_E \to \infty \\ C_E \to 0}} = \frac{V}{F} = g_{33} \cdot \frac{T}{A} \cdot \frac{1}{1 + \frac{C_E}{C_a}}$	
Sensitivity S_Q ($C_E >> C_a$)	$S_Q(E)\Big\vert_{\substack{R_E \to \infty \\ C_E \to 0}} = \frac{V}{F} = d_{33} \cdot \frac{T}{A} \cdot \frac{1}{1 + \frac{C_E}{C_a}}$	
Frequency limit (Open Circuit)	$f_r = \frac{1}{2p} \cdot \sqrt{\frac{\frac{1}{s_{33}^E} \cdot \frac{A}{h}}{M + \frac{1}{3} \cdot m}}$	
Frequency limit (Short Circuit) $s_{33}^D = (1 - k_{33}^2) \cdot s_{33}^E$	$f_r = \frac{1}{2p} \cdot \sqrt{\frac{\frac{1}{(1 - k_{33}^2) \cdot s_{33}^E} \cdot \frac{A}{h}}{M + \frac{1}{3} \cdot m}}$	

Piezoelectric accelerometers permit the measurements of mechanical vibrations when the force which generates the mechanical vibration is also causing a certain mechanical displacement of the set-up. When this displacement appear, there is a velocity varying during the time and the acceleration may be measured. On contrary, if the system is perfectly blocked (no displacement) and there is no accelerations, the use of the accelerometer has not sense.

The use of accelerometers measures the acceleration generated for the system being studied and also the accelerations that the environment causes over the system. If the system is subject to important external noise a solution is the use of a second accelerometer measuring only the external acceleration (if this is possible). The subtraction of both magnitudes gives the acceleration of the set-up.

A2.3. Force Sensors

Many force/pressure sensors are well known to the art for using in a multiplicity of diverse applications. The known sensors range from simple spring – actuated devices to elaborate wire and semiconductor strain gages. The majority of the sensor take advantage of the displacement occurs during the application of a force to obtain the force, by means of the Young Modulus of structure deformed. Thus these sensor always introduce a modification in the real conditions of the system being measured. Furthermore, they do not allow the measurement of blocking force.

Each particular type of sensor has other limitations of these *strain* sensors types:

Spring-actuated sensing devices, for example, are difficult to interface with electronic systems and typically suffer from bearing-wear problems. The application of this devices is also limited a very low frequencies due to the bad operation of the spring in high frequency.

Strain gages, of wire, semiconductor or other type, generally require careful mounting and elaborate temperature compensation; the output drift of such strain gage sensors often requires manual output zeroing and use in a bridge configuration, manufacture with the customary bridge configuration. Manufacture with the customary bridge configuration is itself relatively expensive. Electronic control technology for such diverse products as home appliances and automobile engines requires a force/pressure sensor which is not extremely reliable, but also relatively inexpensive to produce.

A2.3.1. Description

Piezoelectric force sensors are very stiffness sensors that allow the measurement of dynamic forces without almost incorporating displacement in the system. Nevertheless their application in not possible in static events, although quasi-static measurements may be measured when coupled into high impedance charge or voltage amplifiers.

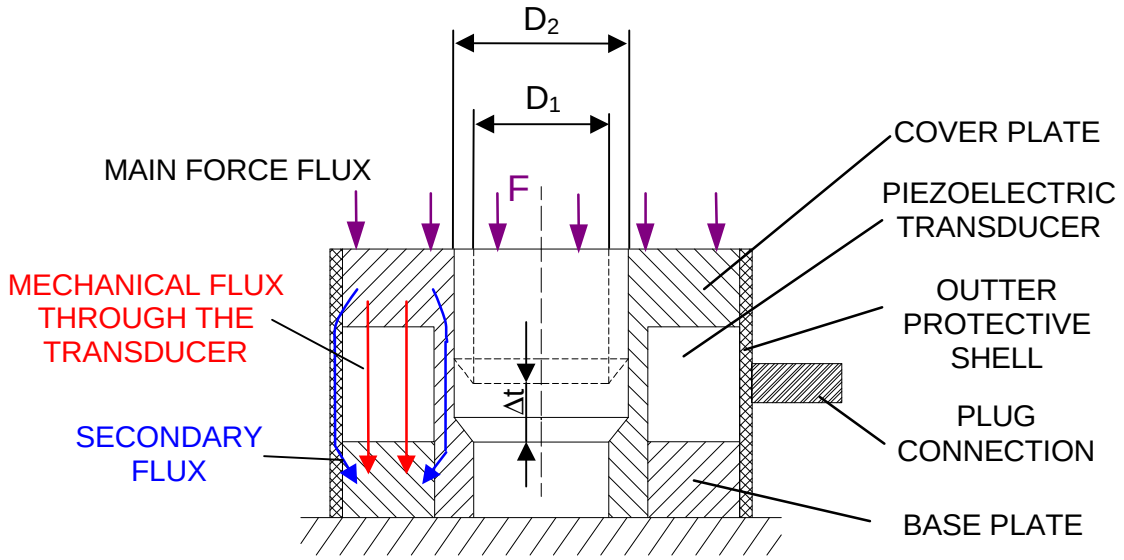

Figure A2.6. *A typical force sensor*

A typical structure of a force sensor is illustrates in Figure A2.6. The transducer consist of the cover plate, base plate, electromechanical transducer, adjustable parallel force element, outer protective shell and plug connection. Of the force flux P introduced onto the cover plate, the main part is led through the electromechanical transducer element, the adjustable secundary

flux through the parallel force element, and a small secondary flux through the protective shell. This shell may be designed as a preloading element.

Also fitted on it is the plug, which provides the electrical connection for the force transducer element. Approximate adjustment of the assembled is accomplished by slightly altering the boring depth Δt, though the engineer may also prefer to retain a constant boring depth and obtain fine adjustment to the required sensitivity by slightly varying the boring diameter D, By adjusting the parallel force element in this way, the division between the main and secondary forces fluxes is altered, resulting in a change of sensitivity because a larger part of force P to be measured is led through the electromechanical transducer element, increasing its sensitivity.

A2.3.2. Operation

If a force F is applied over a piezoelectric force transducer, an electrical charge will appear in their electrodes with a value indicated by equation A2.24.

$$Q = -d_{33} \cdot F \tag{A2.24}$$

This charge is completely independent of transducer dimensions and hence of its tolerances. However, if n discs are stacked and connected electrically in parallel the result will be:

$$Q = -n \cdot d_{33} \cdot F \tag{A2.25}$$

Under open circuit conditions, the open circuit voltage on a disc of thickness t is given by:

$$U_3 = -g_{33} \cdot t \cdot T_3 \tag{A2.26}$$

In the case of the stack, the discs are connected in parallel, so the resulting voltage is the same. The advantage of a stack is more charge, higher capacitance and thus a lower impedance.

• Path of Force transmission

When the mentioned dynamic force is applied onto the cover plate of the force sensor, there are several paths for transmission of the force. Only a part of this flux will arrive to excite the piezoelectric transducer. The structure of each type of sensor housing will determine the percentage of main flux arriving to the piezoelectric material.

Many mounting configurations permit or require multiple pats of static (or average) force transmission between the point of application and the transducer element. These static paths can be viewed as combinations of spring elements in parallel or in series. The masses of the elements and any dissipative (i.e. damping) forces between the elements are initially neglected.

The stiffnesses and the arrangement of the spring elements together with the placement of the load-measuring device within the assembly, determine the effective static sensitivity of the transducer. This sensitivity is often different from the nominal sensitivity of the transducer as given by the manufacturer.

In Figure A2.7, a **single series path** exists between the point of application of the force and the frame. Placing a transducer along the path yields a satisfactory measurement of the average value of the applied load, F. Thus:

$$F = F_T = F_S = F_C \tag{A2.27}$$

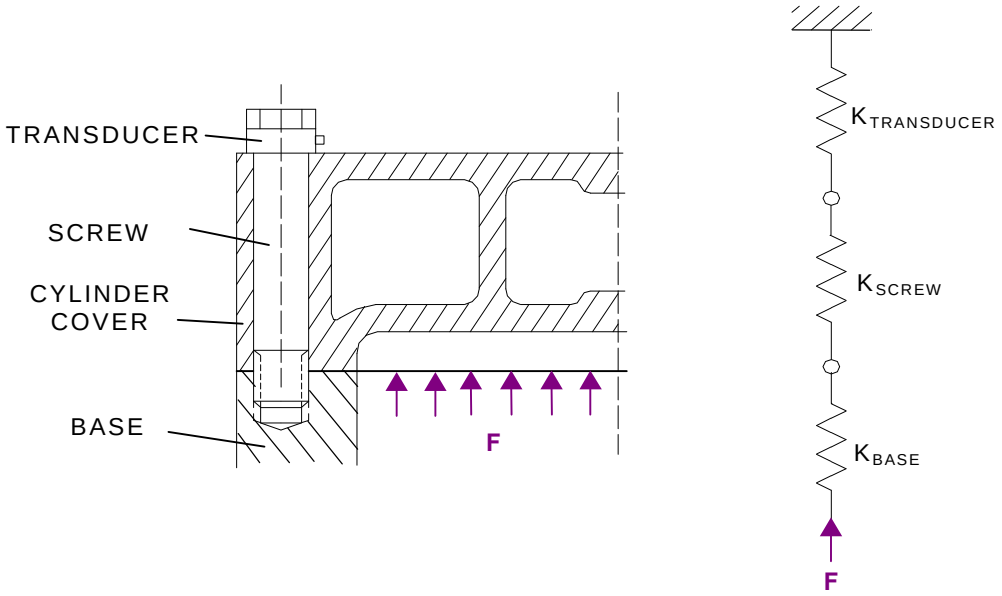

Figure A2.7. *Single series path of force transmission*

In Figure A2.8, two examples of bearing force measurement is shown. In this case, two parallel paths exist between the point of application and the base. The stiffnesses of the members are also shown schematically. Thus, the force F, is divided between the flange/machine screw series combination, and the transducer with stiffness K_T. The combined stiffness of the machine screw and flange is indicated in equation A2.28:

$$K_e = \frac{K_S \cdot K_F}{K_S + K_F} \tag{A2.28}$$

which is approximately equal to K_S since generally, the flange stiffness is likely to be much greater than the stiffness of the machine screw. Therefore:

$$F = F_T + F_S = K_T \cdot X_2 + K_S \cdot X_2 \tag{A2.29}$$

Since the deflections of the machine screw and transducer due to the applied load are equal, the fraction of the load, F, carried by the transducer is:

$$\frac{F_T}{F} = 1 - \frac{K_S}{K_S + K_T} \tag{A2.30}$$

In order to fully utilise the sensitivity of the transducer, its stiffness must be considerably greater than that of the machine screw. The stiffness of the flange, K_F, and the stiffness of the housing, K_H, do not affect the measurement. It should be noted, however, that the stiffness of the individual elements is often difficult to calculate. An in situ calibration of the set-up using static, step unit, or very low frequency time-varying forces is likely to be necessary for each set-up.

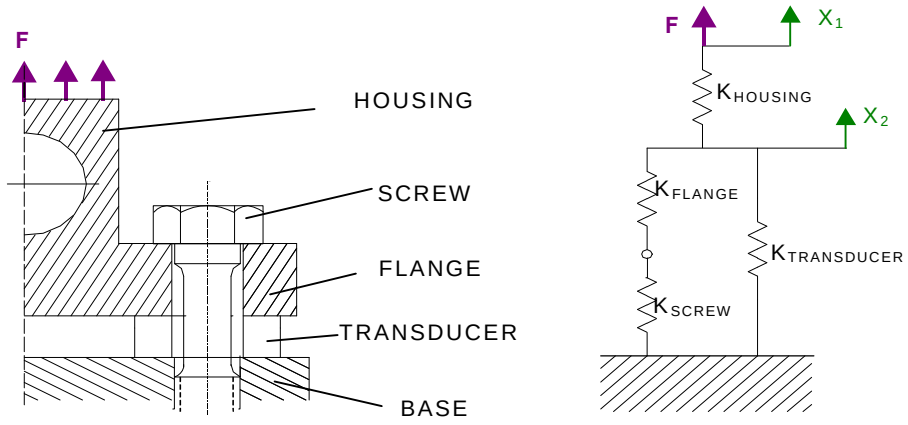

Figure A2.8. *Parallel static path of force transmission*

• Inertial Effects (Dynamic Paths)

The above examples ignore the fact that the housing and other elements also possess mass. In dynamic loading situations, some fraction of the applied load goes to accelerating the mass of the intervening structure between the point of load application and the transducer. This has the effect of reducing the force that appears across the transducer, forming an additional parallel **dynamic path**, similar to the parallel static path discussed above. If one examines the bearing load problem in Figure A2.8 above, it is possible to model the measurement system as shown in Figure A2.9. The effective mass includes the mass of the housing, the mass of the transducer, and a fraction of the mass of the screw.

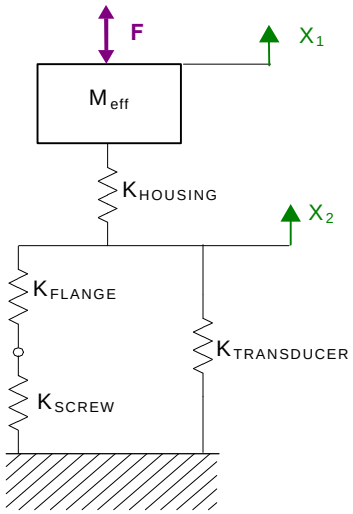

Figure A2.9. *Force path with inertial effects*

Summing the forces acting on the mass and setting them equal to the mass times the vertical acceleration of the centre of gravity, one obtains the force acting through the transducer:

$$F_T = F - F_S - M_{eff} \cdot \ddot{X}_1 \qquad \text{(A2.31)}$$

Again, it has been assumed that $K_F >> K_S$. Equation A2.31 shows that both static and dynamic pats exist around the transducer. The dynamic path also alters the phase of the signal seen by the transducer. Since, in the frequency domain, the acceleration increases as the square of the

frequency, (for a given displacement), the mass-acceleration term becomes progressively larger as the frequency range of the measurement is increased.

One can minimise this dynamic effect by placing the transducer as close as possible to the application point, thereby, minimising the effective mass. However, that choice is not always available. Alternately, one can often compensate for this term by measuring the acceleration with an accelerometer, multiplying by a constant, (the effective mass), and substracting this signal electronically from the measured force signal. Another procedure would be to calibrate the system dynamically by applying a known impact or shaker force in place of the load, F. using this information one could design a compensator circuit (inverse filter) so as to produce a linear dynamic response over an extended frequency range. Finally, one caould adjust the data after storage in a computer after the measurements have been carried out. Although these latter procedures can be quite cumbersome, and involve the noisy operation of electronic differentiation, they are sometimes necessary.

In general, the intervening structure can exhibit more complicated dynamic behaviour than the simple mass spring combination discussed above. Damping forces, existing at joins and elsewhere, although generally intervening structure within the frequency range of interest. While, in principle, compensation is possible by some of the same techniques as were discussed above, serious practical difficulties may be encountered.

Also the base side of the transducer will not usually be stationary, as it has been assumed up to now. Fortunately, base motion does not affect the dynamic calibration considerations discussed above. The main effect of the base motion is to alter the particular value of the acceleration, $\ddot{X}$, that would be required for the mass compensation discussed above.

- **Comments**

Accurate high frequency dynamic force measurements can pose significant challenges to the experimenter. it is often difficult to compensate for any inertial effects other than those due to translations of obvious rigid-body elements. The need for in-situ dynamic calibration of most set-ups over their entire frequency range of intended operation can hardly be overemphasised, if credible data is to be produced. At the very last one should know the usable frequency range of a given measurement set-up. The upper frequency limit is seldom determined by the transducer itself but rather by the intervening elements between the point of load application and the transducer, mounting and alignment of transducer elements within an experimental set-up.

References

[1] Andres Soom, John Kubler, *Measurement of Dynamic Forces*, Kistler Instrument Corporation, Technical Note K20.220.

[2] Great Britain Patent GB1496919, *Adaptable force transducer*, Solicited by: Kistler Instrument AG, 5-January-1978.

[3] U.S.Patent US4088015, *Force measuring apparatus with mounting arrangement*, Inventor: Wolfer Peter, Solicited by: Kistler Instrumente A.G., 9-May-1978

[4] PCB Piezotronics Catalogue, *Force, piezoelectric sensor selection guide for dynamic measurments*, FSG-605B, PCB, U.S.A. 1994.

[5] PCB Piezotronics Catalogue, *Vibration & shock sensor selection guide*, SCG-601C, PCB, U.S.A. 1994.

SIXTH PART:

SCIENTIFIC PRODUCTION

Undertaken Research

Short-Term Research Visits

- **9/99-12/99** . Materials Develop. Dept.. Murata Manufacturing Co. Ltd., Japan.
- **9/98-12/99** Ceramic Laboratory, Swiss Federal Institute of Technology, Switzerland
- **9/97-12/97** High Voltage Laboratory, University of Southampton, Great Britain.

Publications

Books and Monographs.

- A.Vázquez, "Characterisation of Piezoelectric Ceramics. The method of the resonance-antiresonance." CPDA-ETSEIB, UPC, Barcelona, May 1998.
- R.Bosch, A.Vázquez, J.Álvarez, "The Piezoelectric Transformer. A feasible transducer for measuring high voltage". CPDA-ETSEIB, UPC, Barcelona, January 1997.

Articles Published (or to be published)

A. Piezoelectric Applications

- P.Durán Martín, A.Vázquez, D.Damjanovic, *Production and Characterisation Rainbow Piezoelectric Actuators. Advantages from Other Tradicional Devices.* IV Reunión Nacional de ELECTROCERÁMICA and II Conferencia Iberoamericana, Madrid 3-4 June 1999. To be published at Boletin de la Ceramica y Vidrio.
- A.V. Carazo, R. Bosch, Piezoelectric Non-resonant Transformer to Measure High Voltage, Journal of the European Ceramic Society 19 (6-7) (1999) pp. 1275-1279. (in English)
- A.Vázquez, R.Bosch, *Piezoelectric non-resonant transformer to measure high-voltage in distribution networks.* Proceedings of Hispano-French Conference on Piezoelectric Applications, CAP'98, Barcelona 29-30 October 1998, pp. 99-102. (in Spanish)
- A.Vázquez, R.Bosch, *Transformador Piezoeléctrico para Medidas de Altas Tensiones.* Proceedings of the "III Jornadas Latinoamericanas en Alta Tensión y Aislamiento Eléctrico, ALTAE". Universidad Simón Bolivar, Caracas, Venezuela, 28-31 Oct. 97. (in Spanish)
- A.Vázquez, R.Bosch, *Transformador Piezoeléctrico para Medida de Altas Tensiones. Investigaciones en el seno de la UPC*. 5as Jornadas Hispano-Lusas de Ingeniería Eléctrica, Salamanca, Spain, 3-5 July 1997. (in Spanish)
- A.Vázquez, R.Bosch, J.Álvarez, *Medida de tensiones de distribución en M.T. utilizando la piezoelectricidad.* Revista ELECTRA, Barcelona, June 1997. (in Spanish)

B. Space Charge Measurement

- A. Vazquez, G. Chen, A.E. Davies, R. Bosch, *Space Charge Measurement Using Pulsed Electroacoustic Technique and Signal Recovery*, Journal of the European Ceramic Society 19 (6-7) (1999) pp. 1219-1222. (in English)

Patents

- Patent ES2118042: "Piezoelectric non resonant transformer to measure high voltages and its working procedure". R.Bosch, J.Álvarez, A.Vázquez. U.P.C. Spain 01-09-98.